UNIVERSIDAD AUTÓNOMA DE MADRID

MEMORIA DE TESIS DOCTORAL

Phenomenological and Cosmological Aspects of Axions and Other Nambu-Goldstone Bosons

Autor:
Fernando Arias-Aragón

Supervisor:
Dr. Luca Merlo

Tesis presentada para la obtención del título de Doctor en Física Teórica

en

Departamento de Física Teórica, Universidad Autónoma de Madrid
y
Instituto de Física Teórica, UAM-CSIC

2021/06/18

Instituto de
Física
Teórica
UAM-CSIC

A mis familias, la de sangre y la elegida.
A Yves, la luz de mis días.

PUBLICATION LIST

During the development of this thesis the following scientific articles were published:

- **The Minimal Flavour Violating Axion**
  F. Arias-Aragon, L. Merlo
  JHEP 10 (2017) 168, [arXiv:1709.07039].

- **Data Driven Flavour Model**
  F. Arias-Aragon, C. Bouthelier-Madre, J.M. Cano, L. Merlo
  Eur.Phys.J.C 80 (2020) 9, 854, [arXiv:2003.05941].

- **Cosmic Imprints of XENON1T Axions**
  F. Arias-Aragon, F. D'Eramo, R.Z. Ferreira, L. Merlo, A. Notari
  JCAP 11 (2020) 025, [arXiv:2007.06579].

- **Neutrino Masses and Hubble Tension via a Majoron in MFV**
  F. Arias-Aragon, E. Fernandez-Martinez, M. Gonzalez-Lopez, L. Merlo
  Eur.Phys.J.C 81 (2021) 1, 28, [arXiv:2009.01848].

- **Production of Thermal Axions across the ElectroWeak Phase Transition**
  F. Arias-Aragon, F. D'Eramo, R.Z. Ferreira, L. Merlo, A. Notari
  JCAP 03 (2021) 090, [arXiv:1709.07039].

The following conference proceedings were also published:

- **The minimal flavour violating Axion and its effect on ΔN_{eff}**
  F. Arias-Aragon
  Conference Proceeding, 54th Rencontres de Moriond on Electroweak Interactions and Unified Theories.

- **Production of Thermal Axions across the ElectroWeak Phase Transition**
  F. Arias-Aragon
  Conference Proceeding, 40th International Conference on High Energy Physics
  PoS ICHEP2020 (2021), 586. DOI: 10.22323/1.390.0586.

Abstract

Though the Standard Model of Particle Physics is an impressive theory with countless phenomena correctly predicted, it still presents some open problems. In this thesis we explore the power of some Nambu-Goldstone Bosons to deal with two of these problems: the Strong CP Problem and the Flavour Puzzle, while studying at the same time some of their cosmological features.

The Strong CP Problem is addressed at the same time as part of the Flavour Puzzle with an invisible QCD Axion arising from the Minimal Flavour Violation ansatz. This model explains the mass ratios for third-generation fermions while providing a solution to the Strong CP Problem and possible DM candidate, the Minimal Flavour Violating Axion.

Neutrino masses are then addressed with a Majoron that also alleviates the Hubble tension and can arise from Minimal Flavour Violation, compatible thus with the previous model. This model also presents a relatively light new scalar and heavy neutrinos below the usual Type-I see-saw scale, with interesting phenomenology at colliders and beam dump experiments.

Finally, we study the impact hot axions can have on the number of relativistic degrees of freedom. Performing a rigorous and smooth analysis across the Electroweak Phase Transition, we study both a model-independent scenario and three specific models: DFSZ, KSVZ and the previously presented Minimal Flavour Violating Axion. Additionally, the compatibility of this observable with the XENON1T excess is considered. Results measurable by the CMB-S4 experiment, some compatible with axion cold Dark Matter, are obtained.

Contents

List of Figures

List of Tables

Abbreviations

BR	**B**ranching **R**atio
BSM	**B**eyond **S**tandard **M**odel
CMB	**C**osmic **M**icrowave **B**ackground
CP	**C**harge conjugation and **P**arity
DM	**D**ark **M**atter
DFSZ	**D**ine-**F**ischler-**S**rednicki-**Z**hitnitsky
EW	**E**lectro**w**eak
EWPT	**E**lectro**w**eak **P**hase **T**ransition
EWSB	**E**lectro**w**eak **S**ymmetry **B**reaking
FN	**F**roggatt-**N**ielsen
HEP	**H**igh **E**nergy **P**hysics
KSVZ	**K**im-**S**hifman-**V**ainshtein-**Z**akharov
MFV	**M**inimal **F**lavour **V**iolation
MFVA	**M**inimal **F**lavour **V**iolation **A**xion
NEDM	**N**eutron **E**lectric **D**ipole **M**oment
NGB	**N**ambu-**G**oldstone **B**oson
NP	**N**ew **P**hysics
PNGB	**P**seudo-**N**ambu-**G**oldstone **B**oson
PQWW	**P**eccei-**Q**uinn-**W**einberg-**W**ilczek
QCD	**Q**uantum **C**hromo**d**ynamics
QCDPT	**Q**uantum **C**hromo**d**ynamics **P**hase **T**ransition
QFT	**Q**uantum **F**ield **T**heory
SM	**S**tandard **M**odel
SSB	**S**pontaneous **S**ymmetry **B**reaking
VEV	**V**acuum **E**xpectation **V**alue

Introducción

Cuando pensamos en la fenomenología de física de partículas es fácil considerarla como jugar con un puzle: quienes trabajamos en este campo perseguimos la comprensión de una imagen completa de la naturaleza, algo que describa todos los fenómenos observables sin dejar atrás ninguna pieza o romper las reglas que describe cómo se conectan. Esas piezas toman la forma de partículas, mientras que las simetrías, ya sean gauge, globales o Poincaré, discretas o continuas, pueden ser consideradas como las condiciones a satisfacer cuando montamos el puzle.

El puzle que mejor funciona y es más completo hasta la fecha en física de partículas es el Modelo Estándar [1–4]. Con 37 tipos de piezas y tres conjuntos de reglas ha sido capaz de reproducir casi todos los fenómenos observados en física de partículas. Ensamblar este puzle correctamente implica usar todas las piezas disponibles, de todas las formas posibles que satisfagan las reglas. Esto se traduce en escribir todos los términos renormalizables en la Lagrangiana que satisfagan las tres simetrías gauge, el grupo de Poincaré y las simetrías discretas de conjugación de carga, paridad e inversión temporal (CPT).

Los ladrillos del Modelo Estándar son los siguientes: tres generaciones de campos de materia fermiónica con los mismos números cuánticos pero distinta masa; estos campos se dividen a su vez en quarks y leptones, con tres tipos de quarks-arriba de carga eléctrica positiva y tres quarks-abajo negativamente cargados, mientras que los leptones se clasifican en los leptones (negativamente) cargados y sus correspondientes neutrinos, eléctricamente neutros. En el sector bosónico pueden identificarse dos grupos: el bosón de Higgs, responsable del mecanismo de generación de masa conocido como el mecanismo Brout-Englert-Higgs [5–9], y los bosones de gauge, portadores de tres de las cuatro fuerzas fundamentales del Universo. La fuerza de

color y la electromagnética están asociadas a bosones sin masa, los gluones y fotones respectivamente, mientras que la fuerza débil es mediada por tres bosones masivos: dos bosones W con carga eléctrica, uno positivo y otro negativo, y el bosón neutral Z.

A pesar del innegable éxito de este puzle al que llamamos Modelo Estándar quedan aún, afortunadamente para quienes trabajamos en física de partículas, cosas con las que no puede reconciliarse de forma natural. Estos son los llamados problemas abiertos del Modelo Estándar y pueden dividirse en dos categorías: los problemas teóricos, que pueden considerarse partes de la imagen resultante del puzle que parecen extrañas de algún modo, y los indicios experimentales, nuevas partes de la imagen que se han observado pero no tienen cabida en el puzle del Modelo estándar sin alterar su composición, introduciendo nuevas piezas y/o reglas dictando su interconexión.

Finalmente, es importante considerar también cómo el puzle que conocemos hoy en día llegó a ser tal. Por hoy literalmente queremos decir *ahora*, en un sentido cosmológico: la forma en que las piezas se conectan, así como las propias piezas disponibles para montar el puzle, han cambiado a lo largo del tiempo. El Modelo Estándar a temperatura cero es lo que hemos discutido hasta el momento: el Universo es ahora muy *frío* (en torno a 2.7 K) y respeta la simetría de color y el electromagnetismo, las simetrías gauge que sobreviven a temperaturas bajas; además, los quarks no existen libres hoy en día: están confinados en partículas compuestas llamadas hadrones, como protones, neutrones y piones. Sin embargo, retrocediendo en el tiempo y, por tanto, yendo hacia temperaturas más altas, cruzamos la transición de fase de la Cromodinámica Cuántica que marca el comienzo de la época de confinamiento para los quarks, además del punto de Ruptura Espontánea Electrodébil, por encima de la cual la fuerza débil y la de hipercarga aparecen como dos simetrías distintas.

Es importante tener esto en cuenta peusto que, cuando intentamos resolver varios problemas podemos introducir nuevas piezas en el paradigma, y ellas pueden a su vez tener un impacto en la historia térmica del Universo y en cómo todo evolucionó en el tiempo. En esta tesis afrontaremos varios problemas abiertos del Modelo Estándar, intentando proporcionar conexiones entre ellos y finalizaremos considerando un observable concreto que puede haber sido alterado a través de la evolución del Universo.

La estructura de este trabajo se divide en dos partes diferenciadas. En la primera mitad, el Capítulo 1 proporciona una visión global del Modelo Estándar, sus problemas abiertos y la historia térmica del Universo. En el Capítulo 2 discutimos los detalles de cómo el sabor

es particularmente interesante hoy en día, con indicios tanto teóricos como experimentales apuntando hacia nueva física allí, mientras que el Capítulo 3 se centra en uno de los problemas abiertos del Modelo Estándar más intrigantes: el Problema de CP Fuerte. Tras discutir los fundamentos de este problema de *fine-tuning*, discutiremos algunas posibles soluciones con el axión como uno de los principales candidatos. En la segunda parte de esta tesis presentaremos nuestro trabajo original. El Capítulo 4 introduce un modelo que aborda el Problema de CP Fuerte y el puzle de sabor quark. En el Capítulo 5 conectamos el sabor en el sector de neutrinos con una anomalía cosmológica mediante un Majoron y, finalmente, el Capítulo 6 estudia el impacto de axiones en los grados de libertad relativistas cuando son producidos térmicamente.

Introduction

When thinking of particle physics phenomenology it is easy to consider it as toying with a puzzle: we phenomenologists pursue the comprehension of a full image of nature, something that can describe all the observable phenomena without leaving any piece behind or breaking the rules that describe how to connect them. Those pieces will take the form of particles, whereas the symmetries, be them gauge, global or Poincaré, discrete or continuous, can be regarded as the conditions to be satisfied when sticking them together.

The best-working and most complete puzzle up to date in particle physics is the Standard Model (SM) [1–4]. With 37 types of pieces and three sets of rules it has been able to reproduce almost all observed phenomena in particle physics. Doing the puzzle correctly means using all the pieces available, in all possible combinations that satisfy the rules. This is translated in writing all renormalizable terms in the Lagrangian that satisfy all three gauge symmetries, the Poincaré group and the discrete symmetries of charge conjugation, parity and time reversal (CPT).

The building blocks of the SM are the following: three generations of fermionic matter fields with the same quantum numbers but different masses; these fields can be divided in quarks and leptons, with up-type quarks being positively charged and down-type quarks negatively, whereas leptons can be classified as (negatively) charged leptons and their corresponding electrically chargeless neutrinos. In the boson sector one can identify two groups: the Higgs boson, which is responsible for the mass generation mechanism known as the Brout-Englert-Higgs mechanism [5–9], and the gauge bosons, carriers of three out of the four fundamental forces of the Universe. The colour and electromagnetic force are associated to massless gauge bosons, the gluons and the photon respectively, whereas the weak force is mediated via three massive bosons: the two charged W bosons, one positive and one negative, and the neutral Z boson.

Despite the undeniable success of this puzzle we call the SM there are still, fortunately for us particle physicists, things that it cannot accommodate naturally. These are the so-called open problems of the SM model and can be divided in two categories: the theoretical problems, which could be regarded as places in the picture resulting of the whole puzzle that look strange in some way, and the experimental issues, new parts of the picture that have been observed but have no place in the SM puzzle without altering its composition, introducing new pieces and/or rules governing their connection.

Finally, it is important to consider also how the puzzle that we know today came to be. By today we literally mean *now*, in a cosmological sense: the way in which the pieces connect, as well as what puzzle parts are free to be used as building blocks has changed with the course of time. The SM at zero temperature is what we have discussed until now: the Universe is now *cold* (about 2.7 K) and respects colour symmetry as well as electromagnetism, the gauge symmetries that survive at low temperatures; additionally, quarks do not exist freely nowadays: they are confined to composite particles called hadrons, like protons, neutrons and pions. However, going back in time and, therefore, towards higher temperatures, we cross the QCD phase transition (QCDPT), which marks the beginning of quark confinement, as well as the point of Electroweak Symmetry Breaking (EWSB), above which the weak force and hypercharge appear as two separate symmetries.

It is important to take this into account since, when trying to solve several problems one may introduces new pieces in the picture, and they in turn may have an impact on the thermal history of the Universe and how everything evolved in time. In this thesis we will indeed approach several open issues of the SM, trying to provide for links connecting them and finish by considering a specific observable which may have be altered through the evolution of the Universe.

The structure of this work can be divided in two different parts. In the first half, Chapter 1 will provide for an overview of the SM, its open problems and the thermal history of the Universe. In Chapter 2 we discuss the details on how flavour is particularly interesting nowadays, as both theoretical and experimental hints point towards new physics (NP) there, whereas Chapter 3 focuses on one of the most intriguing theoretical problems of the SM: the Strong CP Problem. After discussing the fundamentals of this fine-tuning problem, we will discuss some possible solutions concluding with the axion as one of the strongest candidates. In the second part of this thesis we will present our original work. Chapter 4 introduces a model that tackles

both the Strong CP Problem and the quark flavour puzzle. Chapter 5 links the flavour problem in the neutrino sector with a cosmological anomaly via a Majoron and, finally, Chapter 6 studies the impact of axions on the relativistic degrees of freedom when produced thermally.

Chapter 1

The well established picture in High Energy Physics

In this first chapter let us take a look at the puzzle that has worked the best in High Energy Physics (HEP) until now. In order to do so, we will go over what parts it is built with and how they are assembled, as well as the missing pieces or weird spots in the SM picture, finishing the chapter with an overview of the evolution in time of our Universe.

1.1 The Standard Model of Particle Physics

The Standard Model of Particle Physics is the result of decades of a huge collaborative effort in the HEP community, converging in the birth of a solid framework that is able to explain (almost) all high energy phenomena. Merging Quantum Field Theory (QFT) and Special Relativity, it describes elemental particles as excitations of quantum fields, as well as three of the four fundamental forces of the Universe: the strong or colour interaction, the weak force and hypercharge. These forces are described in the form of gauge symmetries, local transformations than can act on any field charged under said symmetry. The gauge symmetry group of the Standard Model at high energies is

$$\mathcal{G}_{SM} = SU(3)_C \times SU(2)_L \times U(1)_Y, \tag{1.1}$$

where the groups correspond respectively to the colour, weak and hyperforce gauge symmetries. At lower energies, the weak and hypercharge gauge symmetries are broken down spontaneously, remaining then only the colour interaction and electromagnetism:

$$\mathcal{G}_{SM} \xrightarrow{SSB} SU(3)_C \times U(1)_{EM}. \tag{1.2}$$

The particles in the SM can be divided in fermions and bosons. In the fermion sector we find another subdivision, depending on whether they are colour triplets (quarks) or colour singlets (leptons). Regarding quarks, there exist three families of up-type quarks, with electric charge $+\frac{2}{3}e$, and three down-type quarks negatively charged with $-\frac{1}{3}e$. These are the up, charm and top quarks and down, strange and bottom quarks respectively.

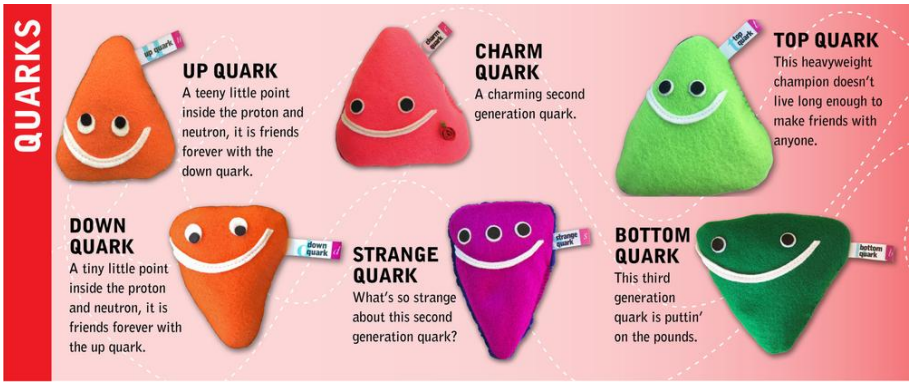

FIGURE 1.1: Quarks of the Standard Model, plush representation by The Particle Zoo

The classification in the lepton sector is a bit different: three massive leptons with electric charge -1, the electron, muon and tau, are accompanied by their corresponding electrically chargeless, and almost massless, neutrino.

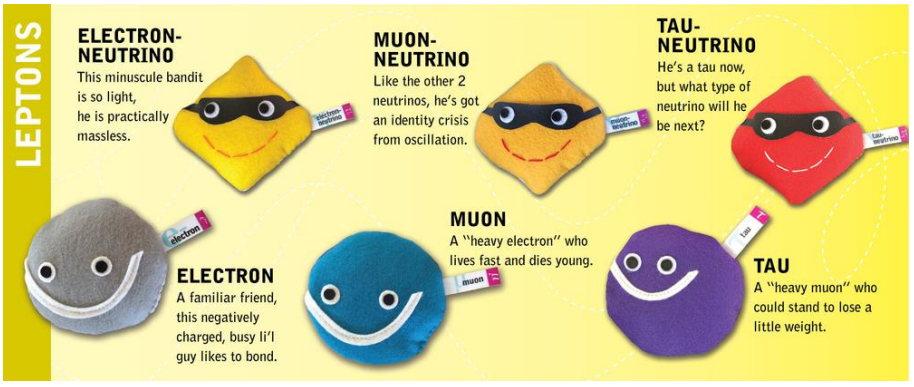

FIGURE 1.2: Plushes representing the leptons in the SM by The Particle Zoo

Finally, the bosonic sector includes the force carriers, the eight gluons G^a_μ, $a = 1, ..., 8$, the three carriers of the weak force, W^i_μ, $i = 1, ..., 3$, and the B_μ boson. In addition to them, the Higgs boson H responsible for the mechanism generating mass for all particles is the only scalar in the SM. After it takes a VEV and EWSB takes place, the weak and hypercharge bosons rearrange themselves in the massive $W^\pm$ and Z bosons and the massless photon.

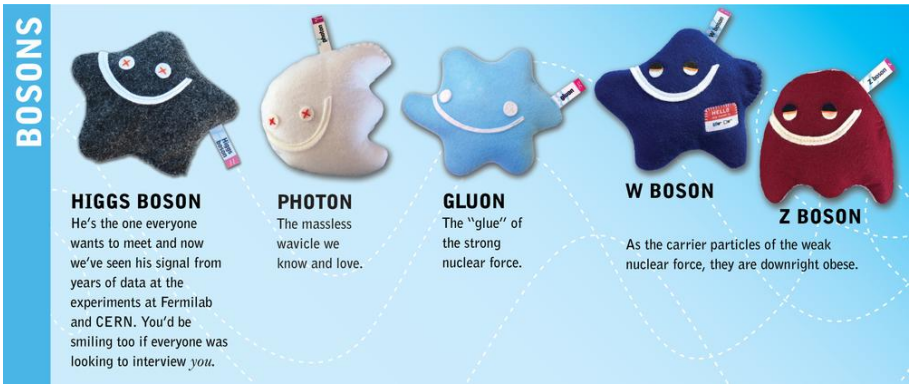

FIGURE 1.3: Higgs boson and force carriers as seen by The Particle Zoo

All these particles and their interactions are encoded in the Lagrangian of the Standard Model. In order to write it, fermions are described using Weyl fields with a well defined chirality and specific representations under the gauge group $\mathcal{G}_{SM}$. These fields are the left-handed quark and lepton weak doublets, q^i_L and l^i_L respectively, and their right-handed weak singlets counterparts, u^i_R, d^i_R and e^i_R for up quarks, down quarks and charged leptons. In all these fields, the index $i = 1, 2, 3$ refers to the three generations existing for each type of fermion.

In the Table 1.1 we show the representation of all SM fields under the whole symmetry group, which need to be taken into account when writing the Lagrangian.

	$SU(3)_C$	$SU(2)_L$	$U(1)_Y$
q_{Li}	**3**	**2**	$\frac{1}{6}$
l_{Li}	**1**	**2**	$-\frac{1}{2}$
u_{Ri}	**3**	**1**	$\frac{2}{3}$
d_{Ri}	**3**	**1**	$-\frac{1}{3}$
e_{Ri}	**3**	**1**	-1

	$SU(3)_C$	$SU(2)_L$	$U(1)_Y$
G^a_μ	**8**	**1**	0
W^i_μ	**1**	**3**	0
B_μ	**1**	**1**	0
H	**1**	**2**	$\frac{1}{2}$

TABLE 1.1: Quantum number for all the fields present in the Standard Model

Using these fields as building blocks we write the SM Lagrangian, which can be divided in three pieces: the kinetic terms for all fields, the Yukawa Lagrangian where fermions couple to the Higgs boson and finally the Higgs scalar potential.

$$\mathscr{L}_{SM} = \mathscr{L}_{Kinetic} + \mathscr{L}_{Yukawa} + V(H), \tag{1.3}$$

Let us study them separately, starting with the kinetic Lagrangian, that contains all gauge interactions.

$$\begin{aligned}\mathscr{L}_{Kinetic} = i\left(\bar{q}_{Li}\not{D}q_{Li} + \bar{u}_{Ri}\not{D}u_{Ri} + \bar{d}_{Ri}\not{D}d_{Ri} + \bar{l}_{Li}\not{D}l_{Li} + \bar{e}_{Ri}\not{D}e_{Ri}\right) \\ - \frac{1}{4}G^a_{\mu\nu}G^{a\mu\nu} - \frac{1}{4}W^i_{\mu\nu}W^{i\mu\nu} - \frac{1}{4}B_{\mu\nu}B^{\mu\nu} + \left(D^\mu H\right)^\dagger D_\mu H,\end{aligned} \tag{1.4}$$

where summation over repeated indices is assumed. The covariant derivate that ensures gauge invariance, acting on a generic field charged under the whole $\mathcal{G}_{SM}$ with hypercharge Y_ψ, is $D_\mu = \partial_\mu - ig_sT_aG^a_\mu - ig\tau_iW^i_\mu - ig'Y_\psi B_\mu$, where $T_a = \frac{\lambda_a}{2}$ and $\tau_i = \frac{\sigma_i}{2}$ are the $SU(3)_C$ and $SU(2)_L$ generators respectively with λ_a and σ_i being the Gell-Mann and Pauli matrices. The standard Feynman slashed notation is used, meaning $\not{D} = D_\mu\gamma^\mu$, with γ^μ are the 4 gamma or Dirac matrices; additionally, in the expression for the covariant derivative, the parameters g_s, g and g' represent the gauge coupling constants for the colour, weak and hypercharge forces respectively. Finally, the gauge kinetic terms are formed with the field strenght tensors that are defined as follows:

$$\begin{aligned}G^a_{\mu\nu} &= \partial_\mu G^a_\nu - \partial_\nu G^a_\mu + g_s f^{abc}G^b_\mu G^c_\nu, \\ W^i_{\mu\nu} &= \partial_\mu W^i_\nu - \partial_\nu W^i_\mu + g\varepsilon^{ijk}W^j_\mu W^k_\nu, \\ B_{\mu\nu} &= \partial_\mu B_\nu - \partial_\nu B_\mu,\end{aligned} \tag{1.5}$$

where f^{abc} are the $SU(3)_C$ structure constants and ε^{ijk} is the Levi-Civita symbol, structure constants of $SU(2)_L$.

Next, we find the Yukawa Lagrangian, responsible for the fermion mass and mixing generation.

$$\mathscr{L}_{Yukawa} = -\bar{q}_LY_u\tilde{H}u_R - \bar{q}_LY_dHd_R - \bar{l}_LY_eHe_R + \text{h.c.}, \tag{1.6}$$

where the fermion fields without generation index represent triplets containing all three generations, $\tilde{H} = i\sigma_2H^*$ and the Yukawa matrices Y_u, Y_d and Y_e are generic 3×3 complex matrices.

After EWSB, these terms provide for the quark and charged lepton mass matrices which can be diagonalized by rotating the fermion fields introducing the Cabibbo-Kobayashi-Masukawa (CKM) matrix in the interaction term with the W bosons. The details on masses and mixings will further be discussed in the next chapter, studying the hierarchies present in the quark and lepton sector, as well as the need for neutrino masses given their observed oscillations.

Finally, the Higgs potential is very simple and can be expressed as

$$V\left(H\right) = -\mu^2 H^\dagger H + \lambda (H^\dagger H)^2, \tag{1.7}$$

where the values of the parameters μ and λ control the spontaneous symmetry breaking mechanism. For $\mu^2 > 0,\ \lambda > 0$ the value of the field that minimizes the potential is different from zero, namely $v = \frac{\mu}{\sqrt{\lambda}}$, resulting in the spontaneous breaking of the weak and hypercharge gauge symmetries.

With only 18 free parameters, the SM has been able to predict many properties of all fundamental particles and their interactions, which have been tested and proved right up to an extreme accuracy, like the W and Z boson masses or countless cross-sections describing many possible processes. The last of these experimental tests that further validated the SM was the discovery of a spin-0 particle compatible with being the Higgs boson in 2012; nine years later, following analyses still find this particle to have the same characteristics as the predicted scalar, making the SM puzzle seemingly complete. From the proton stability to the beta decay, from the nuclear processes in stars that provide for light to their death that populates the universe with all elements in the periodic table, all these phenomena are gathered in the picture the SM generates, shining splendidly.

However, not all that glitters is gold. The closeness and apparent perfection of the SM is robust, as experiments and observations have shown until now, but this also poses a threat on its stability: if any new piece were to be observed, or if one wanted to give an explanation to some things that look awkward in the SM picture, modifications to it may easily destroy all that it has achieved.

In the next section we will discuss that indeed, there are some aspects of the SM that seem to require an additional explanation beyond, which will be called the theoretical problems of the SM, as well as experimental measurements that contradict or escape the predicted behaviour of the universe according to the SM content. We will dedicate the following pages

to discussing some of these issues, that work as motivation for us phenomenologists to enlarge and change the HEP puzzle, aiming for its evolution towards a more complete theory.

1.2 Theoretical problems of the SM

As we have discussed until now, the SM is an extremely successful theory, but not perfect yet. In fact, there are some aspects of it that, without requiring any additional experimental measurement, point towards the necessity of an extension.

These are the so-called theoretical problems, and the main four ones are the Strong CP Problem, the Flavour Puzzle, the Hierarchy Problem and the inclusion of Gravity in the quantum theory. In this thesis we will address the first two, so they will have a chapter on their own, but let us discuss briefly the other two as they are extremely interesting as well.

1.2.1 The Hierarchy Problem

The Standard Model is a very appealing theory which has only one energy scale: the Higgs VEV. This is itself related to the only mass parameter appearing in the SM, $v = \frac{\mu}{\sqrt{\lambda}}$, as well as to the Z and W boson mass and, of course, to the Higgs one as follows:

$$m_W = \frac{1}{2} v g,\ m_Z = \frac{1}{2} v \sqrt{g^2 + g'^2},\ m_H = \sqrt{2\lambda} v. \tag{1.8}$$

The measurement of these masses, together with the Fermi coupling constant obtained from muon decay, allows to extract a value for the Higgs VEV $v \approx 246$ GeV and self coupling $\lambda \simeq 0.13$, meaning that the mass parameter in the potential has a value of around $|\mu| \simeq 88.4$ GeV. These values are of course the result of rectifying the bare potential with all quantum corrections; a simple one-loop computation shows that the mass parameter μ is sensitive to the cut-off scales of NP, namely $\delta\mu^2 \propto \Lambda^2$. Taking this into account, any scale $\Lambda \gg$ TeV will imply that the bare parameter μ^2_{bare} must be extremely fine-tuned so that the addition of quantum corrections arrive precisely at the value inferred through experimental measurements.

This scale can be interpreted as the mass of any heavy particle appearing in any BSM physics, but in any case it can also be regarded at the energy scale at which the theory breaks

down. Even if there were no BSM physics, which as we will see cannot be the case, one would expect the quantum theory to break down as the energy approaches the Planck scale, meaning $\Lambda \sim M_{Pl} \sim 10^{19}$ GeV. A back-of-the-envelope computation shows that for a scale of that order the cancellation between the bare parameter and its quantum correction must be exact up to roughly 35 decimals, which is an astonishing level of fine-tuning.

One possible way to avoid this so-called big hierarchy problem, where the Higgs mass is expected at the Planck scale, is to have NP at a relatively low scale, like the TeV, and have this new physics protect the Higgs mass from other larger scales. Some of the most popular ways to do this are through Supersymmetry, where scalar counterparts of the SM fermions cancel their loop contributions, or by considering that the Higgs is not a fundamental particle, but a composite state of new fermionic degrees of freedom that live at the scale $\Lambda \sim$ TeV. Some other possibilities are considering Technicolor, extra dimensions or relaxion models, but a plethora of proposals are out in the wild, scouting for a possibility to settle this troubling spot of the SM puzzle.

The specific value of the Higgs mass parameter μ, which fixes the scale of both its mass and its VEV unless λ departs greatly from being $\mathcal{O}(1)$, is very relevant for an additional issue, which is the stability of the vacuum of our Universe. With the current measurements of both the top and the Higgs masses, and under the assumption that only the SM is present, the best-fit value implies that our Universe is in fact meta-stable, with total stability only achieved at the $2-3\sigma$ level as it can be seen in Fig. 1.4 [10].

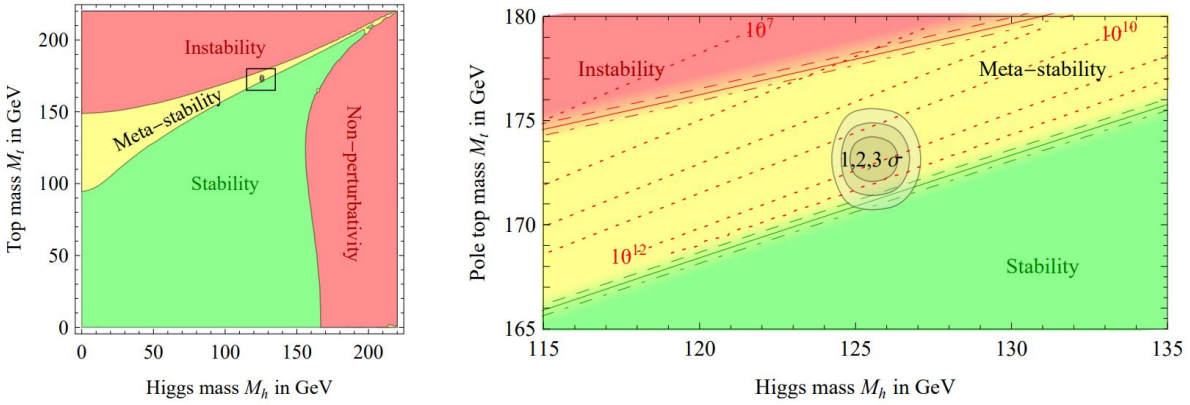

FIGURE 1.4: Stability, meta-stability and instability regions as computed in [10]. On the right, a zoom-in of the region where the SM lives is shown, with at least 2σ being needed to enter the stability area.

It can be unsettling to think that our Universe could someday undergo tunnel effect to a different vacuum if it were to be meta-stable, supossing a sudden change in the masses of all particles and probably ending all chemistry and life itself. However, it is also exciting to look for possible explanations of this very precise value of the Higgs mass and reconcile it with the stability observed (until now) of our Universe.

1.2.2 Gravity: A whole different puzzle?

The SM success is founded on the merging of a quantum theory with special relativity, leading to the quantum description of particles, fields and interactions through the QFT. This is indeed a huge achievement but, however, is not able to include all known interactions: gravity is left out of the picture the SM puzzle creates.

The issue with gravity increases when one tries to calculate the vacuum energy density, which translates into the Cosmological Constant Λ that appears in Einstein's equations of General Relativity (GR). When one computes the zero-point energy in our Universe it is found to be $\mathcal{O}\left(M_{Pl}^4\right)$, which departs the astounding amount of about 120 orders of magnitudes from the inferred value of Λ from the accelerated expansion of the Universe.

This represents another huge fine-tuning problem that, together with the impossibility to renormalize GR as it would imply infinite counterterms, requires new approaches towards a quantum theory that includes gravity consistently even at high energies. String theories, for example, represent one of such endeavours by proposing a UV theory from which one has to recover the correct behaviour at low energies, which is what is proving to be troublesome. The other possibility is to follow a bottom-up approach in which the metric gets treated as a field, giving birth to the graviton, and a canonical quantization is attempted, like in loop quantum gravity, where modifications of the Einstein-Hilbert action are required in the pursuit of a fully renormalizable QFT.

Apart from these popular efforts, other strategies also exist, like the models of Emergent Gravity where this force is considered to be non-fundamental and requires for a thermodynamic approach, but up to today no observation seems to point towards any specific direction. The high energies at which gravity is expected to be relevant in particle physics makes it specially difficult to look for hints, but including gravity in the HEP picture still provides for an exciting challenge in the field of theoretical physics.

1.3 Experimental observations not fitting the SM puzzle

So far, we have discussed the theoretical issues present in the SM, things that are not included in the picture or spots that look weird, the so-called fine-tuning problems. Some people may want to invoke the Anthropic Principle to shrug some of these problems off, by arguing that parameters have the values they do because otherwise life would not be viable and therefore no one would be present to study physics at all.

However, apart from that argument having its own deficits, we of course will not take that easy route, as we will try to provide for dynamical solutions of some problems. Additionally, not only theoretical problems populate the SM; currently, there are several experimental measurements which are completely irreconcilable with the predictions of the SM. These are the experimental hints that point towards BSM physics, and cannot be disregarded in any way.

These observation are the observation of neutrino oscillations, that require neutrinos to be massive, the fact that our Universe is composed of matter with essentially no anti-matter to be observed, the nature of Dark Matter as the responsible for structure formation in the Universe and other astrophysical phenomena and, finally, the origin of Dark Energy, driving force of the accelerated expansion in our Universe.

Though in this thesis we will only address directly neutrino masses and, very tangentially, dark matter, let us discuss briefly all of them as they represent the pieces that absolutely break the SM puzzle, asking for a reformulation that includes everything in a better theory.

1.3.1 Neutrino Oscillations

Neutrinos in the Standard Model appear exclusively in the left-handed lepton doublet. As they are missing a right-handed counterpart, a mass term is forbidden by gauge invariance and chirality, meaning that neutrinos are exactly massless in the SM.

However, the discovery of neutrino oscillations that lead to a Nobel Prize in 2015 established firmly the existence of neutrino masses. Their propagating states are not the flavour one, but mass eigenstates which carry all three flavours in different proportions.

FIGURE 1.5: Plush representation of the neutrinos mass eigenstates from The Particle Zoo.

Neutrino masses can in fact be parametrized through an operator of dimension 5, widely known as the Weinberg operator [11]

$$\mathcal{O}_W = \frac{\left(\bar{l}_L^c \tilde{H}^*\right)\left(\tilde{H}^\dagger l_L\right)}{\Lambda_{LN}}, \tag{1.9}$$

that breaks Lepton Number (LN) at a scale Λ_{LN}. The physics that give rise to this operator are still unknown, and in the next chapter we shall discuss the most used idea: the Seesaw Mechanism. In addition to neutrinos having masses, their nature as Dirac or Majorana particle represents another enigma that is also trying to be uncovered through the search for neutrinoless double beta ($0\nu\beta\beta$) decay.

1.3.2 Baryon Asymmetry of the Universe

Our observable universe is composed almost entirely out of baryonic matter and radiation. Opposed to this, antibaryonic matter also exists, but we only observe it in a small portion through some phenomena like cosmic rays.

In a perfectly symmetric Universe, the baryon-to-photon ratio should be zero. This is essentially the difference in baryonic and antibaryonic matter densities divided by the radiation density, $\eta = \frac{n_B - n_{\bar{B}}}{n_\gamma}$. However, this parameter is measured to be indeed different from zero, thus establishing that our Universe is not matter-antimatter symmetric. This fact is what receives the name of the baryon or matter-antimatter asymmetry problem.

For there to be a process in which matter and anti-matter are produced differently three conditions must be satisfied. These are the so-called Sakharov conditions, which are: baryon number must be violated, as well as C and CP symmetries, and finally the process must take place out of thermal equilibrium.

Though in the SM baryon number is violated non-perturbatively through the weak sphalerons, and both C and CP are broken by the phases in the CKM quark mixing matrix, the amount of asymmetry achieved this way is not enough, and therefore new BSM physics is required such that, under Sakharov conditions, the correct η is reproduced. In this direction go many of the proposals like EW baryogenesis or baryogenesis through leptogenesis, where in the case of the latter the asymmetry is produced first in the lepton sector and then translated into baryonic asymmetry through the sphalerons. As no physics beyond the SM have been observed, there is no preferred model yet, but the interplay between the baryon asymmetry of the Universe and other SM problems may help us decide in which direction we should go.

1.3.3 Dark Matter

Dark matter (DM) is arguably the most famous "known uknown" of the SM. One of the clearest hints towards the existence of DM is the observation of rotation curves in spiral galaxies. Considering only the visible matter in those galaxies, the predicted curve of the velocity as a function of the radius of the galaxy decreases with the square root of the radius. However, observations did not follow this trend, with the velocity becoming relatively constant with the radius.

This phenomenon can be explained if an additional matter component is added to the galaxy, with a profile that is not gathered at its centre but becomes denser at larger radius, which receives the name of dark halo. Apart from this observation, there is much more evidence of the existence of additional matter: the bullet cluster, structure formation in the Universe, baryon acoustic oscillations (BAO) or the CMB angular power spectrum are just some examples of experimental facts that call for the existence of DM.

The properties that this new type of matter needs to display are very specific: it must be stable, massive, electrically neutral (or almost) and with very weak interactions with the SM, so that it is very difficult to detect, hence obtaining the name of *dark* matter. It must also represent

about 27% of the total energy budget of the Universe, whereas baryonic (visible) matter only amounts to 5%.

There are many candidates for particle DM, like the weakly interacting massive particle (WIMP) predicted by supersymmetric theories which, unfortunately (or not) has not been measured where it was expected. This prompted the community to propose other candidates, and nowadays there is a very large catalogue of them, including primordial black holes, sterile neutrinos and other more exotic options. In this work, however, we will comment on the possibility of a particle proposed for the solution of another problem being DM: the QCD axion.

1.3.4 Dark Energy

If DM was the most famous "known unknown", dark energy could be called the "unknown unknown" in HEP. The energy budget of the Universe discussed in the previous section was missing a good chunk, about 68% of the total energy which has to be dark energy according to the accelerated expansion observed in our Universe.

This new form of energy, that must have a negative pressure in order to drive the accelerated expansion, remains a mystery until now. Whether its nature is simply explained by the (very small) cosmological constant, by a new scalar field whose potential varies in time or by some modifications in how gravity works is something still under study through many experiments that try to give some insight on this riddle.

1.4 The thermal history of our Universe: Λ_{CDM}

In this last section of the first chapter let us go briefly over how the SM puzzle came to be and evolved in time. This evolution is described in what is usually called the Standard Cosmological Model Λ_{CDM}, which owns its name to the cosmological constant Λ driving the accelerated expansion of the Universe and Cold Dark Matter (CDM), that allows for the formation of structure, like the superclusters of galaxies where stellar systems will develop afterwards.

The main principle that governs modern cosmology is the Cosmological Principle, which states that there is nothing special with our or any location in the Universe, translating more specifically in the homogeneity and isotropy of the Universe. This principle is described

through the Friedmann-Robertson-Walker (FRW) metric which, in natural units, can be written as follow:

$$ds^2 = dt^2 - R^2(t)\left(\frac{dr^2}{1-kr^2} + r^2\left(d\theta^2 + \sin^2\theta d\phi^2\right)\right), \tag{1.10}$$

where $R(t)$ is the scale factor of the Universe that measures its relative expansion relating proper and comoving distances and k measures the curvature of the Universe, vanishing for a flat Universe as ours appears to be.

Combining this metric together with Einstein's equations[1], yields the equations of motion for our Universe, called the Friedmann equations:

$$H^2 = \left(\frac{\dot{R}}{R}\right)^2 = \frac{8\pi G_N \rho}{3} - \frac{k}{R^2} + \frac{\Lambda}{3}, \tag{1.11}$$

$$\frac{\ddot{R}}{R} = \frac{\Lambda}{3} - \frac{4\pi G_N}{3}\left(\rho + 3p\right), \tag{1.12}$$

where ρ and p are the energy density and isotropic pressure respectively of the energy-momentum tensor, G_N is Newton's constant and $H = \frac{\dot{R}}{R}$ is the Hubble parameter. Once one knows the dominant piece in the Universe energy density, together with its equation of state, it is possible to solve the previous equations arriving at an expression for $H(t)$ which describes how distances in the Universe evolve in time, whether it expands or contracts or remains static.

Just like the particles running free in the Universe, the dominant form of energy has also varied over time. In particular, Λ_{CDM} assumes that the Universe suffered an early inflationary epoch, when space suddenly expanded greatly, which provides for a natural explanation of why the Universe today is apparently flat and isotropic: the early Universe was in thermal equilibrium and it may had some curvature, but after inflation it got "flattened" and regions that previously were in thermal equilibrium suddenly became causally disconnected.

After inflation, the Universe became dominated by radiation, when the energy density could be written considering all relativistic particles:

$$\rho = \left(\sum_B g_B + \frac{7}{8}\sum_F g_F\right)\frac{\pi^2}{30}T^4, \tag{1.13}$$

[1]Here it is also assumed that matter behaves as a perfect fluid, meaning its energy-momentum tensor is $T_{\mu\nu} = -pg_{\mu\nu} + (p+\rho)u_\mu u_\nu$.

where g_B and g_F are respectively the bosonic and fermionic degrees of freedom available at temperature T. These degrees of freedom diminish as the Universe gets colder and more and more particles become non-relativistic.

During this radiation dominated era, many important events must have taken place in the Universe: first, after inflation, baryogenesis is necessary in order to populate the Universe with matter, as opposed to antimatter. After this, at a temperature around the Higgs VEV, the Electroweak Phase Transition (EWPT) takes place, going from a symmetric phase where all particles were massless to a broken phase, generating masses and with only colour and electromagnetism as the remaining gauge symmetries. Then, at about 100 MeV, another phase transition happens, the QCD one where quarks and gluons are no longer free and enter bound states like pions and other hadrons.

As the Universe keeps getting colder, neutrinos decouple from the plasma. They become a radiation component frozen at their decoupling temperature $T \sim 1$ MeV. At around this temperature, electrons and positrons annihilate, pumping entropy into the photons in the plasma, heating it a little with respect to neutrinos. Therefore, for as long as neutrinos remain relativistic, their temperature T_ν is related to the photon temperature T:

$$T_\nu = \left(\frac{4}{11}\right)^{1/3} T. \tag{1.14}$$

Shortly after this, Big Bang Nucleosynthesis (BBN) occurs, with protons and neutrons forming nuclei like deuterium, Helium and Lithium. This is the last big event before matter takes over from radiation, dominating the energy density of the Universe at around $T \sim 0.8$ eV followed by the recombination of nuclei and electrons and photon decoupling at $T \sim 0.3$ eV.

These photons that decoupled became what we know today as the Cosmic Microwave Background (CMB), one of the most powerful tools in modern cosmology. This background of photons at $T_{CMB} = 2.7255 \pm 0.0006$ K [12] has been measured with an amazing precision as shown in Fig. 1.6, and is used as a probe for new physics in many ways as it is sensitive to things like the curvature or the matter and dark energy content of the Universe.

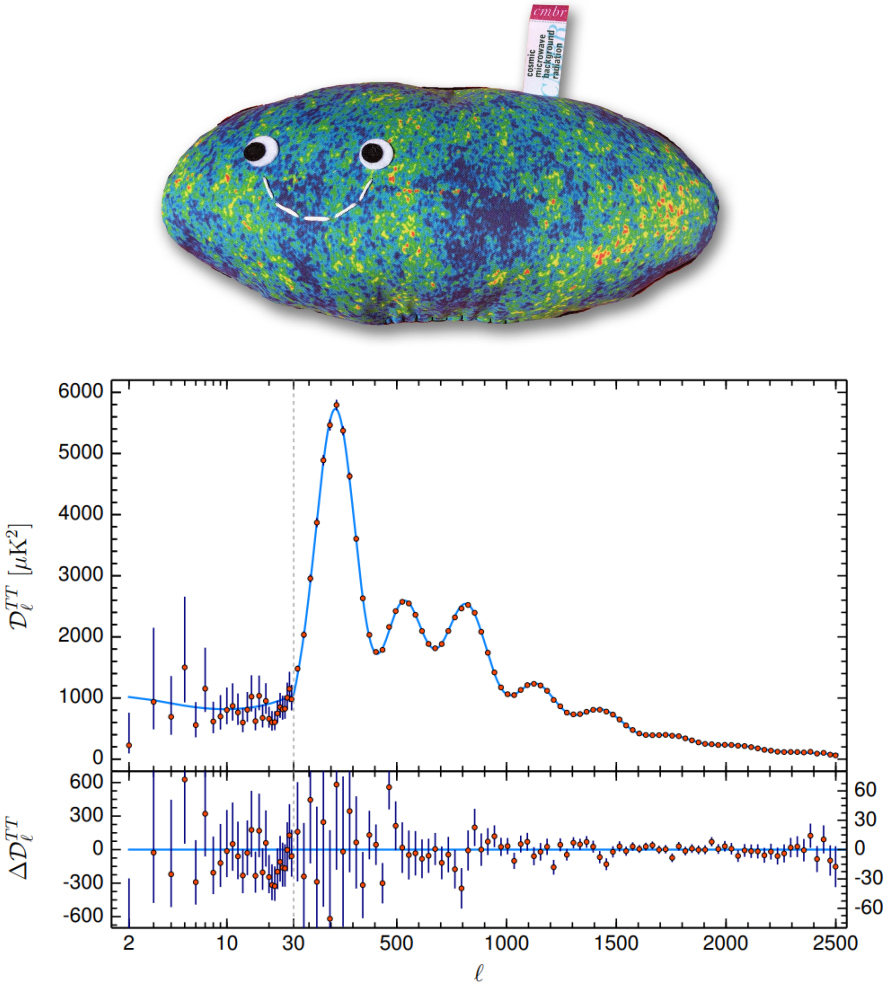

FIGURE 1.6: (Top) CMB real image in the shape of a pillow from The Particle Zoo. (Bottom) Measurement of the CMB power spectrum by the Planck Collaboration [13].

In this thesis there is a specific observable that will become relevant and can be inferred from the CMB, which is the effective number of neutrinos N_{eff}. This magnitude can be regarded as a parametrization of the number of relativistic species in the Universe, and is related to the total radiation energy density, ρ_{rad} via the following equation:

$$\rho_{rad} = \rho_\gamma \left(1 + \frac{7}{8}\left(\frac{T_\nu}{T_\gamma}\right)^{4/3} N_{eff}\right), \tag{1.15}$$

with ρ_γ being the photon energy density and $\frac{T_\nu}{T_\gamma} = \frac{4}{11}$ from Eq. 1.14. In the SM, $N_{eff} = 3.045$ [14] but any additional relativistic species introduced would modify this number as we will study later.

Finally, the Universe kept getting older and colder, when at $T \sim 0.33$ meV until not too long ago (in cosmological scale) dark energy dominated over matter. This is the era in which we live now, and thanks to what the accelerated expansion of the Universe has been measured. This implies that we live in a very exciting moment in time, where the expansion is accelerated, confirming the existence of dark energy whatever it actually is, but it is not so severe that stars and galaxies are already out of reach for us to study them.

Chapter 2

Missing pieces in the flavour sector

In this chapter we will address one sector of the SM where several hints for NP have appeared over the years: the flavour sector. In HEP, flavour is the term used to refer the different type of quarks and leptons that exist in the SM, not to be mistaken with families: there are six flavours of quarks and another six flavours of leptons, both of them arranged in three families. Each flavour can have different properties, like different masses and mixing with other flavours, which are fixed by experimental observations but present no dynamical explanation in the SM.

In the recent years, many anomalies in the flavour sector have sprung up across several observables, like the so-called B anomalies. In this set of measurements, transitions from bottom quarks to either charm or strange quarks with leptons involved, seem to deviate from the SM prediction, where the only difference is the masses which in most cases can be neglected. These observables, mediated by the W boson in the SM, appear to indicate that some BSM physics is coupling differently to different flavours of quarks and/or leptons, and thus has sparked great interest in the community.

Together with this experimental tensions, the lack of a dynamical explanation for the masses, mixings and CP breaking phases in the SM, as well as the existence of neutrino masses themselves, make flavour one of the most intriguing sectors in the SM, and as such we will tackle it through several flavoured models in this thesis.

2.1 The Flavour Puzzle

As we have discussed just now, the flavour sector in the SM is accumulating attention for several reasons. These motivations can be divided in the B anomalies, which will not be addressed in this work, the Flavour Puzzle and the BSM Flavour Problem. For starters, let us describe the flavour sector itself, which will lead us to what is called the Flavour Puzzle.

As we showed in the previous chapter, masses for quarks and charged leptons are generated from Eq. 1.6 after the Electroweak (EW) symmetry is broken spontaneously by the Higgs VEV, finding the following piece in that Lagrangian:

$$\underset{\text{After EWSB}}{\mathscr{L}_{Yuk} \supset \mathscr{L}_m} = -\bar{u}_L Y_u \frac{v}{\sqrt{2}} u_R - \bar{d}_L Y_d \frac{v}{\sqrt{2}} d_R - \bar{e}_L Y_e \frac{v}{\sqrt{2}} e_R + \text{h.c.}. \tag{2.1}$$

In that equation, one must remember that the Yukawa matrices are completely generix 3×3 complex matrices in flavour space and, therefore, are not necessarily diagonal. In order to diagonalize them and find what will be identified as the fermion mass matrices one can rotate the fermion fields in flavour space in the following way[2]:

$$f_L \to U_L^{f\dagger} f_L, \; f_R \to U_R^{f\dagger} f_R \quad f = u, d, e, \tag{2.2}$$

such that

$$\hat{Y}_f = U_L^f Y_f U_R^{f\dagger}, \tag{2.3}$$

where the hatted Yukawa matrices are already diagonal and real and the rotation matrices $U^f_{(L,R)}$ are unitary matrices. After this rotation, we can already identify the mass matrices:

$$\hat{M}_f = \frac{v}{\sqrt{2}} \hat{Y}_f, \tag{2.4}$$

where the hat is again used in the mass matrix to explicitly state that it is diagonal.

Notice that this transformation of the fields leaves the whole Lagrangian except for one part: the W coupling to quarks. From within the kinetic term of the left-handed quark doublet q_L the covariant derivative includes the following piece:

[2]This can also be regarded as a change of basis, going from $f'_{(L,R)} = U^f_{(L,R)} f_{L,R}$, but for the sake of notation simplicity we are dropping the prime in the non-diagonal basis.

$$\bar{q}_L \not{D} q_L \supset -ig\bar{q}_L\gamma^\mu\tau_i W^i_\mu q_L \supset -ig\left(\bar{u}_L\gamma^\mu W^+_\mu d_L - \bar{d}_L\gamma^\mu W^-_\mu u_L\right), \tag{2.5}$$

which after the rotation becomes

$$-i\frac{g}{\sqrt{2}}\left(\bar{u}_L\gamma^\mu U^u_L W^+_\mu U^{d\dagger}_L d_L - \bar{d}_L\gamma^\mu U^d_L W^-_\mu U^{u\dagger}_L u_L\right), \tag{2.6}$$

with $W^\pm_\mu = \frac{W^1_\mu \mp iW^2_\mu}{\sqrt{2}}$. From this last equation we can identify the Cabbibo-Kobayashi-Maskawa or CKM matrix that describes the mixing in the quark sector:

$$V_{CKM} = U^u_L U^{d\dagger}_L = \begin{pmatrix} V_{ud} & V_{us} & V_{ub} \\ V_{cd} & V_{cs} & V_{cb} \\ V_{td} & V_{ts} & V_{tb} \end{pmatrix} \tag{2.7}$$

This matrix has 9 complex entries and is, in the SM, unitary by construction. Its elements have been measured with great precision, and the full matrix can be parametrized using three rotation angles and one CP violating phase. These angles and phase can be expressed in terms of four real parameters in what is called the Wolfenstein parametrization, used to test the unitarity of the CKM matrix through what is called the unitarity triangle of the CKM, which becomes also a tool to constrain BSM physics. Here we present the measured values of both their modulus and each of the quark masses[3] [15]:

$$\begin{pmatrix} |V_{ud}| & |V_{us}| & |V_{ub}| \\ |V_{cd}| & |V_{cs}| & |V_{cb}| \\ |V_{td}| & |V_{ts}| & |V_{tb}| \end{pmatrix} = \begin{pmatrix} 0.97370 \pm 0.00014 & 0.2245 \pm 0.0008 & 0.00382 \pm 0.00024 \\ 0.221 \pm 0.004 & 0.987 \pm 0.011 & 0.0410 \pm 0.0014 \\ 0.0080 \pm 0.0003 & 0.0388 \pm 0.0011 & 1.013 \pm 0.0030 \end{pmatrix} \tag{2.8}$$

$$\begin{gathered} m_u = 2.16^{+0.49}_{-0.26}\,\text{MeV}, \quad m_c = 1.27 \pm 0.02\,\text{GeV}, \quad m_t = 172.76 \pm 0.30\,\text{GeV}, \\ m_d = 4.67^{+0.48}_{-0.17}\,\text{MeV}, \quad m_s = 93^{+11}_{-\ 5}\,\text{MeV}, \quad m_b = 4.18^{+0.03}_{-0.02}\,\text{GeV}. \end{gathered} \tag{2.9}$$

Just by looking at both the masses and the mixing matrix, it is possible to observe hierarchies: the range of quark masses spans for around five orders of magnitude, when in principle

[3] Notice that quark masses depend on the renormalization scheme used in the theory, as well as on the energy scale at which they are computed. The masses shown here were computed in the $\overline{\text{MS}}$ scheme, with $\mu)2$ GeV for the three lightest quarks, $\mu = m_q$ for $q = c, b$ and direct measurements for the top quark.

they could be of the same order of magnitude. Additionally, the CKM matrix is very close to the identity, which looks a bit odd considering it comes from the product of to unitary matrices that are used in the diagonalization of completely generic matrices.

The hierarchy in the masses and the peculiar structure of the CKM matrix are the essence of the flavour puzzle, but it is further understood when one looks at the leptonic sector. Disregarding for now neutrino masses, as they are absent in the SM, the rotation in Eq. 2.2 that diagonalizes the charged lepton mass matrix does not introduce a mixing matrix analogous to the CKM since the rotation can be reabsorbed by a new rotation U_L^ν on the left-handed neutrino field.

However, as we discussed in the previous chapter, neutrinos have been shown to be massive, albeit slightly so when compared to the rest of the SM particles. In order to write a neutrino mass term, it is mandatory to extend the SM spectrum with m new neutrino states with right-handed (RH) chirality, N_R, allowing us to write the following terms in the Lagrangian:

$$\mathscr{L}_\nu = \bar{l}_L \tilde{H} Y_\nu N_R + \frac{1}{2} \bar{N}_R M_N N_R^c + \text{h.c.}, \tag{2.10}$$

where Y_ν is a generic $3 \times m$ complex matrix and M_N is an $m \times m$ symmetric matrix and that, after EWSB, includes the neutrino mass Lagrangian

$$\mathscr{L}_\nu \supset \mathscr{L}_{M_\nu} = \bar{\nu}_L M_D N_R + \frac{1}{2} \bar{N}_R M_N N_R^c + \text{h.c.}, \tag{2.11}$$

with $M_D = \frac{v}{\sqrt{2}} Y_\nu$.

Notice that we did not only write the usual Dirac mass term, the first one in the previous equation, but also an additional one. Since left-handed neutrinos transform non-trivially only under $SU(2)_L \times U(1)_Y$ and $\bar{l}_L \tilde{H}$ is already a SM gauge singlet, the new states N_R are complete gauge singlets, which allows for what is called the Majorana mass term, the second one in Eq. 2.10.

In order to be able to find all the $3 + m$ neutrino mass eigenstates it is convenient to rearrange Eq. 2.10 in such a way that only one mass matrix appears. This can be done by rearranging the neutrino states in a vector of dimension $3 + m$, namely $\nu = \begin{pmatrix} \nu_L \\ N_R^c \end{pmatrix}$ which allows to write the following mass Lagrangian:

$$\mathscr{L}_{M_\nu} = \frac{1}{2}\bar{\nu}^c \begin{pmatrix} 0 & M_D^* \\ M_D^\dagger & M_N \end{pmatrix} \nu + \text{h.c.} = \bar{\nu}^c M_\nu \nu + \text{h.c.}. \tag{2.12}$$

This matrix, as any symmetric matrix, can be diagonalized with just one hermitian rotation, U^ν such that

$$\nu \to U^{\nu\dagger}\nu, \quad \hat{M}_\nu = U^{\nu *} M_\nu U^{\nu\dagger}, \tag{2.13}$$

where $\hat{M}_\nu$ is a diagonal matrix containing the $3+m$ neutrino masses.

This rotation, as it also happened in the quark sector, introduces a mixing matrix in the charged-current interaction of leptons with the W boson: the Pontecorvo-Maki-Nakagawa-Sakata, or PMNS, matrix, which governs over flavour changing processes involving leptons, including neutrino oscillations. For $m = 3$, this matrix contains 3 angles and one CP violating phase, as did the CKM matrix, but presents 2 additional Majorana phases as long as $M_N \neq 0$. In the case where $M_N = 0$ these Majorana phases can be reabsorbed through a rotation, defining neutrinos as Dirac particles as opposed to Majorana in the other scenario. For the Dirac case, the PMNS matrix can be expressed as follows in terms of its three angles $\theta_{12},\ \theta_{13},\ \theta_{23}$ and its CP violating phase δ_{CP}.

$$\begin{aligned} U_{PMNS} &= \begin{pmatrix} U_{e1} & U_{e2} & U_{e3} \\ U_{\mu 1} & U_{\mu 2} & U_{\mu 3} \\ U_{\tau 1} & U_{\tau 2} & U_{\tau 3} \end{pmatrix} \\ &= \begin{pmatrix} c_{12}c_{13} & s_{12}c_{13} & s_{13}e^{-i\delta_{CP}} \\ -s_{12}c_{23} - c_{12}s_{13}s_{23}e^{i\delta_{CP}} & c_{12}c_{23} - s_{12}s_{13}s_{23}e^{i\delta_{CP}} & c_{13}s_{23} \\ s_{12}s_{23} - c_{12}s_{13}c_{23}e^{i\delta_{CP}} & -c_{12}s_{23} - s_{12}s_{13}c_{23}e^{i\delta_{CP}} & c_{13}c_{23} \end{pmatrix}, \end{aligned} \tag{2.14}$$

where $s_{ij} = \sin\theta_{ij}$ and analogously $c_{ij} = \cos\theta_{ij}$.

Whereas the quark sector has been very well characterized, the lepton sector is still lacking some information in the neutrino parameters. Though charged lepton masses are very well measured [15], extremely so in the case of the electron and the muon, the absolute scale of neutrino masses is still unknown, despite experiments like KATRIN [16] aiming at it and cosmology setting strong constraints on the sum of the three masses, with the lightest neutrino being massless still being a possibility.

$$m_e = 0.5109989461 \pm 0.0000000031\ \text{MeV}, \quad m_\mu = 105.6583745 \pm 0.0000024\ \text{MeV}, \quad m_\tau = 1776.86 \pm 0.12\ \text{MeV}. \tag{2.15}$$

The mass difference between the three light neutrino states have been measured with good accuracy, but only one of them is known to be positive. The sign of the lightest-to-heaviest neutrino mass difference is still undetermined, being positive for what is called normal ordering (NO) and negative for inverted ordering (IO). In Table 2.1 we present the current values for the three angles, the CP violating phase and the two mass splittings given by the NuFIT collaboration [17], both for normal and inverted ordering, with compatible results also found by the groups in Refs. [18, 19].

	NO	IO
θ_{12} (°)	$33.44^{+0.77}_{-0.74}$	$33.45^{+0.78}_{-0.75}$
θ_{23} (°)	$49.2^{+0.9}_{-1.2}$	$49.3^{+0.9}_{-1.1}$
θ_{13} (°)	8.57 ± 0.12	8.60 ± 0.12
δ_{CP} (°)	197^{+27}_{-24}	282^{+26}_{-30}
Δm^2_{21} (10^{-5} eV^2)	$7.42^{+0.21}_{-0.20}$	$7.42^{+0.21}_{-0.20}$
Δm^2_{3l} (10^{-3} eV^2)	$+2.517^{+0.026}_{-0.028}$	-2.498 ± 0.028

TABLE 2.1: Best fit for the neutrino oscillation parameters obtained by the NuFIT collaboration.

By looking at the mixing angles in the PMNS matrix it can be seen that, as the smallest of them is about 9°, the texture of the lepton mixing matrix y more *anarchical* than the very hierarchical CKM matrix. Additionally, charged lepton masses are spread through almost 5 orders of magnitude, with neutrino masses being extremely small, below the eV level [16].

This is the nature of the flavour puzzle: the absence of a dynamical explanation for the huge range of fermion masses together with the very different mixing patterns in the quark and lepton sector. In Fig. 2.1, we show the CKM and PMNS matrices, with their entries being represented by circles whose radii are equal to each entry divided by the largest one. Then, in Table 2.2 together with a table with the ratio of all masses divided by the top mass, which in all cases except for the neutrinos corresponds to the Yukawa of each fermion.

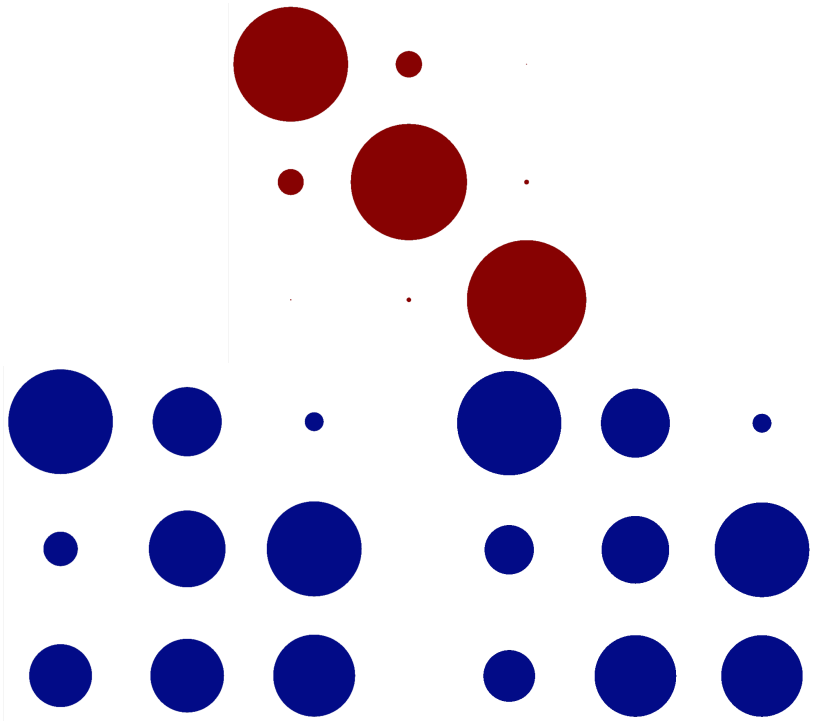

FIGURE 2.1: CKM matrix (top) and PMNS matrix for NO (bottom left) and inverted ordering (bottom right), with the circles being a representation of the modulus of each element.

	First Generation	Second Generation	Third Generation
Up-type quarks	$\mathcal{O}(10^{-5})$	$\mathcal{O}(10^{-2})$	1
Down-type quarks	$\mathcal{O}(10^{-5})$	$\mathcal{O}(10^{-3})$	$\mathcal{O}(10^{-2})$
Charged Leptons	$\mathcal{O}(10^{-6})$	$\mathcal{O}(10^{-3})$	$\mathcal{O}(10^{-2})$
Neutrinos	$0 - \mathcal{O}(10^{-11})$	$\mathcal{O}(10^{-11})$	$\mathcal{O}(10^{-11})$

TABLE 2.2: Masses (normalized by the top mass) for the three generations of all SM fermions. Normal ordering has been assumed so that the first generation neutrino is the lightest one.

In the following sections we will discuss some widely proposed solutions to one or several aspects of the flavour puzzle, starting with the particularly small neutrino masses and moving towards a more generic approach towards all hierarchies in the flavour sector. Finally, we will comment in the second half of this chapter the consequences of modifying flavour with BSM physics and how to stay safe from these dangers.

2.1.1 The See-Saw Mechanism

As we have commented previously, and a RH counterpart for neutrinos is not within the SM particle spectrum, neutrino masses cannot be accommodated in the SM without departing from renormalizability or adding new particles. In the first case, if one gives up on having a renormalizable theory, it is possible to include the Weinberg Operator that, with only SM fields, provides a source for neutrino masses. However, this needs a UV completion that gives rise to that effective operator. Following the idea of maintaining renormalizability implies adding new particles to the SM. This can be done still conserving Lepton Number, the Dirac case, that implies the neutrino Yukawa to be strikingly small in order to account for their tiny neutrino masses, increasing the fine-tuning level in the particle physics.

If in turn one allows LN to be explicitly broken, a Majorana mass term for the new fields can be introduced that can help with the smallness of neutrino masses, giving rise to the so-called See-Saw (SS) mechanism. The main idea behind this is the introduction of a large scale that, just like two children in a see-saw, *pushes* neutrino masses up to lighter values. Depending on the specific particle that is introduced to generate the Weinberg operator after it is integrated out three classical types of see-saws can be identified.

The simplest one of them, in terms of the complexity of the new particle and its interactions, is the so-called Type-I SS, where a number of right-handed neutrinos are introduced, being singlets under the whole SM gauge group. This is the case that is depicted in Eq. 2.10 that leads to the neutrino mass matrix shown in Eq. 2.12. In the limit where $M_N \gg M_D$, which for a Yukawa $\mathcal{O}(1)$ implies $M_N \gg v$, the diagonalization of M_ν yields the following masses for light and heavy neutrinos, m_ν and m_N respectively, the following expressions:

$$m_\nu \sim M_D M_N^{-1} M_D^T, \quad m_N \sim M_N, \tag{2.16}$$

which requires $M_N \sim 10^{14}$ GeV in order to reproduce a light neutrino mass scale $m_\nu \sim \mathcal{O}(\text{eV})$.

This same mechanism works if the fermion introduced is not a full singlet of the SM gauge group, but transforms as a triplet, Σ, under $SU(2)_L$ as the products $\mathbf{2} \times \mathbf{2} \times \mathbf{3}$ and $\mathbf{3} \times \mathbf{3}$ both contain a singlet. This allows for both a Yukawa and Majorana term, analogous to the type-I singlet case, to be written in the Lagrangian, resulting in the same expression for light neutrino masses.

A slightly different solution appears when one considers the inclusion of a new scalar instead of a fermion. By adding a weak triplet scalar, Δ, to the SM particle content the following terms appear within the Lagrangian associated to this field:

$$\mathscr{L}_\Delta \supset \bar{l}_L^c i\sigma_2 \Delta Y_\Delta l_L + m_\Delta^2 \mathrm{Tr}(\Delta^\dagger \Delta) + \mu_\Delta H^T \tilde{\Delta} H + \mathrm{h.c.} \tag{2.17}$$

imposing a hypercharge for Δ of $Y_\Delta = 2$ in order to ensure full gauge invariance and $\tilde{\Delta} = i\sigma_2 \Delta^*$ analogously to the previously defined $\tilde{H}$.

This new scalar field gets a VEV $v_\Delta = \frac{\mu_\Delta v^2}{\sqrt{2} m_\Delta^2} \ll v$, with the generated neutrino mass being

$$m_\nu = Y_\Delta v_\Delta = Y_\Delta \frac{\mu_\Delta v^2}{\sqrt{2} m_\Delta^2}, \tag{2.18}$$

which can be made naturally small with $Y_\Delta \sim \mathcal{O}(1)$ by choosing the appropriate values for μ_Δ and m_Δ. The enriched scalar spectrum in this type of SS leads to many constraints, both from colliders and non-collider observations, which may compromise the naturalness of Y_Δ but still allow for a less fine-tuned Yukawa than the $\mathcal{O}(10^{-11})$ required for Dirac neutrinos in the absence of a SS mechanism.

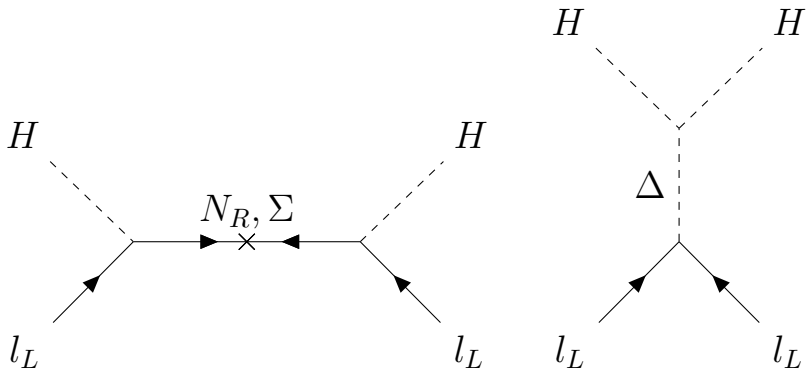

FIGURE 2.2: Feynman diagrams for the type-I and III SS on the left, with the one for the type-II SS on the right.

In Fig. 2.2 we show the Feynman diagrams for the type-I or III and type-II SS that, after integrating out the heavy particle, lead to the Weinberg operator. Apart from these three standard types of SS, where the light neutrino masses in all cases are inversely proportional to some new heavy mass parameter, there are some other proposals. In frameworks like the the inverse and linear SS the lepton number breaking scale, which in the standard SS is M_N, can

be lowered thanks to the introduction of more than one flavour of right-handed neutrino and the textures that generates in M_ν.

Though the SS mechanisms can account for the smallness of the overall scale of neutrino masses, while the structure of the PMNS matrix and the mass splittings still lack a dynamical explanation and have to be accommodated through the extra parameters that the Majorana and Yukawa matrices introduce.

In the next section we will discuss frameworks that do attempt to provide for an explanation to these hierarchies in the mixings and mass ratios. These strategies can be used in the neutrino sector, but also address the flavour problem in the charged lepton and quark sectors, and they all are based in the use of global symmetries.

2.1.2 Discrete and continuous flavour symmetries

As we discussed already in the introduction and first chapter of this thesis, symmetries are the *rules* we must respect when *building our particle puzzle*. In this sense, they may seem restrictive, but this reasoning can be flipped and try to use new symmetries to explain the hierarchies present in the flavour sector.

This approach has been followed by many phenomenologists, leading to the developing of many models that implement flavour symmetries to reproduce the mass ratios and mixing hierarchies. These models can be broadly classified according to the type of flavour symmetry they use: they can be either gauge or global, discrete or continuous, Abelian or non-Abelian. Though gauged flavour symmetries are indeed an interesting research subject[4], we will provide here an overview only on the trajectory of global flavour symmetries as those will be the ones used in the original work presented here later.

Discrete flavour symmetries [25–32] became particularly interesting in the early ages of neutrino oscillation measurements. The so-called atmospheric angle, θ_{23}, was measured to be very close to 45°, with tau and muon neutrinos oscillating maximally. This angle could be explained with a Z_2 symmetry that predicts at the same time a vanishing reactor angle, $\theta_{13} = 0^\circ$. This approach evolved into more complex symmetries, like the discrete non-Abelian A_4 or S_4, which predict what was called the tri-bimaximal mixing [33, 34], with $\sin^2\theta_{12} = \frac{1}{3}$ in addition to the previous prediction from the Z_2 symmetry.

[4] Examples of this are found in Refs. [20–24]

While the solar angle θ_{12} predicted agreed with data, the reactor angle was measured to be clearly non-zero, rendering the tri-bimaximal mixing together with other proposals that predicted $\theta_{13} = 0$, unattractive. After the determination of the three mixing angles in the neutrino sector, in particular a relatively large reactor angle [35–39], new proposals appeared trying to accommodate these observations, either by considering other textures, modifying to the previously predicted one or including new less minimal flavour symmetries.

Apart from the neutrino sector, quark and charged lepton masses have also been addressed with discrete flavour symmetries. As an example, in Ref. [40] a supersymmetric model is presented using the double covering of A_4, T', which has the features of A_4 models in the lepton sector together with realistic results for quark masses and mixings not found in the simple A_4 models.

Departing from the discrete approach, continuous flavour symmetries have proven to be a really powerful tool to tackle the flavour puzzle. One possibility is considering non-Abelian continuous symmetries, like $U(3)^n$ groups as in Minimal Flavour Violation [41, 42], which will be discussed in depth later on, or $U(2)^n$ models [43, 44] where the third generation of fermions is singled out, as well as a combination of $U(2)^n \times U(3)^m$ as discussed in Ref. [45], one of the papers produced during this thesis that will not be addressed in this document.

All these models with continuous non-Abelian symmetries share the treatment of the Yukawa matrices, which become spurions: non-dynamical fields that transform non-trivially under a certain symmetry. In particular, the SM Yukawas transform under the non-Abelian part part of the $U(N)$, i.e. under $SU(N)$, in a certain representation that can vary from model to model. This ensures the flavour invariance of the Lagrangian, together with that of any higher dimensional operator created, that must include the appropriate combination of Yukawa insertions. Additionally, the Yukawa spurions can be promoted to dynamical scalar fields and their potential can be constructed, restricted by the combinations allowed by the Yukawas representations. This potential can then be minimized in search for a solution that explains the SM masses and mixing hierarchies.

These models have great predictability when promoting the spurions to scalars thanks to a reduction of the free parameters, but may find it difficult to include a minimum which explains the observed mass and hierarchies and is not too highly fine tuned. An alternate approach is the one followed by the so-called Froggatt-Nielsen models [46–49] where the continuous flavour symmetry used is Abelian. These models accommodate easier the observed masses,

but have a higher number of free parameters and, additionally, lose the renormalizable appeal of the non-Abelian models.

In these models, an Abelian $U(1)_{FN}$ flavour symmetry is imposed in the Lagrangian, with each fermion of type $f = u, d, q, e, N, l$ and generation $i = 1, 2, 3$ has a charge x_i^f. Together with the inclusion of a scalar field Φ, dubbed flavon, with a $U(1)_{FN}$ charge of, without loss of generality, $x_\Phi = -1$ each Yukawa term can be made flavour invariant in the following fashion:

$$\left(\frac{\Phi}{\Lambda}\right)^{x_j^{f_R} - x_i^{f_L}} \bar{f}_{L_i} H Y_f^{ij} f_{R_j}, \tag{2.19}$$

with $f_L = q, l$, $f_R = u, d, e, N$ and where Λ represents the energy cutt-off of the effective field theory described by these non-renormalizable Yukawa operators.

After the spontaneous breaking of $U(1)_{FN}$ through the VEV of Φ, v_Φ, the masses and mixing hierarchies are ruled by a small parameter $\varepsilon = \frac{v_\Phi}{\sqrt{2}\Lambda}$, while the entries of the Yukawa matrices remain free, with their natural $\mathcal{O}(1)$ value being specially attractive. Notice that these models produce a Nambu-Goldstone Boson (NGB) from the breaking of $U(1)_{FN}$ that, in general, can have flavour violating couplings to fermions, what translates in strong limits to these type of models from processes like flavour violating meson decays. The danger these type of observables pose on BSM models is what is usually called the BSM Flavour Problem.

2.2 The BSM Flavour Problem

When modifying the particle content of the SM in order to solve some of its open problems new states may be observed through resonant searches, together with indirect effects these states can have through loop processes. Flavour physics is particularly sensitive to the latter, as in the SM all flavour violating processes are mediated by the W and therefore suppressed by the CKM matrix elements.

There is one particular type of processes which is strongly suppressed, and that is the one involving flavour changing neutral currents (FCNC); in other words, processes with a flavour change but where the initial and final states possess the same electric charge. As there are no electrically neutral flavour couplings in the SM, FCNC processes must necessarily occur at the one loop level. Such processes include rare decays, like $B_S^0 \to \mu^+\mu^-$ in Fig. 2.3 or meson

oscillations like $K^0 - \bar{K}^0$ in Fig. 2.4, described by the so-called box diagrams or by the penguin diagrams.

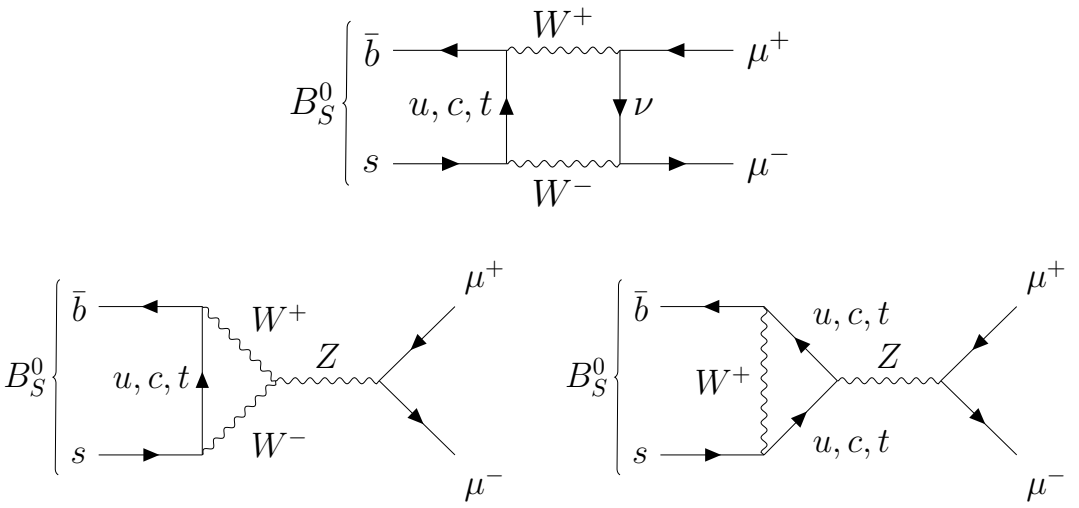

FIGURE 2.3: One-loop diagrams describing the $B_S^0 \to \mu^+\mu^-$ decay, with the box diagram above and the penguin ones on the bottom.

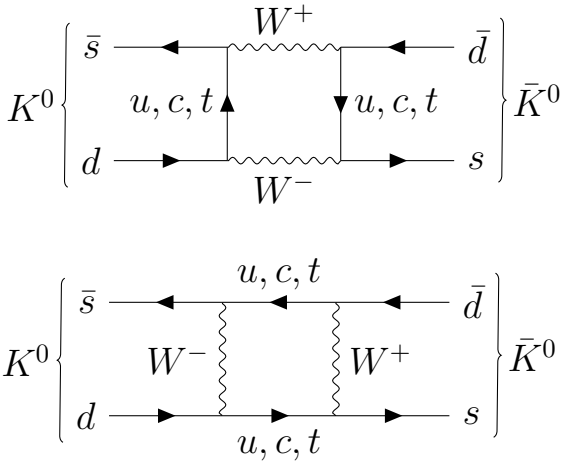

FIGURE 2.4: One-loop diagrams for the kaon oscillation $K^0 - \bar{K}^0$.

The loop nature of these processes already implies an important suppression, but it becomes further so when the unitarity of the CKM matrix is taken into account: when summing the contributions of the three quarks running in the loop, due to the CKM unitarity, they exactly cancel except up to masses effects. This is what is known as the GIM mechanism, and it can imply stronger suppressions in these type of processes.

The extremely small presence of these processes in the SM implies that any BSM contribution which may impact them should be easily measurable. These NP contributions can be

parametrized by the scale Λ that delimits up to when the SM is a good EFT, without considering explicitly the new degrees of freedom. As we commented before, the hierarchy problem asks for a low NP scale, of order $\Lambda \sim \mathcal{O}(\text{TeV})$, but measurements of meson mixing, through observables like ε_K, lepton mixing, like $\mu \to e$ conversion in nuclei and CP-violation observables, like EDMs, set a limit on the scale $\Lambda \gtrsim \mathcal{O}(10^4 \text{ TeV})$ [50, 51].

This large scale, and the generically large effects that one could expect when new flavour physics are considered, are indeed worrying as it seems to point in the direction that NP in the flavour sector cannot be arbitrarily large. Such is the nature of the BSM flavour problem, and in the next section we will present a framework that allows for an elegant way to protect our models against this danger.

2.2.1 Minimal Flavour Violation

When looking for a way to allow new flavour physics while satisfying experimental constraints but still maintain a low NP scale, the Minimal Flavour Violation (MFV) framework [41] was developed. The main assumption of MFV lies in considering that the only source of flavour and CP violation in any NP model is that of the SM, i.e. the Yukawas. This implies that, in the limit of vanishing Yukawa couplings, a flavour symmetry group $\mathcal{G}_F$ can be identified by looking at the kinetic terms of all fermion fields [42]:

$$\mathcal{G}_F = U(3)_{q_L} \times U(3)_{u_R} \times U(3)_{d_R} \times U(3)_{l_L} \times U(3)_{e_R}, \tag{2.20}$$

where for now we are considering massless neutrinos.

This assumption follows the direction of the non-Abelian continuous flavour symmetry models we discussed before: the Yukawa matrices of the SM must become spurions that transform non-trivially under the non-Abelian symmetry subgroup $\mathcal{G}_F^{NA} \subset \mathcal{G}_F$ in order to ensure full invariance of the Lagrangian, while their background value (spurious analogue of the scalar VEV) they take must reproduce the observed masses and mixings in the SM.

$$\begin{gathered} Y_u \to \mathcal{Y}_u \sim (\mathbf{3}, \bar{\mathbf{3}}, \mathbf{1}, \mathbf{1}, \mathbf{1}), \quad Y_d \to \mathcal{Y}_d \sim (\mathbf{3}, \mathbf{1}, \bar{\mathbf{3}}, \mathbf{1}, \mathbf{1}), \\ Y_e \to \mathcal{Y}_e \sim (\mathbf{1}, \mathbf{1}, \mathbf{1}, \mathbf{3}, \bar{\mathbf{3}}), \end{gathered} \tag{2.21}$$

$$\langle \mathcal{Y}_u \rangle = c_t V_{CKM}^\dagger \text{diag}\left(\frac{m_u}{m_t}, \frac{m_c}{m_t}, 1\right), \quad \langle \mathcal{Y}_d \rangle = c_b \text{diag}\left(\frac{m_d}{m_b}, \frac{m_s}{m_b}, 1\right), \\ \langle \mathcal{Y}_e \rangle = c_\tau \text{diag}\left(\frac{m_e}{m_\tau}, \frac{m_\mu}{m_\tau}, 1\right), \tag{2.22}$$

with c_t, c_b and c_τ numeric factors smaller than 1.

The power of this procedure appears when considering non-renormalizable operators that may encode new flavour physics. These operators must be constructed flavour invariant and, as such, they will include appropriate powers of the Yukawa matrices. These Yukawa matrices carry the SM flavour hierarchies, meaning that the new operators will be Yukawa suppressed, mimicking the GIM mechanism present already in the SM. When matching the flavour observables with the predictions made through MFV operators the scale of NP goes from hundreds or thousands of TeVs [50] as discussed before (when generic BSM operators were assumed) to even a few TeVs [20–24, 42, 52–57].

These framework has of course its drawbacks as well: the top Yukawa is contained in a spurion and, as such, is reproduced by a background value. However, it is close to one, so this could pose a threat on the perturbative character of the scheme. Additionally, it is necessary to give a dynamical origin to said background values; this is something that has indeed been attempted with positive results but not complete: after promoting the spurions to scalar fields, minima have been found that include non-vanishing masses for the heavier quarks and leptons, two massive neutrinos and small mixing in the quark sector. The lepton sector requires a special treatment as, as we will see in the final section of this chapter, the naïve symmetry obtained from the kinetic terms lacks predictive power.

2.2.2 Minimal Lepton Flavour Violation

MFV in the lepton sector requires for a more detailed discussion, as neutrino masses are not present in the SM. In a first step, the minimal field content (MFC) scenario, only the non-renormalizable Weinberg operator is considered.

$$\mathcal{O}_W = \frac{\left(\bar{l}_L^c \tilde{H}^*\right) \mathcal{G}_\nu \left(\tilde{H}^\dagger l_L\right)}{\Lambda_{LN}}, \tag{2.23}$$

where $\mathcal{G}_\nu$ is a spurion that transforms under $SU(3)_{l_L}$ as a $\bar{\mathbf{6}}$, such that its background value reproduces neutrino masses:

$$\langle \mathcal{G}_\nu \rangle = \frac{\Lambda_{LN}}{v^2} U^T \hat{m}_\nu U, \tag{2.24}$$

with U the PMNS matrix.

One would, however, like to work in a renormalizable scenario. After extending the SM into a Type-I SS with 3 RH neutrinos, the symmetry gets an additional $SU(3)_{N_R}$ factor coming from their kinetic term. In this case, looking at Eq. 2.10 one can see that two spurions appear, namely:

$$Y_\nu \to \mathcal{Y}_\nu \sim (\mathbf{1}, \mathbf{1}, \mathbf{1}, \mathbf{3}, \mathbf{1}, \bar{\mathbf{3}}), \quad M_N \to \mu_{LN} \mathcal{Y}_N \sim (\mathbf{1}, \mathbf{1}, \mathbf{1}, \mathbf{1}, \mathbf{1}, \bar{\mathbf{6}}), \tag{2.25}$$

where μ_{LN} is a mass scale extracted from M_N such that the spurion $\mathcal{Y}_N$ is dimensionless and all its entries are at most 1.

In the limit where $\mu_{LN} \gg v$ the light neutrino masses can be identified in the same fashion as in Eq. 2.16 as follows:

$$m_\nu \simeq \frac{v^2}{2\mu_{LN}} \mathcal{Y}_\nu \mathcal{Y}_N^{-1} \mathcal{Y}_\nu^T, \tag{2.26}$$

which must reproduce light neutrino masses once the spurions acquire a background value, meaning

$$\langle \mathcal{Y}_\nu \rangle \langle \mathcal{Y}_N^{-1} \rangle \langle \mathcal{Y}_\nu^T \rangle = \frac{2\mu_{LN}}{v^2} U^T \hat{m}_\nu U. \tag{2.27}$$

Notice that, in this case, there is not a single spurion related to neutrino masses and mixings, but a combination of two of them. This implies that it is not possible to unambiguously identify the elements of the spurions in terms of neutrino masses and the PMNS matrix elements. More so, when one considers neutrino flavour operators to match with observables, we find that the spurions entering said operators are $\mathcal{Y}_\nu$, $\mathcal{Y}_N$ and their hermitian conjugates instead of their transposed. As a consequence of this fact, flavour processes can not be described in terms of neutrino masses and mixings either, losing therefore the predictivity MFV harnessed in the quark sector.

As a way to bypass this loss of predictive power, a modification of the flavour symmetry assumed in the lepton sector was proposed. This implies in particular considering a slightly

smaller lepton flavour symmetry group $\mathcal{G}_L^{NA} \subset \mathcal{G}_F^{NA}$, such that the combination of spurions appearing in the light neutrino masses and flavour observables were the same.

The first of these modifications [58, 59] considers restricting the symmetry in the RH neutrino sector and imposing CP conservation.

$$\mathcal{G}_L^{NA} \to SU(3)_{l_L} \times SU(3)_{e_R} \times SO(3)_{N_R} \times CP. \tag{2.28}$$

As a consequence of CP conservation in the lepton sector, the spurions are automatically real meaning in particular that $\mathcal{Y}_\nu^\dagger = \mathcal{Y}_\nu^T$[5]. Additionally, the reduction of the N_R flavour symmetry, going from a unitary group to an orthogonal one, is equivalent to considering that the three heavy neutrinos are mass degenerate, which translates in terms of the spurion to $\mathcal{Y}_N \propto \mathbb{1}$. With these assumptions, the expression for light neutrino masses is simplified to

$$m_\nu \simeq \frac{v^2}{2\mu_{LN}} \mathcal{Y}_\nu \mathcal{Y}_\nu^T. \tag{2.29}$$

Thanks to these conditions, the only spurion combinations that appear in flavour relevant operators are $\mathcal{Y}_e$ and $\mathcal{Y}_\nu \mathcal{Y}_\nu^T$, which allows for them to be rewritten in terms of lepton masses and mixings, recovering the predictive power previously lost.

The other proposal to render Minimal Lepton Flavour Violation (MLFV) predictive is to consider that the RH neutrinos transform under the same symmetry as the LH lepton doublet [60]. In terms of the symmetry, this means considering

$$\mathcal{G}_L^{NA} \to SU(3)_{l_L + N_R} \times SU(3)_{e_R}. \tag{2.30}$$

As a consequence of this choice, the neutrino Yukawa is automatically flavour invariant, with $\mathcal{Y}_\nu$ being a singlet under the whole flavour symmetry group. As such, it is a unitary matrix [61, 62] that can therefore be rotated to the identity matrix through a RH neutrino flavour rotation. Consequently, light neutrino masses reduce now to

[5] This is not entirely true, as CP conservation only requires the Majorana phases to be either 0, π or 2π. However, Majorana phases of π do not result in real Yukawas. The CP conservation imposed here is a bit stronger than the usual one, forbidding this value for the Majorana phases.

$$m_\nu \simeq \frac{v^2}{2\mu_{LN}} \mathcal{Y}_N^{-1}, \tag{2.31}$$

while flavour violating effects are now written exclusively in terms of $\mathcal{Y}_e$ and $\mathcal{Y}_N$, allowing them to be expressed in terms of lepton masses and mixings, recovering thus the predictive power of MFV. In both cases, the constraints on NP considering the present available data on flavour changing processes in the lepton sector are as low as a few TeV [58–60, 63–66].

In this thesis we will present two flavour models that follow the philosophy of MFV, protecting them against the BSM flavour problem. Additionally, we will show how the Abelian part of the MFV flavour symmetry group can be used to solve other problems of the SM, increasing its appeal beyond a mere defence against possible flavour bounds.

Chapter 3

The Strong CP Problem

When we wrote the SM Lagrangian we followed some rules: one has to write all possible terms which are renormalizable (up to dimension 4) that respect all gauge symmetries and Lorentz invariance. In principle, one could think that all the terms we showed in eqs. (1.4, 1.6, 1.7) are all of the possible terms that respect the rules. However, there are three more terms that could be added to the SM Lagrangian without breaking renormalizability nor gauge or Lorentz symmetry. These terms involve only the gauge fields and are the following:

$$\mathscr{L}_{X\tilde{X}} = \theta_{QCD}\frac{\alpha_s}{8\pi}G^{a\mu\nu}\tilde{G}^a_{\mu\nu} + \theta_W\frac{\alpha_W}{8\pi}W^{i\mu\nu}\tilde{W}^i_{\mu\nu} + \theta_Y\frac{\alpha_Y}{8\pi}B^{\mu\nu}\tilde{B}_{\mu\nu}, \tag{3.1}$$

where $\tilde{X}_{\mu\nu} = \frac{1}{2}\varepsilon_{\mu\nu\alpha\beta}X^{\alpha\beta}$ is the dual of the field strength tensor for each gauge group, with $\varepsilon^{\mu\nu\alpha\beta}$ being the fully antisymmetric tensor satisfying $\varepsilon^{1230} = 1$.

The terms appearing in the previous equation are indeed gauge and Lorentz invariant, breaking only CP symmetry. However, CP is not a conserved symmetry in the SM Lagrangian either, since the phases in the Yukawa matrices already break it, so one may wonder why should these terms not be considered. They all share in fact one peculiarity which is being proportional to a total derivative, namely

$$\frac{\alpha_X}{8\pi}X^{a\mu\nu}\tilde{X}^a_{\mu\nu} = \partial_\mu K^\mu;\ K^\mu = \frac{\alpha_X}{4\pi}\varepsilon^{\mu\nu\alpha\beta}\left(X^a_\nu\partial_\alpha X^a_\beta + \frac{1}{3}f_{abc}X^a_\nu X^b_\alpha X^c_\beta\right), \tag{3.2}$$

where K^μ is the so called Chern-Simons current and the last term in its expression only exists for non-Abelian symmetries.

Taking this into consideration, one could naïvely apply Gauss' Theorem together with the condition of gauge fields being null at infinity or a gauge transformation of 0, expecting that term to vanish after it is integrated by parts. This happens in fact for Abelian gauge groups, rendering the hypercharge term unphysical. However, that is not the case for the colour and weak forces. As we will see in the next section, the QCD vacuum presents non-trivial solutions for the gauge configuration called instantons that allow it to have physical consequences.

The most relevant of said consequences is the presence of a non-vanishing neutron electric dipole moment d_n (nEDM) [67, 68], a magnitude that has been measured with a stunning accuracy. The θ_{QCD} parameter is related to this observable as follows

$$d_n \sim \theta_{QCD} \times 10^{-16}\ \text{e} \cdot \text{cm}. \tag{3.3}$$

Current measurements are able to set a very stringent limit on this observable [69–71] to be below $d_n \lesssim \mathcal{O}(10^{-26})$ e · cm, which translates into an upper limit on the θ_{QCD} parameter:

$$\theta_{QCD} \lesssim \mathcal{O}(10^{-10}), \tag{3.4}$$

which is an extremely small value for a dimensionless parameter, something that does not happen in any other place of the SM picture, constituting the so-called Strong CP Problem. Let us start first with discussing the details of how CP is broken by the strong sector, together with quark masses, and studying a little bit the QCD vacua.

3.1 CP Invariance in the QCD Lagrangian and the Chiral Anomaly

As already discussed, besides the θ_{QCD} term there is an additional source of CP violation in the Yukawa sector. Let us consider for now a simple case with just one quark mass matrix M. In its diagonal form, the masses could still have an overall phase, so that it can be written

$$M = \text{diag}\left(m_j e^{i\alpha_j}\right), \tag{3.5}$$

where the index j runs for all the quarks considered.

In the limit of small phases, the quark mass term can be rewritten as:

$$\bar{q}Mq = m_j \cos\alpha_j \bar{q}_j q_j - i m_j \sin\alpha_j \bar{q}_j \gamma_5 q_j \simeq m_j \bar{q}_j q_j - i m_j \alpha_j \bar{q}_j \gamma_5 q_j, \tag{3.6}$$

with $\gamma_5 = i\gamma_0\gamma_1\gamma_2\gamma_3$ the fifth Dirac matrix that anti-commutes with all Dirac matrices.

The last term in the previous equation constitutes an additional source of CP violation in our Lagrangian and, as we will show in the following, it is in fact related to the θ_{QCD} term through the Chiral Anomaly.

For the sake of simplicity, let us consider the case of only one quark with complex mass $M = me^{i\alpha}$. The Lagrangian for this quark is

$$\mathscr{L}_{Dirac} = \bar{q}\left(i\not{D} - M\right) q. \tag{3.7}$$

Considering only this Lagrangian it is easy to think of a rotation that allows us to make the quark mass real, namely:

$$U(1)_A: \quad q \to e^{-i\gamma_5 \frac{\alpha}{2}} q, \qquad\qquad \bar{q} \to \bar{q} e^{-i\gamma_5 \frac{\alpha}{2}}, \tag{3.8}$$

which, at first order in the small parameter α, transforms the previous Lagrangian in the following way:

$$\begin{aligned}
\mathscr{L}_{Dirac} \xrightarrow{U(1)_A} & \bar{q}\left(1 - i\gamma_5\frac{\alpha}{2}\right)\left(i\not{D} - M\right)\left(1 - i\gamma_5\frac{\alpha}{2}\right) q \\
& \approx \mathscr{L}_{Dirac} - \bar{q}\left(i\not{D} - M\right) i\frac{\alpha}{2}\gamma_5 q - i\bar{q}\gamma_5\frac{\alpha}{2}\left(i\not{D} - M\right) q \\
& = \mathscr{L}_{Dirac} + \frac{\alpha}{2}\bar{q}\left(\not{D}\gamma_5 + \gamma_5\not{D}\right) + iM\alpha\bar{q}\gamma_5 q \\
& = \mathscr{L}_{Dirac} + iM\alpha\bar{q}\gamma_5 q \approx \mathscr{L}_{Dirac} + im\alpha\bar{q}\gamma_5 q,
\end{aligned} \tag{3.9}$$

where the last term exactly cancels the imaginary term of Eq. 3.6, rendering the mass quark real.

This is the effect of the transformation at the classical level. However, it was shown that this kind of transformation does not leave the measure of the path integral invariant. As we will see now, the impact of this non-invariance of the path integral leads to the appearance of a term analogue to the θ_{QCD} one.

The breaking at the quantum level of the axial $U(1)_A$ is an issue that has been widely studied in the context of the neutral pion decay to photons [72, 73] or the mass of the η' meson. This non-conservation of the axial current $j_A^\mu = \bar{q}\gamma^\mu\gamma_5 q$ receives the name of chiral, axial or ABJ anomaly [74, 75], and can be explained through the computation of the triangle diagram shown in Fig. 3.1.

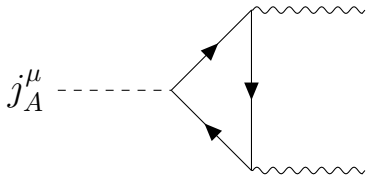

FIGURE 3.1: Triangle diagram that breaks the axial $(1)_A$ symmetry.

In this work, however, we will follow a parallel approach to this anomaly, as proposed by Fujikawa [76], where the anomaly is shown through the non-invariance of the measure of the path integral, the functional integral that gathers all information of the QFT being treated. Let us first write the path integral

$$\mathcal{Z} = \int \mathfrak{D}\bar{q}\mathfrak{D}q\, e^{i\int d^4x \bar{q}\left(i\not{D} - M\right)q}, \tag{3.10}$$

and the transformation, generalized with a parameter that may depend on space-time coordinates,

$$\begin{aligned} q &\to e^{-i\theta(x)\gamma_5} q \xrightarrow{\theta \ll 1} (1 - i\theta(x)\gamma_5)\, q, \\ \bar{q} &\to \bar{q} e^{-i\theta(x)\gamma_5} \xrightarrow{\theta \ll 1} q\,(1 - i\theta(x)\gamma_5), \end{aligned} \tag{3.11}$$

which translates in the following change of the Lagrangian

$$\mathscr{L} = \bar{q}\left(i\not{D} - M\right)q \to \mathscr{L} + \bar{q}\not{\partial}(\theta(x))\gamma_5 q + i2M\bar{q}\gamma_5 q. \tag{3.12}$$

Let us now express the quark fields in terms of eigenstates of the dirac operator $i\not{D}$ in the following way:

$$\left(i\not{D}\right)\phi_m = \lambda_m \phi_m. \qquad q = \sum_n a_n \phi_n(x), \qquad \bar{q} = \sum_n \phi_n^\dagger(x)\bar{b}_n, \tag{3.13}$$

where ϕ_n is the nth eigenstate of the Dirac operator with its eigenvalue λ_n. In this field expansion, the coefficients a_n and b_n are Grassman variables where the fermion character of the quark field is contained, while the eigenstates $\phi_n(x)$ include within them all Lorentz dependence and satisfy the normalization $\int d^4x \phi_m^\dagger \phi_n = \delta_{mn}$.

The measure of the integral after this expansion, before and after the axial transformation, can be expressed as:

$$\mathfrak{D}\bar{q}\mathfrak{D}q = \prod_n da_n d\bar{b}_n \to \mathfrak{D}\bar{q}'\mathfrak{D}q' = \prod_n da'_n d\bar{b}'_n, \tag{3.14}$$

which are related as usual for Grassman variables:

$$\prod_m da'_m = \mathcal{J}^{-1} \prod_n da_n, \tag{3.15}$$

where $\mathcal{J}$ is the Jacobian of the transformation. By using the definition and normalization relation of the Dirac operator eigenstates, one can find the Jacobian in the following way:

$$\begin{aligned}
&q = \sum_n a_n \phi_n(x) \to \sum_n a_n \left(1 - i\theta(x)\gamma_5\right) \phi_n(x) = q' = \sum_m a'_m \phi_m(x), \\
&\sum_m a'_m \int d^4x \phi_j^\dagger(x)\phi_m(x) = \sum_n a_n \int \left(1 - i\theta(x)\gamma_5\right) \phi_j^\dagger(x)\phi_n(x), \\
&\sum_m a'_m \delta_{jm} = \sum_n a_n \left(\delta_{jn} - i \int d^4x \theta(x) \phi_j^\dagger(x)\gamma_5\phi_n(x)\right), \\
&a'_j = \sum_n a_n \left(\mathbb{1} - i \int d^4x \theta(x) \phi_j^\dagger(x)\gamma_5\phi_n(x)\right).
\end{aligned} \tag{3.16}$$

From the last line of this equation, the Jacobian of the transformation is directly obtained as:

$$\begin{aligned}
\mathcal{J}^{-1} = \det\left(\mathbb{1} + C_{nj}\right) \approx \exp\left(Tr\left(C_{nj}\right)\right)^{-1}, \quad \text{with} \quad C_{nj} = -i \int d^4x \theta(x) \sum_n \phi_j^\dagger \gamma_5 \phi_n(x), \\
\mathcal{J} \approx \exp\left(i \int d^4x \theta(x) \sum_n \phi_j^\dagger(x)\gamma_5\phi_n(x)\right).
\end{aligned} \tag{3.17}$$

The Jacobian contains a divergent sum, and thus needs to be regularized somehow. A possibility is to introduce a cut-off as Fujikawa proposed:

$$\sum_n \phi_n^\dagger \gamma_5 \phi_n = \lim_{M\to\infty} \sum_n \phi_n^\dagger(x)\gamma_5\phi_n(x) e^{-\frac{\lambda_n^2}{M^2}} \qquad (|\lambda_n| \ll M). \tag{3.18}$$

Taking into account that λ_n are the eigenvalues of the Dirac operator, we can rewrite the previous equation as follows:

$$\lim_{M\to\infty}\sum_n \phi_n^\dagger(x)\gamma_5 e^{\frac{-(i\not{D})^2}{M^2}}\phi_n(x) = \lim_{M\to\infty}\left\langle x\left|Tr\left(\gamma_5 e^{-\frac{(i\not{D})^2}{M^2}}\right)\right|x\right\rangle, \tag{3.19}$$

where $\not{D}^2$ can be rearranged into the following form.

$$\begin{aligned}\not{D}^2 &= \gamma_\mu D^\mu \gamma_\nu D^\nu = \frac{1}{2}\left(\{\gamma_\mu,\gamma_\nu\}+[\gamma_\mu,\gamma_\nu]\right)D^\mu D^\nu \\ &= D^2 + \frac{1}{4}\left[\gamma_\mu,\gamma_\nu\right]\left[D^\mu,D^\nu\right],\end{aligned} \tag{3.20}$$

where we used the commutation relation for gamma matrices, $\{\gamma_\mu,\gamma_\nu\} = 2g_{\mu\nu}$, together with the decomposition in symmetric and anti-symmetric parts for a tensor. For simplicity and as we look for the colour anomaly, let us consider only the gluon part of the covariant derivative.

$$[D_\mu, D_\nu] = -ig_s\frac{\lambda_a}{2}G^a_{\mu\nu}, \tag{3.21}$$

With these expressions, we can expand Eq. 3.19 up to second order in $\frac{g_s G^{\mu\nu}}{M}$, reaching the following:

$$\begin{aligned}&\lim_{M\to\infty}\left\langle x\left|Tr\left(\gamma_5 e^{-\frac{(i\not{D})^2}{M^2}}\right)\right|x\right\rangle = \lim_{M\to\infty}\left\langle x\left|Tr\left(\gamma_5 e^{\frac{D^2 - i\frac{g_s}{4}\frac{\lambda_a}{2}[\gamma_\mu,\gamma_\nu]G^{a\,\mu\nu}}{M^2}}\right)\right|x\right\rangle \approx \\ &\lim_{M\to\infty}\left\langle x\left|Tr\left(\gamma_5\left(1 + i\frac{g_s}{4M^2}\frac{\lambda_a}{2}\left[\gamma_\mu,\gamma_\nu\right]G^{a\mu\nu} - \frac{g_s^2}{32M^4}\left(\frac{\lambda_a}{2}\left[\gamma_\mu,\gamma_\nu\right]G^{a\mu\nu}\right)^2\right)e^{\frac{D^2}{M^2}}\right)\right|x\right\rangle.\end{aligned} \tag{3.22}$$

The zeroth and first order of the expansion vanish as a consequence of the relations $Tr\left(\gamma_5\right) = 0$ and $Tr\left(\gamma_5\gamma_\mu\gamma_\nu\right) = 0$. For the second order, the trace over the $SU(3)$ generators will yield $Tr\left(\frac{\lambda_a}{2}\frac{\lambda_b}{2}\right) = \frac{1}{2}\delta_{ab}$, and using $Tr\left(\gamma_5\gamma_\mu\gamma_\nu\gamma_\alpha\gamma_\beta\right) = -i4\varepsilon_{\mu\nu\alpha\beta}$ plus some rearrangement of the terms, we find the following:

$$
\begin{aligned}
&\lim_{M\to\infty} -\left\langle x \left| Tr\left(\gamma_5\left(\frac{g_s^2}{32M^4}\left(\frac{\lambda_a}{2}\left[\gamma_\mu,\gamma_\nu\right]G^{a\mu\nu}\right)^2\right)e^{\frac{D^2}{M^2}}\right)\right| x\right\rangle \\
&= \lim_{M\to\infty} i\frac{g_s^2}{4M^4}\varepsilon_{\mu\nu\alpha\beta}G^{a\mu\nu}G^{a\alpha\beta}\left\langle x\left|e^{\frac{D^2}{M^2}}\right|x\right\rangle \\
&= \lim_{M\to\infty} i\frac{g_s^2}{2M^4}G^{a\mu\nu}\tilde{G}^a_{\mu\nu}\left\langle x\left|e^{\frac{\partial^2}{M^2}}\right|x\right\rangle \\
&= -\frac{\alpha_s}{8\pi}G^{a\mu\nu}\tilde{G}^a_{\mu\nu} = \sum_n \phi_n^\dagger(x)\gamma_5\phi_n(x),
\end{aligned}
\tag{3.23}
$$

where $\tilde{G}^a_{\mu\nu} = \frac{1}{2}\varepsilon^{\mu\nu\alpha\beta}G^a_{\alpha\beta}$ and we used the value of the matrix element $\left\langle x\left|e^{\frac{\partial^2}{M^2}}\right|x\right\rangle = \frac{iM^4}{16\pi^2}$. Finally, the expression for the Jacobian of the transformation is found:

$$
\mathcal{J} = e^{-i\int d^4x\theta(x)\frac{\alpha_s}{8\pi}G^{a\mu\nu}\tilde{G}^a_{\mu\nu}}. \tag{3.24}
$$

The transformed path integral can now be written, using Eq. 3.24 and Eq. 3.12, obtaining thus the Lagrangian after the chiral rotation:

$$
\begin{aligned}
\mathcal{Z} &= \int \mathfrak{D}\bar{q}'\mathfrak{D}q' e^{i\int d^4x\mathscr{L}'\left(\bar{q}',q'\right)} \\
&= \int \mathfrak{D}\bar{q}\mathfrak{D}q\mathcal{J}^{-2}e^{i\int d^4x\bar{q}\left(i\not{D}-M\right)q+\bar{q}\not{\partial}\left(\theta(x)\right)\gamma_5 q+i2M\theta\bar{q}\gamma_5 q} \\
&= \int \mathfrak{D}\bar{q}\mathfrak{D}q e^{i\int d^4x\mathscr{L}-\theta(x)\left(\partial_\mu\left(\bar{q}\gamma^\mu\gamma_5 q\right)-i2M\bar{q}\gamma_5 q-\frac{\alpha_s}{4\pi}G^{a\mu\nu}\tilde{G}^a_{\mu\nu}\right)},
\end{aligned}
\tag{3.25}
$$

where one term has been integrated by parts to take out $\theta(x)$ as a common factor. Taking now derivatives with respect to $\theta(x)$, we obtain the equation of motion for the axial current $j_5^\mu = \bar{q}\gamma^\mu\gamma_5 q$:

$$
\partial_\mu j_5^\mu = i2M\bar{q}\gamma_5 q + \frac{\alpha_s}{4\pi}G^{a\mu\nu}\tilde{G}^a_{\mu\nu}. \tag{3.26}
$$

We come now to the origin of the chiral anomaly: both quark masses and a QCD term coming from the non-invariance of the metric break the conservation of the axial current. Notice that in Eq. 3.25 appears a term with the same form that had the CP strong violating term of Eq. 3.1. This translates in the observable parameter being, instead of θ_{QCD}, the following combination:

$$
\bar{\theta} = \theta_{QCD} + 2\theta(x) \tag{3.27}
$$

In order to cancel the imaginary mass term appearing in Eq. 3.6, the parameter $\theta(x)$ must be chosen as $\theta = \frac{\alpha}{2}$. This, apart from making the mass real, would imply that the observable $\bar{\theta}$ is now:

$$\bar{\theta} = \theta_{QCD} + \alpha. \tag{3.28}$$

Extending this result to the SM, where not only one quark but three up-type and three down-type quarks exist, yields the following result where all phases are considered:

$$\bar{\theta} = \theta_{QCD} + \text{Arg}\left(\text{Det}\left(M_u M_d\right)\right), \tag{3.29}$$

with $M_{u,d} = Y_{u,d}\frac{v}{\sqrt{2}}$ are the quark mass matrices in the non-diagonal and complex basis.

Considering the physical parameter comes from both the strong and weak sector the Strong CP Problem becomes even more worrying: why should to parameters coming from different sectors cancel up to such a high order as imposed by the limits on nEDM? One could also wonder if the $W^{i\mu\nu}\tilde{W}^i_{\mu\nu}$ term in Eq. 3.1 also results in a "Weak CP Problem". However, this is not the case as $SU(2)_L$ only acts on left-handed fields and through a Baryon Number rotation the θ_W can be removed.

Summarizing, the only term that has physical consequences and represents a fine tuning problem in the SM is that of the $\bar{\theta}$ term. In order to give a dynamical explanation to its tiny value there are many proposals, but the most popular one, and one of the cores of this thesis, is the use of an axion. In the next section we will indeed detail the axion mechanism, but first we will review other proposals to solve the Strong CP Problem that do not require the presence of an axion to provide a more complete view of the situation.

3.2 Axionless solutions to the Strong CP Problem

As we have discussed, the Strong CP Problem is a fine-tuning problem in the SM that has lead to a great activity in the field. There are many proposals that aim to solve it, but they can be broadly classified in three categories: massless quark solutions, Nelson-Barr models and axion models. Let us briefly discuss first the two classes of axionless solutions and, afterwards, provide some details about the axion solution.

3.2.1 Massless quarks

By simply looking at Eq. 3.29 it is easy to see why a massless quark proposal helps with the Strong CP Problem: if only one of the eigenvalues of the quark matrices is zero, its determinant also vanishes. With this, the only remaining parameter is therefore θ_{QCD} which can then be rotated away via a chiral rotation without any effect anywhere else in the Lagrangian.

This solution is indeed extremely simple and satisfying, or so it would be were not for the fact that quark masses are very well studied. Even for the lightest of them, current data and lattice simulations set it at the MeV scale, ruining this potential solution.

Despite the original idea being currently ruled out, the proposal evolved and found its way into new models, sparking interest again in this type of solutions. One example is that of Ref. [77] where a mirror QCD′ sector is included, such that its $\bar{\theta}'$ is aligned with the SM one through a Z_2 symmetry, and where massless quarks can live undetectable for us, predicting at the same time new coloured states at the TeV scale.

3.2.2 Nelson-Barr models

An alternative solution to the Strong CP Problem is considering that CP is indeed a symmetry of the Lagrangian, broken spontaneously, forbidding therefore the existence of the $\bar{\theta}$ parameter before its breaking. These type of models, also called Nelson-Barr models following the original idea by Ann E. Nelson [78] and Stephen M. Barr [79], must account somehow for the observed CP violation present in the SM, while keeping $\bar{\theta} = 0$ at tree level.

Though this can be achieved as shown in Ref. [80] by extending the SM with additional EW singlet quarks that mix with the SM ones through extra EW singlet scalars that take complex VEVs, breaking thus spontaneously CP symmetry, some difficulties can arise. Additional symmetries may be required to forbid some couplings among the new fields and between those and the SM fields, or otherwise a non vanishing $\mathrm{Arg}\left(\mathrm{Det}\left(M_u M_d\right)\right)$ would be generated.

Additional issues include fine-tuning among the model parameters as well as a possible generation of $\bar{\theta}$ by high-dimensional operators or through loop corrections. Some of these ailments can be cured by invoking supersymmetry (SUSY) though they may still find some trouble in radiative corrections. An example of a supersymmetric model derived from the Nelson-Barr mechanism is the one in Ref. [81] where a non-renormalziation theorem protects

$\bar{\theta}$ from getting large loop corrections, but other variations are still being published in the literature, keeping the Nelson-Barr idea still relevant.

3.3 An elegant solution: the axion

As we have already seen, there are various proposals to solve the Strong CP Problem. However, one which is particularly appealing, as we will discuss, that has tremendous experimental searches looking for it and that will be crucial in this thesis is the axion. The original proposal was by Roberto Peccei and Helen Quinn [82, 83] where the $\bar{\theta}$ parameter becomes a dynamical field and an new global symmetry, $U(1)_{PQ}$, connects it with the gluon field through the chiral anomaly.

The Peccei-Quinn symmetry $U(1)_{PQ}$ is broken spontaneously by a field that carries PQ charge, giving rise to a Nambu-Goldstone Boson, the axion, a, [84, 85]. This NG boson couples to gluons through the chiral anomaly as follows:

$$\mathscr{L}_{aGG} = \frac{a}{f_a}\frac{\alpha_s}{8\pi}G^{a\mu\nu}\tilde{G}^a_{\mu\nu}, \tag{3.30}$$

where f_a is the so-called axion decay constant. This term is completely analogue to the one in Eq. 3.1, with the theta parameter becoming now

$$\theta_{eff} = \bar{\theta} + \frac{a}{f_a}. \tag{3.31}$$

Non-perturbative QCD effects give rise to a potential for the axion which has approximately the following shape:

$$V_{eff} \sim 1 - \sqrt{1 + \cos\left(\bar{\theta} + \frac{a}{f_a}\right)}, \tag{3.32}$$

which dynamically drives the minimum to be CP conserving:

$$\langle a \rangle = -f_a\bar{\theta}. \tag{3.33}$$

With just the introduction of one new symmetry and one extra field the Strong CP Problem is easily solved. This solution of course has its own difficulties, namely the PQ quality problem. This is the name that receives the sensitivity of the axion potential to be shifted; additional explicit breakings of the PQ symmetry could move the minimum away from its CP conserving value, which is something that could happen since gravity is expected to break global symmetries. This issue is particularly dangerous for large values of the axion decay constant, which are usually required as we will discuss in a while.

On top of this, the $U(1)_{PQ}$ symmetry may not be broken down entirely in general, but a Z_n symmetry may be left after PQ SSB. When this happens, several degenerate vacua can appear in the early universe, creating bubbles with different values of $\langle a \rangle$ that can give rise to a network of domain walls and cosmic string which, when produced after inflation, could dominate the Universe and overclose it. This is what constitutes the so-called axion domain wall problem, and is another interesting research topic associated to axions.

Despite the axion quality and domain wall problems being extremely exciting issues for model building, it is beyond the scope of this thesis, so we will limit ourselves to discussing in the following pages the most common axion models and motivating them, starting with the original one: the Peccei-Quinn-Weinberg-Wilczek axion.

3.3.1 The PQWW Axion

The Peccei-Quinn-Weinberg-Wilczek (PQWW) axion is considered within the SM gauge group $SU(3)_C \times SU(2)_L \times U(1)_Y$, and is identified within the phase of the Higgs field when a new $U(1)_{PQ}$ is spontaneously broken. However, only one Higgs doublet is not enough to solve the Strong CP Problem, as for the Yukawas to be invariant under the PQ symmetry it is needed that up-type quarks and down-type quarks have opposite charges, which would imply a vanishing contribution to the $G^{a\mu\nu}\tilde{G}^a_{\mu\nu}$ term of the anomaly. Consequently, the model must be extended with two Higgs doublets, so that each one of them couples only to up or down quarks and the Yukawas can be made invariant under $U(1)_{PQ}$ without making the $aG^{a\mu\nu}\tilde{G}^a_{\mu\nu}$ coupling disappear.

With two Higgs weak doublets H_d and H_u, with hypercharges $Y(H_d) = \frac{1}{2}$ and $Y(H_u) = -\frac{1}{2}$ respectively, the most generic potential that can be built [86] is found to be:

$$\begin{aligned} V(H_d, H_u) = &- \mu_1^2 H_d^\dagger H_d - \mu_2^2 H_u^\dagger H_u + \sum_{i,j} a_{i,j} H_i^\dagger H_i H_j^\dagger H_j \\ &+ \sum_{i,j} b_{i,j} H_i^\dagger \tilde{H}_j \tilde{H}_j^\dagger H_i + \sum_{i \neq j} \left(c_{i,j} H_i^\dagger H_j H_i^\dagger H_j + h.c. \right), \end{aligned} \tag{3.34}$$

In the previous equation, $a_{i,j}$ and $b_{i,j}$ are real and symmetric, while $c_{i,j}$ is hermitian. Such potential is invariant under a $U(1)$ symmetry, provided H_d and H_u have opposite charges, but this is just the usual gauge $U(1)_Y$.

Peccei and Quinn included an additional constraint by considering $c_{ij} = 0$. This makes the potential completely invariant under:

$$H_d \xrightarrow{U(1)_{PQ}} e^{i\theta x_{H_d}} H_d, \qquad H_u \xrightarrow{U(1)_{PQ}} e^{i\theta x_{H_u}} H_u, \tag{3.35}$$

where θ is the parameter of the transformation. The Higgs doublets H_d and H_u will develop a VEV in the lower and upper component of the doublet respectively, so that H_d couples to down quarks and H_u to up-type quarks. Taking this into account, the quark Yukawa can be written as follows:

$$\mathscr{L}_Y^q = - \left(Y^d \bar{q}_L H_d d_R + Y^u \bar{q}_L H_u u_R \right) + h.c., \tag{3.36}$$

where, in order to be invariant under $U(1)_{PQ}$, the quark fields must transform as:

$$u \xrightarrow{U(1)_{PQ}} e^{-i\frac{\theta}{2} x_{H_u} \gamma_5} u, \quad d \xrightarrow{U(1)_{PQ}} e^{-i\frac{\theta}{2} x_{H_d} \gamma_5} d. \tag{3.37}$$

The axion will appear as a specific linear combination of the pseudoscalar parts of H_u and H_d. These fields can be written in the two following ways:

$$\begin{aligned} H_d &= \frac{v_d + h_d(x)}{\sqrt{2}} e^{i\frac{p_d^a(x)\sigma_a}{v_d}} \begin{pmatrix} 0 \\ 1 \end{pmatrix} = \begin{pmatrix} H_d^+(x) \\ \frac{v_d + h_d(x) + i p_d^0(x)}{\sqrt{2}} \end{pmatrix}, \\ H_u &= \frac{v_u + h_u(x)}{\sqrt{2}} e^{i\frac{p_u^a(x)\sigma_a}{v_u}} \begin{pmatrix} 1 \\ 0 \end{pmatrix} = \begin{pmatrix} \frac{v_u + h_u(x) + i p_u^0(x)}{\sqrt{2}} \\ H_u^-(x) \end{pmatrix}, \end{aligned} \tag{3.38}$$

where v_i are the VEV of the fields, h_i, p_i^a and p_i^0 are real scalar fields and H_d^+ and H_u^- are complex scalar fields, the charged parts that have vanishing VEV. In this equation, σ_a are the three Pauli matrices, acting as a basis of $SU(2)$.

Now, let us look into the covariant derivative of these fields, focusing only on the neutral pseudo-scalar parts. Considering the polar form of the field yields

$$\begin{aligned} D_\mu H_d &\supset \frac{v_d + h_d}{\sqrt{2}} \left(\partial_\mu + i g_Y Y B_\mu + i g_W \frac{\sigma_a}{2} W_\mu^a\right) e^{i\frac{p_d^a \sigma_a}{v_d}} \begin{pmatrix} 0 \\ 1 \end{pmatrix} \\ &\supset \left(-i\frac{\partial_\mu p_d^0}{v_d} + i\frac{g_Y}{2} B_\mu - \frac{g_W}{2} W_\mu^3\right) H_d \\ &= -i\left(\frac{\partial_\mu p_d^0}{v_d} + \frac{g}{2} Z_\mu\right) H_d. \end{aligned} \tag{3.39}$$

Here, it has been used the definition of the electroweak gauge boson $Z_\mu = \frac{g_W W_\mu^3 - g_Y B_\mu}{g}$, with $g = \sqrt{g_Y^2 + g_W^2}$. We find for H_u analogously:

$$\begin{aligned} D_\mu H_u &\supset \frac{v_u + h_u}{\sqrt{2}} \left(\partial_\mu + i g_Y Y B_\mu + i g_W \frac{\sigma_a}{2} W_\mu^a\right) e^{i\frac{p_u^a \sigma_a}{v_u}} \begin{pmatrix} 1 \\ 0 \end{pmatrix} \\ &\supset \left(i\frac{\partial_\mu p_u^0}{v_u} - i\frac{g_Y}{2} B_\mu + \frac{g_W}{2} W_\mu^3\right) H_u \\ &= i\left(\frac{\partial_\mu p_u^0}{v_u} + \frac{g}{2} Z_\mu\right) H_u. \end{aligned} \tag{3.40}$$

With this, we can write the neutral pseudoscalar part of the kinetic terms as follows:

$$\sum_i D_\mu H_i^\dagger D^\mu H_i \supset \frac{v_d^2}{2}\left(\frac{\partial_\mu p_d^0}{v_d} + \frac{g}{2} Z_\mu\right)^2 + \frac{v_u^2}{2}\left(\frac{\partial_\mu p_u^0}{v_u} + \frac{g}{2} Z_\mu\right)^2. \tag{3.41}$$

Let us consider now the following change of basis for the pseudoscalar fields:

$$\begin{aligned} &p_d^0 = \cos(\alpha)\rho - \sin(\alpha)\chi,\ p_u^0 = \sin(\alpha)\rho + \cos(\alpha)\chi; \\ &\rho = \cos(\alpha)p_d^0 + \sin(\alpha)p_u^0,\ \chi = -\sin(\alpha)p_d^0 + \cos(\alpha)p_u^0, \end{aligned} \tag{3.42}$$

where α is the mixing angle between the two fields. For simplicity, the cosine and sine of this angle will be referred to as just c and s respectively. Using this in Eq. 3.41 and expanding the

squares, we find:

$$\begin{aligned}
&\frac{v_d^2}{2}\left(\frac{\partial_\mu p_d^0}{v_d}+\frac{g}{2}Z_\mu\right)^2+\frac{v_u^2}{2}\left(\frac{\partial_\mu p_u^0}{v_u}+\frac{g}{2}Z_\mu\right)^2 \\
&=\frac{v_d^2}{2}\left(\frac{c\partial_\mu\rho-s\partial_\mu\chi}{v_d}+\frac{g}{2}Z_\mu\right)^2+\frac{v_u^2}{2}\left(\frac{s\partial_\mu\rho+c\partial_\mu\chi}{v_u}+\frac{g}{2}Z_\mu\right)^2 \\
&=\frac{v^2}{8}g^2Z_\mu Z^\mu+\frac{1}{2}\left(\partial_\mu\rho\partial^\mu\rho+\partial_\mu\chi\partial^\mu\chi\right)+\frac{g}{2}Z^\mu\left[\partial_\mu\rho\left(cv_d+sv_u\right)+\partial_\mu\chi\left(cv_u-sv_d\right)\right],
\end{aligned} \tag{3.43}$$

with $v^2=v_d^2+v_u^2$.

From this last equation, we can identify one of the combinations as the NGB eaten by the Z boson, while the remaining one will become the axion. Let us consider a $U(1)_Z$ transformation defined for the Z boson, which charge is $Q_Z=I_3-Y$. The two Higgs fields will be charged under this transformation with $Q_Z\left(H_d\right)=-1$ and $Q_Z\left(H_u\right)=1$. In terms of the fields ρ and χ this means:

$$\rho\xrightarrow{U(1)_Z}\rho+\left(sv_u-cv_d\right)\theta,\qquad\qquad \chi\xrightarrow{U(1)_Z}\chi+\left(sv_d+cv_u\right)\theta. \tag{3.44}$$

One of these particles, that will be identified with the axion, can be chosen neutral under the $U(1)_Z$ as it is orthogonal to the NGB absorbed by the Z boson. If ρ is taken to be neutral, the mixing angle is found to be:

$$Q_Z\left(\rho\right)=0\Rightarrow\tan\alpha=\frac{v_d}{v_u}, \tag{3.45}$$

so that the fields ρ and χ can be rewritten in the following way:

$$\rho=\frac{v_up_d^0+v_dp_u^0}{v},\ \chi=\frac{-v_dp_d^0+v_up_u^0}{v}. \tag{3.46}$$

Following the same logic with the $U(1)_{PQ}$ symmetry, with the axion being the one charged and the other combination neutral, we find:

$$\begin{gathered}
\rho\xrightarrow{U(1)_{PQ}}\rho+\theta\frac{\left(x_{H_d}+x_{H_u}\right)v_dv_u}{v},\ \chi\xrightarrow{U(1)_{PQ}}\chi+\theta\frac{-x_{H_d}v_d^2+x_{H_u}v_u^2}{v}; \\
Q_{PQ}\left(\chi\right)=0\Rightarrow\frac{x_{H_d}}{x_{H_u}}=\frac{v_u^2}{v_d^2}.
\end{gathered} \tag{3.47}$$

Finally, we can identify ρ with the axion a and normalize the Higgs charges as $x_{H_d}+x_{H_u} = 1$,obtaining the following PQ transformation for the axion:

$$a \xrightarrow{U(1)_{PQ}} a + \theta \frac{v_d v_u}{v}. \tag{3.48}$$

From this equation it is straightforward to identify the axion decay constant f_a. If the Higgs fields VEVs are considered to be of the same order and equal to the usual EW Higgs VEV $v \approx 246\ GeV$, the result is:

$$f_a = \frac{v_d v_u}{v} \approx 246\ GeV. \tag{3.49}$$

Such a value for the axion scale is currently ruled out, since that is the scale suppressing the axion coupling to fermions and, with such a low value, the axion should have been observed already. The necessity appears, then, for alternative models that make the axion a bit more elusive: the so-called invisible axion models.

3.3.2 Invisible axions: the DFSZ and KSVZ frameworks

We will devote this section to the study of these alternative models that aim to salvage the original idea by Peccei and Quinn. In order to do so, it is necessary to introduce a new scale f_a much larger than the EW one for the axion to escape experimental bounds. These models received the name of invisible axion models [87, 88] and the classical proposals are classified in two sets of models. These two frameworks differ from each other on their particle content and the way in which the axion couples to gluons. The first of them takes the PQWW axion model as a starting point and extends it with an additional EW singlet complex scalar that carries PQ charge, whereas the second considers only a single Higgs doublet, singlet under $U(1)_{PQ}$, and includes an additional complex scalar and a new heavy quark field, carrying PQ charge both of these BSM fields and therefore coupling to gluons through the new quark species.

The first framework we will discuss is the so-called Dine-Fischler-Srednicki-Zhitnitsky model [89, 90], or DFSZ for short, and it is a next step in the direction of the PQWW axion model. In this scenario, the SM quark Yukawas contain two Higgs fields, H_u and H_d that couple to up-type quarks and down-type quarks respectively, as shown in the equation below.

$$\mathscr{L}_Y \supset Y_u \bar{q}_L H_u u_r + Y_d \bar{q}_L H_d d_r + \text{h.c.}. \tag{3.50}$$

Additionally, a new scalar field ϕ, full SM gauge singlet, is introduced. The two Higgs doublets and the new scalar all transform under the $U(1)_{PQ}$ symmetry as follows:

$$H_u \to e^{i\theta x_u} H_u, \quad H_d \to e^{i\theta x_d} H_d, \quad \phi \to e^{i\theta x_\phi} \phi. \tag{3.51}$$

With this symmetry transformation, we can build the most general scalar potential as shown here:

$$\begin{aligned} V(\phi, H_u, H_d) = {} & \lambda_u \left(|H_u|^2 - V_u^2 \right)^2 + \lambda_d \left(|H_d|^2 - V_d^2 \right)^2 + \lambda \left(|\phi|^2 - V^2 \right)^2 \\ & + \left(a |H_u|^2 + b |H_d|^2 \right) |\phi|^2 + c \left(H_u^i \varepsilon_{ij} H_d^j \phi^2 + h.c. \right) \\ & + d \left| H_u^i \varepsilon_{ij} H_d^j \right|^2 + e \left| H_u^* H_d \right|^2, \end{aligned} \tag{3.52}$$

where ε_{ij} is the fully anti-symmetric tensor for 2 dimensions. Imposing PQ invariance in this potential translates in the following condition for their PQ charges, normalized as in the PQWW model:

$$x_u + x_d = 1 = -2x_\phi \tag{3.53}$$

This automatically defines the new scalar field charge to be $x_\phi = -\frac{1}{2}$. The VEV of this new scalar field, v_ϕ is free, and can be chosen much larger than the EW scale so that:

$$v_\phi \gg \sqrt{v_u^2 + v_d^2} = v \approx 246\ GeV. \tag{3.54}$$

Analogously to the procedure followed in the PQWW model, we can write the fields as:

$$\begin{gathered} \phi_u = \frac{1}{\sqrt{2}} \begin{pmatrix} v_u + \eta^u + i\xi_1^u \\ \eta_2^u + i\eta_3^u \end{pmatrix}, \quad \phi_d = \frac{1}{\sqrt{2}} \begin{pmatrix} \eta_2^d + i\eta_3^d \\ v_d + \eta^d + i\xi_1^d \end{pmatrix}, \\ \phi = \frac{1}{\sqrt{2}} \left(v_\phi + \eta^\phi + i\xi^\phi \right), \end{gathered} \tag{3.55}$$

where η_i and χ_i are all real scalar fields.

The NGB eaten by the Z boson is now found to be:

$$\chi = \frac{v_u \xi_1^u - v_d \xi_1^d}{v}, \tag{3.56}$$

and when it is chosen to be neutral under the $U(1)_{PQ}$, the charges are:

$$x_u = \frac{v_d^2}{v^2}, \quad x_d = \frac{v_u^2}{v^2}. \tag{3.57}$$

The axion will now, however, be a combination of the previous PQ axion ρ and the pseudo-scalar part of the new field ϕ, η^ϕ. To find this, first its transformation under $U(1)_{PQ}$ is:

$$\phi \xrightarrow{U(1)_{PQ}} e^{-i\frac{\theta}{2}}\phi \Rightarrow \xi^\phi \xrightarrow{U(1)_{PQ}} \xi^\phi - \frac{f_\phi}{2}\theta, \tag{3.58}$$

and we can write the unitary transformation describing this combination in terms of the mixing angle φ:

$$\begin{aligned} a &= \cos(\varphi)\,\rho - \sin(\varphi)\,\xi^\phi, \quad b = \sin(\varphi)\,\rho + \cos(\varphi)\,\xi^\phi; \\ \rho &= \cos(\varphi)\,a + \sin(\varphi)\,b, \quad \xi^\phi = -\sin(\varphi)\,a + \cos(\varphi)\,b. \end{aligned} \tag{3.59}$$

Finally, we study how these combinations transform under the PQ symmetry:

$$\begin{aligned} a &\xrightarrow{U(1)_{PQ}} a + \left(\cos(\varphi)\frac{v_d v_u}{v} + \sin(\varphi)\frac{v_\phi}{2}\right)\theta, \\ b &\xrightarrow{U(1)_{PQ}} b + \left(\sin(\varphi)\frac{v_d v_u}{v} - \cos(\varphi)\frac{v_\phi}{2}\right)\theta, \end{aligned} \tag{3.60}$$

from where we can identify the mixing angle φ by making b neutral, and the new axion a can finally be written in terms of the other fields and VEVs:

$$\begin{aligned} Q_{PQ}(b) = 0 \Rightarrow \tan\varphi &= \frac{v_\phi v}{v_u v_d}, \\ a = \frac{2v_u v_d\left(v_u\xi_1^d + v_d\xi_1^u\right) - v_\phi v^2 \xi^\phi}{v\sqrt{v^2 v_\phi^2 + 4v_u^2 v_d^2}} &\xrightarrow{v_\phi \gg v_u, v_d} -\xi^\phi. \end{aligned} \tag{3.61}$$

From eqs. (3.60) and (3.61), the value of the new DFSZ axion scale is found to be:

$$f_a = \frac{\sqrt{v_\phi^2 v^2 + 4v_u^2 v_d^2}}{2v} \xrightarrow{v_\phi \gg v_u, v_d} \frac{v_\phi}{2}. \tag{3.62}$$

Thus, with the addition of just one more scalar singlet the PQWW has been taken to a much higher energy scale, well above the EW one and beyond current experimental bounds for large enough f_ϕ.

Let us look now into the second possibility, the KSVZ axion. In this case, Kim [91], Shifman, Vainshtein and Zakharov [92], considered the possibility of enlarging the SM particle spectrum with a new EW singlet heavy quark, Q, of mass m_Q and a complex scalar field σ, singlet of the whole SM gauge group. In this case, all SM particles are neutral under $U(1)_{PQ}$, while the new fields carry PQ charge:

$$Q \xrightarrow{U(1)_{PQ}} e^{-i\gamma_5\theta}Q, \quad \sigma \xrightarrow{U(1)_{PQ}} e^{-i2\theta}\sigma, \tag{3.63}$$

forbidding the appearance of a bare mass term for the Q quark of the type $\bar{Q}Q$. However, one can write a Yukawa involving both Q and σ, together with a scalar potential, that respect the PQ symmetry:

$$\begin{aligned} \mathscr{L}_Y &= -Y_Q Q_L^\dagger \sigma Q_R - Y_Q^* Q_R^\dagger \sigma^* Q_L, \\ V(H,\sigma) &= -\mu_H^2 H^\dagger H - \mu_\sigma^2 \sigma^*\sigma + \lambda_H \left(H^\dagger H\right)^2 + \lambda_\sigma (\sigma^*\sigma)^2 + \lambda_{H\sigma} H^\dagger H \sigma^*\sigma. \end{aligned} \tag{3.64}$$

From here, the mass of the heavy quark, assuming real Yukawas, is deduced to be $m_Q = \frac{Y_Q v_\sigma}{\sqrt{2}}$.

The axion is easy to identify in this case, as the angular part of the field σ, that has a VEV v_σ that lies way above the EW scale, so it is again an invisible axion.

$$\sigma = \frac{v_\sigma + s(x)}{\sqrt{2}} e^{i\frac{a}{v_\sigma}}, \quad \langle\sigma\rangle = \frac{v_\sigma}{\sqrt{2}} \gg v \approx 246\ GeV. \tag{3.65}$$

Despite this axion not coupling at tree level to the SM fermions q, it actually does it via an anomaly, as shown in Fig. 3.2:

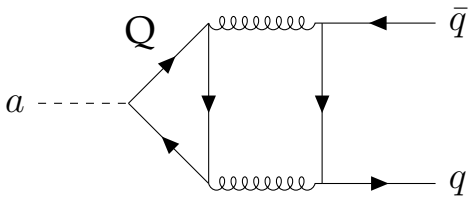

FIGURE 3.2: Effective coupling of a KSVZ axion to SM quarks.

With this, the KSVZ axion emerges as another possibility for an invisible QCD axion that solves the Strong CP Problem and still has coupling to SM quarks, though further suppressed.

An interesting general prediction for all these QCD axion models is the relation between its decay constant. As a consequence of the required axion-gluon coupling. This prediction

can be evaluated to be [93]:

$$m_a = 5.691(51)\left(\frac{10^9 \text{ GeV}}{f_a}\right) \text{ meV}. \tag{3.66}$$

Considering the usually large values, larger than $\mathcal{O}(10^9 \text{ GeV})$, for f_a required to escape current experimental bounds as we will show in the next chapter, a common feature of all QCD axions is their light mass, below the meV level.

We have shown in this section the staple of axions regarding the Strong CP Problem. However, axions are a very interesting theoretical particle as they actually have potential interest in many other sectors of HEP, and we will discuss a bit these other places where axions can be relevant in the following section.

3.3.3 Axion ubiquity beyond the Strong CP Problem

Axions arose as a very compelling solution to the Strong CP Problem, but the current interest in them is not limited to solving that fine-tuning problem. Axions are for starters a general prediction of string theory [94–101], one of the best candidates for UV theory that includes gravity together with the SM gauge forces.

But one of the most interesting features of axions, that actually came naturally as a surprise, is the fact that they are a very interesting candidate for particle cold dark matter. Given the low mass and greatly suppressed interactions expected from QCD axions, they are stable by construction and, additionally, they may be produced non-thermaly through the so-called misalignment mechanism or via the decay of topological defects (domain walls and cosmic strings). These axions can indeed constitute all of the DM in a region of the parameter space that is still allowed by experimental constraints [102].

The realization of this fact has given birth to a huge experimental and observational task force looking for the axion through several ways. An example of a lab experiment looking for axions are Light-shining-through-wall (LSW) experiments like OSQAR where the axion-photon coupling is used in trying to convert photons from a laser into axions so that they go through a wall, and then back into photons for detection. On the more astrophysical side, helioscopes like CAST, that point a telescope under earth towards the sun, aim to detect axions produced within our star; another probe are haloscopes like ADMX, which try to measure the

axion dark matter halo in which we live if axions are indeed what constitute the DM in our Universe.

These and many other collaborations are aiming to look for the axion within the band expected from QCD axions, but also outside of it, since the idea of axion-like particles (ALPs) has become increasingly relevant in the last years. These particles share the shift symmetry of the axion, but are free from the restrictive relation between its mass and decay constant that QCD axions must satisfy.

On the theoretical side, and besides string theory, axions are being used as tools to tackle problems other than the Strong CP one. Some examples of this fact are models where the axion is related to the inflaton, others where it is used towards Grand Unification, the so-called Majoron models where the breaking of the PQ symmetry and lepton number (LN) give rise to a majoron-axion mixture and flavoured axion models like the axiflavon or flaxion.

In this thesis we will deal with this last case, studying the possible interplay of the Strong CP Problem and the Flavour sector as we propose a model where the axion is introduced within the MFV framework in the following chapter, while in Chapter 5 we study the complementarity between this MFV axion and a Majoron that helps alleviate the Hubble tension. Finally, in Chapter 6 we will study one possible cosmological signature of axions where, in the case they are produced thermally, can impact the effective number of neutrinos of our Universe, together with its compatibility with a recent excess observed by the DM experiment XENON1T.

Chapter 4

A flavourful axion: The Minimal Flavour Violating Axion

As we have argued already, the flavour sector of the SM asks for an explanation to its hierarchies. If one rejects the anthropic proposal, one of the most appealing ways to tackle the flavour puzzle is by introducing flavour symmetries.

In this chapter, based in the published paper of Ref. [103], we will present a flavour model where we will follow the FN proposal, with an Abelian symmetry in order to explain some of the hierarchies in the fermion masses of the SM. In order to protect our model from the BSM Flavour Problem we will embed the Abelian flavour symmetry in the Minimal Flavour Violation framework. While in MFV NGBs are usually avoided by gauging part of the symmetry group [20–24, 65, 104], in this work we tried to go in the opposite direction and use a NGBs arising within MFV to address a different SM open problem: the Strong CP Problem, with the axion arising from the Abelian part of the $U(3)^5$ symmetry in MFV, that we will call the Minimal Flavour Violating Axion (MFVA).

The MFVA departs from the traditional QCD axion and from the so-called invisible axions [89–92] in the fact that its transformation properties under the PQ symmetry are determined by the flavour structure of the SM fermions. Its associated phenomenology will be discussed in the context of astrophysics, collider searches and in flavour observables, with the principal focus being on meson decays.

The MFVA is also clearly different from the so-called Axiflavon or Flaxion [105, 106], based on Ref. [107]. Whereas the Axiflavon is the NGB arising from a FN symmetry under which every generation is charged differently, and therefore presents flavour violating couplings to fermions, the MFVA appears from a symmetry which treats in the same way the three generation, but differently up quarks, down quarks and leptons. This implies that the MFVA will have flavour conserving, but non-universal, coupling to fermions, leading to a radically different prediction in observables like meson decays.

Let us now start by discussing the fact that a PQ symmetry can easily be identified within the MFV symmetry group, and then proceed by detailing the mechanism which will explain part of the fermion mass hierarchies.

4.1 Peccei-Quinn symmetry within MFV

Let us remember that in the modern realisation of MFV [42, 58–60, 66], the SM fermionic kinetic terms exhibit a $U(3)^5$ flavour symmetry. In this work we will make use of the fact that the symmetry group can be decomposed into the product of an Abelian and a non-Abelian factor, $\mathcal{G}_F^{\rm NA} \times \mathcal{G}_F^{\rm A}$, as follows

$$\begin{aligned} \mathcal{G}_F^{\rm NA} &\equiv SU(3)_{q_L} \times SU(3)_{u_R} \times SU(3)_{d_R} \times SU(3)_{l_L} \times SU(3)_{e_R} \\ \mathcal{G}_F^{\rm A} &\equiv U(1)_B \times U(1)_L \times U(1)_Y \times U(1)_{PQ} \times U(1)_{e_R}\,. \end{aligned} \tag{4.1}$$

In the previous expressions, B and L refer to the Baryon and Lepton numbers, Y to the Hypercharge, PQ to the PQ symmetry, while the last Abelian symmetry factor corresponds to rotations on only the e_R fields.

As we discussed in Chapter 2, the Yukawa matrices must become now spurions, $\mathcal{Y}_i$, that transform under the non-Abelian part of the symmetry group. In previous work [108–111], it was shown that the non-Abelian symmetry $\mathcal{G}_F^{NA}$ can deal exclusively with the explanation of the inter-generation hierarchies, but is unable to predict the overall coefficients c_i. In this work, however, we will show how the ratios m_b/m_t and m_τ/m_t, i.e. c_b/c_t and c_τ/c_t in the previous expressions, can be elegantly explained following the philosophy of the FN models: we will impose one of the symmetries within $\mathcal{G}_F^A$ as a true symmetry of the Lagrangian, while its charges can be chosen such that the only renormalizable terms invariant under this Abelian factor are the ones of the up-type quarks, while those describing down-type quarks

and charged leptons are forbidden at dimension 4. These terms are written after rejecting renormalizability, by including a new field, the flavon Φ, that transforms under this Abelian factor, re-establishing the invariance under the symmetry.

The strategy of this work is to identify $U(1)_{PQ}$ as the symmetry that[6], among those in $\mathcal{G}_F^{\rm A}$, will explain the intra-generation hierarchies: Baryon and Lepton numbers and Hypercharge are fixed by definition, whereas $U(1)_{e_R}$ could only explain the ratio m_τ/m_t. Though we could use two symmetries, in a sort of double FN mechanism, this would require two different flavons. However, we will remain as minimal as possible, use only $U(1)_{PQ}$ as a symmetry respected by the Lagrangian, since all fermions can be charged under that symmetry and explain the top-bottom and top-tau mass ratios.

Let us write the more generic Yukawa Lagrangian allowed by the PQ symmetry, without considering first any specific charge assignment.

$$\begin{aligned}\mathscr{L}_Y = &-\left(\frac{\Phi}{\Lambda_\Phi}\right)^{x_u-x_q}\bar{q}_L\widetilde{H}\mathcal{Y}_u u_R-\left(\frac{\Phi}{\Lambda_\Phi}\right)^{x_d-x_q}\bar{q}_L H\mathcal{Y}_d d_R+\\ &-\left(\frac{\Phi}{\Lambda_\Phi}\right)^{x_e-x_l}\bar{l}_L H\mathcal{Y}_e e_R\,,\end{aligned} \tag{4.2}$$

where x_i are the PQ charges of the $i=u,d,l$ field[7] and, without loss of generality, the charge of the flavon Φ has been fixed to -1.

The known Yukawa matrices are recovered after the flavon takes a VEV $\langle\Phi\rangle=\frac{v_\Phi}{\sqrt{2}}$ and the Yukawa spurions get their background values.

$$\begin{gathered}Y_u=\varepsilon^{x_u-x_q}\langle\mathcal{Y}_u\rangle\qquad Y_d=\varepsilon^{x_d-x_q}\langle\mathcal{Y}_d\rangle\\ Y_e=\varepsilon^{x_e-x_l}\langle\mathcal{Y}_u\rangle\,,\end{gathered} \tag{4.3}$$

$$\begin{gathered}\langle\mathcal{Y}_u\rangle=c_t V_{CKM}^\dagger\text{diag}\left(\frac{m_u}{m_t},\frac{m_c}{m_t},1\right),\quad \langle\mathcal{Y}_d\rangle=c_b\text{diag}\left(\frac{m_d}{m_b},\frac{m_s}{m_b},1\right),\\ \langle\mathcal{Y}_e\rangle=c_\tau\text{diag}\left(\frac{m_e}{m_\tau},\frac{m_\mu}{m_\tau},1\right),\end{gathered} \tag{4.4}$$

[6] In Ref. [112] was discussed a similar approach, with gauged non-Abelian symmetries and two distinct Abelian symmetries explain the ratio between the third family quark masses. However, the phenomenology and spectrum obtained there differs with respect to the one discussed in Refs. [20, 23] and here.

[7] The mixed use of a PQ flavon Φ and of the Yukawa spurions $\mathcal{Y}_i$ may be puzzling. Indeed, at this level of the discussion, it is equivalent introducing a dynamical flavon Φ or treating its effects via a PQ spurion (see Ref. [60] for the latter case). Similarly, the Yukawa spurions may be promoted to be dynamical fields (see Refs. [108–111]). The discussion that follows and the results presented in this section are not affected by this choice. Instead, the necessity to describe the breaking of the PQ symmetry through a dynamical flavon resides in the origin of the MFV axion, as it will be explained in the Sect. 4.2.

where $\varepsilon \equiv v_\Phi/\sqrt{2}\Lambda_\Phi$ and we have reminded there the spurions background value as written in Chapter 2.

From here, we can read the ratios of the third-generation fermions in terms of the parameter ε and the PQ charges:

$$\begin{aligned} m_b/m_t &\simeq \varepsilon^{x_d - x_u} \\ m_\tau/m_t &\simeq \varepsilon^{x_e - x_l - x_u + x_q}\,, \end{aligned} \tag{4.5}$$

where we have neglected the ratios of the c_i parameters since they are all expected to be $\mathcal{O}(1)$.

Considering the value of the top mass is given by Eqs. 4.2, 4.3 and 4.4 to be $c_t \varepsilon^{x_u - x_q} \frac{v}{\sqrt{2}}$, while the measured value is roughly $\frac{v}{\sqrt{2}}$, we can see that $c_t \simeq 1$ and therefore no power of ε should appear in the top Yukawa. The simplest choice of charges for this to happen is the following:

$$x_q = x_u = 0 \tag{4.6}$$

for the quark doublets and up-quark singlets PQ charges. Consequently, we can find the remaining charges by imposing that the ε suppression accounts for the mass ratios of the fermions in the third generation.

$$\begin{aligned} x_d &\simeq \log_\epsilon(m_b/m_t) \\ x_e - x_l &\simeq \log_\epsilon(m_\tau/m_t) \end{aligned} \tag{4.7}$$

where ε is still unknown, and its value depends on the specific ultraviolet theory that gives rise to the low-energy Lagrangian in Eq. 4.2. Considering that it should remain a perturbative parameter, and that the value of v_Φ is not expected to be so much smaller than Λ_Φ (without a dynamical mechanism to explain it), we will take ε in the range $[0.01,\ 0.3]$, consistent previous FN models [48, 49]. The logarithm in Eq. 4.7 relaxes the dependence on the exact value of ε: for ε inside its preferred interval, x_d and $x_e - x_l$ must be in the interval $[1,\ 4]$.

In order to give a benchmark that we can use in the phenomenological analysis, let us consider the parameter to be order the Cabibbo angle, i.e. $\varepsilon \sim 0.23$, which translates in the following charges for down quarks and charged leptons:

$$x_d = 3 \quad x_e - x_l = 3. \tag{4.8}$$

The charges x_e and x_l cannot be specifically determined beyond their difference exclusively using charged lepton masses and quark mixings. However, by looking at the neutrino sector we can find an additional condition: the PQ invariance of the Weinberg operator implies that this operator is written with $2x_l$ insertions of the flavon Φ,

$$\mathscr{L}_5 = \left(\frac{\Phi}{\Lambda_\Phi}\right)^{2x_l} \times \frac{\left(\overline{l_L^c}\widetilde{H}^*\right)\mathcal{G}_\nu\left(\widetilde{H}^\dagger l_L\right)}{\Lambda_L}\,, \tag{4.9}$$

where Λ_L is the scale of lepton number violation and $\mathcal{G}_\nu$ is the spurion field described in Chapter 2, whose background value $\langle\,\mathcal{G}_\nu\rangle \equiv g_\nu$ contains the information of the neutrino mass eigenvalues and the PMNS mixing matrix (see Ref. [58, 66] for details). Considering that the eigenvalues of g_ν are not larger than 1 to ensure perturbativity (as for c_i in Eq. 4.4), an upper bound on Λ_L can be identified:

$$\Lambda_L \simeq \frac{v^2}{2}\frac{g_\nu\,\epsilon^{2x_l}}{\sqrt{\Delta m^2_{\text{atm}}}} \lesssim 6\times 10^{14}\ \text{GeV}\times\epsilon^{2x_l}\,, \tag{4.10}$$

where Δm^2_{atm} is the atmospheric neutrino mass squared difference.

In Ref. [66] (see Fig. 1) it is shown that, for $x_l = 0$, there is some parameter space for this model probed by the current data on the $\mu \to e$ conversion in golden nuclei. Additionally, one can easily see that for $x_l = 2$ and $\epsilon = 0.23$ there is essentially no parameter space accessible by current experiments or prospects in the near future. Considering this constraint, and in order to maintain some predictability, we will consider only $x_l = 0$ and $x_l = 1$ in the phenomenological analysis that follows. Summarising, two scenarios will be studied[8]:

$$\begin{aligned} &\text{S0:} \quad x_q = 0 = x_u = x_l\,, \qquad\qquad x_d = 3 = x_e, \\ &\text{S1:} \quad x_q = 0 = x_u\,, \quad x_l = 1\,, \quad x_d = 3\,, \quad x_e = 4\,. \end{aligned} \tag{4.11}$$

[8]The stability of a generic choice for these charges under the renormalisation group evolution has been discussed in Ref. [113], specially considering the impact on axion couplings, which will be the subject of the next section. These effects could be relevant if the axion scale f_a is relatively small, while for the values considered here they can be neglected.

4.2 The MFV Axion

Once all the symmetries and charges at play in our model have been established, we are in condition to study the origin of the axion. Considering the flavon to be a complex scalar field, once it acquires a VEV it can be written in the following way:

$$\Phi = \frac{\rho + v_\Phi}{\sqrt{2}} e^{ia/v_\Phi} \,, \tag{4.12}$$

where ρ is the radial component and a, which is identified as the axion, is the the angular one.

The full scalar potential of the model presents three distinct parts:

$$V\left(H,\Phi\right) = -\mu^2|H|^2 + \lambda|H|^4 - \mu_\Phi^2|\Phi|^2 + \lambda_\Phi|\Phi|^4 + \lambda_{H\Phi}|H|^2|\Phi|^2 \,. \tag{4.13}$$

In a part of the parameter space, the pure Φ-dependent scalar potential has a minimum corresponding to a non-vanishing VEV for Φ, $v_\Phi^2 = \mu_\Phi^2/\lambda_\Phi$.

If v_Φ is much larger than the EW scale, this may represent a problem for the EW symmetry breaking (EWSB) mechanism: indeed the quartic $|H|^2|\Phi|^2$ coupling would contribute to the quadratic term of the pure H-dependent potential,

$$\mu^2 \to \mu'^2 \equiv \mu^2 - \lambda_{H\Phi} v_\Phi^2 \,. \tag{4.14}$$

If no *ad hoc* cancellation between these two terms is invoked and for arbitrary values of $\lambda_{H\Phi}$, the new mass parameter μ' resides at the same, large scale of v_Φ. In order to reproduce the expected value of the EW VEV, $v \equiv 245$ GeV fixed through the W gauge boson mass, it is then necessary to require a large value of the Higgs quartic coupling λ, describing in this way a strongly interacting scenario with a non-linearly realised EWSB mechanism. This is an intriguing possibility, especially considering the recent interest in non-SM descriptions of the Higgs sector, such as composite Higgs models [114–122], dilaton models [123–130], or general effective Lagrangians [55, 131–147].

On the other side, if v_Φ is close to the EW scale, then no tuning is required and the EWSB mechanism would work as in the SM (see for example Refs. [148, 149]). In the phenomenological section, both the cases will be discussed.

Through this chapter, v_Φ will be considered sufficiently large to consider the radial component ρ as a heavy degree of freedom: it can be safely integrated out from the low-energy Lagrangian, leaving the axion a as the only light degree of freedom remaining from Φ. The low-energy Lagrangian of the model can therefore be written as the sum of the following different terms:

$$\begin{aligned}\mathscr{L} =& \mathscr{L}_{Kin}^{\text{SM}} + \frac{1}{2}\,\partial_\mu a\,\partial^\mu a + \mu'^2|H|^2 - \lambda|H|^4 + \\ &- e^{i(x_u - x_q)a/v_\Phi}\overline{q}_L\widetilde{H}Y_u u_R - e^{i(x_d-x_q)a/v_\Phi}\overline{q}_L H Y_d d_R + \\ &- e^{i(x_e-x_l)a/v_\Phi}\overline{l}_L H Y_e e_R + c_\nu^{(5)} e^{2i\,x_l\,a/v_\Phi}\left(\overline{l_L^c}\widetilde{H}^*\right)\left(\widetilde{H}^\dagger l_L\right) \\ &+ \theta_{QCD}\frac{\alpha_s}{8\pi}G^{a\mu\nu}\widetilde{G}^a_{\mu\nu}\,.\end{aligned} \tag{4.15}$$

where

$$c_\nu^{(5)} \equiv \epsilon^{2x_l}\frac{\langle \mathscr{I}_\nu\rangle}{\Lambda_L} = -\frac{2}{v^2}m_\nu\,. \tag{4.16}$$

Some comments are in order. The Yukawa matrices are the ones defined in Eq. 4.3, with $c_\nu^{(5)}$ is the coefficient of the Weinbeng operator and m_ν is the neutrino mass matrix in the flavour basis. The specific choice of the PQ charges in Eq. 4.11 has not been implemented yet, to keep the discussion general for now.

It is straightforward to rewrite the Lagrangian in the basis where the axion-fermion couplings are derivative. The resulting Lagrangian consists of the SM Lagrangian modified by the addition of interactions with the axion that read

$$\delta\mathscr{L} = \frac{1}{2}\,\partial_\mu a\,\partial^\mu a - c_{a\psi}\frac{\partial_\mu a}{2v_\Phi}\overline{\psi}\gamma^\mu\gamma_5\psi - M_\nu e^{2i\,x_l\,a/v_\Phi}\overline{\nu_L^c}\nu_L\,, \tag{4.17}$$

where $\psi = \{u,\, d,\, e\}$ and the coefficients are

$$\begin{aligned} c_{au} &= x_q - x_u \\ c_{ad} &= x_q - x_d \\ c_{ae} &= x_l - x_e\,. \end{aligned} \tag{4.18}$$

At the quantum level, the derivative of the axial current is non-vanishing as we showed in Chapter 3, giving rise to the following effective axion-gauge boson couplings: in the physics

basis for the gauge bosons

$$\begin{aligned}\delta\mathscr{L}_{\text{eff}} \supset & -\frac{\alpha_s}{8\pi}\, c_{agg}\frac{a}{v_\Phi} G^{a\mu\nu}\widetilde{G}^a_{\mu\nu} - \frac{\alpha_{em}}{8\pi}\, c_{a\gamma\gamma}\frac{a}{v_\Phi} F^{\mu\nu}\widetilde{F}_{\mu\nu} + \\ & -\frac{\alpha_{em}}{8\pi}\, c_{aZZ}\frac{a}{v_\Phi} Z^{\mu\nu}\widetilde{Z}_{\mu\nu} - \frac{\alpha_{em}}{8\pi}\, c_{a\gamma Z}\frac{a}{v_\Phi} F^{\mu\nu}\widetilde{Z}_{\mu\nu} + \\ & -\frac{\alpha_{em}}{8\pi}\, c_{aWW}\frac{a}{v_\Phi} W^{+\mu\nu}\widetilde{W}^-_{\mu\nu}\,,\end{aligned} \tag{4.19}$$

where $X_{\mu\nu} = \partial_\mu X_\nu - \partial_\nu X_\mu$ for $F_{\mu\nu}$, $Z_{\mu\nu}$ and $W_{\mu\nu}$, and $G^a_{\mu\nu} = \partial_\mu G^a_\nu - \partial_\nu G^a_\mu + g_s f^{abc} G^b_\mu G^c_\nu$, and the coefficients have the following expressions:

$$\begin{aligned} c_{agg} &= 3(c_{au} + c_{ad}), \quad c_{aWW} = \frac{3}{2s^2_\theta}\left(3\left(c_{au} + c_{ad}\right) + c_{ae}\right), \\ c_{aZZ} &= \frac{t^2_\theta}{4}\left(17c_{au} + 5c_{ad} + 15c_{ae}\right) + \frac{3}{4t^2_\theta}\left(3(c_{au} + c_{ad}) + c_{ae}\right), \\ c_{a\gamma Z} &= \frac{t_\theta}{4}\left(17c_{au} + 5c_{ad} + 15c_{ae}\right) - \frac{3}{4t_\theta}\left(3(c_{au} + c_{ad}) + c_{ae}\right), \\ c_{a\gamma\gamma} &= 2(4c_{au} + c_{ad} + 3c_{ae}), \end{aligned} \tag{4.20}$$

with, for the sake of notation simplicity, $t_\theta \equiv \tan\theta_W$, $s_\theta \equiv \sin\theta_W$ and $s_{2\theta} \equiv \sin 2\theta_W$, being θ_W the Weinberg angle. The coefficients of the anomalous terms contain the contributions from all the fermions with a non-vanishing PQ charge.

The MFV axion solves the Strong CP problem in exactly the same way as the traditional QCD axion: the θ_{QCD} parameter can be absorbed by a shift transformation of the axion. The only condition that must be satisfied is that $c_{agg} \neq 0$, which is consistent with Eq. 4.11, that explains the top Yukawa coupling of order 1 and the smallness of the bottom mass with respect to the top mass.

Table 4.1 reports the values of the c_{ai} coefficients of the axion couplings to fermions and gauge field strengths in the physical basis for the two scenarios described in Eq. 4.11. As the coefficients in Eq. 4.20 depend only on charge differences, the values for the anomaly couplings are the same values for both the scenarios. Of particular interest is that the ratio between the axion coupling to photons and that to gluons, which is typically a free parameter [150–155], is exactly fixed to $8/3$, as in the original DFSZ invisible axion model.

	x_l	x_e	c_{au}	c_{ad}	c_{ae}	c_{agg}	$c_{a\gamma\gamma}$	c_{aZZ}	$c_{a\gamma Z}$	c_{aWW}
$S0$	0	3	0	-3	-3	-9	-24	-35.8	8.8	-81
$S1$	1	4	0	-3	-3	-9	-24	-35.8	8.8	-81

TABLE 4.1: Values of the coefficients of the axion couplings to fermions and gauge boson field strengths in the physical basis for the two scenarios identified in Eq. 4.11, where the normalisation is defined in Eqs. (4.17) and (4.19).

Notice that the common notation adopted in the literature makes use of effective couplings that can be expressed in terms of the c_{ai} coefficients as follows:

$$\begin{aligned} g_{agg} &\equiv \frac{\alpha_s}{2\pi}\frac{c_{agg}}{v_\Phi} \equiv \frac{\alpha_s}{2\pi}\frac{1}{f_a} \\ g_{ai} &\equiv \frac{\alpha_{\rm em}}{2\pi}\frac{c_{ai}}{v_\Phi} = \frac{\alpha_{\rm em}}{2\pi}\frac{c_{ai}}{c_{agg}}\frac{1}{f_a}\,, \end{aligned} \tag{4.21}$$

where $i = \{\gamma\gamma,\, ZZ,\, \gamma Z,\, WW\}$ and the traditional notation for the axion decay constant f_a has been introduced. In the QCD axion case, where it is light, a mixing with the η and π^0 mesons arises below the QCD phase transition. This modifies the axion-photon coupling at low energies, that can be redefined as follows [88, 156–159]

$$g_{a\gamma\gamma} \equiv \frac{\alpha_{\rm em}}{2\pi}\frac{1}{f_a}\Big(c_{a\gamma\gamma} - 1.92(4)\Big)\,. \tag{4.22}$$

4.3 Phenomenological Features

In this section we will study the phenomenology of this Minimal Flavour Violating Axion, starting with a review of the bounds on axion couplings to fermions and gauge bosons, identifying the most relevant ones for our case, then we will proceed with a discussion regarding its mass and conclude with a comparative analysis considering the Axiflavon as a benchmark for other flavoured axion model.

Several studies have been performed to constrain the axion couplings to SM fermions and gauge bosons [160–185]. Two recent summaries can be found in Refs. [186, 187]. These bounds strongly depend on the axion mass, that also determines its decay length. The main results will be reported in this section, translating the distinct constraints into limits on the axion scale f_a.

Coupling to photons:

Astrophysical, cosmological and low-energy terrestrial data provides the strongest bounds on the axion coupling to photons (the latest constraints have been recently published in Ref. [184]): the upper bounds on the effective couplings can be summed up as [186, 187]

$$\begin{aligned}
|g_{a\gamma\gamma}| &\lesssim 7\times10^{-11}\ \text{GeV}^{-1} && \text{for} && m_a \lesssim 10\ \text{meV},\\
|g_{a\gamma\gamma}| &\lesssim 10^{-10}\ \text{GeV}^{-1} && \text{for} && 10\ \text{meV} \lesssim m_a \lesssim 10\ \text{eV},\\
|g_{a\gamma\gamma}| &\ll 10^{-12}\ \text{GeV}^{-1} && \text{for} && 10\ \text{eV} \lesssim m_a \lesssim 0.1\ \text{GeV},\\
|g_{a\gamma\gamma}| &\lesssim 10^{-3}\ \text{GeV}^{-1} && \text{for} && 0.1\ \text{GeV} \lesssim m_a \lesssim 1\ \text{TeV}\,.
\end{aligned} \tag{4.23}$$

Notice that the bounds for masses between 10 eV and 0.1 GeV, which include the so-called MeV window, come from (model dependent) cosmological data [176]. On the other side, for masses larger than the TeV, no constraint is present. Finally, for the mass range $0.1\ \text{GeV} \lesssim m_a \lesssim 1\ \text{TeV}$, the bounds may be improved by two order of magnitudes with dedicated analyses on BaBar data and at Belle-II [174, 181, 185].

These bounds can be translated in terms of f_a through Eq. 4.21: taking $\alpha_{\text{em}} = 1/137.036$,

$$\begin{aligned}
f_a &\gtrsim 1.2\times10^{7}\ \text{GeV} && \text{for} && m_a \lesssim 10\ \text{meV},\\
f_a &\gtrsim 8.7\times10^{6}\ \text{GeV} && \text{for} && 10\ \text{meV} \lesssim m_a \lesssim 10\ \text{eV},\\
f_a &\gg 8.7\times10^{8}\ \text{GeV} && \text{for} && 10\ \text{eV} \lesssim m_a \lesssim 0.1\ \text{GeV},\\
f_a &\gtrsim 3\ \text{GeV} && \text{for} && 0.1\ \text{GeV} \lesssim m_a \lesssim 1\ \text{TeV}\,.
\end{aligned} \tag{4.24}$$

The first three bounds take into account the effects of the axion mixing with the π^0 [159].

Coupling to gluons:

Collider mono-jet searches [173, 174, 178, 182] and axion-pion mixing effects [160, 162] allows to extract bounds on the axion couplings with gluons:

$$\begin{aligned}
|g_{agg}| &\lesssim 1.1\times10^{-5}\ \text{GeV}^{-1} && \text{for} && m_a \lesssim 60\ \text{MeV},\\
|g_{agg}| &\lesssim 10^{-4}\ \text{GeV}^{-1} && \text{for} && 60\ \text{MeV} \lesssim m_a \lesssim 0.1\ \text{GeV},
\end{aligned} \tag{4.25}$$

that can be translated into constraints on f_a,

$$\begin{aligned} f_a &\gtrsim 1.7 \times 10^3 \text{ GeV} \quad \text{for} \quad m_a \lesssim 60 \text{ MeV}, \\ f_a &\gtrsim 188 \text{ GeV} \quad \text{for} \quad 60 \text{ MeV} \lesssim m_a \lesssim 0.1 \text{ GeV}, \end{aligned} \tag{4.26}$$

taking $\alpha_s(M_Z^2) = 0.1184$.

Couplings to massive gauge bosons (collider):

Considering LHC data with $\sqrt{s} = 13$ TeV, dedicated analyses on Mono-W ($pp \to aW(W \to \mu\nu_\mu)$) and mono-$Z$ ($pp \to aZ(Z \to ee)$) channels put bounds on axion couplings to two W's and to two Z's: for $0.1 \lesssim m_a \lesssim 1$ GeV [182],

$$\begin{aligned} |g_{aWW}| &\lesssim 1.6 \times 10^{-3} \text{ GeV}^{-1}, \\ |g_{aZZ}| &\lesssim 8 \times 10^{-4} \text{ GeV}^{-1}. \end{aligned} \tag{4.27}$$

A complementary analysis on LEP data [188, 189] on the radiative Z decays leads to a bound on the $a\gamma Z$ coupling [185]:

$$|g_{a\gamma Z}| \lesssim 6.4 \times 10^{-5} \text{ GeV}^{-1}. \tag{4.28}$$

For both $S0$ and $S1$ scenarios, these bounds on the effective couplings translate into the following constraints on f_a:

$$\begin{aligned} (aWW) \qquad & f_a \gtrsim 6.4 \text{ GeV}, \\ (aZZ) \qquad & f_a \gtrsim 5.7 \text{ GeV}, \\ (aZ\gamma) \qquad & f_a \gtrsim 17.8 \text{ GeV}. \end{aligned} \tag{4.29}$$

The previous bounds hold for an axion that escapes the detector and therefore is considered as missing energy in the data analysis. If instead the axion mass is sufficiently large and/or its characteristic scale f_a is sufficiently low, the axion may decay within the detector and the previous limits cannot be taken into consideration.

Considering the possibility of an axion decaying into two photons, that is typically the dominant channel, LEP data [188, 189] on the decay $Z \to 3\gamma$ has been used to constrain axion couplings with the axion decaying inside the detector. A bound on $a\gamma Z$ coupling follows from

Ref. [185]: assuming that a decays only into two photons,

$$|g_{a\gamma Z}| \lesssim 6 \times 10^{-4}\ \text{GeV}^{-1}\,, \tag{4.30}$$

for axion masses in the interval $m_{\pi^0} \lesssim m_a \lesssim 10$ GeV and

$$|g_{a\gamma Z}| \lesssim 2 \times 10^{-4}\ \text{GeV}^{-1}\,, \tag{4.31}$$

for $10\ \text{GeV} \lesssim m_a \lesssim 91.2$ GeV. Considering explicitly the values for the axion couplings, the corresponding limit on f_a reads

$$\begin{aligned} f_a &\gtrsim 1.8\ \text{GeV} \qquad \text{for} \qquad m_{\pi^0} \lesssim m_a \lesssim 10\ \text{GeV}, \\ f_a &\gtrsim 5.3\ \text{GeV} \qquad \text{for} \quad 10\ \text{GeV} \lesssim m_a \lesssim 91.2\ \text{GeV}\,. \end{aligned} \tag{4.32}$$

A dedicated analysis with LHC data on the same observable may improve these bounds by one order of magnitude [186].

Couplings to fermions and W's (flavour):

Studies on Compton scattering of axions in the Sun, axionic recombination and de-excitation in ions and axion bremsstrahlung [168] set very strong bounds on axion couplings to electrons for masses below ~ 80 keV. Similar constraints are inferred from Compton conversion of solar axions [165] for masses up to ~ 10 MeV. Considering these, the following bound on the axion-electron coupling is found:

$$\frac{c_{ae}}{c_{agg} f_a} \lesssim 5.2 \times 10^{-8}\ \text{GeV}^{-1} \quad \text{for} \quad 1\ \text{eV} \lesssim m_a \lesssim 10\ \text{MeV}\,. \tag{4.33}$$

Even more stringent limits arise from observation of Red Giants [170, 190, 191], but for a smaller range of masses:

$$\frac{c_{ae}}{c_{agg} f_a} \lesssim 8.6 \times 10^{-10}\ \text{GeV}^{-1} \quad \text{for} \quad m_a \lesssim 1\ \text{eV}\,. \tag{4.34}$$

When considering the explicit value of the c_{ae} coefficient, which is the same for the two PQ charge scenarios, these constraints translate into bounds on the axion scale:

$$\begin{aligned} f_a &\gtrsim 3.9 \times 10^8 \text{ GeV} \quad \text{for} \quad m_a \lesssim 1 \text{ eV}, \\ f_a &\gtrsim 6.4 \times 10^6 \text{ GeV} \quad \text{for} \quad 1 \text{ eV} \lesssim m_a \lesssim 10 \text{ MeV}. \end{aligned} \tag{4.35}$$

Rare meson decays provide strong constraints of axion couplings to quarks and to two W gauge bosons. For masses below ~ 0.2 GeV, the most relevant observable is $K^+ \to \pi^+ a(a \to \text{inv.})$, whose branching ratio is limited to be [164]:

$$\mathcal{B}_{K^+ \to \pi^+ a(a \to \text{inv.})} < 7.3 \times 10^{-11}. \tag{4.36}$$

For larger masses up to a few GeVs, the $B^+ \to K^+ a(a \to \text{inv.})$ decay provides the most stringent bound [167]:

$$\mathcal{B}_{B^+ \to K^+ a(a \to \text{inv.})} < 3.2 \times 10^{-5}. \tag{4.37}$$

As the axion does not couple to up-type quarks ($c_{au} = 0$), the two decays $K^+ \to \pi^+ a$ and $B^+ \to K^+ a$ can only occur at 1-loop level with the axion arising from the interaction with the internal W propagator. The constraints that can be inferred on g_{aWW} reads [181]:

$$\begin{aligned} |g_{aWW}| &\lesssim 3 \times 10^{-6} \text{ GeV}^{-1} \quad \text{for} \quad m_a \lesssim 0.2 \text{ GeV}, \\ |g_{aWW}| &\lesssim 10^{-4} \text{ GeV}^{-1} \quad \text{for} \quad 0.2 \text{ GeV} \lesssim m_a \lesssim 5 \text{ GeV}, \end{aligned} \tag{4.38}$$

that can be translated in terms of f_a expliciting the value of c_{aWW},

$$\begin{aligned} f_a &\gtrsim 3.5 \times 10^3 \text{ GeV} \quad \text{for} \quad m_a \lesssim 0.2 \text{ GeV} \\ f_a &\gtrsim 105 \text{ GeV} \quad \text{for} \quad 0.2 \text{ GeV} \lesssim m_a \lesssim 5 \text{ GeV}. \end{aligned} \tag{4.39}$$

Focussing now on processes that receive 1-loop contributions with down-type quark in the internal lines, such as D-meson hadronic decays, no interesting bound can be extracted. The $D^+ \to \pi^+ a(a \to \text{inv.})$ and $D_s^+ \to K^+ a(a \to \text{inv.})$ decays are proportional to a combination of c_{ad} and c_{aWW}. However, for $f_a \gtrsim 105$ GeV as identified above, the branching ratios of these processes are smaller than 10^{-12}, impossible to probe experimentally in the near future.

Finally, a recent bound from $\Upsilon \to a\gamma$ has been extracted considering bounds from BaBar and Belle [192–194]. Considering that $g_{a\gamma\gamma} \ll c_{ad}$, a bound on c_{ad}/f_a can be extracted as reported in Ref. [195]:

$$\frac{c_{ad}}{c_{agg} f_a} \lesssim 4 \times 10^{-4}\ \text{GeV}^{-1}\,, \tag{4.40}$$

for an axion of $m_a = \mathcal{O}(1)$ GeV. This limit can be translated in terms of f_a as

$$f_a \gtrsim 830\ \text{GeV}\,. \tag{4.41}$$

The previous bounds are valid only for a stable axion at detector size. If instead the axion further decays, present data from $b \to sg$ or $b \to sq\bar{q}$ from CLEO collaboration [196] allows to put a bound on axion couplings to b quarks:

$$\frac{c_{ad}}{c_{agg} f_a} \lesssim 5 \times 10^{-4}\ \text{GeV}^{-1}\,, \tag{4.42}$$

for $0.4 \lesssim m_a \lesssim 4.8$ GeV. This constraint translates into a bound on f_a that reads

$$f_a \gtrsim 667\ \text{GeV}\,. \tag{4.43}$$

Similar bounds can be inferred with a future analysis on $B^\pm \to K^\pm a(\to 2\gamma)$ at Belle-II [181]. In the case the branching ratio for this observables is measured at the level of 10^{-6}, values of f_a as large as 550 GeV in the aWW coupling could be tested.

Axion flavor conserving couplings to third generation quarks:

Stellar cooling data imply bounds on axion couplings to top and bottom quarks [197]. In general, this constraint applies on the effective axion coupling with electrons, which is the sum between the tree-level coupling with electrons and the loop-induced contributions proportional to the axion couplings with any other fermion. Under the assumption that only one coupling is non-vanishing at a time, and in particular the tree level coupling with electrons is zero, then

$$\frac{c_{agg} f_a}{c_t} \gtrsim 1.2 \times 10^9\ \text{GeV} \qquad\qquad \frac{c_{agg} f_a}{c_b} \gtrsim 6.1 \times 10^5\ \text{GeV}\,, \tag{4.44}$$

for axion masses in the range $m_a \lesssim 10$ keV. Since our model has vanishing coupling to up-quaks, we can only extract a limit from the bound on the bottom coupling, which translates

to:

$$f_a \gtrsim 2 \times 10^5 \text{ GeV}\,. \tag{4.45}$$

Axion couplings to nucleons:

Neutron star and Supernova 1987A cooling data provide bounds on axion coupling with neutrons and nuclei. The physical process consists in the neutron or nucleus bremsstrahlung, respectively, and the corresponding bounds read

$$\frac{c_{agg} f_a}{c_{an}} \gtrsim 1.21 \times 10^9 \text{ GeV [198, 199]} \qquad \frac{c_{agg} f_a}{\sqrt{c_{ap}^2 + c_{an}^2}} \gtrsim 1.67 \times 10^9 \text{ GeV [200, 201]}\,, \tag{4.46}$$

$$\frac{c_{agg} f_a}{\sqrt{c_{ap}^2 + 0.61 c_{an}^2 + 0.53 c_{ap} c_{an}}} \gtrsim 1.03 \times 10^9 \text{ GeV [202]}\,, \tag{4.47}$$

where c_{an} and c_{ap} stand for the effective coupling of axion to neutrons and protons and are expressed in terms of the axion-quark couplings as follows:

$$\begin{aligned} c_{an} &= -0.02 c_{agg} + 0.88 c_d - 0.39 c_u - 0.038 c_s - 0.012 c_c - 0.009 c_b - 0.0035 c_t, \\ c_{ap} &= -0.47 c_{agg} + 0.88 c_u - 0.39 c_d - 0.038 c_s - 0.012 c_c - 0.009 c_b - 0.0035 c_t. \end{aligned} \tag{4.48}$$

The first terms refer to the axion coupling to gluons, while the others to the corresponding axion-fermion couplings. These bounds are rather strong, but should be taken with caution: from one side they are model dependent and from the other hold under the current knowledge of the complicated Supernova physics and neutron stars. In our model, these bounds translate respectively into

$$f_a \gtrsim 3.12 \times 10^8 \text{ GeV}, \qquad f_a \gtrsim 1.15 \times 10^9 \text{ GeV}\,, \tag{4.49}$$

$$f_a \gtrsim 6.23 \times 10^8 \text{ GeV}\,. \tag{4.50}$$

Axion flavor violating couplings to third generation quarks:

While our model is flavour conserving and these bounds do not apply, it is interesting to review the limits set on flavour-violating axion couplings for the sake of completeness. These couplings are strongly constrained from processes like rare decays or meson oscillations. An example of these processes are $B^+ \to \pi^+ a$ decay and $B^0 - \bar{B}^0$ oscillations, from where a bound

can be obtained on the vector and axial axion coupling, respectively, to bottom and down quarks [203–205]:

$$\frac{c_{agg} f_a}{c^V_{bd}} > 1.1 \times 10^8 \text{ GeV} \qquad \frac{c_{agg} f_a}{c^A_{bd}} > 2.6 \times 10^6 \text{ GeV}. \tag{4.51}$$

Analogously, from the processes $B^{+,0} \to K^{+,0} a$ and $B^{+,0} \to K^{*+,0} a$ bounds on the vector and axial couplings to bottom and strange quarks can be obtained [167]:

$$\frac{c_{agg} f_a}{c^V_{bs}} > 3.3 \times 10^8 \text{ GeV} \qquad \frac{c_{agg} f_a}{c^A_{bs}} > 1.3 \times 10^8 \text{ GeV}. \tag{4.52}$$

Bounds of flavor violating couplings involving the top quark are obtained in the same fashion as for the flavor conserving ones: considering the contribution at one loop to the process $K^+ \to \pi^+ a$ of a top-up and top-charm coupling it is possible to extract the following bounds [164]:

$$\frac{c_{agg} f_a}{c_{tu}} > 3 \times 10^8 \text{ GeV} \qquad \frac{c_{agg} f_a}{c_{tc}} > 7 \times 10^8 \text{ GeV}. \tag{4.53}$$

The axion mass and the ALP scenario:

Without an explicit soft breaking source of the shift symmetry, a mass term for the MFV axion may arise, as for the traditional QCD axion, from non-perturbative dynamics: the axion mixing with neutral mesons induces a contribution which is estimated to be [92, 206, 207]

$$m_a \sim 6 \, \mu\text{eV} \left(\frac{10^{12} \text{ GeV}}{f_a} \right) , \tag{4.54}$$

and not much larger than a few eV. Additional contributions may arise *à la* KSVZ axion in the presence of exotic fermions that couple to the axion. Exotic fermions are typically present when constructing the underlying theory originating the effective terms in Eq. 4.2 (see for example Ref. [208]) or are required from anomaly cancellation conditions in models with gauged flavour symmetries [20–24, 65, 104]: the largest mass contribution originated in these cases is of hundreds of eV, for values of the axion scale f_a close to the TeV. Even considering possible contributions of this kind, one can safely conclude that the MFV axion mass is smaller than the keV, unless explicit shift symmetry breaking sources are introduced in the scalar potential. For these mass values the strongest constraints arise from the axion coupling to photons, Eq. 4.24, and to electrons, Eq. 4.35: the axion scale is necessarily larger than $\sim 10^{10}$ GeV and $\sim 10^9$ GeV, preventing any possibility to detect the MFV axion at colliders or in flavour searches.

On the other side, if a signal of detection that may be interpreted in terms of an axion is seen, it may be compatible with the MFV axion at the price of invoking an explicit breaking of the shift symmetry (gravitational and/or Planck-scale effects [209–212] are examples of unavoidable explicit breaking sources, but the corresponding mass contributions are tiny): in this case, the relation between the axion mass and its scale gets broken and the bounds aforementioned may be avoided. In the common language, this eventuality is refereed to as Axion-like-particle (ALP) framework, that received much attention from the community in the last years.

In what follows, this last scenario will be considered, assuming a MFV axion mass much larger than the eV region. For masses of the order of the GeV, the stringent bounds from the $a\gamma\gamma$ and aee couplings are easily evaded, and the next most sensitive observables are those from collider and flavour. For even larger masses, no bounds at all exist at present.

By increasing the axion mass and/or lowering the scale f_a, however, its decay length decreases, and the axion may decay within the detector: in this case, some of the previous listed bounds cannot apply anymore. The distance travelled by an axion after being produced can be expressed in the following way [182]:

$$d \approx \frac{10^4}{c_{ai}^2} \left(\frac{\text{MeV}}{m_a}\right)^4 \left(\frac{f_a}{\text{GeV}}\right)^2 \left(\frac{|p_a|}{\text{GeV}}\right) \text{ m}\,, \tag{4.55}$$

where the typical momentum considered is of 100 GeV. Selecting a benchmark region with $m_a \simeq 1$ GeV and $f_a = 1$ TeV, the axion may decay into two photons, two gluons, or two light fermions. Once considering the values for c_{ai} as reported in Tab. 4.1, the dominant channel is the radiative one (see i.e. Ref. [187] for the relevant expressions of the axion decays). The decay length for this benchmark axion turns out to be slightly larger than 1 mm. The most sensitive observables to the this ALP is $b \to sg$ from CLEO collaboration and $Z \to 3\gamma$ from LEP and LHC experiments: indeed, these processes are sensitive to values of f_a up to ~ 1 TeV.

Comparison with the Axiflavon:

The Axiflavon [105, 106] is the axion arising in the context of the FN mechanism and has flavour violating couplings, in the mass basis for fermions, predicted in terms of the FN charges, up to $\mathcal{O}(1)$ uncertainties. This represents a major difference with respect to the MFV axion: the presence of flavour violating couplings induces tree-level flavour changing neutral

current processes, such as the meson decays described in the previous section. To satisfy the present bounds on K and B decays, the axion scale f_a needs to be of the order of 10^{10} GeV [106], that approximatively coincides with the values necessary to pass the very strong bounds on the $a\gamma\gamma$ and aee couplings. The Axiflavon is therefore an example of visible QCD axion, as it predicts low-energy flavour effects, despite the very large value of the axion scale f_a. On the other side, no signals are expected at colliders, as indeed effects in mono-W and mono-Z channels, and in the Z boson width are expected to be tiny and not appreciable neither in the future phases of LHC nor in next generation of linear/circular colliders. A final comment that helps distinguishing between the MFV axion and the Axiflavon is the prediction for the ratio between the axion coupling to photons and that to gluons: in the first model this ratio is strictly predicted to be $8/3$, while in the second one it may vary within the range $[2.4,\ 3]$.

In this chapter we have presented a model with an axion, that solves the Strong CP Problem as the usual QCD axion, which has flavour non-universal but conserving couplings to SM fermions. This axion arose as the consequence of a PQ symmetry embedded in the MFV symmetry group, with the mass ratio of the third generation fermions explained via this Abelian symmetry while the MFV framework protects the model from the BSM flavour problem.

In the case this MFVA is a QCD axion, its main phenomenology coincides with that of invisible axions: astrophysical and cosmological observables give interesting limits on the axion coupling to photons and electrons. If, on the other hand, an explicit breaking of the axion shift symmetry is considered, we would be talking about a Minimal Flavour Violating ALP, that may result in relevant phenomenology at colliders and flavour searches.

Though this model deals with the Strong CP Problem and (part of) the quark flavour puzzle in a very minimal and natural way, the lightness of neutrino masses is not discussed here. In the next chapter based on the publication from Ref. [213], however, we will show a model with a Majoron, also embedded in the MFV scheme ad therefore compatible with the axion shown in this chapter, that not only provides a dynamical explanation for the light neutrino masses and helps alleviating the interesting cosmological anomaly related to the Hubble parameter.

Chapter 5

A MFV Majoron: Neutrino masses and the H_0 tension

There is nowadays a considerable tension between late-time, local probes of the present rate of expansion of the Universe, that is the Hubble constant H_0, and its value inferred through the standard cosmological model ΛCDM from early Universe observations. Local measurements, from type-Ia supernovae and strong lensing, tend to cluster at similar values of H_0, significantly larger than those preferred by cosmic microwave background (CMB) and baryon acoustic oscillations probes. The strongest tension, estimated at the level of $4-6\,\sigma$ [214, 215] depending on the assumptions performed, is between the `Planck` inferred measure from the CMB spectrum [13] and the one obtained by the SH_0ES collaboration [216] from supernovae measurements.

Although the solution to this discrepancy might be related to systematics in the measurements (notably the callibration of the supernovae distances) or, more interestingly, point to a modification of the cosmological model, it may instead be provided by particle physics, as already discussed in the literature (see for example [217–230]). In particular, Ref. [226] suggests that a Majoron that couples to light neutrinos could reduce the tension in the determination of H_0. It is then interesting to investigate whether this setup is compatible with possible explanations of other open problems in the Standard Model of particle physics (SM): the focus of this paper is to study the compatibility with Type-I Seesaw mechanism to explain the lightness of the active neutrinos, with specific flavour symmetries to describe the flavour puzzle and with the presence of an axion to solve the Strong CP problem.

The Majoron, called ω hereafter, is the Nambu-Goldstone boson (NGB) associated to the spontaneous breaking of lepton number (LN) [231–234], which is only accidental within the SM and breaks down at the quantum level. It naturally arises in the context of the Type-I Seesaw mechanism, where the Majorana mass term, instead of being a simple bilinear of the right-handed (RH) neutrino fields N_R, is a Yukawa-like term that couples N_R to a scalar field that carries a LN charge, labelled as χ in the following. Once this scalar field develops a vacuum expectation value (VEV), then LN is spontaneously broken, a Majorana neutrino mass term is generated and the Majoron appears as a physical degree of freedom of the spectrum.

If a Dirac term that mixes N_R and the left-handed (LH) lepton doublets l_L is also present in the Lagrangian, small masses for active neutrinos are generated at low energies, according to the Type-I Seesaw mechanism.

At low-energies, the Majoron ω acquires a coupling with ν_L, labelled as $\lambda_{\omega\nu\nu}$. For Majoron masses

$$m_\omega \in [0.1,\, 1]\ \text{eV} \tag{5.1}$$

and $\lambda_{\omega\nu\nu}$ in the range

$$\lambda_{\omega\nu\nu} \in [5\times 10^{-14},\, 10^{-12}]\,, \tag{5.2}$$

the tension on the Hubble constant is reduced [226]. Indeed, for such small Majoron-neutrino mixings and Majoron masses, Majorons only partially thermalize after Big Bang Nucleosynthesis (BBN) or never thermalize [235], enhancing the effective number of neutrino species N_{eff} by at least 0.03 and at most 0.11, values that may be tested with CMB-S4 experiments [236]. Moreover, a non-vanishing $\lambda_{\omega\nu\nu}$ would reduce neutrino free-streaming, modifying the neutrino anisotropic stress energy tensor [237]. This has an impact in the CMB that results in modifying the posterior for the Hubble constant: as shown in Ref. [226], the inclusion of Majoron-neutrino interactions slightly shifts the central value of H_0, but largely broadens its profile reducing the H_0 tension to 2.5σ. For larger couplings, $\lambda_{\omega\nu\nu} > 10^{-12}$, these effects are too large and excluded by the same `Planck` data.

Interestingly, Ref. [226] found that the best χ^2 in a Markov Chain Monte Carlo corresponds to Majoron mass and coupling as in Eqs. 5.1 and 5.2 and $\Delta N_{\text{eff}} = 0.52 \pm 0.19$. The uncertainty in the last observable is very large and $\Delta N_{\text{eff}} = 0$ is compatible within 3σ. However, values close to the central one can be achieved if a thermal population of Majorons is produced

in the early Universe and is not diluted during inflation. This may occur if the reheating temperature is larger than the RH neutrino masses [226]. Alternatively, other relativistic species, such as axions [238–241], may contribute to ΔN_{eff} and their presence may justify such a large value.

The existence of both Majorana and Dirac terms, the achievement of the correct scale for the active neutrino masses and at the same time the alleviation of the Hubble tension via the Majoron strongly depend on the LN charge assignments of l_L, N_R and χ. In particular, fixing the LN of l_L to unity, then the LN of the RH neutrinos needs to have opposite sign with respect to the LN of the scalar field χ. This model presents interesting phenomenological features. On one hand, the heavy neutrinos are expected to be relatively light, with masses at the MeV or GeV scales, opening up the possibility to be studied at colliders. Moreover, the presence of the Majoron may also have other consequences distinct from the Hubble tension. In particular, its couplings to photons and electrons are constrained by CAST and Red Giant observations, respectively, while, due to its coupling to the Higgs, the Majoron may contribute to the invisible Higgs decay, strongly constrained by colliders.

Sect. 5.1 illustrates the mechanism to produce a Majoron that alleviates the H_0 tension together with a correct scale for the active neutrino masses. In Sect. 5.2, this mechanism is introduced in a setup that correctly describes the flavour puzzle of the SM and at the same time produces a QCD axion that solves the Strong CP problem, while Sect. 5.3 gathers the phenomenological signatures of this model.

5.1 The Majoron Mechanism

To produce a Majoron and explain the lightness of the active neutrinos, one can consider a Type-I Seesaw mechanism where the Majorana mass is dynamically generated by the spontaneous breaking of LN. The SM spectrum is extended by three RH neutrinos [9] and a singlet scalar field χ that only transforms under LN. The LN charge assignments can be read in Tab. 5.1, where l_L, N_R and χ have already been defined, and e_R refers to the RH charged leptons. Notice that L_χ and L_N are integer numbers and are not completely free, but must obey a series of constraints that will be made explicit in the following.

[9] The case with only two RH neutrinos is also viable, and correspondingly the lightest active neutrino would be massless.

Field	$U(1)_L$ Charge
l_L, e_R	1
N_R	$-L_N$
χ	L_χ

TABLE 5.1: LN assignments. Fields that are not listed here do not transform under LN.

The most general effective Lagrangian in the neutrino sector invariant under LN is the following [10]:

$$-\mathscr{L}_\nu = \left(\frac{\chi}{\Lambda_\chi}\right)^{\frac{1+L_N}{L_\chi}} \bar{l}_L \tilde{H} \mathcal{Y}_\nu N_R + \frac{1}{2}\left(\frac{\chi}{\Lambda_\chi}\right)^{\frac{2L_N - L_\chi}{L_\chi}} \chi \bar{N}_R^c \mathcal{Y}_N N_R + \text{h.c.}\,, \tag{5.4}$$

where H is the SM Higgs doublet, $\tilde{H} = i\sigma_2 H^*$, Λ_χ is the cut-off scale up to which the effective operator approach holds, and $\mathcal{Y}_\nu$ is a dimensionless and complex matrix, while $\mathcal{Y}_N$ is dimensionless, complex and symmetric. A first condition on $L_{N,\chi}$ arises from requiring that all the terms are local:

$$\frac{1+L_N}{L_\chi}\,, \frac{2L_N - L_\chi}{L_\chi} \in \mathbb{N}\,. \tag{5.5}$$

In the LN broken phase, the field χ can be parametrized as

$$\chi = \frac{\sigma + v_\chi}{\sqrt{2}} e^{i\frac{\omega}{v_\chi}}, \tag{5.6}$$

where the angular part ω is the NGB identified as a Majoron, σ is the radial component and v_χ is its VEV. Notice that the scale appearing in the denominator of the exponent is also v_χ in order to obtain canonically normalized kinetic terms for the Majoron. A useful notation that

[10] Other terms can be added to this Lagrangian inserting $\chi^\dagger$ instead of χ. However, once the terms in Eq. 5.4 are local, then their siblings with $\chi^\dagger$ would not be local and therefore cannot be added to the Lagrangian. The only exception is the term

$$\frac{1}{2}\left(\frac{\chi}{\Lambda_\chi}\right)^{\frac{2L_N + L_\chi}{L_\chi}} \chi^\dagger \bar{N}_R^c \mathcal{Y}_N N_R\,, \tag{5.3}$$

that however only provides a suppressed correction with respect to the Majorana term written in Eq. 5.4 and for this reason it can be neglected.

will be employed in the following is the ratio of the χ VEV and the cut-off scale:

$$\varepsilon_\chi = \frac{v_\chi}{\sqrt{2}\Lambda_\chi}. \tag{5.7}$$

This parameter ε_χ is expected to be smaller than 1 in order to guarantee a good expansion in terms of $1/\Lambda_\chi$. Consequently, the χ VEV, which represents the overall scale of the LN breaking, is expected to be smaller that the scale Λ_χ, where New Physics should be present and is responsible for generating the expression in Eq. 5.4.

Once the electroweak symmetry is also spontaneously broken, i.e. after the SM Higgs develops its VEV that in the unitary gauge reads

$$H = \frac{h+v}{\sqrt{2}}\,, \tag{5.8}$$

where h is the physical Higgs and $v \simeq 246$ GeV, masses for the active neutrinos are generated according to the Type-I Seesaw mechanism:

$$\mathscr{L}_\nu^{\text{low-energy}} = \frac{1}{2}\bar{\nu}_L\, m_\nu\, \nu_L^c + \text{h.c.} \qquad \text{with} \qquad m_\nu = \frac{\varepsilon_\chi^{\frac{2+L_\chi}{L_\chi}} v^2}{\sqrt{2}v_\chi}\mathcal{Y}_\nu\mathcal{Y}_N^{-1}\mathcal{Y}_\nu^T\,. \tag{5.9}$$

In the basis where the charged lepton mass matrix is already diagonal, the neutrino mass matrix can be diagonalized by the PMNS matrix U:

$$\hat{m}_\nu \equiv \text{diag}\,(m_1,\, m_2,\, m_3) = U^\dagger\, m_\nu\, U^*\,. \tag{5.10}$$

The overall scale for the active neutrino masses can be written in terms of the parameter ε_χ, the ratio of the VEVs and the product $\mathcal{Y}_\nu\mathcal{Y}_N^{-1}\mathcal{Y}_\nu^T$:

$$\frac{\varepsilon_\chi^{\frac{2+L_\chi}{L_\chi}} v^2}{\sqrt{2}v_\chi}\mathcal{Y}_\nu\mathcal{Y}_N^{-1}\mathcal{Y}_\nu^T \simeq \sqrt{|\Delta m^2_{\text{atm}}|}\,, \tag{5.11}$$

where $\Delta m^2_{\text{atm}} = 2.514^{+0.028}_{-0.027} \times 10^{-3}$ eV^2 for the Normal Ordering (NO) of the neutrino mass spectrum and $\Delta m^2_{\text{atm}} = -2.497 \pm 0.028 \times 10^{-3}$ eV^2 for the Inverted Ordering (IO) [17].

The heavy neutrinos, that mostly coincide with the RH neutrinos, have a mass matrix that in first approximation can be directly read from the Lagrangian in Eq. 5.4,

$$M_N \simeq \varepsilon_\chi^{\frac{2L_N - L_\chi}{L_\chi}} \frac{v_\chi}{\sqrt{2}} \mathcal{Y}_N \,. \tag{5.12}$$

The overall scale for the heavy neutrinos must be larger than the overall scale of the active neutrinos, in order for the Seesaw approximation to hold:

$$\varepsilon_\chi^{\frac{2L_N - L_\chi}{L_\chi}} \frac{v_\chi}{\sqrt{2}} \mathcal{Y}_N \gg \sqrt{|\Delta m^2_{\text{atm}}|} \,. \tag{5.13}$$

On the other hand, the electroweak and LN breakings give rise to the Majoron Lagrangian that can be written as follows:

$$\begin{aligned} \mathscr{L}_\omega =& \frac{1}{2}\partial_\mu\omega\partial^\mu\omega + \frac{1}{2}m^2_\omega\omega^2 - i\frac{1+L_N}{L_\chi}\varepsilon_\chi^{\frac{1+L_N}{L_\chi}} \frac{v}{\sqrt{2}v_\chi}\bar{\nu}_L\mathcal{Y}_\nu N_R\omega + \\ & - i\frac{L_N}{L_\chi}\frac{\varepsilon_\chi^{\frac{2L_N - L_\chi}{L_\chi}}}{\sqrt{2}}\bar{N}^c_R\mathcal{Y}_N N_R\omega + \text{h.c.}\,, \end{aligned} \tag{5.14}$$

where the m^2_ω term parametrizes the Majoron mass introduced here as an explicit breaking of its corresponding shift symmetry. At low energy, a direct coupling of the Majoron to the active neutrinos emerges after performing the same transformations that gave rise to the mass matrix in Eq. 5.9:

$$\mathscr{L}_\omega^{\text{low-energy}} \supset i\frac{\lambda_{\omega\nu\nu}}{2}\omega\bar{\nu}_L\nu^c_L + \text{h.c.}^{11} \qquad \text{with} \qquad \lambda_{\omega\nu\nu} = 2\frac{m_\nu}{L_\chi v_\chi} \,. \tag{5.15}$$

From the results in Ref. [226], shown in Eq. 5.2, it is then possible to infer a bound on the product $L_\chi v_\chi$, once taking $\sqrt{\Delta m^2_{\text{atm}}}$ as the overall scale for the neutrino masses:

$$|L_\chi| v_\chi \simeq \frac{2\sqrt{|\Delta m^2_{\text{atm}}|}}{\lambda_{\omega\nu\nu}} \in [0.1,\, 2]\ \text{TeV} \,. \tag{5.16}$$

Adopting this relation and substituting it within the expressions in Eqs. 5.11 and 5.13, new conditions can be found:

$$|L_\chi|\varepsilon_\chi^{\frac{2+L_\chi}{L_\chi}}\mathcal{Y}_\nu\mathcal{Y}_N^{-1}\mathcal{Y}_\nu^T \simeq \frac{2\sqrt{2}}{\lambda_{\omega\nu\nu}}\frac{|\Delta m^2_{\text{atm}}|}{v^2} \in [1.2\times10^{-13},\, 2.4\times10^{-12}] \,, \tag{5.17}$$

$$\frac{\varepsilon_\chi^{\frac{2L_N - L_\chi}{L_\chi}}}{|L_\chi|}\mathcal{Y}_N \gg \frac{\lambda_{\omega\nu\nu}}{\sqrt{2}} \simeq 3.5\times10^{-14} \,. \tag{5.18}$$

[11] This expression coincides with the one in Ref. [226] once identifying ω with ϕ and $\lambda_{\omega\nu\nu}$ with λ.

The following choice of charge assignments leads to a completely renormalizable Lagrangian and thus deserves special mention:

$$\text{CASE R:} \qquad L_N = -1 \qquad \text{and} \qquad L_\chi = -2\,, \tag{5.19}$$

such that the powers of the ratio χ/Λ_χ in Eq. 5.4 are not present in either the Dirac and the Majorana terms. The relation in Eq. 5.16 and the two conditions in Eqs. 5.17 and 5.18 further simplify:

$$\text{Eq. 5.16} \longrightarrow \quad v_\chi \simeq \frac{\sqrt{|\Delta m^2_{\text{atm}}|}}{\lambda_{\omega\nu\nu}} \in [0.05,\, 1]\ \text{TeV}\,, \tag{5.20}$$

$$\text{Eq. 5.17} \longrightarrow \quad \mathcal{Y}_\nu \mathcal{Y}_N^{-1} \mathcal{Y}_\nu^T \simeq \frac{\sqrt{2}}{\lambda_{\omega\nu\nu}} \frac{|\Delta m^2_{\text{atm}}|}{v^2} \in [1.2 \times 10^{-13},\, 2.4 \times 10^{-12}]\,, \tag{5.21}$$

$$\text{Eq. 5.18} \longrightarrow \quad \mathcal{Y}_N \gg \frac{2\lambda_{\omega\nu\nu}}{\sqrt{2}} \simeq 7 \times 10^{-13}\,. \tag{5.22}$$

The first expression fixes a range of values for v_χ. While the third expression represents a lower bound on the overall scale of $\mathcal{Y}_N$, the second one implies that the product $\mathcal{Y}_\nu \mathcal{Y}_N^{-1} \mathcal{Y}_\nu^T$ should be tuned to a very small value in order to reproduce the lightness of the active neutrinos.

For values of $L_{N,\chi}$ different from the previous ones, the Lagrangian is necessarily non-renormalizable. An interesting question is whether the extremely small values of the product $\mathcal{Y}_\nu \mathcal{Y}_N^{-1} \mathcal{Y}_\nu^T$ can be avoided exploiting the suppression in ε_χ from the new physics scale Λ_χ, similarly to the Froggatt-Nielsen approach to the flavour puzzle [46]. Considering first the case in which $L_{N,\chi} > 0$, then the only available possibilities are

$$\begin{aligned} &\text{CASE NR1:} \qquad L_N = 1 \qquad \text{and} \qquad L_\chi = 1, \\ &\text{CASE NR2:} \qquad L_N = 1 \qquad \text{and} \qquad L_\chi = 2\,. \end{aligned} \tag{5.23}$$

The corresponding values for v_χ, ε_χ, the overall scale for the heavy neutrinos $\langle M_N \rangle$ and the cut-off scale Λ_χ are reported in Tab. 5.2.

	L_N	L_χ	v_χ	ε_χ	$\langle M_N \rangle$	Λ_χ
CASE NR1	1	1	$[0.1, 2]$ TeV	$[0.49, 1.4] \times 10^{-4}$	$[3.5, 200]$ MeV	$[1.4 - 11] \times 10^3$ TeV
CASE NR2	1	2	$[0.05, 1]$ TeV	$[2.4, 11] \times 10^{-7}$	$[35.4, 707]$ GeV	$[1.4 - 6.5] \times 10^5$ TeV

TABLE 5.2: Parameter ranges in the two phenomenologically interesting scenarios.

From Eq. 5.17, it can be seen that ε_χ gets smaller for larger values of L_χ (unless tuning the product $\mathcal{Y}_\nu \mathcal{Y}_N^{-1} \mathcal{Y}_\nu^T$ as in CASE R discussed above, a possibility to be avoided in the present discussion): although this is not a problem by itself, it hardens the constraint in Eq. 5.18. It follows that for larger values of L_N and L_χ satisfying the locality conditions in Eq. 5.5, the overall scale of the heavy neutrino masses would be as small as the one of active neutrinos and therefore the expansion in the Type-I Seesaw mechanism would break down.

In the case when $L_N > 0$ and $L_\chi < 0$, it is possible to obtain the same results listed above substituting χ by $\chi^\dagger$ in the Lagrangian in Eq. 5.4: in this case, the signs in the denominators of the exponents would be flipped, compensating the negative sign of L_χ. The opposite case, $L_N < 0$ and $L_\chi > 0$, is not allowed by the locality conditions.

For $L_{N,\chi} < 0$, besides the possibility of CASE R, only another choice is allowed by the locality conditions: $(L_N = -1, L_\chi = -1)$. However, this case would require $\varepsilon_\chi \gg 1$, leading to an even more extreme fine-tuning than in CASE R without the appeal of renormalizability.

The condition in Eq. 5.16, corresponding to Eq. 5.2, is only one of the ingredients necessary to lower the H_0 tension. A second relevant requirement is Eq. 5.1, regarding the Majoron mass. For the sake of simplicity, it has been introduced directly in the Majoron Lagrangian in Eq. 5.14 as en effective term. Its origin has been widely discussed in the literature and constitutes in itself an interesting research topic. Any violation of the global LN symmetry would induce a mass for the Majoron. An obvious example are gravitational effects, which are expected to break all accidental global symmetries. Estimations of their size from non-perturbative arguments via wormhole effects [212] fall too short of their required value. Conversely, their size from Planck-suppressed effective operators [242] would result in too large a mass, although several possibilities have been discussed that could prevent the lower dimension operators from being generated [243–250]. These options were originally introduced as a solution to the axion quality problem. A simpler possibility, given the singlet nature of the N_R, is an explicit breaking of LN via a Majorana mass term at the Lagrangian level. The Majoron would thus develop a mass slightly below this breaking scale from its coupling to the N_R through self-energy diagrams. In this work we will remain agnostic to the origin of the Majoron mass, and a value consistent with Eq. 5.1 will be assumed.

Besides the Majoron, also the radial component of χ is present in the spectrum and does play a role modifying the Higgs scalar potential. Indeed, the most general scalar potential containing H and χ can be written as

$$V(H,\chi) = -\mu^2 H^\dagger H + \lambda \left(H^\dagger H\right)^2 - \mu_\chi^2 \chi^* \chi + \lambda_\chi \left(\chi^* \chi\right)^2 + g H^\dagger H \chi^* \chi \,. \tag{5.24}$$

The minimization of such potential leads to VEVs for the two fields that read

$$v^2 = \frac{4\lambda_\chi \mu^2 - 2g\mu_\chi^2}{4\lambda\lambda_\chi - g^2}\,, \qquad\qquad v_\chi^2 = \frac{4\lambda\mu_\chi^2 - 2g\mu^2}{4\lambda\lambda_\chi - g^2}\,. \tag{5.25}$$

The parameters of this scalar potential need to be such that v takes the electroweak value and v_χ acquires the values in Tab. 5.2.

Due to the mixed quartic term, the two physical scalar fields h and σ mix in the broken phase and the mass matrix describing this mixing is given by

$$\mathcal{M}^2 = \begin{pmatrix} 2\,\lambda\, v^2 & g\, v\, v_\chi \\ g\, v\, v_\chi & 2\,\lambda_\chi\, v_\chi^2 \end{pmatrix}\,. \tag{5.26}$$

The two eigenvalues that arise after diagonalising this mass matrix are the following

$$M_{h,\sigma}^2 = \lambda v^2 + \lambda_\chi v_\chi^2 \pm \left(\lambda v^2 - \lambda_\chi v_\chi^2\right)\sqrt{1+\tan^2 2\vartheta}\,, \tag{5.27}$$

where

$$\tan 2\vartheta = \frac{g\, v\, v_\chi}{\lambda_\chi v_\chi^2 - \lambda v^2}\,. \tag{5.28}$$

The lightest mass in Eq. 5.27 corresponds to the eigenstate mainly aligned with the SM Higgs, while the heaviest state is mainly composed of the radial component of χ. Its mass can be as small as a few hundreds GeV or much larger than the TeV. From the relation between the mixed quartic coupling g and the physical parameters,

$$g = \frac{M_\sigma^2 - M_h^2}{2\, v\, v_\chi} \sin 2\vartheta\,, \tag{5.29}$$

it is possible to straightforwardly study the dependence of M_σ with the other model parameters. Notice that the mixing parameter ϑ is constrained by LHC data to be [251]

$$\sin^2\vartheta \lesssim 0.11\,, \tag{5.30}$$

from a $\sqrt{s} = 13$ TeV analysis of Higgs signal strengths with 80 fb^{-1} of integrated luminosity.

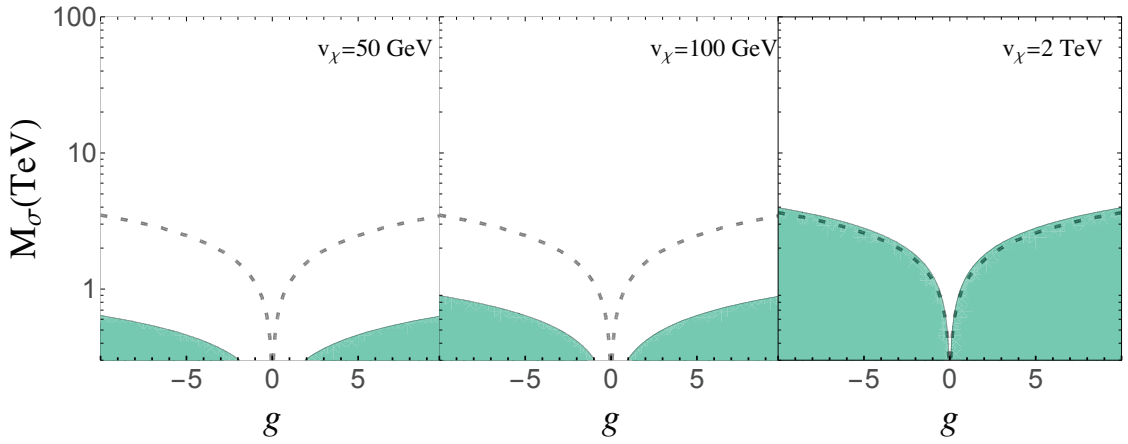

FIGURE 5.1: M_σ *vs.* g parameter space, fixing $v = 246$ GeV, $M_h = 125$ GeV and taking three values for LN breaking scale, $v_\chi = \{50 \text{ GeV}, 100 \text{ GeV}, 2 \text{ TeV}\}$. The white area is the one allowed by the bound in Eq. 5.30, while the green region is the excluded one. The dashed line correspond to the bound in Eq. 5.48, being the area above such line allowed.

As shown in Fig. 5.1, M_σ can reach very large values, without requiring any fine-tuning on g. On the contrary, very small M_σ can only be achieved for g close to zero. It is then natural to focus on the case in which σ is massive enough to be safely integrated out. This will be the case in the rest of the chapter.

The mechanism illustrated in this section allows to soften the H_0 tension explaining at the same time the lightness of the active neutrinos. In the next section, this mechanism will be embedded into the same flavour framework as the model in Chapter 4, that allows to account for the Flavour Puzzle, without violating any bounds from flavour observables, and also contains a QCD axion that solves the Strong CP Problem.

5.2 The Majoron arising from MFV

In Chapter 2 we discussed the power of the Minimal Flavour Violation ansatz, that protects NP models from the BSM Flavour problem. In Chapter 4 we showed that an axion can in fact arise within that framework naturally, solving the Strong CP Problem with additional interesting Phenomenology. In this section we will discuss how a Majoron can also arise naturally together with the MFVA. Let us remember that, with the inclusion of RH neutrinos, the

MFV symmetry group is

$$\mathcal{G}_F = U(3)^6 \,, \tag{5.31}$$

whose Abelian subgroup can be rearranged, provided that the new combinations are still linearly independent, identifying among them Baryon Number, LN, weak hypercharge and the Peccei-Quinn symmetry:

$$\mathcal{G}_F^A = U(1)_B \times U(1)_L \times U(1)_Y \times U(1)_{PQ} \times U(1)_{e_R} \times U(1)_{N_R} \,. \tag{5.32}$$

In the model described in this section, fermion charges under baryon number and hypercharge are assigned as in the SM, while the LN charges are given in Tab. 5.1, while PQ charges are those described in the two scenarios of Eq. 4.11. Finally, the last two symmetries in Eq. 5.32 do not play any role in this model and are explicitly broken. The LN appearing within this Abelyan subgroup is imposed on the Lagrangian, with the consequent Majoron appearing after its SSB.

As discussed in Chapter 2, MFV in the lepton sector requires for modifications to the initial $U(3)^6$ in order to recover predictability. The solutions that have been proposed are to assume $\mathcal{Y}_N \propto \mathbb{1}$ [58, 59] or to consider $\mathcal{Y}_\nu$ as a unitary matrix [60]. In the following we will recapitulate briefly these approaches, and show the expression for light neutrino masses in each of these two scenarios when the Majoron mechanism described in this chapter is also considered.

I): $\mathcal{G}_L^{NA} \to SU(3)_{l_L} \times SU(3)_{e_R} \times SO(3)_{N_R} \times CP$ [58, 59].

Under the assumption that the three RH neutrinos are degenerate in mass, i.e. $\mathcal{Y}_N \propto \mathbb{1}$, then the non-Abelian symmetry associated to the RH neutrinos, $SU(3)_{N_R}$, is broken down to $SO(3)_{N_R}$. With the additional assumption of no CP violation in the lepton sector, forcing Y_ν to be real, the expression for the active neutrino mass in Eq. 5.9 simplifies to

$$m_\nu = \frac{\varepsilon_\chi^{\frac{2+L_\chi}{L_\chi}} v^2}{\sqrt{2} v_\chi} \mathcal{Y}_\nu \mathcal{Y}_\nu^T \,, \tag{5.33}$$

and all flavour changing effects involving leptons can be written in terms of $\mathcal{Y}_\nu \mathcal{Y}_\nu^T$ and Y_e.

Diagonalising m_ν corresponds to diagonalising the product $\langle \mathcal{Y}_\nu \rangle \langle \mathcal{Y}_\nu \rangle^T$ and, given the fact that the the lepton mixing angles are relatively large, then no hierarchies should be expected among the entries of $\langle \mathcal{Y}_\nu \rangle \langle \mathcal{Y}_\nu \rangle^T$, contrary to what happens in the quark case.

Note that some setups, such as the so-called sequential dominance scenarios, obtain large mixing angles even if there exists a strong hierarchy among the Yukawa couplings [252]. However, this possibility is disfavoured by the general philosophy of MLFV. In the same spirit, the overall scale of this product is of $\mathcal{O}(1)$, as any explanation of the neutrino masses should reside in the model itself, and not be due to any fine-tuning.

II): $\mathcal{G}_L^{NA} \to SU(3)_{l_L+N_R} \times SU(3)_{e_R}$ [60].

Assuming that the three RH neutrinos transform as a triplet under the same symmetry group of the lepton doublets,

$$l_L, N_R \sim (\mathbf{3},\, 1)_{\mathcal{G}_L^{NA}} \qquad\qquad e_R \sim (1,\, \mathbf{3})_{\mathcal{G}_L^{NA}}\,, \tag{5.34}$$

then Schur's Lemma guarantees that $\mathcal{Y}_\nu$ transforms as a singlet of the symmetry group. Then, Y_ν is a unitary matrix [61, 62], which can always be rotated to the identity matrix by a suitable unitary transformation acting only on the RH neutrinos. The only meaningful quantities in this context are $\mathcal{Y}_e$ and $\mathcal{Y}_N$, so neutrino masses and lepton mixings are encoded uniquely into Y_N,

$$m_\nu = \frac{\varepsilon_\chi^{\frac{2+L_\chi}{L_\chi}} v^2}{\sqrt{2} v_\chi} \mathcal{Y}_N^{-1}\,. \tag{5.35}$$

As for the previous case, the diagonalisation of the active neutrino mass coincides with the diagonalisation of $\langle \mathcal{Y}_N \rangle^{-1}$, that therefore does not present any strong hierarchy among its entries. Moreover, its overall scale should be $\mathcal{O}(1)$ according to the MLFV construction approach.

Summarising, the Majoron together with axion constitute the natural Abelian completion of MFV scenarios. The Majoron does not affect (at tree level) the physics associated to the axion and the quark and charged lepton flavour physics. Thus, this model, besides describing fermion masses and mixings and solving the Strong CP problem, is able to alleviate the Hubble tension with the only inclusion of three RH neutrinos and two extra singlet scalars. In particular, as no fine-tuning is allowed within this approach on $\langle \mathcal{Y}_\nu \rangle$ or $\langle \mathcal{Y}_N \rangle$, then only CASE NR1 and CASE NR2 are viable in the MFV framework. In the following section, the analysis of this model will be completed with the study of its phenomenological signatures.

5.3 Phenomenological Aspects

The only tree-level coupling of the Majoron is to neutrinos. However, at quantum level, couplings to gauge bosons, other SM fermions and the Higgs are originated.

Coupling to photons

The searches for very light pseudoscalars, usually addressed to axions, can also apply to Majorons. In the range of masses in Eq. 5.1, the strongest constraints on the effective coupling to photons are set by CAST [184], which establishes the upper bound

$$\lambda_{\omega\gamma\gamma} \lesssim 10^{-10}\ \text{GeV}^{-1}\,, \tag{5.36}$$

where $\lambda_{\omega\gamma\gamma}$ is defined as

$$\mathscr{L}_{\omega}^{\text{low-energy}} \supset \frac{1}{4}\,\lambda_{\omega\gamma\gamma}\,\omega\,F^{\mu\nu}\tilde{F}_{\mu\nu} \tag{5.37}$$

with $\widetilde{F}_{\mu\nu} \equiv \frac{1}{2}\epsilon_{\mu\nu\rho\sigma}F^{\rho\sigma}$.

As the Majoron does not couple at tree-level to charged particles, then the process $\omega \to \gamma\gamma$ occurs only at two loops. Ref. [253] provides an estimate for its decay width: under the assumption $m_\omega \ll m_e$,

$$\Gamma_{\omega\to\gamma\gamma} = \frac{\alpha^2}{1536^2\pi^7}\frac{m_\omega^7}{v^2 m_e^4}\left(\text{Tr}\left(\frac{m_D m_D^\dagger}{v v_\chi}\right)\right)^2 \tag{5.38}$$

where $\alpha \equiv e^2/4\pi$ and with m_D the Dirac neutrino mass matrix.

Computing the same process by means of the effective couplings in Eq. 5.37,

$$\Gamma_{\omega\to\gamma\gamma} = \frac{\lambda_{\omega\gamma\gamma}^2 m_\omega^3}{32\pi} \tag{5.39}$$

it is then possible to match the two expressions for the $\omega \to \gamma\gamma$ decay width providing the expression for the $\lambda_{\omega\gamma\gamma}$ coupling:

$$\lambda_{\omega\gamma\gamma} = \frac{\alpha m_\omega^2}{384\sqrt{2}\pi^3 m_e^2 v_\chi}\epsilon_\chi^{\frac{2+2L_N}{L_\chi}}\,\text{Tr}\left(\mathcal{Y}_\nu\mathcal{Y}_\nu^\dagger\right)\,. \tag{5.40}$$

Tab. 5.3 shows the numerical estimations for the predicted values of the Majoron coupling to photons, assuming that the trace gives an $\mathcal{O}(1)$ number, as already discussed: the experimental bound is still far from the theoretical prediction.

	$\lambda_{\omega\gamma\gamma}$	$\lambda_{\omega ee}$	$\lambda_{\omega\nu\nu}$
CASE NR1	$[10^{-39}, 10^{-36}]$ GeV^{-1}	$[10^{-25}, 10^{-24}]$	$[10^{-14}, 10^{-12}]$
CASE NR2	$[10^{-34}, 10^{-32}]$ GeV^{-1}	10^{-20}	
Exp. Upper bounds	10^{-10} GeV^{-1}	10^{-13}	10^{-5}

TABLE 5.3: Predictions for the Majoron effective couplings to electrons, photons and neutrinos, for the window of the parameter space where Hubble tension is alleviated. In the last line, the corresponding experimental upper bounds.

Coupling to electrons.

Astrophysical measurements can also constrain Majoron couplings. Ref. [170] provides an upper bound on the Majoron effective coupling to electrons

$$\mathscr{L}_{\omega}^{\text{low-energy}} \supset i\,\lambda_{\omega ee}\,\omega\,\bar{e}\,e\,, \tag{5.41}$$

based on observations on Red Giants:

$$\lambda_{\omega ee} < 4.3 \times 10^{-13}\,. \tag{5.42}$$

The decay width of the Majoron to two electrons reads [253]

$$\Gamma_{\omega ee} \simeq \frac{1}{8\pi}|\lambda_{\omega ee}|^2\, m_\omega\,, \tag{5.43}$$

where

$$\lambda_{\omega ee} \simeq \frac{1}{8\pi^2}\frac{m_e}{v}\left(\left(\frac{m_D m_D^\dagger}{v v_\chi}\right)_{11} - \frac{1}{2}\text{Tr}\left(\frac{m_D m_D^\dagger}{v v_\chi}\right)\right)\,, \tag{5.44}$$

with $(\ldots)_{11}$ standing for the $(1,1)$ entry of the matrix in the brackets. Substituting explicitly the expression for m_D, the coupling becomes

$$\lambda_{\omega ee} = \frac{1}{16\pi^2}\frac{m_e}{v_\chi}\epsilon_\chi^{\frac{2+2L_N}{L_\chi}}\left(\left(\mathcal{Y}_\nu\mathcal{Y}_\nu^\dagger\right)_{11} - \text{Tr}\left(\mathcal{Y}_\nu\mathcal{Y}_\nu^\dagger\right)\right)\,. \tag{5.45}$$

Assuming as before that the elements of the product $\mathcal{Y}_\nu \mathcal{Y}_\nu^\dagger$ are $\mathcal{O}(1)$ numbers, also the Majoron-electron coupling is predicted to be much smaller than the corresponding experimental bound, as shown in Tab. 5.3.

Coupling to neutrinos. Majoron emission in $0\nu\beta\beta$ decays.

The tree level coupling of the Majoron to neutrinos does not have an impact only on cosmology, but may be relevant for low-energy terrestrial experiments. In particular, searches for neutrinoless-double-beta decay could also be sensitive to processes in which Majorons are produced, such as in KamLAND-Zen [254] and NEMO-3 [255] experiments.

Current measurements set a lower bound on the half-life of the neutrinoless-double-beta decay of the order of 10^{24} years. In the particular case discussed here, where the Majoron could only be produced by the annihilation of two neutrinos (see Fig. 5.2), this bound can be translated into a constraint on the Majoron-neutrino coupling [256], such that

$$\lambda_{\omega\nu\nu} < 10^{-5}\,, \tag{5.46}$$

where $\lambda_{\omega\nu\nu}$ is defined in Eq. 5.15.

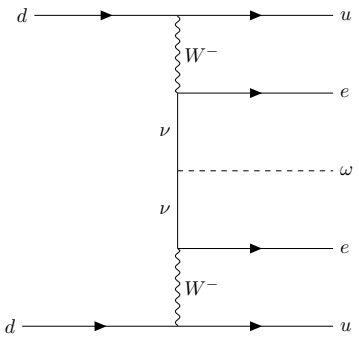

FIGURE 5.2: Feynman Diagram for the neutrinoless-double-beta decay with the emission of a Majoron.

The predicted value of the Majoron-neutrino coupling can be read out in Tab. 5.3 and it is much smaller than the corresponding experimental value and the bound from `Planck` [226] ($\lambda_{\omega\nu\nu} < \mathcal{O}(10^{-12})$).

Coupling with the SM Higgs. Higgs invisible decay.

The Majoron-Higgs coupling follows due to the mixing between the radial component of χ and the physical Higgs, as described at the end of Sect. 5.1. Indeed, expanding the kinetic term of the field χ, a $\sigma\omega\omega$ coupling arises that induces an effective coupling $h\omega\omega$, via the mixing ϑ. This coupling opens up a new decay channel for the Higgs that contributes to the Higgs invisible decay observable. The width of this process is given by

$$\Gamma_{h\to\omega\omega} = \frac{s_\vartheta^2 M_h^3}{32\pi v_\chi^2} \lesssim 0.8\ \text{MeV}\,, \tag{5.47}$$

where the last inequality has been obtained considering that the invisible Higgs decay width may constitute at most the 19% of its total width [257].

This result can be translated into a strong bound on v_χ, that reads

$$\frac{v_\chi}{|s_\vartheta|} \gtrsim 5\ \text{TeV}\,. \tag{5.48}$$

For a light σ, the mixing would be close to its current upper bound, Eq. 5.30, and v_χ should be larger than ~ 1.5 TeV, which would exclude CASE NR2 and part of the parameter space of CASE NR1, see the dashed line in Fig. 5.1. However, as stated at the end of Sect. 5.1, the assumption made here is that σ is sufficiently heavy to be integrated out and this corresponds to much smaller values of the mixing angle ϑ, relaxing in this way the bound on v_χ.

Heavy Neutrinos

In both cases discussed in Sect. 5.1, the heavy neutrino masses lie in ranges that may lead to detection in various experimental facilities. Neutrinos with masses ranging from tens to hundreds of MeV can be probed and potentially detected at beam dump or even near detectors of neutrino oscillation experiments [258–265], such as DUNE or SHiP, whereas those with masses in the range of tens to hundreds of GeV have interesting prospects of being produced at the LHC or future colliders [259, 266–272].

On the other hand, given their extremely small couplings, the heavy neutrinos produced in the early Universe would not be Boltzmann suppressed when decoupled from the thermal bath, leading to an unacceptably large contribution to the relativistic degrees of freedom of the Universe after their subsequent decay [273–277]. If their decay takes place before the onset

of BBN, the decay products would quickly thermalise and BBN would then proceed as in the standard ΛCDM scenario. However, if the decay of the heavy neutrinos happens after BBN and neutrino decoupling, their contribution to the effective number of neutrinos would be too high and ruled out. If the decay takes place during BBN, the decay products could also alter the production of primordial helium and strong constraints also apply [278–281]. This would be the situation of CASE NR1, for which the neutrino masses and mixings predict decay rates comparable to or larger than the onset of BBN. Conversely, the larger masses that characterize CASE NR2 lead to decays faster than BBN, eluding these cosmological constraints. Hence, BBN and CMB observations disfavor CASE NR1 unless the heavy neutrino decay is faster than BBN in some part of the parameter space or some other modification of the standard ΛCDM scenario is considered. Indeed, if the heavy neutrinos decay after BBN, for heavy neutrino masses in the range $[3.5, 200]$ MeV, then the bound on the mixing is [277]:

$$\sin^2\theta_s \equiv \frac{\langle m_\nu \rangle}{\langle M_N \rangle} \lesssim 10^{-15} - 10^{-17}\,, \tag{5.49}$$

much smaller than the expected value that can be read in Tab. 5.4.

	$\langle M_N \rangle$	$\sin^2\theta_s$	$\Gamma^Z_{N\to 3\nu}$	$\Gamma^\omega_{N\to 3\nu}$
CASE NR1	$[3.5, 200]$ MeV	$[2.5\times10^{-10},\ 1.4\times10^{-8}]$	$\mathcal{O}(10^{-38})$	$\mathcal{O}(10^{-68})$
CASE NR2	$[35.4, 707]$ GeV	$[7.1\times10^{-14},\ 1.4\times10^{-12}]$	$\mathcal{O}(10^{-27})$	$\mathcal{O}(10^{-66})$

TABLE 5.4: Expectation for the heavy neutrino mass and mixing between heavy and active neutrinos.

In this chapter we have presented a model where a Majoron, the NGB of LN, can help alleviate the Hubble tension, from 4.4σ to 2.5σ, while explaining the smallness of active neutrino masses at the same time. This Majoron mechanism is very generic, and can be embedded in several flavour models.

In this thesis in particular we have shown that this Majoron can be found within the MFV framework, and cohexist in fact with the Minimal Flavour Violating axion, the NGB of a PQ symmetry that also deals with the mass ratios of top and bottom quark and the tau charged lepton. In addition to the phenomenology of the MFVA, the existence of this Majoron carries its own phenomenological features.

Though the Majoron couples to neutrinos at tree level, and to electrons and photons at one and two loops respectively, its couplings happen to be so small that it is well below current limits coming from neutrinoless double-beta decay, Red Giant observations and CAST. However,

the extra scalar and the (not so) heavy neutrinos that come together with the Majoron present interesting phenomenology. In particular, the scalar could have masses at the order of tens of TeVs, escaping the bounds from Higgs invisible decay and scalar mixing but light enough to expect it in future colliders, while the heavy neutrinos can be found in the MeV or GeV range, depending the case. Those masses could imply a possible detection in DUNE or SHiP, but also imply cosmological constraints.

These constraint comes from the effective number of neutrinos in the Universe, which is relevant also for the partial solution of the Hubble tension. Though we have discussed the impact on this observable by heavy neutrino decays and the Majoron, we have not discussed the possibility of thermal axions contributing to it. The next chapter will be dedicated to this analysis: we will study the possibility of axions being produced thermally and obtain its impact on the number of relativistic species, as well as its compatibility with the recent anomaly observed by the XENON1T experiment.

Chapter 6

Axion Dark Radiation and ΔN_{eff}

To close this thesis, we will change gears a little bit and study the synergy between particle phenomenology and cosmology through the relativistic degrees of freedom, parametrized by the effective number of neutrinos N_{eff}. We will consider in the first part, based on the publication of Ref. [282], the possibility of axions produced thermaly and its impact on N_{eff}, performing a model independent analysis as well as providing predictions from several phenomenologically interesting axion models. Then, the second half, whose content was published in Ref. [241], will be devoted to the compatibility between this same observable and the anomaly compatible with solar axions observed by the XENON1T collaboration [283]. Finally, we will close the chapter with a reflection on what can be learnt through this observable and the results obtained here.

6.1 Production of thermal Axions across the ElectroWeak Phase Transition

As we have extensively through this thesis, the axion is a very well motivated extension to the SM as it can handle the Strong CP Problem and, at the same time, can become a candidate for the cold DM in our Universe.

The focus of this chapter, however, is on a different and distinct cosmological imprint: scattering and/or decay of particles in the primordial plasma produce relativistic axions [238, 284]. Current bounds on f_a implies that m_a must be roughly below the eV scale. Axions produced at early times are still relativistic at matter-radiation equality and, for $m_a \ll \mathcal{O}(0.1)$ eV as

we consider by neglecting the axion mass, also around recombination. In this case, they would manifest themselves as an additional contribution to the amount of radiation at the time of CMB formation. Upcoming CMB-S4 surveys [236, 285] will improve bounds on this quantity, historically parameterized as an effective number of neutrino species N_{eff}, and can potentially discover a deviation from the SM. The forecasted sensitivity allows to detect the effects of a relativistic species which decoupled at high temperatures, as high as the ElectroWeak Phase Transition (EWPT), making this a new probe of high-energy physics. Motivated by forthcoming data, recent works revisited axion production through various channels and the resulting prediction for N_{eff} [220, 239, 240, 286, 287].

There are, broadly speaking, two classes of axion interactions with visible matter

$$\mathscr{L}_{\text{axion}-\text{int}} \supset \frac{1}{f_a}\left[a\, c_X \frac{\alpha_X}{8\pi} X^{a\mu\nu}\tilde{X}^a_{\mu\nu} + \partial_\mu a\; c_\psi \overline{\psi}\gamma^\mu\psi\right] . \tag{6.1}$$

Operators with gauge bosons $X = \{G,\, W,\, B\}$, present if the PQ symmetry is anomalous under the associated gauge group, are suppressed by a loop factor. We need a coupling to gluons in order to solve the strong CP problem, and we set $c_G = 1$ consistently with Eq. 3.30. Anomalies under the electroweak group are possible but not mandatory. We consider the high-energy theory where SM fermions, $\psi = \{q_L, u_R, d_R, l_L, e_R\}$, have well defined gauge quantum numbers and their interactions with the axion preserve the shift symmetry $a \to a + \text{const}$. Other dimension 5 interactions can be redefined away as explained later in the chapter.

Axion production is efficient when the interaction rate exceeds the Hubble rate H. The latter, assuming an early universe dominated by radiation with temperature T, scales as $H \propto T^2/M_{Pl}$. Hot axions can be produced either via scatterings or decays. Interactions with gauge bosons, the first kind in Eq. 6.1, cannot mediate decays. Coupling to SM fermions, the second kind in Eq. 6.1, could in principle be responsible for production via decays if the fermion bilinear couples fields belonging to different generations. In other words, we need flavour violation in order to have production via unsuppressed tree-level bath particles decays to axions.

Regardless of the production details, the highest value for N_{eff} is reached when axions achieve thermalization with the thermal bath. The resulting abundance in this case depends only on the plasma temperature when they lose thermal contact, and its value is suppressed by the total number of the entropic degrees of freedom g_{*s} at decoupling. If this happens above the EWPT then the resulting N_{eff} is barely within the reach of future surveys [286].

Rates for scattering mediated by interactions with SM gauge bosons scale at high temperatures as $\Gamma_X \simeq \alpha_X^3 T^3/f_a^2$, and these processes are never in thermal equilibrium at the EWPT for $f_a \gtrsim \mathcal{O}(10^8)$ GeV [238, 239]. If axions never thermalize, the prediction for N_{eff} is sensitive to the initial abundance that is presumably set at the stage of reheating after inflation; an accurate calculation requires a treatment of thermal effects at high temperature [239]. Either way, the associated N_{eff} is at the edge of what we can test.

Once considering interactions with fermions, for flavour conserving couplings, the only way to produce hot axions is via scattering. We consider $2 \to 2$ collisions, and these processes always involve two SM fermions and one SM boson besides the axion itself.

At temperatures above the EWPT, we have two options for the SM boson involved. On the one hand, it can be any of the four real component of the Higgs doublet H [12] and the scattering rate in this case scales as $\Gamma_{\psi/H} \simeq c_\psi^2 y_\psi^2 T^3/f_a^2$ [239] with y_ψ the SM fermion Yukawa coupling. For heavy SM fermions, this is larger by a factor $c_\psi^2 y_\psi^2/\alpha_X^3$ compared to scattering mediated by the axion-gauge boson vertex. On the other hand, it can be a transverse gauge boson. The scattering rate in this case is proportional to the mass of the fermion, since there is a chirality flip needed in the process, and this contribution is vanishing because all fermions are massless above the EWPT.

The SM boson involved in the scattering with fermions can be a gauge field only below the EWPT. The associated rate scales as $\Gamma_{\psi/X} \simeq \alpha_X c_\psi^2 m_\psi^2 T/f_a^2$ for temperatures above the fermion mass, where m_ψ^2 reflects the fermion chirality flip mentioned in the paragraph above, and it is exponentially suppressed at lower temperatures. In this case, at temperatures above the fermion mass, the scattering rate grows with the temperature slower than the Hubble rate and thus axion production is saturated when the ratio between interaction and expansion rates is maximal. This happens at temperatures around the fermion mass, and such a ratio is approximately $\Gamma_{\psi/X}/H|_{T=m_\psi} \approx \alpha_X c_\psi m_\psi M_{Pl}/f_a^2$. If this quantity is larger than $\mathcal{O}(1)$ thermalization is achieved, and the final abundance is not affected by our ignorance about the thermal history (assuming reheating above the weak scale) and possible new degrees of freedom and/or interactions at high energy.

Decays of SM fermions provide an additional axion production channel, often the dominant one, if we have flavour violating couplings. The interaction rate is given by the rest

[12] Namely the Higgs boson and what would become the longitudinal components of the weak gauge bosons below the EWPT scale.

frame width of the decaying fermion times a Lorentz dilation factor accounting for the bath kinetic energy, and it scales as $\Gamma_\psi \simeq c_\psi^2 m_\psi^4/(f_a^2 T)$. Axion production is saturated at temperatures around the fermion mass also in this case, and we achieve thermalization if the condition $\Gamma_\psi/H|_{T=m_\psi} \approx c_\psi^2 m_\psi M_{Pl}/f_a^2$ is satisfied.

After this comparison among different production channels, we decide to focus on axion production mediated by its interactions with SM fermions. We analyze processes with third generation quarks. Production via leptons has been studied in Ref. [220], and such an axion abundance can alleviate the current tension in the measurement of the Hubble parameter [288]. A full calculation via the first two quark generations would require a careful treatment of the QCD phase transition (QCDPT) and it is beyond the scope of this thesis. Previous studies have considered production well above [239] and well below [240] the EWPT. We improve earlier treatments by providing a continuous and smooth prediction for N_{eff} across the EWPT.

We introduce the theoretical framework in Sect. 6.1.1, and we describe axion effective interactions considering both flavour conserving and violating couplings. We collect there too all the processes contributing to axion production, and we provide explicit expressions for cross sections and decay widths. In particular, we compute cross section both above and below the EWPT and we match them at this threshold. We feed Boltzmann equations with these quantities and we solve them numerically, presenting predictions for N_{eff} as a function of the fermion couplings in Sect. 6.1.2. We consider both effective interactions as well as explicit UV constructions leading to flavour conserving couplings. Remarkably, our predictions are within the reach of future CMB surveys inside the low-f_a part of the experimentally allowed region. It is to be noted that, in the absence of no big hierarchy in the dimensionless coefficient describing the coupling to photons, we find that the same parameter space will be probed by future terrestrial searches.

6.1.1 Effective Interactions and Production Processes

Axion interactions with SM fields can be written compactly as follows

$$\mathscr{L}^{(a)} = \mathscr{L}^{(a)}_{\text{gauge}} + \mathscr{L}^{(a)}_{\text{matter}} \,, \tag{6.2}$$

where $\mathscr{L}^{(a)}_{\text{gauge}}$ and $\mathscr{L}^{(a)}_{\text{matter}}$ describe couplings with SM gauge bosons and matter fields, respectively. The entire focus of our work is on axion couplings with SM quarks. However, there

are usually relations among different axion interactions once one considers UV complete models. For this reason, we provided an overview of all axion couplings and we summarize their bounds in Sect. 4.3 where one could visualize which parameter space region is not excluded experimentally.

The axion has anomalous couplings to gauge bosons

$$\mathscr{L}^{(a)}_{\text{gauge}} = -\frac{a}{f_a}\left(\frac{\alpha_s}{8\pi}G^a_{\mu\nu}\tilde{G}^{a\,\mu\nu} + c_W\frac{\alpha_W}{8\pi}W^a_{\mu\nu}\tilde{W}^{a\,\mu\nu} + c_B\frac{\alpha_Y}{8\pi}B_{\mu\nu}\tilde{B}^{\mu\nu}\right), \tag{6.3}$$

where $\tilde{W}$, $\tilde{B}$ and $\tilde{G}$ are defined as below Eq. 3.1. These operators should be interpreted as the effects of the presence of any fermion that couples to the axion and are associated to quantum level contributions. As already mentioned in the beginning of Sect. 6.1, the gluon term does not present any free coefficient, in contrast with the EW terms, in order to match with the traditional definition of f_a. Once we integrate-out weak scale states and heavy quarks, the Lagrangian contains axion couplings only to gluons and photons

$$\mathscr{L}^{(a)}_{\text{gauge}} \supset -\frac{a}{f_a}\left(\frac{\alpha_s}{8\pi}G^a_{\mu\nu}\tilde{G}^{a\,\mu\nu} + c_{a\gamma\gamma}\frac{\alpha_{\text{em}}}{8\pi}F_{\mu\nu}\tilde{F}^{\mu\nu}\right), \tag{6.4}$$

where $c_{a\gamma\gamma} = c_B\,\cos\theta_W^2 + c_W\,\sin\theta_W^2$, being θ_W the Weinberg angle. This expression is valid above the scale where strong interactions confine and therefore before the axion mixes with the η and π^0 mesons. However, experimental searches probe the axion-photon coupling at much lower energy scales and therefore this mixing is to be taken into account. We define this coupling as follows:

$$g_{a\gamma\gamma} \equiv \frac{\alpha_{\text{em}}}{2\pi}\frac{1}{f_a}\Big(c_{a\gamma\gamma} - 1.92(4)\Big), \tag{6.5}$$

where the second term in the parenthesis is the model-independent contribution arising from the above mentioned axion mixing with the η' and π^0 mesons [88, 156–159].

We present matter couplings for the case of quarks, but the discussion is analogous if we consider leptons. Axion couplings to quarks can be expressed in different field bases and physical results cannot depend on such a choice. However, the statement that the axion couples without flavour violation is not true in an arbitrary basis. We specify axion couplings to quarks in the "primed basis" defined in App. A where the fields appearing in the Lagrangian are the $SU(2)_L$ quark doublets q'_L, and the $SU(2)_L$ singlets u'_R and d'_R, and where Yukawa interactions take the form of Eq. A.4.

We distinguish between two cases, and we begin from flavour conserving axion-quark interactions

$$\mathscr{L}^{(a)}_{\text{matter}} \supset \mathscr{L}^{(a)}_{\partial-\text{F.C.}} = \frac{\partial_\mu a}{f_a} \sum_{i=1}^{3} \left(c_q \, \overline{q'_{Li}} \gamma^\mu q'_{Li} + c_u \, \overline{u'_{Ri}} \gamma^\mu u'_{Ri} + c_d \, \overline{d'_{Ri}} \gamma^\mu d'_{Ri} \right) , \tag{6.6}$$

where the free coefficients $\{c_q, c_u, c_d\}$ are typically of the same order of magnitude. The universality of quark-axion couplings guarantees that no flavour-changing interactions arise when moving to the quark mass basis. We can see it explicitly after performing the rotation to get mass eigenstates given in Eq. A.5, the unitarity of the CKM matrix ensures that in the mass eigenbasis the fermion couplings are still flavour conserving.

The most general flavour violating part of the Lagrangian above the EWPT can be written in an analogous way to the flavour conserving one as follows

$$\mathscr{L}^{(a)}_{\text{matter}} \supset \mathscr{L}^{(a)}_{\partial-\text{F.V.}} = \frac{\partial_\mu a}{f_a} \sum_{i,j} \left(c_q^{(ij)} \, \overline{q'_{Li}} \gamma^\mu q'_{Lj} + c_u^{(ij)} \, \overline{u'_{Ri}} \gamma^\mu u'_{Rj} + c_d^{(ij)} \, \overline{d'_{Ri}} \gamma^\mu d'_{Rj} \right) , \tag{6.7}$$

where the matrices of coefficients $\left\{ c_q^{(ij)}, c_u^{(ij)}, c_d^{(ij)} \right\}$ have a generic structure in flavour space. Unless we tune the entries of these matrices consistently with CKM factors, couplings are still flavour off-diagonal once we go to the mass eigenstate basis.

We complete this overview on axion couplings by discussing the remaining options. The case of coupling to leptons is analogous, and Ref. [220] exploited their cosmological consequences. Besides interactions with leptons, no other matter couplings can be present in the Lagrangian as an independent operator. The Higgs-axion interaction

$$i \frac{\partial_\mu a}{f_a} H^\dagger \overset{\leftrightarrow}{D^\mu} H \, , \tag{6.8}$$

where $H^\dagger \overset{\leftrightarrow}{D^\mu} H \equiv H^\dagger (D^\mu H) - (D^\mu H)^\dagger H$ is redundant at lowest order in $1/f_a$ as can be shown via a field redefinition. Moreover, axion couplings to pseudo-scalar fermion currents such as

$$i \frac{a}{f_a} \overline{q'_L} \, H \, d'_R \, , \tag{6.9}$$

can be proved to be also redundant.

Multiple processes contribute to the production of hot axions in the early universe, and we list all of them in this section. Binary scatterings control production for the flavour conserving

case since decays are loop and CKM suppressed. We provide the associated scattering cross sections above and below the weak scale, and we match our results across the EWPT. If axion couplings are flavour violating then tree-level decays dominate the production rate, with their associated decay widths shown here as well .

Axion couplings to quarks are a crucial ingredient for our calculations, and we remark how we define them in the "primed basis" where the SM Yukawa interactions take the form in Eq. A.4. One of our main goals is to provide a smooth treatment of production through the EWPT, hence it is convenient to work in the mass eigenbasis.

Cross sections

We start from flavour conserving axion couplings defined in Eq. 6.6 and quantified by the scale f_a and the three dimensionless coefficients $\{c_q, c_u, c_d\}$. As it turns out, scattering cross sections depend only on two linear combinations of them. This can be checked through explicit calculations or via a change of basis. We perform the following rotations where we redefine quark fields by an axion-dependent phase

$$q'_{Li} \to e^{ic_q \frac{a}{f_a}} q'_{Li} \,, \qquad u'_{Rj} \to e^{ic_u \frac{a}{f_a}} u'_{Rj} \,, \qquad d'_{Rj} \to e^{ic_d \frac{a}{f_a}} d'_{Rj} \,. \tag{6.10}$$

These chiral rotations modify several couplings in the Lagrangian. First, they are anomalous and the dimensionless coefficients of axion couplings to gauge bosons in Eq. 6.4 are affected; as already stated above we do not consider these interactions for our processes and we do not need to worry about this effect. Second, we generate new axion derivative couplings equal and opposite to the ones in Eq. 6.6 once we plug the new quark fields defined above in the kinetic terms. Thus axion derivative couplings are not present anymore in the Lagrangian. Third, and crucially for us, the axion field appears in the Yukawa interactions after we plug these field redefinitions into the SM Yukawa Lagrangian, whose explicit expression is given in Eq. A.4, and we find

$$-\mathscr{L}^{(a)}_{Y-\text{F.C.}} = e^{i(c_u - c_q)\frac{a}{f_a}} \overline{q'_L}\, \tilde{H}\, \hat{Y}^u\, u'_R + e^{i(c_d - c_q)\frac{a}{f_a}} \overline{q'_L}\, H\, V_{\text{CKM}}\, \hat{Y}^d\, d'_R + \text{h.c.} \,. \tag{6.11}$$

As anticipated, although there are three different couplings in the theory only two linear combinations of them can appear in scattering amplitudes

$$c_t \equiv -c_q + c_u \,, \tag{6.12}$$

$$c_b \equiv -c_q + c_d \,. \tag{6.13}$$

We label them with the top and bottom quark because we only focus on the third quark generation as explained in the Introduction. The hatted matrices $\hat{Y}^{u,d}$ are diagonal in flavour space, and axion interactions are flavour conserving once we switch to the mass eigenbasis via the rotations given in Eq. A.5.

Scattering cross sections above EWPT

We focus on third generation quarks $\{t_L, b_L, t_R, b_R\} = \{u_{L3}, d_{L3}, u_{R3}, d_{R3}\}$ where we assign new names to left- and right-handed fields. In order to write explicitly their interactions, we parameterize the complex components of the Higgs doublet as follows

$$H = \begin{pmatrix} \chi_+ \\ \chi_0 \end{pmatrix} \,, \qquad\qquad \tilde{H} \equiv i\sigma_2 (H^\dagger)^T = \begin{pmatrix} \chi_0^c \\ -\chi_- \end{pmatrix} \,, \tag{6.14}$$

where we define $\chi_- \equiv \chi_+^\dagger$ and $\chi_0^c \equiv \chi_0^\dagger$. Once we focus on third generation quarks and we consider the Lagrangian in Eq. 6.11 in the mass eigenbasis, namely without the CKM matrix, we find the following axion interactions

$$\begin{aligned} -\mathscr{L}^{(a)}_{Y-\text{F.C.}} = \; & y_t \, e^{i c_t \frac{a}{f_a}} \left[\chi_0^c \, \overline{t_L} t_R - \chi_- \, \overline{b_L} t_R\right] + y_b \, e^{i c_b \frac{a}{f_a}} \left[\chi_+ \, \overline{t_L} b_R + \chi_0 \, \overline{b_L} b_R\right] + \\ & + y_t \, e^{-i c_t \frac{a}{f_a}} \left[\chi_0 \, \overline{t_R} t_L - \chi_+ \, \overline{t_R} b_L\right] + y_b \, e^{-i c_b \frac{a}{f_a}} \left[\chi_- \, \overline{b_R} t_L + \chi_0^c \, \overline{b_R} b_L\right] \,. \end{aligned} \tag{6.15}$$

The processes we are interested in have only one axion field in the external legs, thus we can Taylor expand the exponential functions appearing in the above Lagrangian and only keep terms up to the first order.

In the unbroken electroweak phase, the Higgs VEV is vanishing and all particles are massless. We want to consider processes producing one axion particle in the final state, so the most general binary collisions involve two fermions fields. The other boson in the process can be either a component of the Higgs doublet or a SM gauge boson. However, if we look at the

axion interactions in Eq. 6.15 we see that only the former is possible. There is no $2 \to 2$ scattering with SM gauge bosons; this is manifest in the basis we choose to describe axion couplings. Alternatively, if we insisted on working in the basis where axion is derivatively coupled to SM fermions the amplitude for a $2 \to 2$ is vanishing as it requires a fermion chirality flip that is not possible in the absence of a mass term for the fermion itself.

Axion Production Above EWSB		
Process	CP Conjugate	$\sigma_{ij\to ka} \times 64\pi f_a^2$
$t\bar{t} \to \chi_0 a$	$t\bar{t} \to \chi_0^c a$	$c_t^2 y_t^2$
$b\bar{b} \to \chi_0 a$	$b\bar{b} \to \chi_0^c a$	$c_b^2 y_b^2$
$t\bar{b} \to \chi_+ a$	$b\bar{t} \to \chi_- a$	$c_t^2 y_t^2 + c_b^2 y_b^2$
$t\chi_0 \to ta$	$\bar{t}\chi_0^c \to \bar{t}a$	$c_t^2 y_t^2$
$t\chi_0^c \to ta$	$\bar{t}\chi_0 \to \bar{t}a$	$c_t^2 y_t^2$
$b\chi_0 \to ba$	$\bar{b}\chi_0^c \to \bar{b}a$	$c_b^2 y_b^2$
$b\chi_0^c \to ba$	$\bar{b}\chi_0 \to \bar{b}a$	$c_b^2 y_b^2$
$t\chi_- \to ba$	$\bar{t}\chi_+ \to \bar{b}a$	$c_t^2 y_t^2 + c_b^2 y_b^2$
$b\chi_+ \to ta$	$\bar{b}\chi_- \to \bar{t}a$	$c_t^2 y_t^2 + c_b^2 y_b^2$

TABLE 6.1: Scatterings producing axions above the EWPT. In the first two columns we list the process and its CP conjugate. They have the same cross section, listed on the third column.

We only have processes with the components of the Higgs doublet in Eq. 6.14. The two fermions in the scattering can be either both in the initial state or one in the initial state and the other one in the final state. We classify all possible cases according to where fermions appear. If we consider the first case, we have fermion/antifermion annihilations producing and axion and any of the components of the complex Higgs doublet. The possible processes are listed in the first block of Tab. 6.1; we show the associate CP conjugate on the same row, and we correctly account for both in our numerical analysis. Another possibility is to have just one fermion in the initial state, and the other particle would be a component of the Higgs doublet. The associated processes are listed in the second block of Tab. 6.1. For each process we also provide the scattering cross section. Our contribution proportional to y_t^2 agrees with what was found in Ref. [239].

Scattering cross sections below EWPT

Once the electroweak symmetry is broken, the Higgs field gets a VEV which gives mass to SM particles. We work in unitarity gauge where the Higgs field is parameterized by the following field coordinates

$$H = \begin{pmatrix} 0 \\ \frac{v+h}{\sqrt{2}} \end{pmatrix} , \qquad \tilde{H} \equiv i\sigma_2 (H^\dagger)^T = \begin{pmatrix} \frac{v+h}{\sqrt{2}} \\ 0 \end{pmatrix} , \tag{6.16}$$

where v and h are the VEV and the physical Higgs boson, respectively. In such a gauge, the three remaining (Goldstone) components of the Higgs doublet are eaten up by the massive Z and W bosons. The mass spectrum as a function of the Higgs VEV results in

$$\{m_W, m_Z, m_h, m_f\} = \left\{ \frac{g}{2}, \frac{\sqrt{g^2+g'^2}}{2}, \sqrt{\frac{\lambda}{2}}, \frac{y_f}{\sqrt{2}} \right\} v \, . \tag{6.17}$$

Here, g and g' are the $SU(2)_L$ and $U(1)_Y$ gauge couplings, respectively. The Higgs quartic coupling λ is normalized in such a way that the potential term is $\lambda(H^\dagger H)^2$.

Axion Production Below EWSB					
Process	CP Conjugate	$\sigma_{ij\to ka}$	Process	CP Conjugate	$\sigma_{ij\to ka}$
$t\bar{t} \to ga$	Same	Eq. B.1	$tg \to ta$	$\bar{t}g \to \bar{t}a$	Eq. B.6
$b\bar{b} \to ga$	Same		$bg \to ba$	$\bar{b}g \to \bar{b}a$	
$t\bar{t} \to ha$	Same	Eq. B.2	$th \to ta$	$\bar{t}h \to \bar{t}a$	Eq. B.7
$b\bar{b} \to ha$	Same		$bh \to ba$	$\bar{b}h \to \bar{b}a$	
$t\bar{t} \to Za$	Same	Eq. B.3	$tZ \to ta$	$\bar{t}Z \to \bar{t}a$	Eq. B.8
$b\bar{b} \to Za$	Same	Eq. B.4	$bZ \to ba$	$\bar{b}Z \to \bar{b}a$	Eq. B.9
$t\bar{b} \to W^+a$	$b\bar{t} \to W^-a$	Eq. B.5	$tW^- \to ba$	$\bar{t}W^+ \to \bar{b}a$	Eq. B.10
			$bW^+ \to ta$	$\bar{b}W^- \to \bar{t}a$	Eq. B.11

TABLE 6.2: Scatterings producing axions below the EWPT. We give the process (left column), the CP conjugate (central column) and the reference to the equation with the explicit analytical expression for the scattering cross section.

We list in Tab. 6.2 all processes contributing to axion production in the phase where the electroweak symmetry is broken. As done already above, we provide also the CP conjugate

process as well as the scattering cross section. The explicit expressions are too lengthy to be displayed directly in the table and we give their explicit analytical expressions in App. B.

Matching at the EWPT

We complete our discussion of production via scattering by showing how processes involving the four components of the Higgs doublet, three of which are the longitudinal components of the Z and W bosons below the EWPT, match at the point of electroweak symmetry breaking. For this reason, the Z and W components involved in the following processes are the longitudinal ones and will be denoted with an index L in the rest of this subsection. In the following, we will take the cross sections for the different processes, express all masses in terms of the Higgs VEV and run towards $v \to 0$. The processes that will match are shown in Tab. 6.3.

Processes Above EWPT	Processes Below EWPT
$t\bar{t} \to \chi_0 a \, + \, t\bar{t} \to \chi_0^c a$	$t\bar{t} \to h a \, + \, t\bar{t} \to Z_L a$
$t\bar{b} \to \chi_+ a$	$t\bar{b} \to W_L^+ a$
$b\bar{t} \to \chi_- a$	$b\bar{t} \to W_L^- a$
$t\chi_0 \to ta \, + \, t\chi_0^c \to ta$	$th \to ta \, + \, tZ_L \to ta$
$\bar{t}\chi_0 \to \bar{t}a \, + \, \bar{t}\chi_0^c \to \bar{t}a$	$\bar{t}h \to \bar{t}a \, + \, \bar{t}Z_L \to \bar{t}a$
$t\chi_- \to ba$	$tW_L^- \to ba$
$\bar{t}\chi_+ \to \bar{b}a$	$\bar{t}W_L^+ \to \bar{b}a$
$b\chi_+ \to ta$	$bW_L^+ \to ta$
$\bar{b}\chi_- \to \bar{t}a$	$\bar{b}W_L^- \to \bar{t}a$

TABLE 6.3: Scatterings producing axions involving the Higgs doublet above and below the EWPT. We consider the four components of the Higgs doublet above, and we work in unitary gauge below with the Higgs boson h and the longitudinal components Z_L and W_L of the weak bosons.

- *Neutral annihilations:* $t\bar{t} \to \chi_0 a, \quad t\bar{t} \to \chi_0^c a \, ; \quad t\bar{t} \to h a, \quad t\bar{t} \to Z_L a.$

  When considering the limit in which the Higgs VEV vanishes, the cross sections below EWPT coincide exactly with those above, as expected:

$$\sigma_{t\bar{t}\to\chi_0 a} + \sigma_{t\bar{t}\to\chi_0^c a} = \sigma_{t\bar{t}\to h a} + \sigma_{t\bar{t}\to Z_L a} = \frac{c_t^2 y_t^2}{32\pi f_a^2}. \tag{6.18}$$

- *Neutral scatterings:* $t\chi_0 \to ta, \quad t\chi_0^c \to ta\,; \quad th \to ta, \quad tZ_L \to ta.$
  $\bar{t}\chi_0 \to \bar{t}a, \quad \bar{t}\chi_0^c \to \bar{t}a\,; \quad \bar{t}h \to \bar{t}a, \quad \bar{t}Z_L \to \bar{t}a.$

  In this case, the matching can be expressed as:

$$\begin{aligned} &\sigma_{t\chi_0\to ta} + \sigma_{t\chi_0^c\to ta} = \sigma_{th\to ta} + \sigma_{tZ_L\to ta} = \\ &= \sigma_{\bar{t}\chi_0^c\to \bar{t}a} + \sigma_{\bar{t}\chi_0\to \bar{t}a} = \sigma_{\bar{t}h\to \bar{t}a} + \sigma_{\bar{t}Z_L\to \bar{t}a} = \frac{c_t^2 y_t^2}{32\pi f_a^2}, \end{aligned} \tag{6.19}$$

  where the CP conjugates give indeed the same contribution.

- *Charged annihilations:* $t\bar{b} \to \chi_+ a, \quad b\bar{t} \to \chi_- a\,; \quad t\bar{b} \to W_L^+ a, \quad b\bar{t} \to W_L^- a.$

  Analogously to the neutral case, the charged annihilations can be matched as:

$$\sigma_{t\bar{b}\to\chi_+ a} + \sigma_{b\bar{t}\to\chi_- a} = \sigma_{t\bar{b}\to W_L^+ a} + \sigma_{b\bar{t}\to W_L^- a} = \frac{c_t^2 y_t^2 + c_b^2 y_b^2}{32\pi f_a^2}. \tag{6.20}$$

- *Charged scatterings:* $t\chi_- \to ba, \quad b\chi_+ \to ta\,; \quad tW_L^- \to ba, \quad bW_L^+ \to ta\,.$
  $\bar{t}\chi_+ \to \bar{b}a, \quad \bar{b}\chi_- \to \bar{t}a\,; \quad \bar{t}W_L^+ \to \bar{b}a, \quad \bar{b}W_L^- \to \bar{t}a.$

  Finally, these set of processes match their cross sections as follows:

$$\begin{aligned} &\sigma_{t\chi_-\to ba} + \sigma_{b\chi_+\to ta} = \sigma_{tW_L^-\to ba} + \sigma_{bW_L^+\to ta} = \\ &= \sigma_{\bar{t}\chi_+\to \bar{b}a} + \sigma_{\bar{b}\chi_-\to \bar{t}a} = \sigma_{\bar{t}W_L^+\to \bar{b}a} + \sigma_{\bar{b}W_L^-\to \bar{t}a} = \frac{c_t^2 y_t^2 + c_b^2 y_b^2}{32\pi f_a^2}. \end{aligned} \tag{6.21}$$

Decay widths

The crucial ingredient for axion production via quark decays is the Lagrangian with flavour violating interactions whose explicit expression is given in Eq. 6.7. This channel is active only below the EWPT because it is kinematically forbidden at higher temperatures where all quarks are massless. For this reason, we find it convenient to rewrite it in terms of Dirac quark fields $u = (u_L\ u_R)$ and $d = (d_L\ d_R)$ in the mass eigenstate basis

$$\mathscr{L}^{(a)}_{\partial-\text{F.V.}} = \frac{\partial_\mu a}{f_a} \sum_{i,j} \left[\bar{u}_i \gamma^\mu \left(c_{V_u}^{(ij)} + c_{A_u}^{(ij)} \gamma_5 \right) u_j + \bar{d}_i \gamma^\mu \left(c_{V_d}^{(ij)} + c_{A_d}^{(ij)} \gamma_5 \right) d_j, \right] , \tag{6.22}$$

where we identify the following combinations

$$\left\{ c_{V_u}^{(ij)}, c_{A_u}^{(ij)}, c_{V_d}^{(ij)}, c_{A_d}^{(ij)} \right\} = \frac{1}{2} \times \left\{ c_u^{(ij)} + c_q^{(ij)}, c_u^{(ij)} - c_q^{(ij)}, c_d^{(ij)} + c_q^{(ij)}, c_d^{(ij)} - c_q^{(ij)} \right\} . \tag{6.23}$$

The decay process $q_i \to q_j a$ and its CP conjugate $\bar{q}_i \to \bar{q}_j a$, which can happen for both up- and down-type quarks, have the following decay width

$$\Gamma_{q_i \to q_j a} = \frac{m_i^3}{16\pi f_a^2}\left(c_{V_q}^{(ij)^2} + c_{A_q}^{(ij)^2}\right)\left(1 - \frac{m_j^2}{m_i^2}\right)^3 . \tag{6.24}$$

Here, the ratio $\frac{m_j}{m_i}$ can safely be neglected as it leads to non observable changes in ΔN_{eff}. The decays relevant to our analysis and their CP conjugates are displayed in Tab. 6.4 with their corresponding decay widths.

Axion Production Above EWSB		
Process	CP Conjugate	$\Gamma_{i\to ja} \times 16\pi f_a^2/m_i^3$
$t \to ca$	$\bar{t} \to \bar{c}a$	$c_{V_u}^{(tc)^2} + c_{A_u}^{(tc)^2}$
$t \to ua$	$\bar{t} \to \bar{u}a$	$c_{V_u}^{(tu)^2} + c_{A_u}^{(tu)^2}$
$b \to sa$	$\bar{b} \to \bar{s}a$	$c_{V_d}^{(bs)^2} + c_{A_d}^{(bs)^2}$
$b \to da$	$\bar{b} \to \bar{d}a$	$c_{V_d}^{(bd)^2} + c_{A_d}^{(bd)^2}$

TABLE 6.4: Quark decays producing axions. In the first two columns we list the process and its CP conjugate, and they both have the same decay widths listed on the third column.

6.1.2 Impact of thermal axions on ΔN_{eff}

The physical observable of interest in our work is the effective number of neutrinos N_{eff} induced by hot axions. Big bang nucleosynthesis [289] and CMB experiments [13, 236] probe this quantity, and we focus on the latter case as it is the most sensitive. Here, we first review briefly how to compute N_{eff} from a given axion production source and then we quantify the N_{eff} generated from all processes analysed in the previous section.

The effective number of neutrinos is related to the radiation energy density ρ_{rad} as

$$\rho_{\text{rad}} = \rho_\gamma \left(1 + \frac{7}{8}\left(\frac{T_\nu}{T_\gamma}\right)^4 N_{eff}\right) , \tag{6.25}$$

where ρ_γ is the photon energy density. Any relativistic particle with a non-negligible energy density, like neutrinos or axions, will contribute to N_{eff}. In particular, we are interested in

deviations from the ΛCDM value caused by axions

$$\Delta N_{eff} \equiv N_{eff} - N_{eff}^{\Lambda\text{CDM}} = \frac{8}{7}\left(\frac{11}{4}\right)^{4/3}\frac{\rho_a}{\rho_\gamma}\,, \tag{6.26}$$

with $N_{eff}^{\Lambda\text{CDM}} = 3.046$ and where ρ_a is the axion energy density.

In order to connect with the numerical solutions of Boltzmann equations, we find it convenient to rewrite ΔN_{eff} in terms of the comoving axion abundance $Y_a \equiv n_a/s$. Here, n_a is the axion number density and $s = 2\pi^2 g_{*s} T^3/45$ is the entropy density with g_{*s} the number of entropic degrees of freedom. The photon energy density can also be expressed as follows

$$\rho_\gamma = 2 \times \frac{\pi^2}{30}\left(\frac{45\,s}{2\pi^2 g_{*s}}\right)^{4/3}\,, \tag{6.27}$$

whereas the axion energy density is related to the number density via

$$\rho_a = \frac{\pi^2}{30}\left(\frac{\pi^2 n_a}{\zeta(3)}\right)^{4/3}\,. \tag{6.28}$$

We combine these two equations and find

$$\Delta N_{eff} \simeq 74.85\, Y_a^{4/3}\,, \tag{6.29}$$

where we used the value of g_{*s} at recombination $g_{*s} = 43/11$.

We determine the asymptotic value of the axion number density by solving the associated Boltzmann equation[13]. The differential equation describing how the axion number density evolves with time reads

$$\frac{d}{dt}n_a + 3Hn_a = \left[\sum_S \bar{\Gamma}_S + \sum_D \bar{\Gamma}_D\right]\left(n_a^{\text{eq}} - n_a\right)\,. \tag{6.30}$$

Here, H is the Hubble parameter quantifying the expansion rate of the universe and the superscript "eq" for number density denotes expressions valid when particles are in thermal equilibrium. The two terms on the right hand side denote, respectively, the sum over thermally averaged scattering and decay rates involving the axion and their explicit expressions

[13]The lowest temperature considered when solving the Boltzmann equation can be dangerous if chosen too close to the QCDPT. The effect on the final result due to this parameter is briefly discussed in App. C.

read

$$\bar{\Gamma}_S = \frac{g_i g_j}{32\pi^4 n_a^{\rm eq}} T \int_{s_{min}}^{\infty} ds \, \frac{\lambda(s,m_i,m_j)}{\sqrt{s}} \, \sigma_{ij\to ka}(s) \, K_1\left(\frac{\sqrt{s}}{T}\right) , \tag{6.31}$$

$$\bar{\Gamma}_D = \frac{n_i^{\rm eq}}{n_a^{\rm eq}} \frac{K_1\left(\frac{m_i}{T}\right)}{K_2\left(\frac{m_i}{T}\right)} \Gamma_{i\to ja} \, . \tag{6.32}$$

The function λ is defined as follows

$$\lambda(x,y,z) \equiv \left[x-(y+z)^2\right]\left[x-(y-z)^2\right] , \tag{6.33}$$

whereas the minimum center of mass energy is $s_{min} = \text{Max}\left((m_i+m_j)^2, m_k^2\right)$. The general expression for the equilibrium number density is

$$n_i^{\rm eq} = g_i \frac{m_i^2}{2\pi^2} T K_2\left(\frac{m_i}{T}\right) , \tag{6.34}$$

where g_i stands for the degrees of freedom of the particle i and $K_n(z)$ are the modified Bessel function of the second kind.

We find it convenient to switch to dimensionless variables. We define $x = m/T$, where m is taken to be the mass of the heaviest particle in the process, and the Boltzmann equation for Y_a reads

$$sHx\frac{dY_a}{dx} = \left(1-\frac{1}{3}\frac{\ln g_{*s}}{\ln x}\right)\left(\sum_S \gamma_S + \sum_D \gamma_D\right)\left(1-\frac{Y_a}{Y_a^{\rm eq}}\right) , \tag{6.35}$$

where $\gamma_{D,S} \equiv n_a^{\rm eq}\,\bar{\Gamma}_{D,S}$. We solve now the equation numerically for the different axion production processes. Analytical approximations can be found for the cases below thermal abundance and at large f_a, leading to $\Delta N_{eff} \propto f_a^{-8/3}$ [240].

Model Independent results

We first perform a model-independent operator analysis. For flavour conserving couplings, we switch on separately the top-axion vertex c_t and the bottom-axion vertex c_b, whereas we account for the decay of each quark for flavour violating interactions.

We begin with scatterings and we set $c_i = 1$ throughout this section; this is equivalent to interpreting f_a as f_a/c_i for each specific coupling. One of our main results is a smooth treatment of the EWPT, and this is relevant once one accounts for axion production controlled

by processes with the top (anti-)quark on the external legs. We show in Fig. 6.1 the contribution to ΔN_{eff} from each one of these processes as a function of f_a.

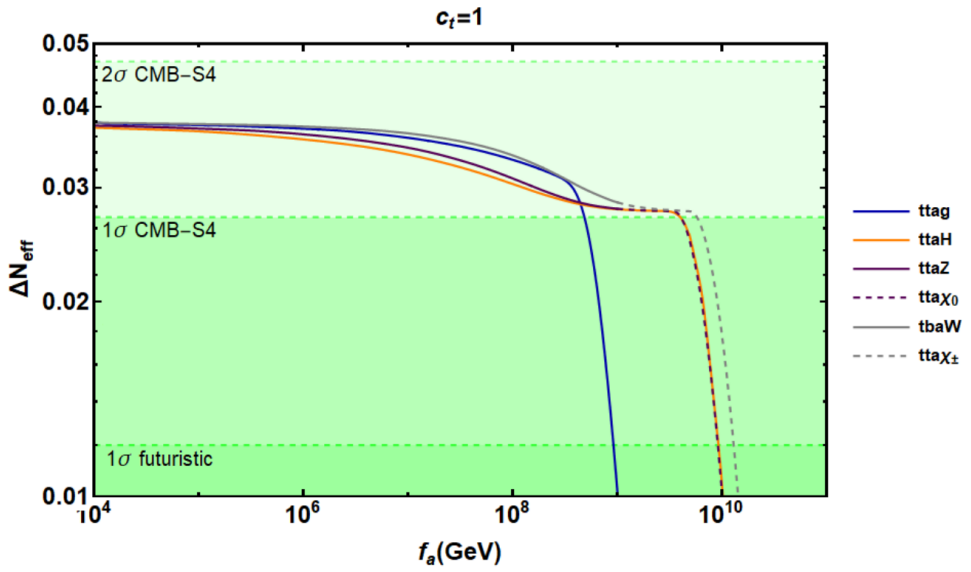

FIGURE 6.1: Contribution to ΔN_{eff} from individual binary scatterings with the top quark involved. The dimensionless coupling is set to $c_t = 1$. Each line denotes all processes with the external legs denoted in the legenda. The initial temperature here is set to $T_I = 10^4$ GeV and the initial axion abundance has been assumed to be zero.

Production via scatterings with gluons is not altered by this threshold. However, processes with longitudinal weak gauge bosons feel this transition since they become massive below the EWPT. Dashed lines correspond to calculations in the electroweak symmetric phase whereas solid lines hold below the EWPT. Our lines for each individual process, with the relevant degrees of freedom at the associated temperature, are indeed smooth across the two phases.

The physical observable is actually the combined effects of these individual lines. We add them up and we show our prediction for ΔN_{eff} in Fig. 6.2 together with the associated quantity from the bottom-axion vertex c_b. Solid lines correspond to the extreme case in which the initial temperature T_I (*i.e.* the reheating temperature, if the Universe went through a stage of Inflation) was very close to the EWPT, and assuming the initial abundance of axions to be zero at $T = T_I$. The opposite extreme case, dot-dashed lines, correspond to an initial thermal abundance of axions at a given initial temperature above the EWPT. Finally, we show predictions from one particular process which remains the same at all temperatures and whose strength grows with the temperature, the purely gluonic $gg \to ga$. In order to take it into account, we

interpolated the result from Ref. [239] and assumed that it decreases always with the same power of temperature, extrapolating the results to lower temperatures.

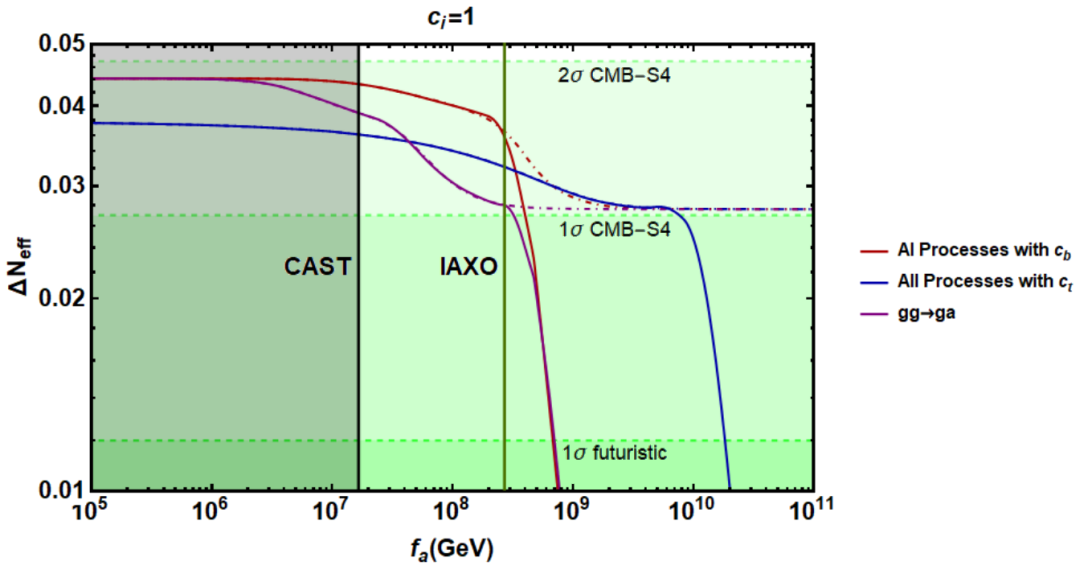

FIGURE 6.2: Impact on ΔN_{eff} following an operator-by-operator analysis: for each line, we consider the axion coupling only to one particle i, with coupling constant $c_i = 1$. The initial temperature here is set to $T_I = 10^4$ GeV and the initial axion abundance has been assumed to be zero (thermal) for the solid (dot-dashed) lines. The CAST limit and IAXO prospect are shown as a shaded region and a vertical green line respectively, assuming $c_{a\gamma\gamma} = 1$.

Fig. 6.2 shows that the axion can thermalize through the scatterings with the top, below or around the EWPT, for $f_a \lesssim 10^{10}$ GeV even with zero initial axion abundance close to the EWPT. This means that, independently of the initial conditions, it is possible to be above the 1σ region of CMB-S4. If one assumes an initial thermal abundance, as shown in the same figure with dot-dashed lines, such initial seed automatically gives a signal of about 1σ, as already stressed in previous works [287].

For both choices of initial conditions, the signal increases as f_a lowers, reflecting the fact that the axion decouples at a lower temperature where the number of degrees of freedom in thermal equilibrium $g_*(T_{\rm dec})$ is smaller. For $f_a \lesssim 10^9$ GeV the processes involving the axion-bottom coupling become efficient and yields a larger ΔN_{eff} which roughly saturates at $\Delta N_{eff}(g_*(m_b))$ for $f_a \lesssim 10^8$ GeV. Finally, we note that the axion-gluon scattering channel is always less efficient than the other scattering channels, except for $f_a \lesssim 5 \times 10^7$ GeV where it becomes more efficient than the axion-top scatterings.

We also show the constraints from CAST [290] and the forecasted sensitivity of IAXO [291, 292]. Although these experiment probe the axion-photon coupling, we can still compare both

forecasts assuming $c_{a\gamma\gamma} = 1$. Interestingly, the parameter space probed by IAXO corresponds to the region where ΔN_{eff} is above the 1σ level. These multiple detection channels will be very useful in case of a detection.

As discussed in the paragraphs above, the initial conditions for our Boltzmann equation evolution depend on whether axions thermalize or not above the EWPT. For example, for $f_a \sim 10^9$ GeV the axion thermalizes already at $T \sim$ TeV due to the interactions with the Higgs [239]. In general, this depends on the value of the reheating temperature. This interplay between the axion scale f_a and the initial (reheating) temperature, when zero initial abundance is assumed for the axion, can be seen more clearly in Fig. 6.3. Here, we show the dependence of ΔN_{eff} on the reheating temperature and f_a by considering purely gluonic processes, which must be present in any QCD axion model, following the procedure from before. The figure shows that the axion always thermalizes, independently of f_a, as long as the reheating temperature is set high enough.

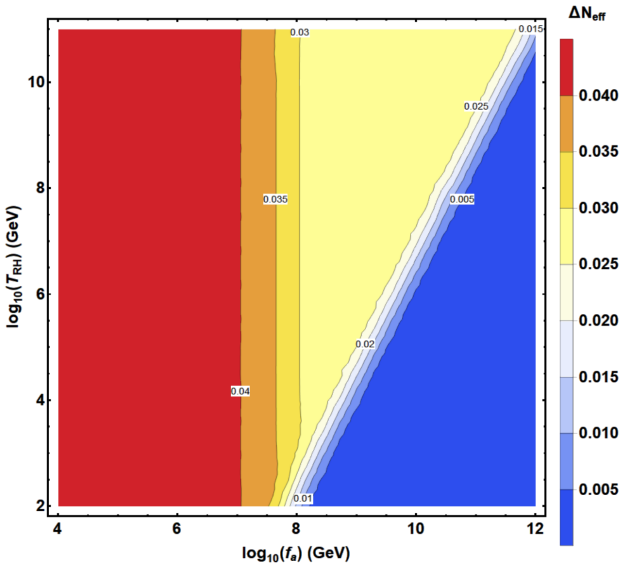

FIGURE 6.3: ΔN_{eff} as a function of f_a and the reheating temperature with initial axion abundance set to zero. In this figure only purely gluonic processes have been included.

Turning now to the possibility of having flavour violating couplings, the interactions in Eq. 6.22 lead to the following possible decays below the EWPT

$$\begin{aligned} t &\to c\,a\,, & t &\to u\,a\,, \\ b &\to s\,a\,, & b &\to d\,a. \end{aligned} \tag{6.36}$$

The decays $c \to u\,a$ and $s \to d\,a$ are not taken into consideration, although they should be significant, because the relevant temperatures here should be around the QCD phase transition, where we do not have control on the complicated strongly coupled physics.

The couplings in Eq. 6.22 also lead to quark annihilation into a W and an axion with non-diagonal flavour transitions: the flavour change may be present in the coupling with the W and/or with the axion. These processes, however, are subdominant with respect to those with only flavour conserving couplings and for these reasons they are not discussed here. The only potentially interesting processes would be $t\,\bar{c} \to Z\,a$ and $t\,\bar{s} \to W\,a$, but the contribution from these processes is of the same order of magnitude as that coming from the processes that involve flavour-conserving couplings, namely $t\,\bar{t} \to Z\,a$ and $t\,\bar{b} \to W\,a$, which were already discussed above. Since the results would be essentially the same, we will not include the analysis of such processes in this work.

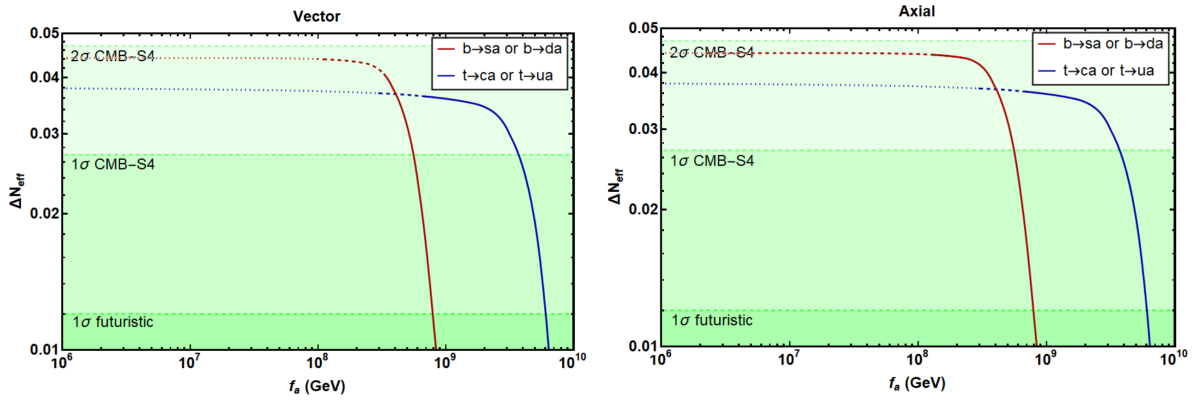

FIGURE 6.4: Effect of quark decays on N_{eff}. The figure on the left (right) assume only vector (axial) couplings, assumed to be equal to one. In these figures solid lines escape all bounds, whereas dotted lines are ruled out. Dashed lines correspond to the situation where one of the two possible decays channels is still allowed.

We show predictions for ΔN_{eff} generated from the different quark decays in Fig. 6.4. As already done before, we switch on only one coupling at a time. Both top decay channels yield the same ΔN_{eff} but they are subject to different bounds, and the same holds for bottom decays. In spite of the strong bounds on flavour violating couplings, given in Ref. [203] and reviewed in Sect. 4.3, the signal is above 1σ in most of the cases.

Finally, we appreciate how the range of PQ breaking scales that could be detected through these hot axions in some frameworks overlap with that of cold axion dark matter. This is true for both scatterings and decays. In particular, if the PQ symmetry is broken after inflation there is an additional contribution to axion dark matter from topological defects. Axions produced

non-thermally through the decays of such defects are cold, and they are a viable dark matter candidate. Although there is a large theoretical uncertainty of this contribution, we claim for the benchmark value $f_a \gtrsim \mathcal{O}(10^9)$ GeV [293, 294] it could be possible to measure both hot and cold axions at the same time.

UV Complete Models

This section is devoted to the analysis of three specific models already discussed in this thesis: the so-called DFSZ model [89, 90], KSVZ model [91, 92] and the Minimal Flavor Violating Axion (MFVA) model [103].

In the DFSZ case, the axion couplings are flavour-blind and, using the notation of Eqs. 6.12 and 6.13, non-vanishing couplings with the top and bottom quarks are present, satisfying the following relation,

$$c_t + c_b = \frac{1}{3}\,. \tag{6.37}$$

In the limit where all the scalar components are heavy, except for what would become the longitudinal components of the gauge bosons, the physical h and the axion, this model matches the general analyses performed in the previous sections. Notice that, dealing with a well-defined model, the $c_{a\gamma\gamma}$ coupling can be predicted in terms of the axion-fermion couplings: $c_{a\gamma\gamma} = 2(4c_t + c_b + 3c_\tau)$, where c_τ is the coupling with leptons and its defined in a similar way as c_t and c_b in Eqs. 6.12 and 6.13. Leptons can couple to the axion as the up-type quarks do or as the down-quarks do, and in general this leads to different values for the axion-photon coupling.

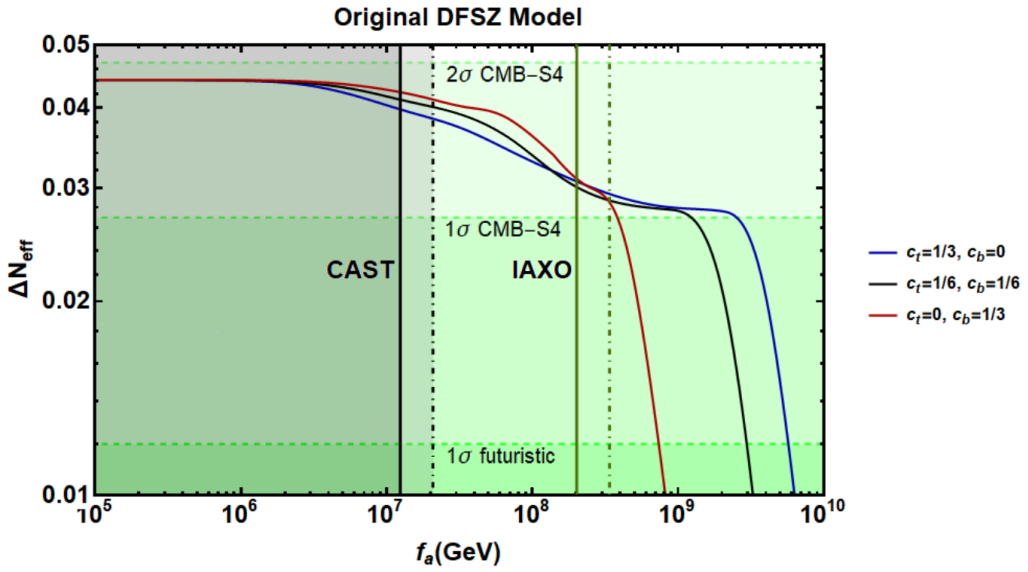

FIGURE 6.5: Total impact on ΔN_{eff} for a classic DFSZ axion. Three benchmarks couplings of the DFSZ axion to top and bottom quarks have been considered. The initial temperature here is set to $T_I = 10^4\, GeV$ and the initial axion abundance has been assumed to be zero. The CAST limit and IAXO prospect are shown: solid (dot-dashed) lines correspond to $c_{a\gamma\gamma} = 8/3\ (2/3)$, when charged leptons couple to the same higgs doublet as the down-quarks (up-quarks) do.

The contributions to ΔN_{eff} for the DSFZ model can be seen in Fig. 6.5. Three representative cases are considered, in order to cover the entire range of values for c_b and c_t: with $c_t = 1/3$ and $c_b = 0$ (in blue in the plot), with $c_t = 0$ and $c_b = 1/3$ (in red), and with $c_t = c_b = 1/6$ (in black). For the CAST limit and IAXO prospect, the continuous line corresponds to the case with the smallest value for $c_{a\gamma\gamma} - 1.92$, while the dot-dashed corresponds to the one with the most restrictive value of $c_{a\gamma\gamma} - 1.92$.

In the KSVZ model, the axion does not couple to the SM fermions at tree-level, but only to exotic quarks that enrich the SM fermionic spectrum. In this case, the only sizeable contribution to ΔN_{eff} arises from the axion coupling to gluons, as axion couplings to SM fermions are induced only at 2-loops and therefore are strongly suppressed. Fig. 6.6 shows the predictions for ΔN_{eff} for this model. The range of axion-photon coupling considered here is $c_{a\gamma\gamma} - 1.92 \in [-0.25,\ 12.75]$, motivated by several possible UV completions of a KSVZ axion [295].

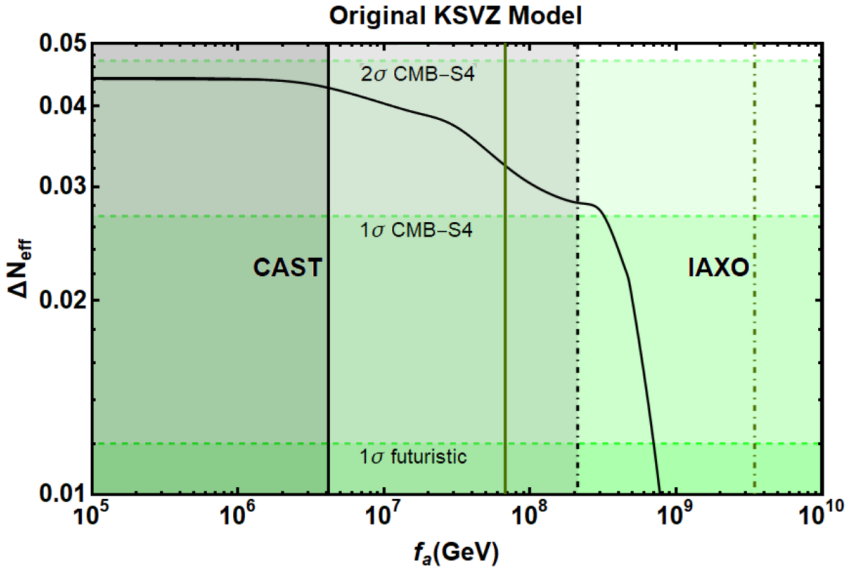

FIGURE 6.6: Total impact on ΔN_{eff} for a classic KSVZ axion. We set the initial temperature $T_I = 10^4\, GeV$ and the initial axion abundance to zero. The CAST limit is shown as a shaded region, with solid lines corresponding to $c_{a\gamma\gamma} - 1.92 = -0.25$ and dot-dashed for $c_{a\gamma\gamma} - 1.92 = 12.75$.

The MFVA model [103], instead, provides an effective description of the axion couplings with SM fields, once the flavour symmetry of the Minimal Flavor Violation framework [41, 42] is implemented in the Lagrangian. The axion couplings to fermions are universal within the same type of quarks and therefore are flavour conserving. Moreover, the axion coupling to up-type quarks is vanishing at leading order, and therefore the largest interactions are with the down-type quarks, and in particular with the bottom, due to Yukawa suppressions. This fact sensibly affects the results presented in the model independent analysis, where the axion-top coupling was dominating all the contributions. In particular, the processes $b + \bar{b} \to g + a$ and $t + \bar{b} \to W^+ + a$ (proportional to the $ab\bar{b}$ coupling), that are proportional to the bottom quark Yukawa, were irrelevant when the axion coupled to the top, but now become crucial, as they are the only important contributions apart from the purely gluonic ones.

The coefficients describing axion couplings with bottoms c_b and with photons $g_{a\gamma\gamma}$ acquire the following values in the MFVA model,

$$c_b = \frac{1}{3}\,, \qquad\qquad g_{a\gamma\gamma} = \frac{\alpha_{\rm em}}{2\pi}\frac{1}{f_a}\left(\frac{8}{3} - 1.92\right)\,, \tag{6.38}$$

and the final result for ΔN_{eff} is shown in Fig. 6.7.

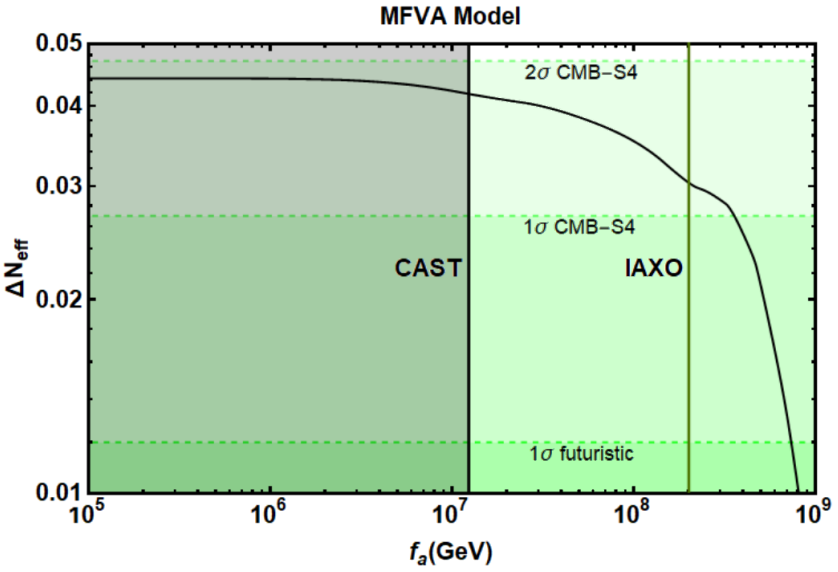

FIGURE 6.7: Total impact on ΔN_{eff} for the MFVA model. The initial temperature here is set to $T_I = 10^4$ GeV and the initial axion abundance is set to zero. The CAST limit and IAXO prospect are shown as a shaded region and a vertical green line, respectively.

As it can be seen, all models give the same contribution at low f_a. At high f_a, instead, the DFSZ model gives the largest abundances since it couples to all SM fermions already at tree level. For such a model one can reach a detectable axion abundance even in the range $f_a \approx 10^9 - 10^{10}$ GeV. If the PQ symmetry is broken after inflation and not restored afterwards, the abundance of cold axion dark matter receives a significant contribution from topological defects [296–299]. The detailed amount from this source suffers a significant theoretical uncertainty [293, 294], but it is worth keeping in mind that in such a low f_a region axion cold dark matter may coexist with detectable hot axions. Within the DFSZ framework, PQ symmetry in the post inflationary scenario has to be broken also explicitly to avoid the domain wall problem [300–303].

Moreover, there is a window for f_a between 10^7 GeV and 2×10^8 GeV that can be explored by IAXO and is also above the 1σ level for the CMB-S4 experiments, where the models can be differentiated. This could imply an exciting opportunity to not only detect an effect of the axion, but also tell apart different invisible axion models.

When considering specific models with flavour violating axion couplings, like the Axiflavon [106] or Flaxion [105], they give a sizeable contribution to $\Delta N_{eff} \gtrsim 0.01$ only for axion scales below $f_a \lesssim 10^9$ GeV, a region which is largely excluded in those models due to the bound coming from the $K^+ \to \pi^+ a$ decay, being therefore irrelevant in this analysis.

6.2 Cosmic Imprints of XENON1T Axions

In this second section of the chapter we will study the compatibility between the observable previously discussed, ΔN_{eff}, and the anomaly observed by the XENON1T experiment. We have already discussed the possibility of looking for axions through its coupling to photons, in colliders and flavour searches and, lastly, through its impact on the thermal history of the Universe, but these are not the only ways to search for axions.

Another promising strategy to discover these particles is by searching for electron recoils induced by the absorptions of axions produced in the Sun. Recently, the XENON1T experiment has reported an excess in the number of electron recoil events in the energy range $1-7\,\mathrm{keV}$ [283]. Among several plausible explanations, solar axions stood up with a 3.5σ statistical significance. However, one should take the solar axion interpretation with the necessary caution. Other signal interpretations that do not require new physics, such as a higher concentration of tritium [283, 304, 305], remain viable. Moreover, the value of the axion-electron coupling favored by XENON1T is in sharp tension with stellar cooling bounds [283, 306] (See also Refs. [307, 308]), though some models appear to be able to escape them [309].

In this section, with the above caveats in mind, we correlate the solar axion interpretation of the XENON1T excess with a distinct cosmological signal, the impact of axions on the effective number of neutrinos, ΔN_{eff}. The observed events inform us that axions couple to electrons, and this leads to the natural expectation that it could couple to other SM fermions as well. We consider a few plausible examples where the axion: (i) couples to all SM fermions with the same strength; (ii) couples at tree level only to one SM fermion and this induces a nonzero coupling to electrons at one loop; (iii) is part of a well defined framework that indeed has couplings to all SM fermions, the DFSZ case [89, 90]. In the following, we will show how thermal axions produced and their effect on ΔN_{eff} in these scenarios may be linked to the XENON1T excess.

We discuss axion production via fermion scattering in Sec. 6.2.1, providing cross sections for the processes contributing to the signal in ΔN_{eff} and the related Boltzmann equations. We consider two main classes of explicit realizations: a non-anomalous ALP coupled to SM fermions in Sec. 6.2.2, and the QCD axion in Sec. 6.2.3. Measuring a non-vanishing contribution to ΔN_{eff} would provide the additional information discussed in Sec. 6.3, while deferring radiatively induced axion couplings to App. D.

6.2.1 Thermal axions production via fermion scattering

We consider axion production via fermion scattering below the electroweak phase transition (EWPT). These processes are mediated by the following dimension 5 contact interactions[14]

$$\mathcal{L}_{a\psi\psi} = \frac{\partial_\mu a}{2f_a} \sum_\psi c_\psi \bar{\psi}\gamma^\mu\gamma^5\psi \,, \tag{6.39}$$

with a and ψ the axion and SM fermions, respectively. The quantity f_a is the axion decay constant, and we implicitly consider microscopic models where the only new degree of freedom accessible below the scale f_a is the axion. The dimensionless coefficients c_ψ encode unknown UV dynamics and can be thought as the result of integrating out heavy physics at energy scales above f_a. They are energy dependent and we provide details of their renormalization group evolution (RGE) in App. D.

There are two leading production channels as we discussed previously in this chapter: fermion/antifermion annihilation ($\bar{\psi}\psi \to Xa$) and Compton-like scattering ($\psi X \to \psi a$, and the same with the antifermion $\bar{\psi}$). The particle X can be either a gluon or a photon depending on whether the SM fermion ψ carries colour charge[15]. For colored fermions, namely SM quarks q, axion production is driven by processes with gluons, whose cross sections read [240]

$$\sigma_{\bar{q}q\to ga} = \frac{c_q^2 g_s^2 x_q}{9\pi f_a^2} \frac{\tanh^{-1}\left(\sqrt{1-4x_q}\right)}{1-4x_q} \,, \tag{6.40}$$

$$\sigma_{qg\to qa} = \frac{c_q^2 g_s^2 x_q}{192\pi f_a^2} \frac{4x_q - 2\ln(x_q) - x_q^2 - 3}{1-x_q} . \tag{6.41}$$

Here, $x_\psi = m_\psi^2/E_{\rm CM}^2$ and $E_{\rm CM}$ is the energy in the center of mass frame. If the SM fermion responsible for axion production is a lepton, processes with photons would dominate and they have cross sections [220]

$$\sigma_{\ell^+\ell^-\to\gamma a} = \frac{c_\ell^2 e^2 x_\ell}{4\pi f_a^2} \frac{\tanh^{-1}\left(\sqrt{1-4x_l}\right)}{1-4x_l} \,, \tag{6.42}$$

$$\sigma_{\ell^\pm\gamma\to\ell^\pm a} = \frac{c_\ell^2 e^2 x_\ell}{32\pi f_a^2} \frac{4x_\ell - 2\ln(x_\ell) - x_\ell^2 - 3}{1-x_\ell} . \tag{6.43}$$

[14] This Lagrangian can be shown to be equivalent to that of Eq. 6.6 after going to the mass basis below the EWPT and using the conservation of the vectorial fermionic current, with $c_\psi = -c_q + c_{u,d}$.

[15] Processes with a Higgs, W or Z boson are also possible but subleading below the EWPT, so they are not considered in this part.

As it is manifest from these expressions and we have discussed previously, cross sections are proportional to m_ψ^2 and therefore lighter fermions need a smaller f_a/c_ψ to thermalize. Since $\Delta N_{eff} \propto g_{*s}(T_D)^{-4/3}$, the later the axion decouples the larger the signal would be; processes with light fermions, if efficient, would give the leading contribution.

We compute the resulting ΔN_{eff} by solving the Boltzmann equation as we did before, stopping the evolution described by the Boltzmann equation at 1 GeV. For production driven by the top quark as well as for the one driven by leptons this is not an issue. However, for the bottom and for the charm this is a potential serious problem, as discussed in App. C. In particular for the charm, axion production is likely to be efficient also below the GeV scale, and since g_{*s} is rapidly changing around that temperature this translates into a significant theoretical uncertainty on the amount of axions. Production via pion scattering [310–313] could give some additional contribution for the values of f_a we are interested in [16]. For these reasons, we should interpret the output of our calculations for bottom and charm as a lower bound on the resulting ΔN_{eff}. Moreover, we assume zero axion abundance at temperatures slightly above the EWPT. An initial abundance could also be present but that would depend on other aspects such the reheating temperature and on the value of g_{*s} at higher temperatures [17].

In the next two sections, we study these processes in various setups corresponding to different choices for UV fermion couplings as well as different relations between them and the ones to SM gauge bosons.

6.2.2 Non-anomalous ALPs

We consider ALPs arising from the spontaneous breaking of a non-anomalous symmetry. For this reason, at the symmetry breaking scale f_a we have only the couplings to fermions in Eq. 6.39 and no couplings to gauge bosons. Nevertheless, dimension 5 couplings to gauge bosons can be generated as a consequence of threshold corrections, proportional to $(m_a/f_a)^2$, once we integrate out SM fermions [187]. ALPs contributing to dark radiation must be relativistic between the epoch of matter-radiation equality and recombination. This results into

[16] Note however that for $f_a \gtrsim 5\times 10^7$ GeV, which is the case for the parameter space region analysed in this paper, Eq. 6.44, the rates given in [311] would give decoupling temperatures above 200 MeV. For these temperatures we enter the QCD phase transition where we cannot assume the existence of thermal pions.

[17] Assuming an initial axion abundance due to scatterings that decouple at $T_D \gg \mathcal{O}(100)$ GeV [238, 239] would simply flatten the curves of the ΔN_{eff} predictions at large f_a to the equilibrium value, which is at most the value obtained assuming the SM with no extra degrees of freedom at such T_D, $\Delta N_{eff} \simeq 0.027$, see [220, 240].

the upper bound $m_a \lesssim \mathcal{O}(0.1)$eV, and threshold corrections are negligible for these masses. We account for coupling to photons in the next section when we study the QCD axion case.

We define each case studied in this section by a choice of Wilson coefficients $c_\psi(f_a)$ at the UV scale f_a. The resulting couplings at low energy, c_ψ, can be found according to the RGE prescription provided in App. D. The low-energy axion-electron interaction that we need in order to address the XENON1T excess lies in the range

$$\frac{f_a}{c_e} \equiv \frac{m_e}{g_{ae}}\bigg|_{\text{XENON1T}} \simeq (1.46 - 1.96) \times 10^8\,\text{GeV}\,. \tag{6.44}$$

This could turn out to be the case both because the axion couples to electrons at the high scale f_a ($c_e(f_a) \neq 0$), or because the low-energy coupling c_e is induced by radiative corrections. In the latter case, we need the fermion couplings at the UV scale illustrated in Fig. 6.8.

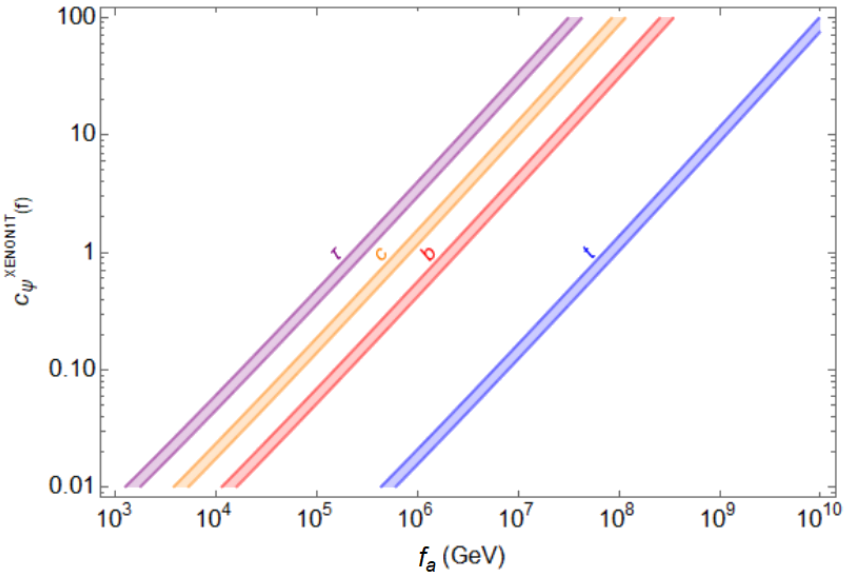

FIGURE 6.8: Relation between the axion-fermion coupling $c_\psi(f)$ at the UV scale and the scale f_a itself that we need in order to generate a radiative coupling to the electron consistent with the XENON1T excess.

Democratic ALP

The first case we consider is the *democratic* ALP where the axion has democratic ($c_\psi \sim 1$) and flavor conserving couplings to all fermions; constraints on flavor violating couplings [203] are too stringent and they do not allow a feasible explanation of the XENON1T excess. This

scenario can be motivated in two different ways: one can assume that all fermions have couplings of order one in the UV, or one can consider an axion-top coupling of order unity in the UV ($c_t(f_a) \sim 1$) and RGE would generate axion couplings $c_\psi \sim 1$ at low energy to all fermions.

We set $c_\psi = 1$ and the signal in ΔN_{eff} is dominated by axion-heavy quark scatterings. We solve the Boltzmann equation with the cross-sections given in Eqs. B.1 and B.6 assuming zero axion abundance at temperatures above the EWPT. The results are shown in Fig. 6.9. For f_a in the XENON1T window the scatterings with the charm and bottom dominate the signal and yield ΔN_{eff} slightly above 0.04.

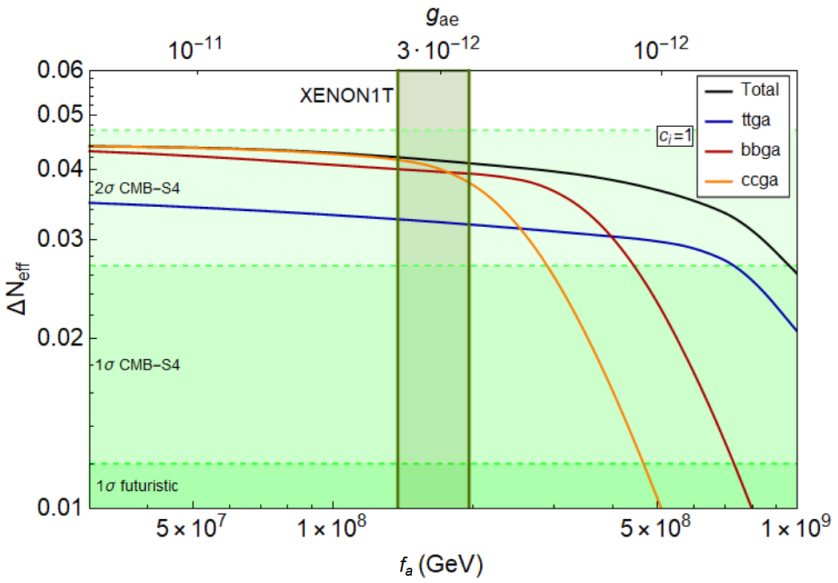

FIGURE 6.9: ΔN_{eff} in the democratic case where the relevant channels are scatterings with heavy quarks c, b, t. We assumed no initial axion abundance above the EWPT and integrated the Boltzmann equation down to 1 GeV to avoid getting too close to strongly coupled regimes. Green bands represent the forecasted sensitivity of CMB-S4 experiments [236]. Notice that the XENON1T window is in tension with the bound $f_a \gtrsim 1.9 \times 10^9$ GeV coming from stellar cooling [314].

Loop-induced electron coupling

The second scenario we study is the one where the axion-electron coupling at low energies is radiatively induced from an axion-fermion coupling ($\psi = \tau, c, b$ or t) at the UV scale. The values of $c_\psi(f_a)$ needed to explain the XENON1T excess are given in Fig. 6.8 for each fermion [18]. For each case, we assume a single $c_\psi(f_a)$ to be nonzero at the UV scale and we solve the Boltzmann equation including all the radiatively induced couplings at low energy.

[18] We do not consider the muon because the coupling needed to generate the correct g_{ae} is of order $c_\mu(f_a)/f_a \sim 10^{-4}\text{GeV}^{-1}$, which is disfavored by about a few orders of magnitude by supernova constraints [220, 315–317].

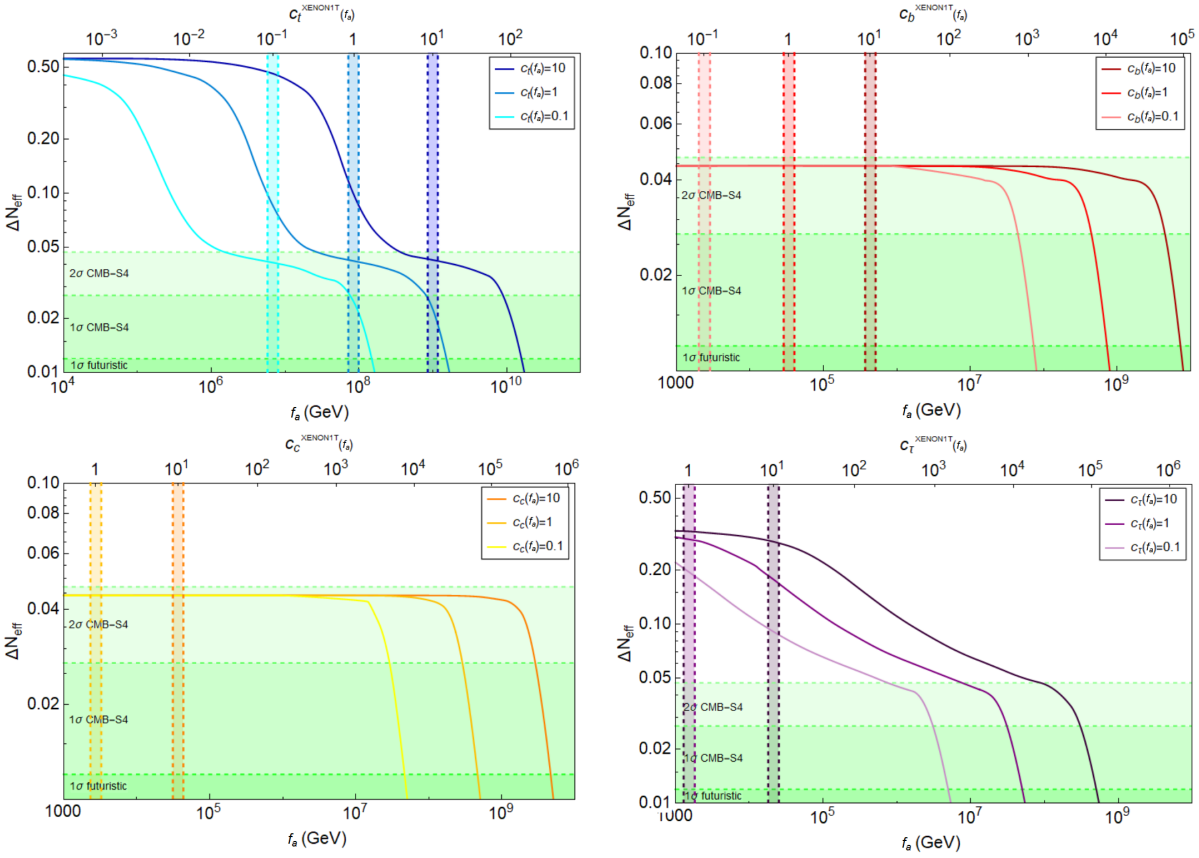

FIGURE 6.10: ΔN_{eff} as a function of f_a for a few values of $c_\psi(f_a)$ in the scenario where the axion-electron coupling is generated at loop-level. We assumed no initial abundance of axions above the EWPT. For quarks we stopped the Boltzmann equation at 1 GeV to avoid getting too close to strongly coupled regimes. The upper horizontal axis indicates the value of $c_\psi(f_a)$ needed for any given f_a to explain the XENON1T excess. Green bands are the forecasted sensitivity of CMB-S4 experiments [236]. Notice that the XENON1T window is in tension with the bound $f_a/c_e \gtrsim 1.9 \times 10^9$ GeV coming from stellar cooling [314].

Our predictions for ΔN_{eff} as a function of f_a for different values of $c_\psi(f_a)$ are shown in Fig. 6.10. In the upper horizontal axis we show the value of $c_\psi(f_a)$ needed to explain the XENON1T excess for the associated value of f_a. The predicted ΔN_{eff} for each fermion is quite sharp in this loop-induced scenario because $c_\psi(f_a)/f_a$ is mostly fixed by the RGE (up to logarithmic corrections and the experimental uncertainty in g_{ae}).

In the case of the top, upper left plot, the XENON1T region corresponds to $\Delta N_{eff} \sim 0.04$ and $f_a = (6 \times 10^6, 10^9)$ GeV for $c_t(f_a)$ in the window $0.1 - 10$. Note that in this case the radiatively induced couplings to others fermions (μ, τ, c and b) are relevant and so we accounted for several channels to produce the axion.

For bottom and charm, respectively upper right and lower left plot, the axion is in thermal equilibrium at 1 GeV for couplings in the XENON1T region. This is the temperature at which

we stop the Boltzmann equation for quarks, and the relic abundance saturates at $\Delta N_{eff} = 13.8\, g_{*s}^{-4/3}|_{T=1\text{GeV}}$ for lower values of f_a. Thus the prediction of $\Delta N_{eff} \simeq 0.044$ should be understood for these cases as a lower bound on the signal. The range of f_a needed to get the right loop-induced c_e is, for the bottom, $f_a = \left(2 \times 10^3, 5 \times 10^5\right)$ GeV for $c_b(f_a) = (0.1, 10)$ and, for the charm, $f_a = \left(2 \times 10^3, 4 \times 10^4\right)$ GeV in the window $c_c(f_a) = (1, 10)$.

Finally, we look at the τ, lower right plot. This case is quite interesting because the axion thermalizes at a much lower temperature and the calculation is still under control since it does not involve QCD. The relative signal is boosted to values of $\Delta N_{eff} \simeq 0.3$ and $f_a = \left(10^3, 3 \times 10^4\right)$ GeV for $c_\tau(f_a) = (1, 10)$. Such a large value of ΔN_{eff} is already now within the 2σ sensitivity region of the latest CMB experiments. In particular, although CMB and LSS data alone do not hint at a non-zero value of ΔN_{eff} [13], when including SH_0ES 2019 local Hubble constant measurement of H_0 [216] there is a shift of the central value towards $\Delta N_{eff} = 0.26^{+0.16}_{-0.15}$ [318] (or $\Delta N_{eff} = 0.28^{+0.16}_{-0.17}$ [319] adding also the Pantheon Supernova dataset) which is in remarkable agreement with the above prediction. Such values will be tested also by forthcoming CMB experiments, such as LiteBIRD [**?**], Simons Observatory [320] and CMB-S4 [236].

6.2.3 QCD axion

In the QCD axion case the non-perturbative axion potential leads to the general relation for its mass, shown in Eq. 3.66, that implies that, for $f_a \sim 10^8$ GeV, the axion is relativistic at the time of CMB decoupling and thus will again contribute to ΔN_{eff}.

There are two benchmark classes of QCD axion models: KSVZ [92] and DFSZ [89, 90]. The former does not have tree-level couplings to SM fermions so it does not seem able to explain the XENON1T excess and satisfy the CAST bound at the same time [283, 290]. Therefore we focus on the DFSZ models whose couplings to quarks satisfy

$$c_U + c_D = \frac{1}{3}\,, \tag{6.45}$$

where c_U is the universal coupling to the up-type quarks and c_D the universal coupling to the down-type ones. The axion may couple to charged leptons as to the up-type quarks or as to the down-type quarks: in what follows, we take the second option for concreteness, as in [283], i.e. $c_E = c_D$, being c_E the universal coupling to the charged leptons.

The DFSZ model also features two Higgs doublets, but the extra Higgs and also the rest of the SM couplings (i.e. with gauge bosons and the physical Higgs) are neglected here, since they would affect axion production only at very high T and would give a subdominant contribution, compared to the production via fermions, which are relevant at lower temperatures, $T_D \approx 1-10$ GeV. The photon-axion coupling in DFSZ model takes the value $c_{a\gamma\gamma} = 8/3$ ($c_{a\gamma\gamma} = 2/3$) if the charged leptons couple to the axion as the down-type (up-type) quarks do; such a coupling is important for experiments that search for axions, but it gives a subdominant contribution to ΔN_{eff}. Finally, there are no RGE effects in this case since we can always choose a basis where the axion appears only inside the quark mass matrix [159].

The contributions to ΔN_{eff} are dominated by scatterings with heavy quarks and can be seen in Fig. 6.11, where three cases are considered: $c_U = 1/3$ and $c_D = 0$ in blue in the plot, $c_U = 0$ and $c_D = 1/3$ in red, and $c_U = 1/6 = c_D$ in black. While the vertical axis represents ΔN_{eff}, the horizontal one stands for f_a or equivalently for $g_{ae}/\cos^2\beta_{\rm DFSZ}$, being $\cos^2\beta_{\rm DFSZ} = x^2/(x^2+1)$ the parameterisation of $x = v_1/v_2$, which is the ratio of the Higgs VEVs.

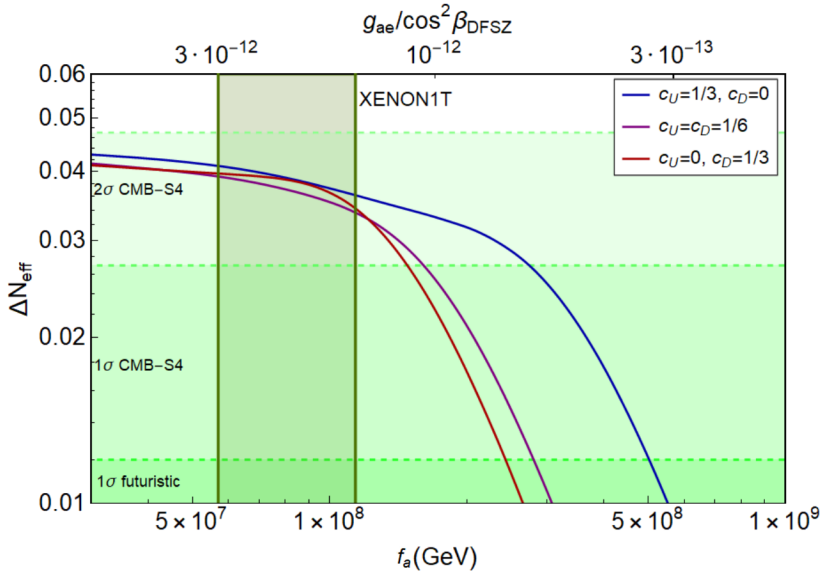

FIGURE 6.11: Prediction for ΔN_{eff} for the DFSZ axion model. Here we show the top, bottom and charm contributions for three different choices of the PQ charges: $c_U = 1/3$ and $c_D = 0$ in blue, $c_U = 0$ and $c_D = 1/3$ in red, and $c_U = 1/6 = c_D$ in purple. We assumed no initial abundance of axions at low temperatures and integrated the Boltzmann equation down to 1 GeV to avoid getting too close to strongly coupled regimes. Green bands are the forecasted sensitivity of CMB-S4 experiments [236]. The XENON1T window is in tension with the bound $f_a/c_E \gtrsim 1.9 \times 10^9$ GeV coming from stellar cooling [314], but escapes the limit $f_a \gtrsim 1.2 \times 10^7$ GeV set by CAST [290]. The XENON1T window for this model could however be just perhaps reached by BabyIAXO (reaching $f_a \sim 5.7 \times 10^7$ GeV) and fully explored by the IAXO experiment [321], that could reach $f_a \sim 2 \times 10^8$ GeV.

6.3 What $\Delta N_{eff} > 0$ can teach us

Having studied the possible contribution to ΔN_{eff} in a model independent approach, followed by the prediction from several axion models and, finally, the correlation of the signal in XENON1T with a potential non-vanishing ΔN_{eff}, let us close this chapter by asking ourselves what we can learn from a non-zero detection of ΔN_{eff}:

No detection, $\Delta N_{eff} \lesssim 0.03$: The axion does not couple to heavy quarks or the coupling is small.

$\Delta N_{eff} \sim 0.03 - 0.05$: A detection of ΔN_{eff} in this window would give a strong hint that the axion couples to at least one of the heavy quarks. In particular, assuming that we know $g_{*s}(T_D)$ with enough precision from latest lattice simulations [322] then in a given model where all the PQ charges are fixed, e.g. DFSZ, the detection in XENON1T would tell us the value of f_a and, consequently, there would be a sharp prediction for ΔN_{eff}. Therefore, in principle one would be able to test if the ratio of PQ charges c_ψ/c_e is indeed the predicted one.

$\Delta N_{eff} \gtrsim 0.05$: In this case axion production could come from different sources: either from the τ with a small f_a or from axion coupling to charm or bottom at temperatures below 1 GeV. In the latter case a reliable calculation of axion production close to the QCD phase transition would be needed.

Through this chapter we have indeed checked that the axion, outstanding candidate for BSM physics, can be looked for through a complementary probe to the usual experiments seeking its detection. Indeed, hot axions can be produced from scatterings or decays of thermal bath particles in the early Universe, and they remain relativistic subsequently until the time of matter/radiation equality and recombination; this is true as long as $m_a \ll \mathcal{O}(0.1)$ eV, as we consider in this chapter by neglecting the axion mass. They would manifest themselves in the CMB anisotropy spectrum as an additional radiation component, parameterized as the number of additional effective neutrinos ΔN_{eff}.

In the previous pages, we studied axions couplings to heavy quarks and we provided rigorous predictions for ΔN_{eff}. We considered flavour conserving couplings, in which case production is controlled by binary collisions, and we also considered flavour violating couplings

leading to axion production via two-body decays. We computed scattering cross sections and decay widths, and we obtained predictions for ΔN_{eff} after solving numerically the Boltzmann equation tracking the axion number density, with smooth predictions across the EWPT.

We studied both the model-independent contribution based on switching on an effective operator at a time as well as specific UV complete models. We found parameter space regions for all cases, typically with PQ breaking scale in the range $f_a \sim (10^9 - 10^{10})$ GeV for order one couplings to fermions, where the predicted signal is comparable to the forecasted 1σ sensitivity of CMB S4 experiments, and it could be detectable by more futuristic experiments.

Additionally, we point out two complementary signals. The values of the PQ breaking scale leading to an observable effect on ΔN_{eff} is consistent with axion cold dark matter. Furthermore, if there is no substantial hierarchy between the dimensionless axion couplings considered in this work and the associated one to photons then future helioscopes are also able to probe this parameter space region. The complementarity of these possible signals makes for a quite fascinating probe into the nature of the axion itself.

Finally, we explored correlated signals of the XENON1T excess in cosmological data, by studying the sizeable contribution to ΔN_{eff} from quarks and leptons. We presented three different motivated setups where such couplings would exist: i) if the axion couples democratically to all fermions in the UV (Fig. 6.9); ii) if the axion-electron coupling compatible with XENON1T is radiatively induced from an axion-(τ, c, b, t) coupling (Fig. 6.10); iii) the DFSZ model of the QCD axion (Fig. 6.11). The largest signal comes from case ii) when the axion couples only to the τ in the UV. In such a case we find in the XENON1T region $f/c_\tau \sim 10^3$ GeV and $\Delta N_{eff} \simeq 0.3$, which interestingly coincides with the recent CMB analyses including supernova data [318, 319]. In the remaining cases the values of f/c_ψ in the XENON1T region are considerably higher, up to $f/c_\psi \sim 10^8$ GeV, and the signal is predicted to be $\Delta N_{eff} \gtrsim 0.04$, which can still be detected at the 2σ level with future CMB-S4 experiments [236].

In all such cases the XENON1T range leads to the possibility of testing axion physics through cosmological data in the coming years, and would allow us to experimentally test the Universe at temperatures of $T \approx 1 - 10$ GeV. This would be a remarkable improvement over our current ability to look at the earliest stage of the universe, going by 3 or 4 orders of magnitude above the present highest experimentally accessible temperature, $T \approx$ MeV, given by nucleosynthesis.

Next-generation detectors such as XENONnT and others [323, 324] will be able to discriminate with high significance between the different interpretations for the excess in the number of electron recoil events at XENON1T. The solar axion interpretation still has to overcome the challenge of being compatible with stellar cooling results but, if it remains firm, it will open a whole new axion window to the universe.

Conclusions

In this thesis we have explored some of the phenomenological and cosmological implications of axions and majorons in the context of two open problems of the SM, namely the Strong CP Problem and the flavour puzzle. Both of the original models presented here, in Chapters 4 and 5 respectively, are connected to the Minimal Flavour Violation scenario that protects them from the danger that flavour models usually suffer: the BSM flavour problem. In Chapter 6, on the other hand, we do not present a particular model, but focus our attention on the cosmological observable ΔN_{eff}, the change in the effective number of neutrinos with respect to the prediction by the SM, and how it can be affected by a population of hot axions produced in the early Universe.

The Strong CP Problem and Quark and Charged Lepton Flavour: The first model here displayed, the Minimal Flavour Violating axion, is a proposal that considers the possibility of finding a natural origin to the PQ symmetry within the MFV symmetry group $\mathcal{G}_F$, without the need to add it ad-hoc. Indeed, it can be seen that within the Abelian subgroup of $\mathcal{G}_F$, a PQ symmetry can be identified, together with BN, LN, hypercharge and an arbitrary rotation of the RH charged leptons, with all these symmetries being linearly independent.

After checking that a PQ symmetry appears naturally in MFV, we introduced a new scalar, the flavon, that breaks it spontaneously. This field is introduced in certain powers within the Yukawa Lagrangian, following the philosophy of Froggatt-Nielsen models, depending on the fermion charges under $U(1)_{PQ}$, which are the same for the three generations but different for up quarks, down quarks and charged leptons. This automatically implies that the axion, NGB of the PQ symmetry and pseudo-scalar part of the flavon, develops flavour conserving non-universal couplings to the SM fermions, suppressed by its decay constant f_a as usual.

The flavon VEV not only gives rise to the axion but, thanks to the choice of charges made in the model, also explain the mass ratio between the third-generation fermions: top, bottom and tau. The inter-generational hierarchies are reproduced by the background values of the Yukawas, spurions under the non-Abelian parts of $\mathcal{G}_F$, as done usually in MFV.

After providing an overview of the current bounds set on the different couplings of the axion to fermions and gauge bosons, we found that, when treated as a light QCD axion, our Minimal Flavour Violating Axion behaves as the well-known invisible KSVZ and DFSZ axions: the strongest bounds on our axion come from its couplings to electrons and photons, pushing its decay constant f_a to be roughly above 10^9 GeV.

On the other side if, instead, we consider we are dealing with an ALP, the relation between its characteristic scale f_a and its mass is broken, a heavier MFVA(LP) is possible, together with low f_a. When this scenario is confronted with existing bounds, we find that now the most interesting phenomenology is expected at colliders and flavour searches, with possible decays of this ALP happening within detectors for masses around the GeV.

Despite this model presenting an axion with flavour properties, it is clearly distinct from its siblings, the Flaxion or Axiflavon models: in that scenario, the axion produced has couplings to fermions that are flavour-violating, thus existing FCNCs at tree level. As a consequence, these models must satisfy the very stringent bounds set on meson decays, mainly K and B decays, which push the scale to be order 10^{10} GeV even if a heavy mass is considered.

All in all, the MFVA appears as a protected, invisible, flavoured QCD axion, or a heavy flavoured ALP, that not only solves the Strong CP Problem but also explains the top, bottom and tau masses. However, this model disregards completely neutrino masses, which ties in with the next model here presented.

More flavour with a touch of cosmology; neutrino masses and the Hubble tension: An unsatisfied reader may find some solace in the second model contained in this thesis. Whereas the MFVA dealt with quark and charged leptons, in Chapter 5 we presented a Majoron model that, not only explains the smallness of neutrino masses, but also alleviates the Hubble tension while being compatible with the MFVA.

In this new model, spurred by the proposal that light pseudoscalars can help reduce the existing tension between early and late measurements of the Hubble parameter, we studied the

possibility of a Majoron, ω that explains the small scale of neutrino masses with the appropriate mass m_ω and coupling to neutrinos $\lambda_{\omega\nu\nu}$ to help with the cosmological discrepancy. Extending the SM particle spectrum with 3 RH neutrinos and a new complex scalar χ, with LN $-L_N$ and L_χ respectively, a Dirac and Majorana mass term can be written for neutrinos and made invariant under LN with the appropriate insertions of χ over a cut-off scale Λ_χ.

After considering the constraints set by the see-saw approximation, locality, the masses of light neutrinos and the required $\lambda_{\omega\nu\nu}$, we could identify three interesting scenarios. One of them, renormalizable, is however disregarded as it would imply a huge fine tuning in the neutrino Yukawas, against the naturalness followed in this thesis for dimensionless parameters.

The two remaining scenarios, NR1 and NR2, are able to accommodate small neutrino masses without tuning the Yukawas, thanks to powers of the VEV of χ over Λ_χ appearing in the expression for neutrino masses. These two scenarios lead to a Majoron that easily escapes the bounds coming from its coupling to electrons (at one loop), photons (at two loops) and from neutrinoless double-beta decay, while providing interesting phenomenology through the heavy neutrinos and the radial part of χ, σ.

The new scalar σ mixes with the Higgs boson, which implies first that it must satisfy the current limits on a scalar mixing. Additionally, through the kinetic term for χ, it also has a coupling to two Majorons, which can therefore lead to a Higgs invisible decay $h \to \omega\omega$, meaning that limits on the Higgs invisible decay width also must be respected. While one could expect that these constraints would push the new scalar to be super heavy, it is found instead that, without tuning its coupling to the Higgs to zero, it can have masses as low as tens of TeV, being a very exciting candidate to be discovered at future colliders.

On the other hand, the heavy neutrinos present in this model actually are not that heavy: in the case NR1 they are in the MeV to hundreds of MeV range, whereas in scenario NR2 go from tens to almost a several hundreds of GeV. These relatively light masses imply that NR1 heavy neutrinos could be produce at beam dump experiments or detected in near detectors, like DUNE or SHiP, while NR2 heavy neutrinos have masses accessible at LHC or future colliders.

On the contrary, these heavy neutrinos may be too long-lived, so that their decay can lead to a exceedingly high number of relativistic degrees of freedom. In particular, if they decay after BBN, they must satisfy a bound on the light-heavy neutrino mixing angle, which

is strong enough to rule out some scenarios. Indeed, for the parameters of case NR1, heavy neutrino decay happens close or later than BBN, being disfavoured unless in some part of the parameter space the decay is found to happen before BBN or we consider modifications to the cosmological model. NR2 neutrinos, however, decay before BBN so they stay safe from this bound.

Finally, one must note that this Majoron mechanism, to address light neutrino masses and the Hubble tension, is fairly general and, in particular, is perfectly compatible with MFV. Apart from a PQ symmetry, LN also arises as an Abelian part of the whole flavour symmetry group, which can be imposed on the Lagrangian and then broken spontaneously to generate light neutrino masses. Consequently, both the MFVA and the Majoron models can coexist in our Universe, with very rich phenomenology associated to each of them.

Another possible hot relic: thermal axions: As we saw in Chapter 5, extra degrees of freedom can be helpful, as the Majoron for the Hubble tension, or dangerous, as the too long-lived NR1 scenario heavy neutrinos. In the last part of this thesis, Chapter 6, we harnessed the power of this observable, ΔN_{eff}, and checked the possibility for it to be an additional probe for axion searches.

In this chapter we performed a smooth treatment across the EWPT of the effect hot axions produced in the early Universe can have on ΔN_{eff}. Considering both flavour-conserving scatterings and flavour-violating quark decays, and focussing on the third generation of quarks, we listed all processes that are relevant for axion production both above and below EWSB and matched them, as a consistency check.

With the recipe for axion production in hand, we solved the Boltzmann equation in order to find the asymptotic axion abundance, that can be translated into ΔN_{eff}, as a function of its scale f_a. We performed this analysis first in a model-independent way, considering only one axion coupling at a time, and then three specific models: the DFSZ, KSVZ and MFVA frameworks.

We found that, for axions coupling to the top quark as can be the case of the DFSZ model, a signal detectable at the 1σ level by the CMB-S4 experiment is expected for axion scales up to around 10^9 GeV. In the case where the axion does not couple to the top, but it does to bottom quark or at least to gluons, a signal close to the 2σ level is expected around $f_a \sim 10^8$ GeV. This region is still not excluded by CAST, by is within the range expected to be probed by IAXO

in the three models discussed. Interestingly enough, in the window $f_a \sim 10^9 - 10^{10}$ GeV the 1σ signal of hot axions could also coexist with cold DM axions produced through the decay of topological defects, while perhaps being also detectable by future helioscopes, allowing maybe to unravel the nature of the axion if it were to be measured.

Finally, in the last part of this chapter we studied the complementarity of this cosmological probe which is ΔN_{eff} and the recent excess observed by the XENON1T collaboration, compatible with solar axions. In this final part we computed the expected ΔN_{eff} from hot axions in three scenarios: one where the axion couples democratically, with the same strength, to all fermions in the UV; another where it couples only to one fermion in the UV while the axion-electron coupling required by the excess is generated radiatively; and finally, the DFSZ model as example of a QCD axion.

In all cases, the window preferred by the XENON1T excess for f_a corresponds to at least $\Delta N_{eff} \sim 0.04$, close to the 2σ level detection from CMB-S4. But in the case where the axion couples only to tau leptons at tree level the result is much larger: $\Delta N_{eff} \simeq 0.3$ is obtained in this case, a value that interestingly coincides with the recent CMB analyses including supernova data.

What now? The puzzle is far from complete: In this thesis we have focused our attention in one possible new piece for the HEP puzzle, axions and Majorons as example of NGBs, very well motivated for many reasons. With them, we have been able to address a good part of the flavour puzzle, the Strong CP problem and even some cosmological anomalies, finding in the way very interesting phenomenological signatures.

However, this does not mean by far that everything is finished: axion models still present issues, like the quality problem and domain walls; the masses for these NGBs must have specific values in some cases, where gravity can perhaps ruin or save everything. Additionally, there are still other problems we have not addressed, like the hierarchy problem, that are extremely intriguing and satisfying to work on.

There are indeed many other pieces beyond NGBs that one could explore to solve these riddles, trying to get a full and perfect image with the HEP puzzle. However, one may wonder if we are not too restricted by our usual view of things: though toying with this puzzle is deeply fascinating, perhaps we are losing something and we should stop looking for new pieces and, instead, try to look at the picture from a different perspective. Maybe the puzzle was not a flat

static image as we always supposed, maybe it spans directions yet to explore. Let us continue striving and keep playing with the puzzle, always with an open mind!

Conclusiones

En esta tesis hemos explorado algunas de las implicaciones cosmológicas y fenomenológicas de axiones y majorones en el contexto de dos problemas abiertos del Modelo Estándar, a saber, el Problema de CP Fuerte y el puzle del sabor. Los dos modelos presentados, en los Capítulos 4 y 5 respectivamente, están conectados con el argumento de la Violación Mínima de Sabor (MFV por sus siglas en inglés) que los protege del peligro al que están sujetos típicamente los modelos de sabor: el problema del sabor más allá del Modelo Estándar. En el Capítulo 6, por otro lado, no presentamos un modelo en particular, sino que centramos nuestra atención en el observable cosmológico ΔN_{eff}, el incremento en el número efectivo de neutrinos con respecto a lo predicho por el Modelo Estándar, y cómo puede verse afectado por una población de axiones calientes producidos en el Universo primigenio.

El Problema de CP Fuerte y el Sabor de Quarks y Leptones Cargados: El primer modelo aquí dispuesto, el Axión con Violación Mínima de Sabor (MFVA), es una propuesta que considera la posibilidad de encontrar un origen natural a la simetría de Peccei-Quinn (PQ) en el interior del grupo de simetrías de MFV $\mathcal{G}_F$, sin la necesidad de añadirla a mano. En efecto, puede comprobarse que dentro del subgrupo Abeliano de $\mathcal{G}_F$, una simetría PQ puede ser definida, junto con Número Bariónico (BN), Número Leptónico (LN), hipercarga y una rotación arbitraria de los leptones cargados dextrógiros, siendo todas estas simetrías linealmente independientes.

Tras comprobar que una simetría PQ aparece naturalmente en MFV, introdujimos un nuevo escalar, el flavón, que la rompe espontáneamente. Este campo se introduce en ciertas potencias en la Lagrangiana de Yukawa, siguiendo la filosofía de los modelos Froggatt-Nielsen, con una dependencia de las cargas bajo $U(1)_{PQ}$ de los fermiones, las cuales son iguales para las tres generaciones pero distintas para quarks arriba, quarks abajo y leptones cargados. Esto

implica automáticamente que el axion, Bosón de Nambu-Goldstone (NGB) de la simetría PQ y parte pseudo-escalar del flavón, desarrolla acoplamientos a los fermiones del Modelo Estándar que conservan el sabor pero son no-universales, suprimidos como es usual por su constante de decaimiento f_a.

El valor esperado de vacío (VEV) del flavón no sólo da lugar al axión sino que, gracias a la elección de cargas realizada en el modelo, también explica el cociente entre las masas de los fermiones de la tercera generación: cima, fondo y tau. Las jerarquías inter-generacionales son reproducidas por los *background values* de los Yukawas, espuriones bajo las partes no-Abelianas de $\mathcal{G}_F$, como es usual en MFV.

Tras proporcionar un repaso de los límites actuales existentes para los distintos acoplo del axión a fermiones y bosones de gauge, encontramos que, cuando es tratado como un axión de QCD, nuestro MFVA se comporta como los conocidos KSVZ y DFSZ axiones invisibles: los límites más fuertes sobre nuestro axión provienen de sus acoplamientos a electrones y fotones, llevando su constante de decaimiento f_a a estar por encima de 10^9 GeV.

Por otra parte si, en su lugar, consideramos que estamos tratando con una partícula-tipo-axión (ALP), la relación entre su escala característica f_a y su masa se rompe, siendo un MFVA(LP) posible junto con una baja f_a. Cuando esta perspectiva es enfrentada a los límites existentes, encontramos que la fenomenología más interesante se espera en colisionadores y experimentos de sabor, con la posibilidad de un decaimiento de este ALP sucediendo dentro de los detectores para masas alrededor del GeV.

A pesar de que este modelo presenta un axión con propiedades de sabor, es claramente diferente de sus congéneres, los modelos de Flaxion o Axiflavon: en estos casos, el axión producido tiene acoplamientos a los fermiones que violan sabor, existiendo por tanto corrientes neutras que cambian sabor (FCNC) a nivel de árbol. Consecuentemente, estos modelos deben satisfacer los severos límites puestos en decaimiento de mesones, principalmente decaimientos de K y B, que llevan la escala a valores por encima de 10^{10} GeV incluso considerando masas pesadas.

Considerándolo todo, el MFVA aparece como un axión de QCD protegido, invisible y sápido, o bien como un ALP pesado con sabor, que no sólo resuelve el problema de CP fuerte sino también explica las masas del quark cima y fondo y del leptón tau. Sin embargo, este

modelo ignora por completo las masas de los neutrinos, algo que nos lleva al siguiente modelo presentado aquí.

Más sabor con un toque de cosmología; masas de neutrinos y la tensión de Hubble: Alguien insatisfecho leyendo esta tesis puede quizá encontrar algo de solaz en el segundo modelo contenido en esta tesis. Mientras que el MFVA lidiaba con quarks y leptones, en el Capítulo 5 presentamos un modelo de Majoron que, no sólo explica la pequeñez de las masas de los neutrinos, sino que también alivia la tensión de Hubble siendo compatible con el MFVA al mismo tiempo.

En este nuevo modelo, motivados por la propuesta de que pseudo-escalares ligeros pueden ayudar a reducir la tensión existente entre medidas del parámetro de Hubble en el Universo reciente y el primigenio, estudiamos la posibilidad de que un Majoron, ω, explique la baja escala de la masa de los neutrinos con una masa m_ω y acoplamiento a neutrinos $\lambda_{\omega\nu\nu}$ apropiados para ayudar con la discrepancia cosmológica. Extendiendo el espectro de partículas del Modelo Estándar con 3 neutrinos dextrógiros y un nuevo escalar complejo χ, con LN $-L_N$ y L_χ respectivamente, podemos escribir términos de masa de Majorana y Dirac para los neutrinos, además de hacerlos invariantes bajo LN con las inserciones apropiadas de χ dividido por la escala de corte Λ_χ.

Tras considerar la restricción que supone la aproximación del "mecanismo de balancín", localidad, las masas de los neutrinos ligeros y el valor requerido de $\lambda_{\omega\nu\nu}$, pudimos identificar tres casos interesantes. Uno de ellos, renormalizable, es ignorado puesto que implicaría un valor extremadamente pequeño para los Yukawas de los neutrinos, en contra de la naturalidad perseguida en esta tesis para los parámetros adimensionales.

Los dos casos restantes, NR1 y NR2, pueden explicar las pequeñas masas de los neutrinos sin Yukawas ínfimos, gracias a potencias del VEV de χ dividido por Λ_χ que aparecen en la expresión de las masas de los neutrinos. Estos dos escenarios conllevan un Majoron que escapa fácilmente de los límites existentes en su acoplamiento a electrones (a un lazo), fotones (a dos lazos) y en el decaimiento doble-beta sin neutrinos, ofreciendo además una fenomenología interesante a través de los neutrinos pesados y la parte radial de χ, σ.

El nuevo escalar σ se mezcla con el bosón de Higgs, lo que implica primero que debe respetar los límites establecidos para la mezcla de escalares. Adicionalmente, a través del

término cinético de χ, también presenta un acoplamiento a dos Majorones, que puede por consiguiente llevar a un decaimiento invisible del Higgs $h \to \omega\omega$, implicando que debe satisfacerse también el límite de la anchura de desintegración invisible del Higgs. Aunque uno podría esperar que estas restricciones lleven la masa del escalar a ser muy pesada, encontramos que en su lugar, sin fijar su acoplamiento con el Higgs a cero, puede tener masas bajas hasta incluso decenas de TeVs, suponiendo un candidato muy emocionante para descubrimiento en futuros aceleradores.

Por otro lado, los neutrinos pesados presentes en este modelo no son de hecho tan pesados: en el caso NR1 están entre los MeV y las centenas de MeV, mientras que los del escenario NR2 van desde las decenas hasta varias centenas de GeV. Estas masas relativamente ligeras implican que los neutrinos de NR1 podrían producirse en experimentos de *beam dump* o observados en detectores cercanos, como DUNE o SHiP, mientras que los neutrinos de NR2 tienen masas accesibles en el LHC o futuros colisionadores.

Opuestamente, estos neutrinos pueden ser demasiado longevos, de modo que su decaimiento pueda dar lugar a un número inaceptablemente alto de grados de libertad relativistas. En particular, si decaen después de la nucleosíntesis del Big Bang (BBN), deben respetar un límite en la mezcla de neutrinos ligeros y pesados, lo suficientemente restrictiva como para excluir algunos casos. En efecto, para los parámetros del caso NR1, los neutrinos pesados decaen alrededor o después de BBN, estando desfavorecido este caso a no ser que en alguna parte del espacio de parámetros el decaimiento suceda antes de BBN o consideremos modificaciones al modelo cosmológico. Los neutrinos de NR2, sin embargo, decaen antes de BBN por lo que están a salvo de este límite.

Finalmente, uno debe ser consciente de que este mecanismo de Majoron, que explica las masas de los neutrinos ligeros y mejora la tensión de Hubble, es bastante general y, en particular, perfectamente compatible con MFV. Además de la simetría de PQ, LN también aparece en la parte Abeliana del grupo de simetría, de modo que puede ser considerada una simetría de la Lagrangiana y, posteriormente, rota espontáneamente para generar las masas de los neutrinos. Como consecuencia, tanto el MFVA como este modelo de Majoron pueden coexistir en nuestro Universo, con una rica fenomenología asociada a cada uno de ellos.

Otra posible reliquia caliente: axiones térmicos: Tal y como vimos en el Capítulo 5, grados de libertad relativista extra pueden ser de ayuda, como el Majoron para la tensión de Hubble,

o peligrosos, como los longevos neutrinos pesados de NR1. En la última parte de esta tesis, Capítulo 6, aprovechamos el potencial de este observable, ΔN_{eff}, y comprobamos la posibilidad de que suponga una sonda adicional con la que buscar axiones.

En este capítulo realizamos un tratamiento continuo y fluido a través de la transición de fase electrodébil (EWPT) del efecto que axiones calientes producidos en el Universo primigenio pueden tener en ΔN_{eff}. Considerando acoplamientos que conservan sabor en colisiones de quarks, así como otros que lo violan en sus decaimientos, y centrándonos en la tercera generación de quarks, listamos todos los procesos relevantes para la producción de axiones, tanto por encima como por debajo de la EWPT, igualándolos en el punto de EWSB como prueba de consistencia.

Con la receta para la producción de axiones en mano, resolvimos la ecuación de Boltzmann para encontrar la abundancia asintótica de axiones, que puede traducirse en ΔN_{eff}, como función de su escala f_a. Realizamos primero un análisis independiente de modelos, considerando sólo un acoplamiento cada vez, seguido de un estudio del impacto de tres modelos concretos: los marcos DFSZ, KSVZ y MFVA.

Encontramos que, para axiones que se acoplan al quark cima como puede ser el caso del modelo DFSZ, se espera una señal detectable al nivel de 1σ por el experimento CMB-S4 para escalas hasta aproximadamente 10^9 GeV. En el caso de que no se acople al quark cima, pero sí al fondo o al menos a gluones, una señal cerca de 2σ se espera en torno a $f_a \sim 10^8$ GeV. En los tres modelos discutidos, esta región, aún no excluida por CAST, está dentro del rango que se espera explorar con IAXO. Es además llamativo que, en la ventana $f_a \sim 10^9 - 10^{10}$ GeV the 1σ la señal a 1σ de axiones calientes puede coexistir también con axiones fríos que sean Materia Oscura producidos por la desintegración de defectos topológicos, siendo detectables quizás por futuros helioscopios, permitiendo tal vez desentrañar la naturaleza del axión de ser medido.

Finalmente, en la última parte de este capítulo, estudiamos la complementariedad de esta sonda cosmológica que es ΔN_{eff} y el exceso recientemente observado por la colaboración XENON1T, compatible con axiones solares. En esta parte final obtuvimos el ΔN_{eff} esperado de axiones calientes en tres escenarios: uno donde el axión se acopla democráticamente, con la misma intensidad, a todos los fermiones a altas energías; otro donde sólo se acopla a un fermión a altas escalas mientras que se induce radiativamente el acoplamiento al electrón requerido por el exceso; y finalmente, el modelo DFSZ como ejemplo de axión de QCD.

En todos los casos, la ventana preferida por el exceso de XENON1T para f_a corresponde con al menos $\Delta N_{eff} \sim 0.04$, cerca de una detección por CMB-S4 a 2σ. Pero, en el caso en que el axión sólo se acopla al leptón tau a nivel de árbol el resultado es mucho mayor: obtenemos $\Delta N_{eff} \simeq 0.3$ en este caso, un valor que curiosamente coincide con los análisis recientes del CMB que incluyen datos de supernova.

¿Ahora qué? El puzle está lejos de ser completo: En esta tesis hemos focalizado nuestra atención en una posible nueva pieza para el puzle de la Física de Altas Energías, axiones y Majorones como ejemplos de bosones de Nambu-Goldstone, altamente motivados por muchos motivos. Con ellos, hemos conseguido además lidiar con buena parte del puzle del sabor, el Problema de CP Fuerte e incluso algunas anomalías cosmológicas, encontrando por el camino señales fenomenológicas muy interesantes.

Sin embargo, esto no significa ni mucho menos que todo haya terminado: los modelos de axiones presentan problemas, como le problema de la cualidad y los muros de dominios; las masas requeridas para estos NGBs deben tener valores muy concretos en algunos casos, donde gravedad puede quizá arruinarlo o resolverlo todo. Además, hay otros problemas que no hemos considerado, como el problema de la jerarquía, que suponen temas de investigación muy intrigantes.

Hay, sin lugar a dudas, muchas otras piezas además de los NGBs que uno podría considerar para resolver estos enigmas, intentando obtener una imagen completa y perfecta del puzzle de la Física de Altas Energías. Sin embargo, uno puede preguntarse si no estamos tal vez muy limitados por nuestra visión usual de las cosas: aunque jugar con este puzle es profundamente fascinante, quizá estamos perdiéndonos algo y deberíamos dejar de buscar piezas y, tal vez, mirar la imagen desde una perspectiva diferente. Tal vez el puzle no es la imagen plana y estática que siempre supusimos, quizá se extienda en direcciones aún incógnitas. Continuemos esforzándonos y jugando con el puzle, ¡siempre con una mente abierta!

Appendix A

Operator basis for axion couplings to quarks

In this appendix, we define the field basis for SM quarks that we employ in our analysis in Chapter 6. The part of the SM Lagrangian needed for this discussion is the one containing Yukawa interactions. Focusing on quarks, the most generic set of Yukawa terms reads

$$-\mathscr{L}_Y = \overline{q''_L}\,\tilde{H}\,Y^u\,u''_R + \overline{q''_L}\,H\,Y^d\,d''_R + \text{h.c.}\,. \tag{A.1}$$

The fields appearing in the operators above are: $SU(2)_L$ quark doublets q''_L, $SU(2)_L$ quark singlets u''_R and d''_R and the $SU(2)_L$ Higgs doublet field H. Moreover, we define $\tilde{H} \equiv i\sigma_2(H^\dagger)^T$ and $Y^{u,d}$ are generic 3×3 diagonalizable matrices in flavor space. We save the symbol of unprimed fields for quark mass eigenstates defined later.

We diagonalize the Yukawa matrices by performing bi-unitary transformations

$$Y^u = U_L^{u\dagger}\,\hat{Y}^u\,U_R^u\,, \qquad\qquad Y^d = U_L^{d\dagger}\,\hat{Y}^d\,U_R^d\,, \tag{A.2}$$

where the U matrices are unitary and the hatted quantities are diagonal in flavor space. We introduce a new set of prime fields defined as follows

$$q''_L = U_L^{u\dagger}\,q'_L\,, \qquad\qquad u''_R = U_R^{u\dagger}\,u'_R\,, \qquad\qquad d''_R = U_R^{d\dagger}\,d'_R\,, \tag{A.3}$$

The Yukawa Lagrangian in the new basis reads

$$-\mathscr{L}_Y = \overline{q'_L}\,\tilde{H}\,\hat{Y}^u\,u'_R + \overline{q'_L}\,H\,V_{\text{CKM}}\,\hat{Y}^d\,d'_R + \text{h.c.}\,, \tag{A.4}$$

with $V_{\text{CKM}} \equiv U_L^u\,U_L^{d\dagger}$ the CKM matrix. In our study, we always specify axion couplings in the primed field basis for quarks with Yukawa interactions as in Eq. (A.4).

Finally, we identify the quark mass eigenstates, which we denote with unprimed fields, and their relation to the primed fields. First, we identify the components of the quark doublet $q'_L = (u'_L\ d'_L)$. Once the Higgs gets a vacuum expectation value (vev), we identify mass eigenstates by redefining the left-handed down quarks

$$u'_L = u_L\,, \qquad d'_L = V_{CKM}\,d_L\,, \qquad u'_R = u_R\,, \qquad d'_R = d_R\,, \tag{A.5}$$

Flavor eigenstates u'_i coincide with the mass eigenstates u_i, and the b' quark, the only down-quark we are interested in, almost coincides with the b quark up to CKM corrections of order $\mathcal{O}(0.05)$. In contrast to gauge interactions in the primed basis, which are still flavor diagonal, the CKM matrix appears in the fermion charged current once we switch to mass eigenstates

$$J_\mu^- = \overline{u_L}\,\gamma_\mu\,V_{\text{CKM}}\,d_L\,. \tag{A.6}$$

Appendix B

Cross sections below the EWPT

We provide analytical cross sections for the processes listed in Tab. 6.2, and we begin with the first block where the two particles in the initial state are fermions. A quark can find its own antiparticle and annihilate to final states containing one axion particle. If the final state is the gluon we have quark-antiquark annihilations to gluon and axion with a cross section

$$\sigma_{q\bar{q}\to ga} = \frac{c_q^2 g_s^2 m_q^2}{9\pi f_a^2\left(s-4m_q^2\right)} \tanh^{-1}\left(\sqrt{1-\frac{4m_q^2}{s}}\right) , \tag{B.1}$$

where g_s is the strong coupling constant and s is the usual Mandelstam variable denoting the (squared of the) energy in the center of mass frame. Here and below, we denote with the letter $q = \{t, b\}$ a generic third generation quark when it is possible to provide a single expression valid for both cases. If the other SM particle in the final state is the Higgs boson we have

$$\sigma^{\downarrow}_{q\bar{q}\to ha} = \frac{c_q^2 y_q^2\left(s-m_h^2\right)}{64\pi s f_a^2\left(s-4m_q^2\right)}\left(\sqrt{s\left(s-4m_q^2\right)}-4m_q^2\tanh^{-1}\left(\sqrt{1-\frac{4m_q^2}{s}}\right)\right) . \tag{B.2}$$

where the symbol "$\downarrow$" indicates that cross sections are calculated below the EWPT. Likewise, quarks can annihilate with their own antiquarks leading to an axion final state together with the Z boson with cross sections

$$\sigma_{t\bar{t}\to Za} = \frac{c_t^2 g_W^2 m_t^2\sqrt{\frac{1}{s-4m_t^2}}\left(s-m_Z^2\right)}{1152\pi s^{3/2} f_a^2 m_W^2 m_Z^2}\left(4\sqrt{\frac{s}{s-4m_t^2}}\tanh^{-1}\left(\sqrt{1-\frac{4m_t^2}{s}}\right)\left(-m_Z^2\left(9m_t^2+40m_W^2\right)+32m_W^4+17m_Z^4\right)+9m_Z^2\left(s-2m_Z^2\right)\right) , \tag{B.3}$$

$$\sigma_{b\bar{b}\to Za} = \frac{c_b^2 g_W^2 m_b^2\sqrt{\frac{1}{s-4m_b^2}}\left(s-m_Z^2\right)}{1152\pi s^{3/2} f_a^2 m_W^2 m_Z^2}\left(4\sqrt{\frac{s}{s-4m_b^2}}\tanh^{-1}\left(\sqrt{1-\frac{4m_b^2}{s}}\right)\left(-m_Z^2\left(9m_b^2+4m_W^2\right)+8m_W^4+5m_Z^4\right)+9m_Z^2\left(s-2m_Z^2\right)\right) , \tag{B.4}$$

Finally, to complete the first block of the table, we can have a top quark and a bottom antiquark as well as the CP conjugate system annihilating to a final state with an axion and a W boson with cross section

$$\begin{aligned}\sigma_{t\bar{b}\to W^+a} =& \frac{g_W^2\left(s-m_W^2\right)}{128\pi s f_a^2 m_W^2\left(\left(-m_b^2+m_t^2+s\right)^2-4sm_t^2\right)}\left(\left(c_b^2m_b^2+c_t^2m_t^2\right)\left(s-2m_W^2\right)\sqrt{-2m_b^2\left(m_t^2+s\right)+m_b^4+\left(m_t^2-s\right)^2}+\right.\\ &-2c_t^2m_t^2s\left(m_b^2-m_t^2+2m_W^2\right)\coth^{-1}\left(\frac{m_b^2-m_t^2-s}{\sqrt{-2m_b^2\left(m_t^2+s\right)+m_b^4+\left(m_t^2-s\right)^2}}\right)+\\ &+2c_bm_b^2s\left(2c_tm_t^2\coth^{-1}\left(\frac{m_b^2+m_t^2-s}{\sqrt{-2m_b^2\left(m_t^2+s\right)+m_b^4+\left(m_t^2-s\right)^2}}\right)+\right.\\ &\left.\left.\left.+c_b\left(m_t^2-m_b^2+2m_W^2\right)\coth^{-1}\left(\frac{m_b^2-m_t^2+s}{\sqrt{-2m_b^2\left(m_t^2+s\right)+m_b^4+\left(m_t^2-s\right)^2}}\right)\right)\right),\end{aligned} \tag{B.5}$$

We switch to the second block of Tab. 6.2 and we consider when there is just one fermion in the initial and final states. For a gluon in the initial state we find

$$\sigma_{qg\to qa} = \frac{c_q^2g_s^2m_q^2}{192\pi f_a^2s^2\left(s-m_q^2\right)}\left[2s^2\log\left(\frac{s}{m_q^2}\right)+4sm_q^2-m_q^4-3s^2\right]. \tag{B.6}$$

For quark/Higgs boson scattering we have

$$\begin{aligned}\sigma^{\downarrow}_{qh\to qa} =& \frac{c_q^2y_q^2\left(s-m_q^2\right)}{64\pi s f_a^2\left(\left(-m_h^2+m_q^2+s\right)^2-4sm_q^2\right)}\left[\left(-m_h^2+m_q^2+s\right)\sqrt{-2m_h^2\left(m_q^2+s\right)+m_h^4+\left(m_q^2-s\right)^2}+\right.\\ &\left.-2sm_q^2\log\left(-\frac{\sqrt{-2m_h^2\left(m_q^2+s\right)+m_h^4+\left(m_q^2-s\right)^2}-m_h^2+m_q^2+s}{\sqrt{-2m_h^2\left(m_q^2+s\right)+m_h^4+\left(m_q^2-s\right)^2}+m_h^2-m_q^2-s}\right)\right],\end{aligned} \tag{B.7}$$

whereas for the case of a Z boson we find

$$\begin{aligned}\sigma_{tZ\to ta} =& \frac{c_t^2g_W^2m_t^2\left(s-m_t^2\right)}{3456\pi s^2f_a^2m_W^2m_Z^2\sqrt{\left(m_t^2-m_Z^2+s\right)^2-4sm_t^2}}\times\\ &\times\left(\frac{2s^2\left(m_Z^2\left(9m_t^2+40m_W^2\right)-32m_W^4-17m_Z^4\right)\log\left(\frac{-\sqrt{-2m_t^2\left(m_Z^2+s\right)+m_t^4+\left(m_Z^2-s\right)^2}+m_t^2-m_Z^2+s}{\sqrt{-2m_t^2\left(m_Z^2+s\right)+m_t^4+\left(m_Z^2-s\right)^2}+m_t^2-m_Z^2+s}\right)}{\sqrt{-2m_t^2\left(m_Z^2+s\right)+m_t^4+\left(m_Z^2-s\right)^2}}+\right.\\ &\left.+3s\left(m_Z^2\left(3m_t^2+40m_W^2\right)-32m_W^4-8m_Z^4\right)+\left(m_t-m_Z\right)\left(m_t+m_Z\right)\left(-40m_W^2m_Z^2+32m_W^4+17m_Z^4\right)+9s^2m_Z^2\right).\end{aligned} \tag{B.8}$$

$$\sigma_{bZ\to ba} = \frac{c_b^2 g_W^2 m_b^2\left(s-m_b^2\right)}{3456\pi s^2 f_a^2 m_W^2 m_Z^2\sqrt{\left(m_b^2-m_Z^2+s\right)^2-4sm_b^2}}\times$$
$$\times\left(\frac{2s^2\left(m_Z^2\left(9m_b^2+4m_W^2\right)-8m_W^4-5m_Z^4\right)\log\left(\frac{-\sqrt{-2m_b^2\left(m_Z^2+s\right)+m_b^4+\left(m_Z^2-s\right)^2}+m_b^2-m_Z^2+s}{\sqrt{-2m_b^2\left(m_Z^2+s\right)+m_b^4+\left(m_Z^2-s\right)^2}+m_b^2-m_Z^2+s}\right)}{\sqrt{-2m_b^2\left(m_Z^2+s\right)+m_b^4+\left(m_Z^2-s\right)^2}}+\right. \tag{B.9}$$
$$\left.+3s\left(m_Z^2\left(3m_b^2+4m_W^2\right)-8m_W^4+4m_Z^4\right)+(m_b-m_Z)(m_b+m_Z)\left(-4m_W^2m_Z^2+8m_W^4+5m_Z^4\right)+9s^2m_Z^2\right).$$

Finally, if the initial state quark annihilate with a W boson we have the cross sections

$$\sigma_{tW^-\to ba} = \frac{g_W^2\left(s-m_b^2\right)}{384\pi s^2 f_a^2 m_W^2\left(\left(m_t^2-m_W^2+s\right)^2-4sm_t^2\right)}\left(\sqrt{-2m_t^2\left(m_W^2+s\right)+\left(m_W^2-s\right)^2+m_t^4}\left(2c_bc_tm_b^2m_t^2\left(3s+m_W^2-m_t^2\right)+\right.\right.$$
$$+c_b^2m_b^2\left(m_t^4-2m_W^4+m_t^2\left(m_W^2-2s\right)+m_W^2s+s^2\right)+c_t^2m_t^2\left(m_b^2\left(m_t^2-m_W^2-3s\right)+s\left(m_t^2-m_W^2+s\right)\right)\Big)+$$
$$\left.+2s^2c_tm_t^2\left(2c_bm_b^2+c_t\left(m_t^2-m_b^2-2m_W^2\right)\right)\log\left(\frac{m_t^2-m_W^2+s-\sqrt{-2m_t^2\left(m_W^2+s\right)+\left(m_W^2-s\right)^2+m_t^4}}{m_t^2-m_W^2+s+\sqrt{-2m_t^2\left(m_W^2+s\right)+\left(m_W^2-s\right)^2+m_t^4}}\right)\right), \tag{B.10}$$

$$\sigma_{bW^+\to ta} = \frac{g_W^2\left(s-m_t^2\right)}{384\pi s^2 f_a^2 m_W^2\left(\left(m_b^2-m_W^2+s\right)^2-4sm_b^2\right)}\left(\sqrt{-2m_b^2\left(m_W^2+s\right)+\left(m_W^2-s\right)^2+m_b^4}\left(2c_tc_bm_t^2m_b^2\left(3s+m_W^2-m_b^2\right)+\right.\right.$$
$$+c_t^2m_t^2\left(m_b^4-2m_W^4+m_b^2\left(m_W^2-2s\right)+m_W^2s+s^2\right)+c_b^2m_b^2\left(m_t^2\left(m_b^2-m_W^2-3s\right)+s\left(m_b^2-m_W^2+s\right)\right)\Big)+$$
$$\left.+2s^2c_bm_b^2\left(2c_tm_t^2+c_b\left(m_b^2-m_t^2-2m_W^2\right)\right)\log\left(\frac{m_b^2-m_W^2+s-\sqrt{-2m_b^2\left(m_W^2+s\right)+\left(m_W^2-s\right)^2+m_b^4}}{m_b^2-m_W^2+s+\sqrt{-2m_b^2\left(m_W^2+s\right)+\left(m_W^2-s\right)^2+m_b^4}}\right)\right), \tag{B.11}$$

Appendix C

Approaching the QCDPT

Ideally, we should integrate the Boltzmann equation tracking the axion number density all the way down to very low temperatures in order to predict ΔN_{eff}. We have seen why this is not necessary because the axion comoving density reaches an asymptotic value once SM quarks participating in the production start feeling the Maxwell-Boltzmann suppression. So it is enough to stop our Boltzmann equation integration at some IR temperature cutoff that we denote $T_{\rm STOP}$.

The value of the needed $T_{\rm STOP}$ could be dangerous if it is too low. Our analysis is based on perturbative calculations for scattering cross sections and on treating the primordial bath as a gas of weakly-coupled quarks and gluons in thermal equilibrium. This setup is certainly valid at high temperatures around the EWPT, and it loses its validity as we approach the QCDPT. In this appendix, we investigate how robust is our predictions for ΔN_{eff} considering this potential issue.

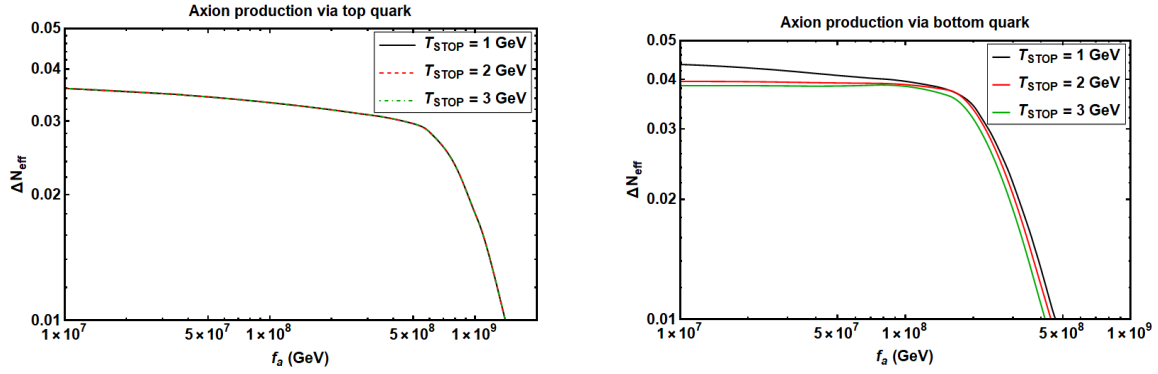

FIGURE C.1: Sensitivity of the ΔN_{eff} prediction on the lowest temperature $T_{\rm STOP}$ reached by our Boltzmann equation integration. We choose values of $T_{\rm STOP}$ close to the QCDPT, and we show results for production via top (left panel) and bottom (right panel) scattering.

We show in Fig. C.1 the prediction for ΔN_{eff} as a function of f_a for axion production via top quark (left panel) and bottom quark (right panel) scatterings. In each panel, we report our prediction for the different values $T_{\rm STOP} = \{1, 2, 3\}$ GeV close to the QCDPT. The result for the top is absolutely stable, and this is not surprising since the top mass is much larger than the typical temperatures around the QCDPT. On the contrary, production via bottom scattering presents some dependence on this temperature and decreasing it leads to slightly higher ΔN_{eff}. However, such a dependence on $T_{\rm STOP}$ is noticeable mostly in the region of very low PQ breaking scales ruled out by experiments. Thus, our results are robust. And, in any case, they could be interpreted as a lower bound on the expected effect on ΔN_{eff} that still ensures perturbativity in the computations.

Appendix D

RGE of axion couplings

As already emphasized in Sec. (6.2.1), the effective axion couplings to SM fermions in Eq. (6.39) are originated at the PQ breaking scale f and at lower energies there are only SM fields and the axion itself. This working assumption allows us to evolve the dimensionless Wilson coefficients c_ψ at lower energy scales by only using known SM interactions. We neglect flavor violating effects and neutrino masses, and the detailed RGE can be found in Refs. [325, 326] where anomalous dimension matrices are derived both above and below the EWPT. We do not consider the RGE of SM couplings and we limit ourselves to the results of a fixed-order calculation. The expressions for the low-energy couplings can be written in terms of simple analytical expressions [197, 327, 328], and at a generic renormalization scale $\mu < f$ they read

$$\begin{aligned} c_\psi(\mu) = c_\psi(f) - T_\psi^{(3)} \times \\ \left[\sum_{m_{\psi'}<\mu} c'_\psi(f) \frac{N_{\psi'}^{(c)} T_{\psi'}^{(3)} \lambda_{\psi'}^2}{2\pi^2} \ln\left(\frac{f}{\mu}\right) + \right. \\ \left. \sum_{m_{\psi'}>\mu} c'_\psi(f) \frac{N_{\psi'}^{(c)} T_{\psi'}^{(3)} \lambda_{\psi'}^2}{2\pi^2} \ln\left(\frac{f}{m_{\psi'}}\right) \right] . \end{aligned} \tag{D.1}$$

Here, $T_\psi^{(3)} = (+1/2, -1/2)$ is the value of the third component of the weak-isospin for the fermion ψ, that also has a Yukawa coupling λ_ψ and number of colors $N_\psi^{(c)}$. The first sum runs over SM fermions with mass below the renormalization scale μ, and thus over degrees of freedom still accessible, whereas the second sum runs over SM fermions heavier than μ that have been integrated out.

In order to address the XENON1T excess, we need a significant low-energy coupling to electrons and its explicit expression in terms of UV couplings results in

$$c_e = c_e(f) + \sum_{\psi'} c'_\psi(f) \frac{N^{(c)}_{\psi'} T^{(3)}_{\psi'} \lambda^2_{\psi'}}{4\pi^2} \ln\left(\frac{f}{m_{\psi'}}\right) , \tag{D.2}$$

with the sum over all SM fermions coupled to the axion.

Agradecimientos

Bueno, ahora sí, ahora llegó el momento. Si hay algo que me resulta fácil a mí es hablar de sentimientos, y después de estos cinco años, cuatro de tesis más uno de máster, emociones acumuladas hay para rato. Así que aviso: se vienen curvas, hora de ser moñas como a mí me gusta. El que avisa no es traidor, así que permitidme vaciarme emocionalmente, va a aparecer aquí hasta el apuntador.

Diría que no sé muy bien por dónde empezar, pero como buena persona obsesiva que soy es mentira porque llevo ya varias semanas pensando en cómo podría darle una estructura medio lógica a esto. Al final lo que se me ha ocurrido es empezar por donde estamos, la tesis, e ir alejándome poco a poco. La persona más cercana a esta tesis, después de mí mismo, es por supuesto mi director, Luca.

Aún recuerdo perfectamente las primeras reuniones para el TFM en tu despacho donde, literalmente, me echaba a temblar. Por muy joven que seas, para un completo amateur de la física teórica como era yo por aquel entonces, imponías bastante. Luego me di cuenta de que en realidad no había por qué asustarse tanto, sobre todo gracias a tu paciencia y lo fácil que es discutir sobre física contigo sin miradas de juicio ni comentarios de reproche cuando me equivocaba en algo. Cuando fue pasando algo más de tiempo, entramos en la colaboración (casi) infinita y probablemente nos sacamos de quicio el uno al otro en más de una ocasión. Pero al final resulta que uno aprende de absolutamente todo, hasta de las experiencias duras, y gracias a todo a lo que me he enfrentado junto a ti soy hoy una persona y un investigador (aunque a veces sienta que me queda grande la palabra) mucho más independiente y con más valor para hacerse escuchar.

A pesar de que hayamos tenidos nuestros momentos de tensión, de no entendernos (ya sea por mi pronunciación y celeridad andaluzas o por tu itañol), me siento súper agradecido de haber aprendido de ti y trabajado contigo. Nunca has tenido problema en reconocer cuando

algo te confundía, y eso me hacía creer que yo tampoco tenía por qué sentirme culpable al no saber algo. Gracias por todas las veces en que has creído en mi, en mi capacidad y en mi resistencia, cuando ni siquiera yo creía que fuera capaz de seguir adelante. Gracias por tu paciencia, especialmente en los comienzos, y por tu comprensión cuando me surgía alguna situación que me impedía estar pendiente del trabajo; valoro mucho que me hayas dado espacio para encontrar mi propio ritmo.

Este último año en concreto, irónicamente porque es cuando menos nos hemos visto, siento que hemos encontrado una dinámica de comunicación y trabajo súper agradable. Ojalá las personas con las que colabore en el futuro me lo pongan así de fácil y, por supuesto, ojalá tú seas una de esas personas en un futuro (espero) no muy lejano. Como ya te he comentado alguna vez, tenemos una charla pendiente cuando todo esto haya acabado, de doctor a doctor, que ya sabes que me encanta escuchar críticas constructivas, jeje.

Distanciándome un poco la tesis, pero sin irme de donde se forjó, encuentro en el IFT muchas otras personas a las que les tengo que agradecer lo que han hecho por mí. Siguiendo todavía en la categoría de "seniors", quería agradecer a Carlos Pena y Sven lo mucho que contribuyen a que el ambiente en el IFT sea siempre tan agradable, gracias por ser tan cercanos y, aunque parezca una tontería, por saludar siempre con una sonrisa por los pasillos. Gracias por la pasión tan genuina que desprendéis por la física, y a Sven en concreto, ¡gracias por estar siempre ahí para echar una mano en los PhenoCoffees!

Hablando de seniors que ayudan en los PhenoCoffees, necesito mencionar a Enrique. No sólo siempre estás ahí para discutir de lo que sea, demostrando lo increíblemente crack que eres y cómo dominas las cosas con una soltura impresionante, sino que siempre lo haces desde una amabilidad, un tacto y una simpatía maravillosas. Cuando pienso en qué tipo de personas me gustaría que formasen la academia en un futuro tengo claro que hacen falta más personas como tú. Además, estos años he tenido la posibilidad de colaborar contigo, y a pesar de que la secretaría del departamento amenace con hacerte añicos y tengas mil responsabilidades, siempre has sacado un rato para nuestras discusiones. Nunca pierdas ese sentido del humor tan característico tuyo (flashbacks a cuando fantaseabas con destruir el universo jugando con vacío del Higgs en el máster).

Gracias también a todas las personas que forman el comité de Equidad, Diversidad e Inclusión del IFT. Gracias a Esperanza, Pilar, Raquel (de ti hablaré después, descuida), Viviana,

Rebeca, Marga y todos los demás. Gracias por no quedaros de brazos cruzados ante las injusticias, ojalá sea una iniciativa que prospere y dure para siempre en el IFT, hasta que deje de ser necesaria.

No sólo de gente que investiga se forma el IFT. Todo el personal de recepción que siempre te recibe con una sonrisa, ¡que hasta se sabe tu nombre! Con la de gente que somos... Especial mención a Chus, increíble artista y mejor persona, a la que deseo muchísima suerte en su trayectoria artística. Gracias también a Rebeca Bello y Chabely: si no fuera por vosotras hasta los pósters de Invisibles arderían espontáneamente. Gracias por estar siempre ahí para echarnos un cable con todas las dudas de papeleos y demás que hemos tenido, por vuestra amabilidad y por hacer la organización de los congresos manejable.

Hablando de Invisibles y estancias no puedo evitar pensar en el mes en Costa Rica. No podría haber tenido mejores huéspedes que Pepe, Alejandro y Joe, ¡aunque nos echaran de un volcán por cierto consejo temerario! Lo que en un principio se me planteaba como una estancia mal recibida, al final acabó siendo una experiencia preciosa donde gracias a vosotros pude disfrutar, aunque sea un poquito, del país y del día a día allí. Gracias también a quienes compartieron esos días conmigo allí, Pablo Quílez y Joey, ¡con quienes me queda pendiente irme de barranquismo algún día!

Y pensando en estancias pienso en la que más disfruté sin lugar a dudas: Japón. Allí tuve la enormísima suerte de coincidir con uno de los previos doctorandos del IFT, Josu. Eso nos evitó ser unos completos marginados ya que al menos hablábamos entre nosotros, y gracias a ti me decidí a hacer aquel genial viaje por Kyoto, Osaka, Nara y, sobre todo, Miyajima. Gracias por evitar que me encerrase en mí mismo y en el trabajo estando en un lugar tan genial, y gracias por echarme un cable cuando me entraban dudas y el pánico con las solicitudes de postdoc. ¡Espero que vuelvan los congresos presenciales y coincidamos de nuevo pronto!

Hablando de congresos y ex-alumni del IFT no puedo obviar Planck 2019 y Víctor y M. Herrero. De nuevo, otras dos personas que siempre han estado ahí para echarme un cable y animarme, ejemplos de gente que sigue en ciencia sin perder sus principios. Gracias por las risas en Planck, por aquella noche de desfase y simplemente por ser como sois: un par de cachos de pan enormes. ¡Espero poder daros un buen abrazo más pronto que tarde!

Volviendo un poco al IFT, y al pasado, siento que tengo que agradecer a mis compis de máster que simplemente estuviesen allí. Andrea, Héctor, Ana, Fabio, Íker, Manu, John y,

por supuesto, Salva, Judit y Raquel. Gracias de corazón por hacer que, en mi primer año en Madrid, pudiese ser yo mismo y por echarme un cable cuando ni siquiera sabía usar LaTeX. A la mayoría os he perdido la pista, pero no por ello guardo con menos cariño todos los recuerdos que compartimos ese año.

Con Salva y Judit he tenido la suerte de compartir no sólo el máster sino despacho durante cuatro años como doctorandos, junto con Fran. Teneros a los tres en el despacho ha hecho que los días en los que parecía que todo se me iba a venir encima, o aquellos en los que directamente me echaba a llorar en el despacho, al final siempre volviese a casa con fuerzas. Gracias por todos los descansitos en el ping-pong para despejarnos, gracias Judit por comentar conmigo los Pokémon Direct y entender mi indignación con Game Freak. Gracias a Fran por tremendas bandas sonoras, como ABBA, que hacías sonar a veces en el despacho. Y gracias, GRACIAS, Salva, por haber compartido conmigo cada paso en la tesis, por aclararme dudas tontas de neutrinos mil veces, por sufrir la burocracia conmigo y simplemente por estar ahí. Ahora ambos nos vamos a tierras galas, así que confío en que podremos seguir en contacto con relativa facilidad, pero sé que pase lo que pase siempre podremos contar el uno con el otro.

Fuera de mi despacho he tenido la suerte de compartir el IFT con muchos otros doctorandos que hacían que los días de trabajo fuesen algo a esperar con ganas. Gracias por el día a día a Pablo Martín, Bris, Gabriel, Mattia, Claudia, Javi Quilis. Gracias a mi hermano de tesis, Gallego, por tener siempre palabras de aliento y ánimo. Gracias Álvaro por educarme un poco en cuerdas y por cierto momento de indignación maravilloso la noche de desfase en Planck. Gracias Raquel, ¡por no odiarme a pesar de mi comentario sobre tu tatuaje cuando apenas te conocía! Es broma, jeje, gracias por haber estado ahí en tantos momentos y congresos, por siempre ser tan dulce. Gracias a Guille por tus vídeos musicales familiares, y por aquella jam session en la que me invitasteis a desinhibirme y simplemente disfrutar de la música. Uga, a ti no sé si debería darte las gracias o pedirte responsabilidad por haberme metido en el infierno de los rogue-likes con Hades, ¡y del rocódromo! Gracias por haber compartido conmigo años de docencia en CIREL, las cosas se me hacen fácil con gente como tú a mi lado.

Gracias también al grupito de doctorandos más jóvenes de feno, Jesús, Jose y Manu. Las organizaciones de los congresos han sido bastante más divertidas gracias a vosotros, así como las cenas. El IFT se queda en buenas manos con doctorandos como vosotros, ¡pero no dinamitéis el PhenoCoffe en mi ausencia! En especial tú, Manu, que nos conocemos.

Abandonando ya el IFT llega el momento de dedicar un ratito a mi casa, mi piso de Alcobendas. Estos cinco años no podrían haber sido tan maravillosos de no ser por mis tres hermanas pequeñas postizas: Ane, Eva y Mari. A vosotras os debo tanto que temo quedarme sin espacio, pero abreviaré. Cenas de gordos, Eurovisión, ¡hasta OT nos hemos tragado juntos! La última época aficionados a la ruleta de la suerte, accidentes varios en la cocina que normalmente acababan con cosas rodando por el suelo, alguna borrachera tonta en el salón. Steven Universe, Avatar, Shingeki no Kyojin (y las microsiestas de Mari), The Office... Hemos compartido tantísimas cosas que sé que siempre nos tendremos los unos a los otros. El piso se me ha hecho bastante vacío estos meses sin vosotras aquí, ¡pero eso hará las reuniones aún más especiales! Os quiero muchísimo.

Aunque hay alguien más a quien conocí en Madrid a quien tengo que agradecerle la vida casi, me gusta dejar lo mejor para el final. Por ahora voy a ir moviéndome poco a poco hacia Sevilla, mi ciudad natal, agradeciendo a alguien a quien conocí allí pero que me persiguió hasta Madrid: Julia. Otra hermana postiza, en este caso de la carrera, de la que no me pienso separar jamás. La conexión que alcanzamos durante esos cuatro años de carrera ya no la rompen ni la distancia ni el tiempo, y cuando me dijiste que te venías a hacer la tesis a Madrid no pude estar más contento. Aunque al final, como suele pasar, nos hemos visto menos de lo que nos habría gustado, cada segundo que hemos compartido siempre tiene un efecto balsámico en mí: saber que puedo confiar en ti para todo me tranquiliza pase lo que pase. También hemos tenido nuestros momentos de diversión, como aquella noche con Carmen en tu piso o el día en Punta con Pepe. Sea el plan que sea, sé que contigo siempre estaré a gusto, gracias por no alejarte nunca.

Ahora me toca hablar de cuatro personitas a las que tengo la mayor parte del tiempo a 500 km de distancia, pero con quienes rara vez pasa un día sin que hable: sí, vosotros, integrantes del Club de Fans de Ganon Rehidratado (tiene narices que haya escrito eso en mi tesis, pero culpa mía por nombrar así al grupo). Antonio, Luis, Glori y Orellana, uno de los pilares de mi cordura durante todo este tiempo. Da igual lo mucho que me estrese la tesis o la vida en general, comentar jueguicos, animes o frikadas varias con vosotros siempre me transporta a un lugar seguro, un espacio donde me siento protegido. Confío en que, en especial a Orellana, os piten los oídos y os dé una subida de azúcar, pero no os hacéis una idea de lo que os quiero y de lo afortunado que me siento por tener amigos como vosotros. Este E3 habrá sido un poco una mierda pero, ¡ya llegarán conferencias que disfrutemos comentando por Discord!

Otro grupo de personas que se originó en Sevilla pero que actualmente está desperdigado por medio mundo. Adri, Carmen, Glou, Marta, Mati y, por supuestísimo, nuestro querido Ramón. Nos conocimos cuando yo era una persona muy distinta, en el instituto, cuando casi era una sombra de quien soy ahora. Y, sin embargo, me aceptasteis por cómo era y desde entonces, para mi sorpresa a veces, habéis sido mis amigos hasta el día de hoy. Aunque ahora está bastante complicado que volvamos a coincidir todos en Dos Hermanas para echar una buena tarde de verano en la piscina de Ramón, por otro lado tenemos casa en Zurich, Barcelona, Londres, Madrid y Dos hermanas. Y, vosotros, la tendréis en Grenoble también próximamente, porque estemos donde estemos siempre nos unirá lo reventados que estamos todos, en el mejor de los sentidos.

No me olvido tampoco de Xtina, Rosa, MPaz y Christian, el otro grupo de chalados que se hicieron mis amigos desde el instituto. Aunque los encuentros ahora sean escasos, siempre que sucedan serán tan maravillosos como siempre, como lo fue la boda de Xtina.

Ya me voy acercando al final de la turra que estoy soltando, y ahora me toca hablar de mis raíces, las de sangre pero sobre todo las que formaron quien soy a día de hoy. En general toda mi familia siempre me ha apoyado en todo lo que he hecho: soy un afortunado, poco importa que haya sido un niño peculiar, que mis decisiones no siempre fueran en la norma general o que mis gustos sean atípicos, mi familia siempre me ha querido y aceptado como tal. Incluso las adiciones más recientes y no de sangre, Juan Antonio y Carmen, han llegado sólo para sumar, dar cariño y apoyo. Gracias a ambos por ser tan maravillosos y por hacer tan felices a mis seres queridos. Pero necesito dedicar unas palabras especiales a vosotros tres, Mamá, Papá y Curro (en tu tesis serás Francisco, pero aquí te aguantas con Curro). Da igual las veces que uno lo diga, porque siempre sonará muy manido, pero es algo que siento hasta en lo más profundo de mi ser, y es que soy quien soy gracias a vosotros tres.

Mamá, tú me has enseñado a sentir, a saber vivir con mi emotividad. Me has enseñado lo que es la perseverancia, me has enseñado a luchar por lo que es justo y a no rendirme. No es sólo que te deba la vida en el sentido biológico de la palabra, es que ESTA vida que llevo, el hecho de que pueda ser feliz conmigo mismo, que me comprenda a mí y a quienes me rodean, todo eso te lo debo a ti. Gracias por todos los debates acalorados que tenemos, gracias por los achuchones que me nos damos siempre que nos vemos, gracias por descubrirme una de mis pasiones: la literatura fantástica. Gracias por haber estado siempre ahí para todo lo que he necesitado, apoyándome, regando mis intereses conforme iban apareciendo. Gracias por

entenderme con la facilidad que te caracteriza, por saber al instante si me ha pasado algo, y por confiarme también tus problemas. Gracias por ser la mejor madre que jamás podría existir, por superarte cada día. Gracias mamá, por todo lo que eres y todo lo que das. Te quiero con todo mi corazón.

Papá, tú no te quedas atrás. Aunque a veces haya podido tener la sensación de que me pudiera faltar un punto de conexión contigo, ni un sólo segundo he notado tu amor lejos. Siempre me has apoyado incondicionalmente, en cada uno de mis pasos, sin dudar de mí ni un segundo. Si no fuera por ti, que me sentabas en tu rodilla frente al ordenador desde que era un enano, puede que jamás hubiera descubierto otra de mis pasiones: los videojuegos. Es más, puede que nunca hubiese estudiado física si no hubiese empezado a interesarme primero por la informática y las matemáticas. A pesar de que no fuera por un motivo alegre, no te haces una idea de lo feliz que me hizo poder compartir unos días contigo, en tu piso, hace algunos meses, y comprobar que en ningún momento se ha perdido esa conexión, que simplemente tenemos una forma distinta de comunicarnos entre nosotros, y que esté donde esté siempre voy a poder contar contigo. Gracias, Papá, te quiero a rabiar.

Y ahora toca el otro, mi hermano mayor, el biólogo más currante (pun intended) del mundo. Tío, Curro, ¿qué te digo? Porque normalmente no te digo mucho lo importante que eres para mí, pero es que es la pura verdad. A pesar de lo pesado que eras y lo mucho que me chinchabas en mi infancia, a pesar de las discusiones que hayamos tenido como cualquier hijo de vecino, hubo un punto de inflexión. Hubo un momento en que o bien yo crecí, o tú me entendiste mejor o simplemente nos encontramos en el camino. Antes de eso siempre estuviste ahí, siempre me protegiste y defendiste cuando hizo falta, pero desde entonces sentí que podía ir a tu lado, y no detrás de ti como me había sentido mucho tiempo. Desde aquel momento, más o menos cuando empezamos a ir juntos a cenar al Anatolia, sentí que de repente contaba con un confidente, con alguien con quien podía compartir cualquier cosa. Verte pelear por seguir en la ciencia, toda la fuerza que desprendes y la atracción magnética que siente hacia ti cualquiera que te conoce... No sabes lo mucho que te admiro, y lo feliz que me hace disfrutar a tu lado de las cosas que ambos logramos, de lo que nos hace ser nosotros. Ojalá puedas venir en persona a mi lectura de tesis y yo pueda ir a la tuya poco después. Gracias, Curro, por ser uno de los motores que me impulsa a seguir adelante.

Y ahora llego al punto que me he estado reservando. Llego ya blandito después de escribir todo lo anterior a corazón abierto, pero aquí quizá me deshaga. Hubo alguien a quien conocí más o menos cuando empezó mi viaje en la investigación, pero que quiero mantener a mi lado durante el resto de mi vida, académica o no.

Yves. Decirte que eres *my Sun and stars* puede ser una chorrada empalagosa sacada de Canción de Hielo y Fuego, pero la metáfora no podría ser más acertada. Es gracias a ti que esta tesis ha salido adelante, porque cuando he estado hundido en la mierda más profunda tú siempre has estado ahí para sacarme, para que un rayito de luz se abra paso entre las nubes. No es que me completes, porque tú me has enseñado que no estaba roto, que no necesitaba que me arreglasen, no. Tú me has querido por como soy, has abrazado cada pedacito de mí, has estado a mi lado cuando pensaba que la cabeza me iba a explotar, cuando no quería nada más que dejar de ser yo mismo. Y aquí sigues, abrazándome como un koala, queriendo compartir tu futuro conmigo.

Gracias por besar mis lágrimas, pero también por escucharme cuando me emociono por cualquier tontería que me ilusiona. Gracias por gochear conmigo, por compartir risas, series, viajes... Por disfrutar del día a día juntos. Gracias por los planes inesperados, por tu sonrisa y tus mimos al despertar juntos. Gracias por tu paciencia, por crecer junto a mí, por abrirte a mí y por la infinita confianza que me regalas. Gracias Yves por haberme esperado cuando me he ido lejos, sin permitir que me sintiese solo ni un solo día. Gracias por enseñarme a llorar de felicidad, de amor, por ofrecerme tus brazos como lugar seguro.

Todo lo que pueda decir es poco, porque estás por todas partes en mi cabeza. Me contentaré con saber que tengo mucho tiempo para decirte lo mucho que te amo día a día, encontrando nuevas formas de ser moñas y simplemente disfrutando de la vida a tu lado. Te amo, Yves, ahora y siempre, y me muero de ganas por ver qué nos depara el futuro juntos, por verte experimentar nuevas cosas y elegir tu camino, confío, a mi lado. Yvernando forever.

Bibliography

[1] S. L. Glashow, *Partial Symmetries of Weak Interactions*, Nucl. Phys. **22** (1961) 579–588. 1, 4

[2] M. Gell-Mann, *A Schematic Model of Baryons and Mesons*, Phys. Lett. **8** (1964) 214–215. 1, 4

[3] S. Weinberg, *A Model of Leptons*, Phys. Rev. Lett. **19** (1967) 1264–1266. 1, 4

[4] A. Salam, *Weak and Electromagnetic Interactions*, Conf. Proc. C **680519** (1968) 367–377. 1, 4

[5] P. W. Higgs, *Broken symmetries, massless particles and gauge fields*, Phys. Lett. **12** (1964) 132–133. 1, 4

[6] P. W. Higgs, *Broken Symmetries and the Masses of Gauge Bosons*, Phys. Rev. Lett. **13** (1964) 508–509. 1, 4

[7] F. Englert and R. Brout, *Broken Symmetry and the Mass of Gauge Vector Mesons*, Phys. Rev. Lett. **13** (1964) 321–323. 1, 4

[8] G. S. Guralnik, C. R. Hagen, and T. W. B. Kibble, *Global Conservation Laws and Massless Particles*, Phys. Rev. Lett. **13** (1964) 585–587. 1, 4

[9] P. W. Higgs, *Spontaneous Symmetry Breakdown without Massless Bosons*, Phys. Rev. **145** (1966) 1156–1163. 1, 4

[10] G. Degrassi, S. Di Vita, J. Elias-Miro, J. R. Espinosa, G. F. Giudice, G. Isidori, and A. Strumia, *Higgs mass and vacuum stability in the Standard Model at NNLO*, JHEP **08** (2012) 098, [arXiv:1205.6497]. 13

[11] S. Weinberg, *Baryon and Lepton Nonconserving Processes*, Phys. Rev. Lett. **43** (1979) 1566–1570. 16

[12] D. J. Fixsen, *The Temperature of the Cosmic Microwave Background*, Astrophys. J. **707** (2009) 916–920, [arXiv:0911.1955]. 20

[13] **Planck** Collaboration, N. Aghanim *et. al.*, *Planck 2018 results. VI. Cosmological parameters*, arXiv:1807.06209. 21, 79, 109, 126

[14] P. F. de Salas and S. Pastor, *Relic neutrino decoupling with flavour oscillations revisited*, JCAP **07** (2016) 051, [arXiv:1606.06986]. 21

[15] **Particle Data Group** Collaboration, P. A. Zyla *et. al.*, *Review of Particle Physics*, PTEP **2020** (2020), no. 8 083C01. 25, 27

[16] M. Aker *et. al.*, *First direct neutrino-mass measurement with sub-eV sensitivity*, arXiv:2105.08533. 27, 28

[17] I. Esteban, M. C. Gonzalez-Garcia, M. Maltoni, T. Schwetz, and A. Zhou, *The fate of hints: updated global analysis of three-flavor neutrino oscillations*, JHEP **09** (2020) 178, [arXiv:2007.14792]. 28, 83

[18] F. Capozzi, E. Lisi, A. Marrone, and A. Palazzo, *Current unknowns in the three neutrino framework*, Prog. Part. Nucl. Phys. **102** (2018) 48–72, [arXiv:1804.09678]. 28

[19] P. F. de Salas, D. V. Forero, C. A. Ternes, M. Tortola, and J. W. F. Valle, *Status of neutrino oscillations 2018: 3σ hint for normal mass ordering and improved CP sensitivity*, Phys. Lett. B **782** (2018) 633–640, [arXiv:1708.01186]. 28

[20] B. Grinstein, M. Redi, and G. Villadoro, *Low Scale Flavor Gauge Symmetries*, JHEP **11** (2010) 067, [arXiv:1009.2049]. 32, 37, 61, 63, 76

[21] T. Feldmann, *See-Saw Masses for Quarks and Leptons in $SU(5)$*, JHEP **04** (2011) 043, [arXiv:1010.2116]. 32, 37, 61, 76

[22] A. J. Buras, L. Merlo, and E. Stamou, *The Impact of Flavour Changing Neutral Gauge Bosons on $\bar{B} - \≫ X_S\gamma$*, JHEP **08** (2011) 124, [arXiv:1105.5146]. 32, 37, 61, 76

[23] A. J. Buras, M. V. Carlucci, L. Merlo, and E. Stamou, *Phenomenology of a Gauged $SU(3)^3$ Flavour Model*, JHEP **03** (2012) 088, [arXiv:1112.4477]. 32, 37, 61, 63, 76

[24] D. Guadagnoli, R. N. Mohapatra, and I. Sung, *Gauged Flavor Group with Left-Right Symmetry*, JHEP **04** (2011) 093, [arXiv:1103.4170]. 32, 37, 61, 76

[25] E. Ma and G. Rajasekaran, *Softly Broken A_4 Symmetry for Nearly Degenerate Neutrino Masses*, Phys. Rev. **D64** (2001) 113012, [hep-ph/0106291]. 32

[26] K. S. Babu, E. Ma, and J. W. F. Valle, *Underlying A_4 Symmetry for the Neutrino Mass Matrix and the Quark Mixing Matrix*, Phys. Lett. **B552** (2003) 207–213, [hep-ph/0206292]. 32

[27] G. Altarelli and F. Feruglio, *Tri-Bimaximal Neutrino Mixing from Discrete Symmetry in Extra Dimensions*, Nucl. Phys. **B720** (2005) 64–88, [hep-ph/0504165]. 32

[28] H. Ishimori, T. Kobayashi, H. Ohki, Y. Shimizu, H. Okada, and M. Tanimoto, *Non-Abelian Discrete Symmetries in Particle Physics*, Prog. Theor. Phys. Suppl. **183** (2010) 1–163, [arXiv:1003.3552]. 32

[29] G. Altarelli, F. Feruglio, and L. Merlo, *Tri-Bimaximal Neutrino Mixing and Discrete Flavour Symmetries*, Fortsch. Phys. **61** (2013) 507–534, [arXiv:1205.5133]. 32

[30] D. Hernandez and A. Smirnov, *Lepton Mixing and Discrete Symmetries*, Phys. Rev. D **86** (2012) 053014, [arXiv:1204.0445]. 32

[31] W. Grimus and P. O. Ludl, *Finite Flavour Groups of Fermions*, J. Phys. **A45** (2012) 233001, [arXiv:1110.6376]. 32

[32] S. F. King and C. Luhn, *Neutrino Mass and Mixing with Discrete Symmetry*, Rept. Prog. Phys. **76** (2013) 056201, [arXiv:1301.1340]. 32

[33] P. F. Harrison, D. H. Perkins, and W. G. Scott, *Tri-Bimaximal Mixing and the Neutrino Oscillation Data*, Phys. Lett. **B530** (2002) 167, [hep-ph/0202074]. 32

[34] Z.-z. Xing, *Nearly Tri Bimaximal Neutrino Mixing and CP Violation*, Phys. Lett. **B533** (2002) 85–93, [hep-ph/0204049]. 32

[35] **T2K** Collaboration, K. Abe *et. al.*, *Indication of Electron Neutrino Appearance from an Accelerator-Produced Off-Axis Muon Neutrino Beam*, Phys. Rev. Lett. **107** (2011) 041801, [arXiv:1106.2822]. 33

[36] **MINOS** Collaboration, P. Adamson *et. al.*, *Improved Search for Muon-Neutrino to Electron-Neutrino Oscillations in Minos*, Phys. Rev. Lett. **107** (2011) 181802, [arXiv:1108.0015]. 33

[37] **Double Chooz** Collaboration, Y. Abe *et. al.*, *Indication for the Disappearance of Reactor Electron Antineutrinos in the Double Chooz Experiment*, Phys. Rev. Lett. **108** (2012) 131801, [arXiv:1112.6353]. 33

[38] **Daya Bay** Collaboration, F. P. An *et. al.*, *Observation of Electron-Antineutrino Disappearance at Daya Bay*, Phys. Rev. Lett. **108** (2012) 171803, [arXiv:1203.1669]. 33

[39] **RENO** Collaboration, J. K. Ahn *et. al.*, *Observation of Reactor Electron Antineutrino Disappearance in the Reno Experiment*, Phys. Rev. Lett. **108** (2012) 191802, [arXiv:1204.0626]. 33

[40] F. Feruglio, C. Hagedorn, Y. Lin, and L. Merlo, *Tri-bimaximal Neutrino Mixing and Quark Masses from a Discrete Flavour Symmetry*, Nucl. Phys. B **775** (2007) 120–142, [hep-ph/0702194]. [Erratum: Nucl.Phys.B 836, 127–128 (2010)]. 33

[41] R. Chivukula and H. Georgi, *Composite Technicolor Standard Model*, Phys. Lett. B **188** (1987) 99–104. 33, 36, 118

[42] G. D'Ambrosio, G. Giudice, G. Isidori, and A. Strumia, *Minimal flavor violation: An Effective field theory approach*, Nucl. Phys. B **645** (2002) 155–187, [hep-ph/0207036]. 33, 36, 37, 62, 118

[43] R. Barbieri, G. Isidori, J. Jones-Perez, P. Lodone, and D. M. Straub, *$U(2)$ and Minimal Flavour Violation in Supersymmetry*, Eur. Phys. J. **C71** (2011) 1725, [arXiv:1105.2296]. 33

[44] G. Blankenburg, G. Isidori, and J. Jones-Perez, *Neutrino Masses and Lfv from Minimal Breaking of $U(3)^5$ and $U(2)^5$ Flavor Symmetries*, Eur. Phys. J. **C72** (2012) 2126, [arXiv:1204.0688]. 33

[45] F. Arias-Aragón, C. Bouthelier-Madre, J. M. Cano, and L. Merlo, *Data Driven Flavour Model*, Eur. Phys. J. C **80** (2020), no. 9 854, [arXiv:2003.05941]. 33

[46] C. D. Froggatt and H. B. Nielsen, *Hierarchy of Quark Masses, Cabibbo Angles and CP Violation*, Nucl. Phys. **B147** (1979) 277–298. 33, 85

[47] W. Buchmuller, V. Domcke, and K. Schmitz, *Predicting θ_{13} and the Neutrino Mass Scale from Quark Lepton Mass Hierarchies*, JHEP **03** (2012) 008, [arXiv:1111.3872]. 33

[48] G. Altarelli, F. Feruglio, I. Masina, and L. Merlo, *Repressing Anarchy in Neutrino Mass Textures*, JHEP **11** (2012) 139, [arXiv:1207.0587]. 33, 64

[49] J. Bergstrom, D. Meloni, and L. Merlo, *Bayesian Comparison of U(1) Lepton Flavor Models*, Phys. Rev. **D89** (2014), no. 9 093021, [arXiv:1403.4528]. 33, 64

[50] G. Isidori, Y. Nir, and G. Perez, *Flavor Physics Constraints for Physics Beyond the Standard Model*, Ann. Rev. Nucl. Part. Sci. **60** (2010) 355, [arXiv:1002.0900]. 36, 37

[51] R. K. Ellis *et. al.*, *Physics Briefing Book: Input for the European Strategy for Particle Physics Update 2020*, arXiv:1910.11775. 36

[52] B. Grinstein, V. Cirigliano, G. Isidori, and M. B. Wise, *Grand Unification and the Principle of Minimal Flavor Violation*, Nucl. Phys. **B763** (2007) 35–48, [hep-ph/0608123]. 37

[53] M. Redi and A. Weiler, *Flavor and CP Invariant Composite Higgs Models*, JHEP **11** (2011) 108, [arXiv:1106.6357]. 37

[54] R. Alonso, M. B. Gavela, L. Merlo, S. Rigolin, and J. Yepes, *Minimal Flavour Violation with Strong Higgs Dynamics*, JHEP **06** (2012) 076, [arXiv:1201.1511]. 37

[55] R. Alonso, M. B. Gavela, L. Merlo, S. Rigolin, and J. Yepes, *Flavor with a Light Dynamical "Higgs Particle"*, Phys. Rev. **D87** (2013), no. 5 055019, [arXiv:1212.3307]. 37, 66

[56] L. Lopez-Honorez and L. Merlo, *Dark Matter Within the Minimal Flavour Violation Ansatz*, Phys. Lett. **B722** (2013) 135–143, [arXiv:1303.1087]. 37

[57] L. Merlo and S. Rosauro-Alcaraz, *Predictive Leptogenesis from Minimal Lepton Flavour Violation*, JHEP **07** (2018) 036, [arXiv:1801.03937]. 37

[58] V. Cirigliano, B. Grinstein, G. Isidori, and M. B. Wise, *Minimal flavor violation in the lepton sector*, Nucl. Phys. B **728** (2005) 121–134, [hep-ph/0507001]. 39, 40, 62, 65, 89

[59] S. Davidson and F. Palorini, *Various definitions of Minimal Flavour Violation for Leptons*, Phys. Lett. B **642** (2006) 72–80, [hep-ph/0607329]. 39, 40, 62, 89

[60] R. Alonso, G. Isidori, L. Merlo, L. A. Munoz, and E. Nardi, *Minimal flavour violation extensions of the seesaw*, JHEP **06** (2011) 037, [arXiv:1103.5461]. 39, 40, 62, 63, 89, 90

[61] E. Bertuzzo, P. Di Bari, F. Feruglio, and E. Nardi, *Flavor Symmetries, Leptogenesis and the Absolute Neutrino Mass Scale*, JHEP **11** (2009) 036, [arXiv:0908.0161]. 39, 90

[62] D. Aristizabal Sierra, F. Bazzocchi, I. de Medeiros Varzielas, L. Merlo, and S. Morisi, *Tri-Bimaximal Lepton Mixing and Leptogenesis*, Nucl. Phys. **B827** (2010) 34–58, [arXiv:0908.0907]. 39, 90

[63] V. Cirigliano and B. Grinstein, *Phenomenology of Minimal Lepton Flavor Violation*, Nucl. Phys. **B752** (2006) 18–39, [hep-ph/0601111]. 40

[64] M. B. Gavela, T. Hambye, D. Hernandez, and P. Hernandez, *Minimal Flavour Seesaw Models*, JHEP **09** (2009) 038, [arXiv:0906.1461]. 40

[65] R. Alonso, E. Fernandez Martínez, M. B. Gavela, B. Grinstein, L. Merlo, and P. Quilez, *Gauged Lepton Flavour*, JHEP **12** (2016) 119, [arXiv:1609.05902]. 40, 61, 76

[66] D. Dinh, L. Merlo, S. T. Petcov, and Vega-Álvarez, *Revisiting Minimal Lepton Flavour Violation in the Light of Leptonic CP Violation*, JHEP **07** (2017) 089, [arXiv:1705.09284]. 40, 62, 65

[67] V. Baluni, *CP Violating Effects in QCD*, Phys. Rev. D **19** (1979) 2227–2230. 42

[68] R. Crewther, P. Di Vecchia, G. Veneziano, and E. Witten, *Chiral Estimate of the Electric Dipole Moment of the Neutron in Quantum Chromodynamics*, Phys. Lett. B **88** (1979) 123. [Erratum: Phys.Lett.B 91, 487 (1980)]. 42

[69] **nEDM** Collaboration, E. P. Tsentalovich, *The nEDM experiment at the SNS*, Phys. Part. Nucl. **45** (2014) 249–250. 42

[70] C. A. Baker *et. al.*, *An Improved Experimental Limit on the Electric Dipole Moment of the Neutron*, Phys. Rev. Lett. **97** (2006) 131801, [hep-ex/0602020]. 42

[71] **nEDM** Collaboration, C. Abel *et. al.*, *Measurement of the Permanent Electric Dipole Moment of the Neutron*, Phys. Rev. Lett. **124** (2020), no. 8 081803, [arXiv:2001.11966]. 42

[72] J. Steinberger, *On the Use of subtraction fields and the lifetimes of some types of meson decay*, Phys. Rev. **76** (1949) 1180–1186. 44

[73] J. S. Schwinger, *On gauge invariance and vacuum polarization*, Phys. Rev. **82** (1951) 664–679. 44

[74] S. L. Adler, *Axial vector vertex in spinor electrodynamics*, Phys. Rev. **177** (1969) 2426–2438. 44

[75] J. S. Bell and R. Jackiw, *A PCAC puzzle: $\pi^0 \to \gamma\gamma$ in the σ model*, Nuovo Cim. A **60** (1969) 47–61. 44

[76] K. Fujikawa, *Path Integral Measure for Gauge Invariant Fermion Theories*, Phys. Rev. Lett. **42** (1979) 1195–1198. 44

[77] A. Hook, *Anomalous solutions to the strong CP problem*, Phys. Rev. Lett. **114** (2015), no. 14 141801, [arXiv:1411.3325]. 49

[78] A. E. Nelson, *Naturally Weak CP Violation*, Phys. Lett. B **136** (1984) 387–391. 49

[79] S. M. Barr, *Solving the Strong CP Problem Without the Peccei-Quinn Symmetry*, Phys. Rev. Lett. **53** (1984) 329. 49

[80] L. Bento, G. C. Branco, and P. A. Parada, *A Minimal model with natural suppression of strong CP violation*, Phys. Lett. B **267** (1991) 95–99. 49

[81] G. Hiller and M. Schmaltz, *Solving the Strong CP Problem with Supersymmetry*, Phys. Lett. B **514** (2001) 263–268, [hep-ph/0105254]. 49

[82] R. D. Peccei and H. R. Quinn, *CP Conservation in the Presence of Instantons*, Phys. Rev. Lett. **38** (1977) 1440–1443. 50

[83] R. D. Peccei and H. R. Quinn, *Constraints Imposed by CP Conservation in the Presence of Instantons*, Phys. Rev. **D16** (1977) 1791–1797. 50

[84] S. Weinberg, *A New Light Boson?*, Phys. Rev. Lett. **40** (1978) 223–226. 50

[85] F. Wilczek, *Problem of Strong P and T Invariance in the Presence of Instantons*, Phys. Rev. Lett. **40** (1978) 279–282. 50

[86] J. E. Kim, *Light Pseudoscalars, Particle Physics and Cosmology*, Phys. Rept. **150** (1987) 1–177. 52

[87] H. Georgi and L. Randall, *Flavor Conserving CP Violation in Invisible Axion Models*, Nucl. Phys. B **276** (1986) 241–252. 55

[88] H. Georgi, D. B. Kaplan, and L. Randall, *Manifesting the Invisible Axion at Low-Energies*, Phys. Lett. **B169** (1986) 73–78. 55, 69, 101

[89] A. R. Zhitnitsky, *On Possible Suppression of the Axion Hadron Interactions. (In Russian)*, Sov. J. Nucl. Phys. **31** (1980) 260. [Yad. Fiz.31,497(1980)]. 55, 61, 116, 120, 126

[90] M. Dine, W. FisCHLer, and M. Srednicki, *A Simple Solution to the Strong CP Problem with a Harmless Axion*, Phys. Lett. **B104** (1981) 199–202. 55, 61, 116, 120, 126

[91] J. E. Kim, *Weak Interaction Singlet and Strong CP Invariance*, Phys. Rev. Lett. **43** (1979) 103. 58, 61, 116

[92] M. A. Shifman, A. I. Vainshtein, and V. I. Zakharov, *Can Confinement Ensure Natural CP Invariance of Strong Interactions?*, Nucl. Phys. **B166** (1980) 493–506. 58, 61, 76, 116, 126

[93] M. Gorghetto and G. Villadoro, *Topological Susceptibility and QCD Axion Mass: QED and NNLO corrections*, JHEP **03** (2019) 033, [arXiv:1812.01008]. 59

[94] E. Witten, *Some Properties of O(32) Superstrings*, Phys. Lett. B **149** (1984) 351–356. 59

[95] J. P. Conlon, *The QCD axion and moduli stabilisation*, JHEP **05** (2006) 078, [hep-th/0602233]. 59

[96] P. Svrcek and E. Witten, *Axions In String Theory*, JHEP **06** (2006) 051, [hep-th/0605206]. 59

[97] K.-S. Choi, H. P. Nilles, S. Ramos-Sanchez, and P. K. S. Vaudrevange, *Accions*, Phys. Lett. B **675** (2009) 381–386, [arXiv:0902.3070]. 59

[98] A. Arvanitaki, S. Dimopoulos, S. Dubovsky, N. Kaloper, and J. March-Russell, *String Axiverse*, Phys. Rev. D **81** (2010) 123530, [arXiv:0905.4720]. 59

[99] B. S. Acharya, K. Bobkov, and P. Kumar, *An M Theory Solution to the Strong CP Problem and Constraints on the Axiverse*, JHEP **11** (2010) 105, [arXiv:1004.5138]. 59

[100] M. Cicoli, M. Goodsell, and A. Ringwald, *The type IIB string axiverse and its low-energy phenomenology*, JHEP **10** (2012) 146, [arXiv:1206.0819]. 59

[101] J. Halverson, C. Long, and P. Nath, *Ultralight axion in supersymmetry and strings and cosmology at small scales*, Phys. Rev. D **96** (2017), no. 5 056025, [arXiv:1703.07779]. 59

[102] D. J. E. Marsh, *Axion Cosmology*, Phys. Rept. **643** (2016) 1–79, [arXiv:1510.07633]. 59

[103] F. Arias-Aragon and L. Merlo, *The Minimal Flavour Violating Axion*, JHEP **10** (2017) 168, [arXiv:1709.07039]. 61, 116, 118

[104] T. Feldmann, C. Luhn, and P. Moch, *Lepton-Flavour Violation in a Pati-Salam Model with Gauged Flavour Symmetry*, JHEP **11** (2016) 078, [arXiv:1608.04124]. 61, 76

[105] Y. Ema, K. Hamaguchi, T. Moroi, and K. Nakayama, *Flaxion: a minimal extension to solve puzzles in the standard model*, JHEP **01** (2017) 096, [arXiv:1612.05492]. 62, 77, 119

[106] L. Calibbi, F. Goertz, D. Redigolo, R. Ziegler, and J. Zupan, *Minimal axion model from flavor*, Phys. Rev. D **95** (2017), no. 9 095009, [arXiv:1612.08040]. 62, 77, 78, 119

[107] F. Wilczek, *Axions and Family Symmetry Breaking*, Phys. Rev. Lett. **49** (1982) 1549–1552. 62

[108] R. Alonso, M. B. Gavela, L. Merlo, and S. Rigolin, *On the Scalar Potential of Minimal Flavour Violation*, JHEP **07** (2011) 012, [arXiv:1103.2915]. 62, 63

[109] R. Alonso, M. B. Gavela, D. Hernandez, and L. Merlo, *On the Potential of Leptonic Minimal Flavour Violation*, Phys. Lett. **B715** (2012) 194–198, [arXiv:1206.3167]. 62, 63

[110] R. Alonso, M. B. Gavela, D. Hernández, L. Merlo, and S. Rigolin, *Leptonic Dynamical Yukawa Couplings*, JHEP **08** (2013) 069, [arXiv:1306.5922]. 62, 63

[111] R. Alonso, M. B. Gavela, G. Isidori, and L. Maiani, *Neutrino Mixing and Masses from a Minimum Principle*, JHEP **11** (2013) 187, [arXiv:1306.5927]. 62, 63

[112] M. E. Albrecht, T. Feldmann, and T. Mannel, *Goldstone Bosons in Effective Theories with Spontaneously Broken Flavour Symmetry*, JHEP **10** (2010) 089, [arXiv:1002.4798]. 63

[113] K. Choi, S. H. Im, C. B. Park, and S. Yun, *Minimal Flavor Violation with Axion-Like Particles*, arXiv:1708.00021. 65

[114] D. B. Kaplan and H. Georgi, $SU(2) \times U(1)$ *Breaking by Vacuum Misalignment*, Phys. Lett. **B136** (1984) 183–186. 66

[115] D. B. Kaplan, H. Georgi, and S. Dimopoulos, *Composite Higgs Scalars*, Phys. Lett. **B136** (1984) 187–190. 66

[116] T. Banks, *Constraints on* $SU(2) \times U(1)$ *Breaking by Vacuum Misalignment*, Nucl. Phys. **B243** (1984) 125–130. 66

[117] K. Agashe, R. Contino, and A. Pomarol, *The Minimal Composite Higgs Model*, Nucl. Phys. **B719** (2005) 165–187, [hep-ph/0412089]. 66

[118] B. Gripaios, A. Pomarol, F. Riva, and J. Serra, *Beyond the Minimal Composite Higgs Model*, JHEP **04** (2009) 070, [arXiv:0902.1483]. 66

[119] J. Mrazek, A. Pomarol, R. Rattazzi, M. Redi, J. Serra, and A. Wulzer, *The Other Natural Two Higgs Doublet Model*, Nucl. Phys. **B853** (2011) 1–48, [arXiv:1105.5403]. 66

[120] R. Alonso, I. Brivio, B. Gavela, L. Merlo, and S. Rigolin, *Sigma Decomposition*, JHEP **12** (2014) 034, [arXiv:1409.1589]. 66

[121] G. Panico and A. Wulzer, *The Composite Nambu-Goldstone Higgs*, Lect. Notes Phys. **913** (2016) pp.1–316, [arXiv:1506.01961]. 66

[122] I. M. Hierro, L. Merlo, and S. Rigolin, *Sigma Decomposition: the Cp-Odd Lagrangian*, JHEP **04** (2016) 016, [arXiv:1510.07899]. 66

[123] E. Halyo, *Technidilaton Or Higgs?*, Mod. Phys. Lett. **A8** (1993) 275–284. 66

[124] W. D. Goldberger, B. Grinstein, and W. Skiba, *Distinguishing the Higgs Boson from the Dilaton at the Large Hadron Collider*, Phys. Rev. Lett. **100** (2008) 111802, [arXiv:0708.1463]. 66

[125] L. Vecchi, *Phenomenology of a Light Scalar: the Dilaton*, Phys. Rev. **D82** (2010) 076009, [arXiv:1002.1721]. 66

[126] S. Matsuzaki and K. Yamawaki, *Is 125 GeV Techni-Dilaton Found at Lhc?*, Phys. Lett. **B719** (2013) 378–382, [arXiv:1207.5911]. 66

[127] Z. Chacko and R. K. Mishra, *Effective Theory of a Light Dilaton*, Phys. Rev. **D87** (2013), no. 11 115006, [arXiv:1209.3022]. 66

[128] Z. Chacko, R. Franceschini, and R. K. Mishra, *Resonance at 125 Gev: Higgs Or Dilaton/Radion?*, JHEP **04** (2013) 015, [arXiv:1209.3259]. 66

[129] B. Bellazzini, C. Csaki, J. Hubisz, J. Serra, and J. Terning, *A Higgslike Dilaton*, Eur. Phys. J. **C73** (2013), no. 2 2333, [arXiv:1209.3299]. 66

[130] P. Hernandez-Leon and L. Merlo, *The Complete Bosonic Basis for a Higgs-Like Dilaton*, arXiv:1703.02064. 66

[131] F. Feruglio, *The Chiral Approach to the Electroweak Interactions*, Int. J. Mod. Phys. **A8** (1993) 4937–4972, [hep-ph/9301281]. 66

[132] R. Contino, C. Grojean, M. Moretti, F. Piccinini, and R. Rattazzi, *Strong Double Higgs Production at the Lhc*, JHEP **05** (2010) 089, [arXiv:1002.1011]. 66

[133] R. Alonso, M. B. Gavela, L. Merlo, S. Rigolin, and J. Yepes, *The Effective Chiral Lagrangian for a Light Dynamical "Higgs Particle"*, Phys. Lett. **B722** (2013) 330–335, [arXiv:1212.3305]. [Erratum: Phys. Lett.B726,926(2013)]. 66

[134] G. Buchalla, O. Catà, and C. Krause, *Complete Electroweak Chiral Lagrangian with a Light Higgs at Nlo*, Nucl. Phys. **B880** (2014) 552–573, [arXiv:1307.5017]. [Erratum: Nucl. Phys.B913,475(2016)]. 66

[135] I. Brivio, T. Corbett, O. J. P. Éboli, M. B. Gavela, J. Gonzalez-Fraile, M. C. Gonzalez-Garcia, L. Merlo, and S. Rigolin, *Disentangling a Dynamical Higgs*, JHEP **03** (2014) 024, [arXiv:1311.1823]. 66

[136] I. Brivio, O. J. P. Éboli, M. B. Gavela, M. C. Gonzalez-Garcia, L. Merlo, and S. Rigolin, *Higgs Ultraviolet Softening*, JHEP **12** (2014) 004, [arXiv:1405.5412]. 66

[137] M. B. Gavela, J. Gonzalez-Fraile, M. C. Gonzalez-Garcia, L. Merlo, S. Rigolin, and J. Yepes, *CP Violation with a Dynamical Higgs*, JHEP **10** (2014) 044, [arXiv:1406.6367]. 66

[138] M. B. Gavela, K. Kanshin, P. A. N. Machado, and S. Saa, *On the Renormalization of the Electroweak Chiral Lagrangian with a Higgs*, JHEP **03** (2015) 043, [arXiv:1409.1571]. 66

[139] I. Brivio, M. B. Gavela, L. Merlo, K. Mimasu, J. M. No, R. del Rey, and V. Sanz, *Non-Linear Higgs Portal to Dark Matter*, JHEP **04** (2016) 141, [arXiv:1511.01099]. 66

[140] B. M. Gavela, E. E. Jenkins, A. V. Manohar, and L. Merlo, *Analysis of General Power Counting Rules in Effective Field Theory*, Eur. Phys. J. **C76** (2016), no. 9 485, [arXiv:1601.07551]. 66

[141] R. Alonso, E. E. Jenkins, and A. V. Manohar, *Sigma Models with Negative Curvature*, Phys. Lett. **B756** (2016) 358–364, [arXiv:1602.00706]. 66

[142] O. J. P. Éboli and M. C. Gonzalez–Garcia, *Classifying the Bosonic Quartic Couplings*, Phys. Rev. **D93** (2016), no. 9 093013, [arXiv:1604.03555]. 66

[143] I. Brivio, J. Gonzalez-Fraile, M. C. Gonzalez-Garcia, and L. Merlo, *The Complete Heft Lagrangian After the Lhc Run I*, Eur. Phys. J. **C76** (2016), no. 7 416, [arXiv:1604.06801]. 66

[144] R. Alonso, E. E. Jenkins, and A. V. Manohar, *Geometry of the Scalar Sector*, JHEP **08** (2016) 101, [arXiv:1605.03602]. 66

[145] **LHC Higgs Cross Section Working Group** Collaboration, D. de Florian *et. al.*, *Handbook of Lhc Higgs Cross Sections: 4. Deciphering the Nature of the Higgs Sector*, arXiv:1610.07922. 66

[146] L. Merlo, S. Saa, and M. Sacristán-Barbero, *Baryon Non-Invariant Couplings in Higgs Effective Field Theory*, Eur. Phys. J. **C77** (2017), no. 3 185, [arXiv:1612.04832]. 66

[147] P. Kozów, L. Merlo, S. Pokorski, and M. Szleper, *Same-sign WW Scattering in the HEFT: Discoverability vs. EFT Validity*, JHEP **07** (2019) 021, [arXiv:1905.03354]. 66

[148] L. Merlo, F. Pobbe, and S. Rigolin, *The Minimal Axion Minimal Linear σ Model*, Eur. Phys. J. C **78** (2018), no. 5 415, [arXiv:1710.10500]. [Erratum: Eur.Phys.J.C 79, 963 (2019)]. 66

[149] J. Alonso-González, L. Merlo, F. Pobbe, S. Rigolin, and O. Sumensari, *Testable axion-like particles in the minimal linear σ model*, Nucl. Phys. B **950** (2020) 114839, [arXiv:1807.08643]. 66

[150] G. F. Giudice, R. Rattazzi, and A. Strumia, *Unificaxion*, Phys. Lett. **B715** (2012) 142–148, [arXiv:1204.5465]. 68

[151] M. Redi and A. Strumia, *Axion-Higgs Unification*, JHEP **11** (2012) 103, [arXiv:1208.6013]. 68

[152] M. Redi and R. Sato, *Composite Accidental Axions*, JHEP **05** (2016) 104, [arXiv:1602.05427]. 68

[153] L. Di Luzio, F. Mescia, and E. Nardi, *Redefining the Axion Window*, Phys. Rev. Lett. **118** (2017), no. 3 031801, [arXiv:1610.07593]. 68

[154] M. Farina, D. Pappadopulo, F. Rompineve, and A. Tesi, *The Photo-Philic QCD Axion*, JHEP **01** (2017) 095, [arXiv:1611.09855]. 68

[155] R. Coy, M. Frigerio, and M. Ibe, *Dynamical Clockwork Axions*, arXiv:1706.04529. 68

[156] D. B. Kaplan, *Opening the Axion Window*, Nucl. Phys. **B260** (1985) 215–226. 69, 101

[157] M. Srednicki, *Axion Couplings to Matter. 1. CP Conserving Parts*, Nucl. Phys. **B260** (1985) 689–700. 69, 101

[158] W. A. Bardeen, R. D. Peccei, and T. Yanagida, *Constraints on Variant Axion Models*, Nucl. Phys. **B279** (1987) 401–428. 69, 101

[159] G. Grilli di Cortona, E. Hardy, J. Pardo Vega, and G. Villadoro, *The QCD Axion, Precisely*, JHEP **01** (2016) 034, [arXiv:1511.02867]. 69, 70, 101, 127

[160] K. Choi, K. Kang, and J. E. Kim, *Effects of η' in Low-Energy Axion Physics*, Phys. Lett. **B181** (1986) 145–149. 69, 70

[161] J. D. Bjorken, S. Ecklund, W. R. Nelson, A. Abashian, C. Church, B. Lu, L. W. Mo, T. A. Nunamaker, and P. Rassmann, *Search for Neutral Metastable Penetrating Particles Produced in the Slac Beam Dump*, Phys. Rev. **D38** (1988) 3375. 69

[162] M. Carena and R. D. Peccei, *The Effective Lagrangian for Axion Emission from Sn1987A*, Phys. Rev. **D40** (1989) 652. 69, 70

[163] G. G. Raffelt, *Astrophysical Axion Bounds*, Lect. Notes Phys. **741** (2008) 51–71, [hep-ph/0611350]. [,51(2006)]. 69

[164] **E949, E787** Collaboration, S. Adler *et. al.*, *Measurement of the K+ –> pi+ nu nu branching ratio*, Phys. Rev. D **77** (2008) 052003, [arXiv:0709.1000]. 69, 73, 76

[165] **Borexino** Collaboration, G. Bellini *et. al.*, *Search for Solar Axions Produced in $p(d,{}^3He)A$ Reaction with Borexino Detector*, Phys. Rev. **D85** (2012) 092003, [arXiv:1203.6258]. 69, 72

[166] A. Friedland, M. Giannotti, and M. Wise, *Constraining the Axion-Photon Coupling with Massive Stars*, Phys. Rev. Lett. **110** (2013), no. 6 061101, [arXiv:1210.1271]. 69

[167] **BaBar** Collaboration, J. Lees *et. al.*, *Search for $B \to K^{(*)}\nu\overline{\nu}$ and invisible quarkonium decays*, Phys. Rev. D **87** (2013), no. 11 112005, [arXiv:1303.7465]. 69, 73, 76

[168] E. Armengaud *et. al.*, *Axion Searches with the Edelweiss-Ii Experiment*, JCAP **1311** (2013) 067, [arXiv:1307.1488]. 69, 72

[169] J. D. Clarke, R. Foot, and R. R. Volkas, *Phenomenology of a Very Light Scalar (100 MeV ≪ m_h ≪ 10 Gev) Mixing with the Sm Higgs*, JHEP **02** (2014) 123, [arXiv:1310.8042]. 69

[170] N. Viaux, M. Catelan, P. B. Stetson, G. Raffelt, J. Redondo, A. A. R. Valcarce, and A. Weiss, *Neutrino and Axion Bounds from the Globular ClusterM **5** (Ngc 5904)*, Phys. Rev. Lett. **111** (2013) 231301, [arXiv:1311.1669]. 69, 72, 92

[171] **XENON100** Collaboration, E. Aprile *et. al.*, *First Axion Results from the Xenon100 Experiment*, Phys. Rev. **D90** (2014), no. 6 062009, [arXiv:1404.1455]. [Erratum: Phys. Rev.D95,no.2,029904(2017)]. 69

[172] A. Ayala, I. Domínguez, M. Giannotti, A. Mirizzi, and O. Straniero, *Revisiting the Bound on Axion-Photon Coupling from Globular Clusters*, Phys. Rev. Lett. **113** (2014), no. 19 191302, [arXiv:1406.6053]. 69

[173] **CMS** Collaboration, V. Khachatryan *et. al.*, *Search for Dark Matter, Extra Dimensions, and Unparticles in Monojet Events in Proton–Proton Collisions at* $\sqrt{s} = 8$ *TeV*, Eur. Phys. J. **C75** (2015), no. 5 235, [arXiv:1408.3583]. 69, 70

[174] K. Mimasu and V. Sanz, *ALPs at Colliders*, JHEP **06** (2015) 173, [arXiv:1409.4792]. 69, 70

[175] M. J. Dolan, F. Kahlhoefer, C. McCabe, and K. Schmidt-Hoberg, *A Taste of Dark Matter: Flavour Constraints on Pseudoscalar Mediators*, JHEP **03** (2015) 171, [arXiv:1412.5174]. [Erratum: JHEP07,103(2015)]. 69

[176] M. Millea, L. Knox, and B. Fields, *New Bounds for Axions and Axion-Like Particles with Kev-Gev Masses*, Phys. Rev. **D92** (2015), no. 2 023010, [arXiv:1501.04097]. 69, 70

[177] N. Vinyoles, A. Serenelli, F. L. Villante, S. Basu, J. Redondo, and J. Isern, *New Axion and Hidden Photon Constraints from a Solar Data Global Fit*, JCAP **1510** (2015), no. 10 015, [arXiv:1501.01639]. 69

[178] **ATLAS** Collaboration, G. Aad *et. al.*, *Search for New Phenomena in Final States with an Energetic Jet and Large Missing Transverse Momentum in PP Collisions at* $\sqrt{s}$ *=8 TeV with the Atlas Detector*, Eur. Phys. J. **C75** (2015), no. 7 299, [arXiv:1502.01518]. [Erratum: Eur. Phys. J.C75,no.9,408(2015)]. 69, 70

[179] G. Krnjaic, *Probing Light Thermal Dark-Matter with a Higgs Portal Mediator*, Phys. Rev. **D94** (2016), no. 7 073009, [arXiv:1512.04119]. 69

[180] W. J. Marciano, A. Masiero, P. Paradisi, and M. Passera, *Contributions of Axionlike Particles to Lepton Dipole Moments*, Phys. Rev. **D94** (2016), no. 11 115033, [arXiv:1607.01022]. 69

[181] E. Izaguirre, T. Lin, and B. Shuve, *A New Flavor of Searches for Axion-Like Particles*, Phys. Rev. Lett. **118** (2017), no. 11 111802, [arXiv:1611.09355]. 69, 70, 73, 74

[182] I. Brivio, M. B. Gavela, L. Merlo, K. Mimasu, J. M. No, R. del Rey, and V. Sanz, *Alps Effective Field Theory and Collider Signatures*, Eur. Phys. J. **C77** (2017), no. 8 572, [arXiv:1701.05379]. 69, 70, 71, 77

[183] M. Bauer, M. Neubert, and A. Thamm, *LHC as an Axion Factory: Probing an Axion Explanation for* $(g-2)_\mu$ *with Exotic Higgs Decays*, Phys. Rev. Lett. **119** (2017), no. 3 031802, [arXiv:1704.08207]. 69

[184] **CAST** Collaboration, V. Anastassopoulos *et. al.*, *New Cast Limit on the Axion-Photon Interaction*, Nature Phys. **13** (2017) 584–590, [arXiv:1705.02290]. 69, 70, 91

[185] M. J. Dolan, T. Ferber, C. Hearty, F. Kahlhoefer, and K. Schmidt-Hoberg, *Revised Constraints and Belle II Sensitivity for Visible and Invisible Axion-Like Particles*, JHEP **12** (2017) 094, [arXiv:1709.00009]. 69, 70, 71, 72

[186] J. Jaeckel and M. Spannowsky, *Probing MeV to 90 GeV Axion-Like Particles with Lep and Lhc*, Phys. Lett. **B753** (2016) 482–487, [arXiv:1509.00476]. 69, 70, 72

[187] M. Bauer, M. Neubert, and A. Thamm, *Collider Probes of Axion-Like Particles*, JHEP **12** (2017) 044, [arXiv:1708.00443]. 69, 70, 77, 122

[188] **L3** Collaboration, M. Acciarri *et. al.*, *Search for Anomalous Z –≫ Gamma Gamma Gamma Events at Lep*, Phys. Lett. **B345** (1995) 609–616. 71

[189] **DELPHI** Collaboration, E. Anashkin *et. al.*, *An Analysis of E+ E- –≫ Gamma Gamma (Gamma) at Lep at S(1/2) Approximately 189-Gev*, in *Proceedings, International Europhysics Conference on High Energy Physics (Eps-Hep 1999): Tampere, Finland, July 15-21, 1999*, 1999. 71

[190] O. Straniero, I. Dominguez, M. Giannotti, and A. Mirizzi, *Axion-electron coupling from the RGB tip of Globular Clusters*, in *13th Patras Workshop on Axions, WIMPs and WISPs*, pp. 172–176, 2018. arXiv:1802.10357. 72

[191] S. A. Díaz, K.-P. Schröder, K. Zuber, D. Jack, and E. E. B. Barrios, *Constraint on the Axion-Electron Coupling Constant and the Neutrino Magnetic Dipole Moment by Using the Tip-RGb Luminosity of Fifty Globular Clusters*, arXiv:1910.10568. 72

[192] **BaBar** Collaboration, B. Aubert *et. al.*, *Search for Invisible Decays of a Light Scalar in Radiative Transitions* $\upsilon_{3S} \to \gamma\, A0$, in *34th International Conference on High Energy Physics*, 7, 2008. arXiv:0808.0017. 74

[193] **BaBar** Collaboration, P. del Amo Sanchez *et. al.*, *Search for Production of Invisible Final States in Single-Photon Decays of* $\Upsilon(1S)$, Phys. Rev. Lett. **107** (2011) 021804, [arXiv:1007.4646]. 74

[194] **Belle** Collaboration, I. S. Seong *et. al.*, *Search for a light CP-odd Higgs boson and low-mass dark matter at the Belle experiment*, Phys. Rev. Lett. **122** (2019), no. 1 011801, [arXiv:1809.05222]. 74

[195] L. Merlo, F. Pobbe, S. Rigolin, and O. Sumensari, *Revisiting the production of ALPs at B-factories*, JHEP **06** (2019) 091, [arXiv:1905.03259]. 74

[196] **CLEO** Collaboration, T. E. Coan *et. al.*, *Flavor - specific inclusive B decays to charm*, Phys. Rev. Lett. **80** (1998) 1150–1155, [hep-ex/9710028]. 74

[197] J. L. Feng, T. Moroi, H. Murayama, and E. Schnapka, *Third Generation Familons, B Factories, and Neutrino Cosmology*, Phys. Rev. **D57** (1998) 5875–5892, [hep-ph/9709411]. 74, 150

[198] J. Keller and A. Sedrakian, *Axions from Cooling Compact Stars*, Nucl. Phys. **A897** (2013) 62–69, [arXiv:1205.6940]. 75

[199] A. Sedrakian, *Axion Cooling of Neutron Stars*, Phys. Rev. **D93** (2016), no. 6 065044, [arXiv:1512.07828]. 75

[200] T. Fischer, S. Chakraborty, M. Giannotti, A. Mirizzi, A. Payez, and A. Ringwald, *Probing Axions with the Neutrino Signal from the Next Galactic Supernova*, Phys. Rev. **D94** (2016), no. 8 085012, [arXiv:1605.08780]. 75

[201] M. Giannotti, I. G. Irastorza, J. Redondo, A. Ringwald, and K. Saikawa, *Stellar Recipes for Axion Hunters*, JCAP **1710** (2017), no. 10 010, [arXiv:1708.02111]. 75

[202] P. Carenza, T. Fischer, M. Giannotti, G. Guo, G. Martínez-Pinedo, and A. Mirizzi, *Improved axion emissivity from a supernova via nucleon-nucleon bremsstrahlung*, JCAP **10** (2019), no. 10 016, [arXiv:1906.11844]. [Erratum: JCAP 05, E01 (2020)]. 75

[203] J. Martin Camalich, M. Pospelov, P. N. H. Vuong, R. Ziegler, and J. Zupan, *Quark Flavor Phenomenology of the QCD Axion*, Phys. Rev. D **102** (2020), no. 1 015023, [arXiv:2002.04623]. 76, 115, 123

[204] **BaBar** Collaboration, B. Aubert *et. al.*, *A search for the decay $B^+ \to K^+ \nu\bar{\nu}$*, Phys. Rev. Lett. **94** (2005) 101801, [hep-ex/0411061]. 76

[205] *Updated fits of the UTfit collaboration at* http://www.utfit.org/UTfit/, . 76

[206] W. A. Bardeen, S. H. H. Tye, and J. A. M. Vermaseren, *Phenomenology of the New Light Higgs Boson Search*, Phys. Lett. **76B** (1978) 580–584. 76

[207] P. Di Vecchia and G. Veneziano, *Chiral Dynamics in the Large N Limit*, Nucl. Phys. **B171** (1980) 253–272. 76

[208] I. de Medeiros Varzielas and L. Merlo, *Ultraviolet Completion of Flavour Models*, JHEP **02** (2011) 062, [arXiv:1011.6662]. 76

[209] S. M. Barr and D. Seckel, *Planck Scale Corrections to Axion Models*, Phys. Rev. **D46** (1992) 539–549. 77

[210] M. Kamionkowski and J. March-Russell, *Planck Scale Physics and the Peccei-Quinn Mechanism*, Phys. Lett. **B282** (1992) 137–141, [hep-th/9202003]. 77

[211] R. Holman, S. D. H. Hsu, T. W. Kephart, E. W. Kolb, R. Watkins, and L. M. Widrow, *Solutions to the Strong CP Problem in a World with Gravity*, Phys. Lett. **B282** (1992) 132–136, [hep-ph/9203206]. 77

[212] R. Alonso and A. Urbano, *Wormholes and Masses for Goldstone Bosons*, arXiv:1706.07415. 77, 86

[213] F. Arias-Aragon, E. Fernandez-Martinez, M. Gonzalez-Lopez, and L. Merlo, *Neutrino Masses and Hubble Tension via a Majoron in MFV*, Eur. Phys. J. C **81** (2021), no. 1 28, [arXiv:2009.01848]. 78

[214] L. Verde, T. Treu, and A. Riess, *Tensions Between the Early and the Late Universe*, arXiv:1907.10625. 79

[215] K. C. Wong *et. al.*, *H0LiCOW XIII. A 2.4% measurement of H_0 from lensed quasars: 5.3σ tension between early and late-Universe probes*, arXiv:1907.04869. 79

[216] A. G. Riess, S. Casertano, W. Yuan, L. M. Macri, and D. Scolnic, *Large Magellanic Cloud Cepheid Standards Provide a 1% Foundation for the Determination of the Hubble Constant and Stronger Evidence for Physics beyond ΛCDM*, Astrophys. J. **876** (2019), no. 1 85, [arXiv:1903.07603]. 79, 126

[217] M. Archidiacono, S. Gariazzo, C. Giunti, S. Hannestad, R. Hansen, M. Laveder, and T. Tram, *Pseudoscalar—Sterile Neutrino Interactions: Reconciling the Cosmos with Neutrino Oscillations*, JCAP **08** (2016) 067, [arXiv:1606.07673]. 79

[218] P. Ko and Y. Tang, *Light Dark Photon and Fermionic Dark Radiation for the Hubble Constant and the Structure Formation*, Phys. Lett. B **762** (2016) 462–466, [arXiv:1608.01083]. 79

[219] E. Di Valentino, C. Bøehm, E. Hivon, and F. R. Bouchet, *Reducing the H_0 and σ_8 tensions with Dark Matter-neutrino interactions*, Phys. Rev. D **97** (2018), no. 4 043513, [arXiv:1710.02559]. 79

[220] F. D'Eramo, R. Z. Ferreira, A. Notari, and J. L. Bernal, *Hot Axions and the H_0 tension*, JCAP **1811** (2018), no. 11 014, [arXiv:1808.07430]. 79, 98, 100, 102, 121, 122, 124

[221] P. Agrawal, F.-Y. Cyr-Racine, D. Pinner, and L. Randall, *Rock 'N' Roll Solutions to the Hubble Tension*, arXiv:1904.01016. 79

[222] P. Agrawal, G. Obied, and C. Vafa, *H_0 Tension, Swampland Conjectures and the Epoch of Fading Dark Matter*, arXiv:1906.08261. 79

[223] S. Alexander and E. McDonough, *Axion-Dilaton Destabilization and the Hubble Tension*, Phys. Lett. B **797** (2019) 134830, [arXiv:1904.08912]. 79

[224] S. Ghosh, R. Khatri, and T. S. Roy, *Dark Neutrino Interactions Phase Out the Hubble Tension*, arXiv:1908.09843. 79

[225] M. Escudero, D. Hooper, G. Krnjaic, and M. Pierre, *Cosmology with A Very Light $L_\mu - L_\tau$ Gauge Boson*, JHEP **03** (2019) 071, [arXiv:1901.02010]. 79

[226] M. Escudero and S. J. Witte, *A Cmb Search for the Neutrino Mass Mechanism and Its Relation to the Hubble Tension*, Eur. Phys. J. C **80** (2020), no. 4 294, [arXiv:1909.04044]. 79, 80, 81, 84, 93

[227] G. B. Gelmini, A. Kusenko, and V. Takhistov, *Hints of Sterile Neutrinos in Recent Measurements of the Hubble Parameter*, arXiv:1906.10136. 79

[228] M. Park, C. D. Kreisch, J. Dunkley, B. Hadzhiyska, and F.-Y. Cyr-Racine, *ΛCDM or self-interacting neutrinos: How CMB data can tell the two models apart*, Phys. Rev. D **100** (2019), no. 6 063524, [arXiv:1904.02625]. 79

[229] C. D. Kreisch, F.-Y. Cyr-Racine, and O. Doré, *The Neutrino Puzzle: Anomalies, Interactions, and Cosmological Tensions*, Phys. Rev. D **101** (2020), no. 12 123505, [arXiv:1902.00534]. 79

[230] T. L. Smith, V. Poulin, and M. A. Amin, *Oscillating Scalar Fields and the Hubble Tension: a Resolution with Novel Signatures*, Phys. Rev. D **101** (2020), no. 6 063523, [arXiv:1908.06995]. 79

[231] Y. Chikashige, R. N. Mohapatra, and R. Peccei, *Spontaneously Broken Lepton Number and Cosmological Constraints on the Neutrino Mass Spectrum*, Phys. Rev. Lett. **45** (1980) 1926. 80

[232] G. Gelmini and M. Roncadelli, *Left-Handed Neutrino Mass Scale and Spontaneously Broken Lepton Number*, Phys. Lett. B **99** (1981) 411–415. 80

[233] H. M. Georgi, S. L. Glashow, and S. Nussinov, *Unconventional Model of Neutrino Masses*, Nucl. Phys. B **193** (1981) 297–316. 80

[234] J. Schechter and J. Valle, *Neutrino Decay and Spontaneous Violation of Lepton Number*, Phys. Rev. D **25** (1982) 774. 80

[235] Z. Chacko, L. J. Hall, T. Okui, and S. J. Oliver, *Cmb Signals of Neutrino Mass Generation*, Phys. Rev. D **70** (2004) 085008, [hep-ph/0312267]. 80

[236] **CMB-S4** Collaboration, K. N. Abazajian *et. al.*, *CMB-S4 Science Book, First Edition*, arXiv:1610.02743. 80, 98, 109, 124, 125, 126, 127, 129

[237] S. Bashinsky and U. Seljak, *Neutrino Perturbations in Cmb Anisotropy and Matter Clustering*, Phys. Rev. D **69** (2004) 083002, [astro-ph/0310198]. 80

[238] E. Masso, F. Rota, and G. Zsembinszki, *On axion thermalization in the early universe*, Phys. Rev. **D66** (2002) 023004, [hep-ph/0203221]. 81, 97, 99, 122

[239] A. Salvio, A. Strumia, and W. Xue, *Thermal axion production*, JCAP **1401** (2014) 011, [arXiv:1310.6982]. 81, 98, 99, 100, 105, 113, 114, 122

[240] R. Z. Ferreira and A. Notari, *Observable Windows for the QCD Axion Through the Number of Relativistic Species*, Phys. Rev. Lett. **120** (2018), no. 19 191301, [arXiv:1801.06090]. 81, 98, 100, 111, 121, 122

[241] F. Arias-Aragon, F. D'Eramo, R. Z. Ferreira, L. Merlo, and A. Notari, *Cosmic Imprints of XENON1T Axions*, JCAP **11** (2020) 025, [arXiv:2007.06579]. 81, 97

[242] E. K. Akhmedov, Z. Berezhiani, R. Mohapatra, and G. Senjanovic, *Planck Scale Effects on the Majoron*, Phys. Lett. B **299** (1993) 90–93, [hep-ph/9209285]. 86

[243] B. A. Dobrescu, *The Strong CP Problem Versus Planck Scale Physics*, Phys. Rev. D **55** (1997) 5826–5833, [hep-ph/9609221]. 86

[244] B. Lillard and T. M. Tait, *A High Quality Composite Axion*, JHEP **11** (2018) 199, [arXiv:1811.03089]. 86

[245] A. Hook, S. Kumar, Z. Liu, and R. Sundrum, *The High Quality QCD Axion and the Lhc*, Phys. Rev. Lett. **124** (2020), no. 22 221801, [arXiv:1911.12364]. 86

[246] K. R. Dienes, E. Dudas, and T. Gherghetta, *Invisible Axions and Large Radius Compactifications*, Phys. Rev. D **62** (2000) 105023, [hep-ph/9912455]. 86

[247] K.-w. Choi, *A QCD Axion from Higher Dimensional Gauge Field*, Phys. Rev. Lett. **92** (2004) 101602, [hep-ph/0308024]. 86

[248] P. Cox, T. Gherghetta, and M. D. Nguyen, *A Holographic Perspective on the Axion Quality Problem*, JHEP **01** (2020) 188, [arXiv:1911.09385]. 86

[249] H. Fukuda, M. Ibe, M. Suzuki, and T. T. Yanagida, *A "gauged" $U(1)$ Peccei–Quinn symmetry*, Phys. Lett. B **771** (2017) 327–331, [arXiv:1703.01112]. 86

[250] C. D. Carone and M. Merchand, *T' models with high quality flaxions*, Phys. Rev. D **101** (2020), no. 11 115032, [arXiv:2004.02040]. 86

[251] **ATLAS** Collaboration, G. Aad *et. al.*, *Combined measurements of Higgs boson production and decay using up to $80\ fb^{-1}$ of proton-proton collision data at $\sqrt{s} = 13$ TeV collected with the ATLAS experiment*, Phys. Rev. D **101** (2020), no. 1 012002, [arXiv:1909.02845]. 87

[252] S. King, *Large mixing angle MSW and atmospheric neutrinos from single right-handed neutrino dominance and U(1) family symmetry*, Nucl. Phys. B **576** (2000) 85–105, [hep-ph/9912492]. 90

[253] C. García-Cely and J. Heeck, *Neutrino Lines from Majoron Dark Matter*, JHEP **05** (2017) 102, [arXiv:1701.07209]. 91, 92

[254] **KamLAND-Zen** Collaboration, A. Gando *et. al.*, *Search for Majorana Neutrinos Near the Inverted Mass Hierarchy Region with Kamland-Zen*, Phys. Rev. Lett. **117** (2016), no. 8 082503, [arXiv:1605.02889]. [Addendum: Phys.Rev.Lett. 117, 109903 (2016)]. 93

[255] R. Arnold *et. al.*, *Final results on ^{82}Se double beta decay to the ground state of ^{82}Kr from the NEMO-3 experiment*, Eur. Phys. J. C **78** (2018), no. 10 821, [arXiv:1806.05553]. 93

[256] R. Cepedello, F. F. Deppisch, L. González, C. Hati, and M. Hirsch, *Neutrinoless Double-β Decay with Nonstandard Majoron Emission*, Phys. Rev. Lett. **122** (2019), no. 18 181801, [arXiv:1811.00031]. 93

[257] **CMS** Collaboration, A. M. Sirunyan *et. al.*, *Search for Invisible Decays of a Higgs Boson Produced Through Vector Boson Fusion in Proton-Proton Collisions at $\sqrt{s} = 13$ TeV*, Phys. Lett. B **793** (2019) 520–551, [arXiv:1809.05937]. 94

[258] D. Gorbunov and M. Shaposhnikov, *How to find neutral leptons of the νMSM?*, JHEP **10** (2007) 015, [arXiv:0705.1729]. [Erratum: JHEP 11, 101 (2013)]. 94

[259] A. Atre, T. Han, S. Pascoli, and B. Zhang, *The Search for Heavy Majorana Neutrinos*, JHEP **05** (2009) 030, [arXiv:0901.3589]. 94

[260] K. Bondarenko, A. Boyarsky, D. Gorbunov, and O. Ruchayskiy, *Phenomenology of GeV-scale Heavy Neutral Leptons*, JHEP **11** (2018) 032, [arXiv:1805.08567]. 94

[261] **SHiP** Collaboration, C. Ahdida *et. al.*, *Sensitivity of the SHiP experiment to Heavy Neutral Leptons*, JHEP **04** (2019) 077, [arXiv:1811.00930]. 94

[262] K. Bondarenko, A. Boyarsky, M. Ovchynnikov, and O. Ruchayskiy, *Sensitivity of the intensity frontier experiments for neutrino and scalar portals: analytic estimates*, JHEP **08** (2019) 061, [arXiv:1902.06240]. 94

[263] P. Ballett, T. Boschi, and S. Pascoli, *Heavy Neutral Leptons from low-scale seesaws at the DUNE Near Detector*, JHEP **20** (2020) 111, [arXiv:1905.00284]. 94

[264] J. M. Berryman, A. de Gouvea, P. J. Fox, B. J. Kayser, K. J. Kelly, and J. L. Raaf, *Searches for Decays of New Particles in the DUNE Multi-Purpose Near Detector*, JHEP **02** (2020) 174, [arXiv:1912.07622]. 94

[265] P. Coloma, E. Fernández-Martínez, M. González-López, J. Hernández-García, and Z. Pavlovic, *GeV-scale neutrinos: interactions with mesons and DUNE sensitivity*, arXiv:2007.03701. 94

[266] F. del Aguila and J. Aguilar-Saavedra, *Distinguishing seesaw models at LHC with multi-lepton signals*, Nucl. Phys. B **813** (2009) 22–90, [arXiv:0808.2468]. 94

[267] S. Antusch and O. Fischer, *Testing sterile neutrino extensions of the Standard Model at future lepton colliders*, JHEP **05** (2015) 053, [arXiv:1502.05915]. 94

[268] F. F. Deppisch, P. Bhupal Dev, and A. Pilaftsis, *Neutrinos and Collider Physics*, New J. Phys. **17** (2015), no. 7 075019, [arXiv:1502.06541]. 94

[269] S. Antusch, E. Cazzato, and O. Fischer, *Sterile neutrino searches at future e^-e^+, pp, and e^-p colliders*, Int. J. Mod. Phys. A **32** (2017), no. 14 1750078, [arXiv:1612.02728]. 94

[270] Y. Cai, T. Han, T. Li, and R. Ruiz, *Lepton Number Violation: Seesaw Models and Their Collider Tests*, Front. in Phys. **6** (2018) 40, [arXiv:1711.02180]. 94

[271] P. Bhupal Dev and Y. Zhang, *Displaced vertex signatures of doubly charged scalars in the type-II seesaw and its left-right extensions*, JHEP **10** (2018) 199, [arXiv:1808.00943]. 94

[272] S. Pascoli, R. Ruiz, and C. Weiland, *Heavy neutrinos with dynamic jet vetoes: multilepton searches at $\sqrt{s} = 14$, 27, and 100 TeV*, JHEP **06** (2019) 049, [arXiv:1812.08750]. 94

[273] K. Sato and M. Kobayashi, *Cosmological Constraints on the Mass and the Number of Heavy Lepton Neutrinos*, Prog. Theor. Phys. **58** (1977) 1775. 94

[274] J. Gunn, B. Lee, I. Lerche, D. Schramm, and G. Steigman, *Some Astrophysical Consequences of the Existence of a Heavy Stable Neutral Lepton*, Astrophys. J. **223** (1978) 1015–1031. 94

[275] P. Hernandez, M. Kekic, and J. Lopez-Pavon, *Low-scale seesaw models versus N_{eff}*, Phys. Rev. D **89** (2014), no. 7 073009, [arXiv:1311.2614]. 94

[276] P. Hernandez, M. Kekic, and J. Lopez-Pavon, *$N_{\rm eff}$ in low-scale seesaw models versus the lightest neutrino mass*, Phys. Rev. D **90** (2014), no. 6 065033, [arXiv:1406.2961]. 94

[277] A. C. Vincent, E. F. Martínez, P. Hernández, M. Lattanzi, and O. Mena, *Revisiting Cosmological Bounds on Sterile Neutrinos*, JCAP **04** (2015) 006, [arXiv:1408.1956]. 94, 95

[278] A. Dolgov, S. Hansen, G. Raffelt, and D. Semikoz, *Cosmological and astrophysical bounds on a heavy sterile neutrino and the KARMEN anomaly*, Nucl. Phys. B **580** (2000) 331–351, [hep-ph/0002223]. 95

[279] O. Ruchayskiy and A. Ivashko, *Restrictions on the lifetime of sterile neutrinos from primordial nucleosynthesis*, JCAP **10** (2012) 014, [arXiv:1202.2841]. 95

[280] G. B. Gelmini, M. Kawasaki, A. Kusenko, K. Murai, and V. Takhistov, *Big Bang Nucleosynthesis constraints on sterile neutrino and lepton asymmetry of the Universe*, arXiv:2005.06721. 95

[281] A. Boyarsky, M. Ovchynnikov, O. Ruchayskiy, and V. Syvolap, *Improved BBN Constraints on Heavy Neutral Leptons*, arXiv:2008.00749. 95

[282] F. Arias-Aragón, F. D'eramo, R. Z. Ferreira, L. Merlo, and A. Notari, *Production of Thermal Axions across the ElectroWeak Phase Transition*, JCAP **03** (2021) 090, [arXiv:2012.04736]. 97

[283] **XENON** Collaboration, E. Aprile *et. al.*, *Excess electronic recoil events in XENON1T*, Phys. Rev. D **102** (2020), no. 7 072004, [arXiv:2006.09721]. 97, 120, 126

[284] M. S. Turner, *Thermal Production of Not SO Invisible Axions in the Early Universe*, Phys. Rev. Lett. **59** (1987) 2489. [Erratum: Phys. Rev. Lett.60,1101(1988)]. 97

[285] K. Abazajian *et. al.*, *CMB-S4 Science Case, Reference Design, and Project Plan*, arXiv:1907.04473. 98

[286] C. Brust, D. E. Kaplan, and M. T. Walters, *New Light Species and the CMB*, JHEP **12** (2013) 058, [arXiv:1303.5379]. 98

[287] D. Baumann, D. Green, and B. Wallisch, *New Target for Cosmic Axion Searches*, Phys. Rev. Lett. **117** (2016), no. 17 171301, [arXiv:1604.08614]. 98, 113

[288] J. L. Bernal, L. Verde, and A. G. Riess, *The trouble with H_0*, JCAP **1610** (2016), no. 10 019, [arXiv:1607.05617]. 100

[289] B. D. Fields, K. A. Olive, T.-H. Yeh, and C. Young, *Big-Bang Nucleosynthesis After Planck*, JCAP **03** (2020) 010, [arXiv:1912.01132]. 109

[290] **CAST** Collaboration, E. Arik *et. al.*, *Probing eV-scale axions with CAST*, JCAP **0902** (2009) 008, [arXiv:0810.4482]. 113, 126, 127

[291] I. G. Irastorza *et. al.*, *Towards a New Generation Axion Helioscope*, JCAP **1106** (2011) 013, [arXiv:1103.5334]. 113

[292] E. Armengaud *et. al.*, *Conceptual Design of the International Axion Observatory (IAXO)*, JINST **9** (2014) T05002, [arXiv:1401.3233]. 113

[293] M. Gorghetto, E. Hardy, and G. Villadoro, *Axions from Strings: the Attractive Solution*, JHEP **07** (2018) 151, [arXiv:1806.04677]. 116, 119

[294] M. Gorghetto, E. Hardy, and G. Villadoro, *More Axions from Strings*, arXiv:2007.04990. 116, 119

[295] L. Di Luzio, F. Mescia, and E. Nardi, *The Window for Preferred Axion Models*, arXiv:1705.05370. 117

[296] A. Vilenkin and A. Everett, *Cosmic Strings and Domain Walls in Models with Goldstone and PseudoGoldstone Bosons*, Phys. Rev. Lett. **48** (1982) 1867–1870. 119

[297] T. Vachaspati, A. E. Everett, and A. Vilenkin, *Radiation From Vacuum Strings and Domain Walls*, Phys. Rev. D **30** (1984) 2046. 119

[298] S. Chang, C. Hagmann, and P. Sikivie, *Studies of the motion and decay of axion walls bounded by strings*, Phys. Rev. D **59** (1999) 023505, [hep-ph/9807374]. 119

[299] C. Hagmann, S. Chang, and P. Sikivie, *Axion radiation from strings*, Phys. Rev. D **63** (2001) 125018, [hep-ph/0012361]. 119

[300] A. Vilenkin, *Gravitational Field of Vacuum Domain Walls and Strings*, Phys. Rev. D **23** (1981) 852–857. 119

[301] P. Sikivie, *Of Axions, Domain Walls and the Early Universe*, Phys. Rev. Lett. **48** (1982) 1156–1159. 119

[302] J. Ipser and P. Sikivie, *The Gravitationally Repulsive Domain Wall*, Phys. Rev. D **30** (1984) 712. 119

[303] A. Vilenkin, *Gravitational Field of Vacuum Domain Walls*, Phys. Lett. B **133** (1983) 177–179. 119

[304] A. E. Robinson, *XENON1T observes tritium*, arXiv:2006.13278. 120

[305] B. Bhattacherjee and R. Sengupta, *Xenon1t excess: Some possible backgrounds*, arXiv:2006.16172. 120

[306] L. Di Luzio, F. Mescia, E. Nardi, P. Panci, and R. Ziegler, *Astrophobic Axions*, Phys. Rev. Lett. **120** (2018), no. 26 261803, [arXiv:1712.04940]. 120

[307] C. Gao, J. Liu, L.-T. Wang, X.-P. Wang, W. Xue, and Y.-M. Zhong, *Re-Examining the Solar Axion Explanation for the Xenon1T Excess*, arXiv:2006.14598. 120

[308] J. Sun and X.-G. He, *Axion-Photon Coupling Revisited*, arXiv:2006.16931. 120

[309] I. M. Bloch, A. Caputo, R. Essig, D. Redigolo, M. Sholapurkar, and T. Volansky, *Exploring new physics with o(kev) electron recoils in direct detection experiments*, arXiv:2006.14521. 120

[310] S. Chang and K. Choi, *Hadronic axion window and the big bang nucleosynthesis*, Phys. Lett. **B316** (1993) 51–56, [hep-ph/9306216]. 122

[311] S. Hannestad, A. Mirizzi, and G. Raffelt, *New cosmological mass limit on thermal relic axions*, JCAP **07** (2005) 002, [hep-ph/0504059]. 122

[312] M. Archidiacono, S. Hannestad, A. Mirizzi, G. Raffelt, and Y. Y. Wong, *Axion hot dark matter bounds after Planck*, JCAP **10** (2013) 020, [arXiv:1307.0615]. 122

[313] M. Millea, *New cosmological bounds on axions in the XENON1T window*, arXiv:2007.05659. 122

[314] L. Di Luzio, M. Fedele, M. Giannotti, F. Mescia, and E. Nardi, *Solar Axions Cannot Explain the Xenon1T Excess*, arXiv:2006.12487. 124, 125, 127

[315] C. Brust, D. E. Kaplan, and M. T. Walters, *New Light Species and the CMB*, JHEP **12** (2013) 058, [arXiv:1303.5379]. 124

[316] R. Bollig, W. DeRocco, P. W. Graham, and H.-T. Janka, *Muons in supernovae: implications for the axion-muon coupling*, arXiv:2005.07141. 124

[317] D. Croon, G. Elor, R. K. Leane, and S. D. McDermott, *Supernova Muons: New Constraints on Z' Bosons, Axions, and ALPs*, arXiv:2006.13942. 124

[318] G. Ballesteros, A. Notari, and F. Rompineve, *The H_0 tension: ΔG_N vs. $\Delta N_{\rm eff}$*, arXiv:2004.05049. 126, 129

[319] M. Gonzalez, M. P. Hertzberg, and F. Rompineve, *Ultralight Scalar Decay and the Hubble Tension*, arXiv:2006.13959. 126, 129

[320] **Simons Observatory** Collaboration, P. Ade *et. al.*, *The Simons Observatory: Science goals and forecasts*, JCAP **1902** (2019) 056, [arXiv:1808.07445]. 126

[321] **IAXO** Collaboration, E. Armengaud *et. al.*, *Physics potential of the International Axion Observatory (IAXO)*, JCAP **06** (2019) 047, [arXiv:1904.09155]. 127

[322] S. Borsanyi *et. al.*, *Calculation of the Axion Mass Based on High-Temperature Lattice Quantum Chromodynamics*, Nature **539** (2016), no. 7627 69–71, [arXiv:1606.07494]. 128

[323] **PandaX** Collaboration, H. Zhang *et. al.*, *Dark matter direct search sensitivity of the PandaX-4T experiment*, Sci. China Phys. Mech. Astron. **62** (2019), no. 3 31011, [arXiv:1806.02229]. 130

[324] **LZ** Collaboration, D. Akerib *et. al.*, *The LUX-ZEPLIN (LZ) Experiment*, Nucl. Instrum. Meth. A **953** (2020) 163047, [arXiv:1910.09124]. 130

[325] A. Crivellin, F. D'Eramo, and M. Procura, *New Constraints on Dark Matter Effective Theories from Standard Model Loops*, Phys. Rev. Lett. **112** (2014) 191304, [arXiv:1402.1173]. 150

[326] F. D'Eramo and M. Procura, *Connecting Dark Matter UV Complete Models to Direct Detection Rates via Effective Field Theory*, JHEP **04** (2015) 054, [arXiv:1411.3342]. 150

[327] F. D'Eramo, B. J. Kavanagh, and P. Panci, *You can hide but you have to run: direct detection with vector mediators*, JHEP **08** (2016) 111, [arXiv:1605.04917]. 150

[328] F. D'Eramo, B. J. Kavanagh, and P. Panci, *Probing Leptophilic Dark Sectors with Hadronic Processes*, Phys. Lett. B **771** (2017) 339–348, [arXiv:1702.00016]. 150